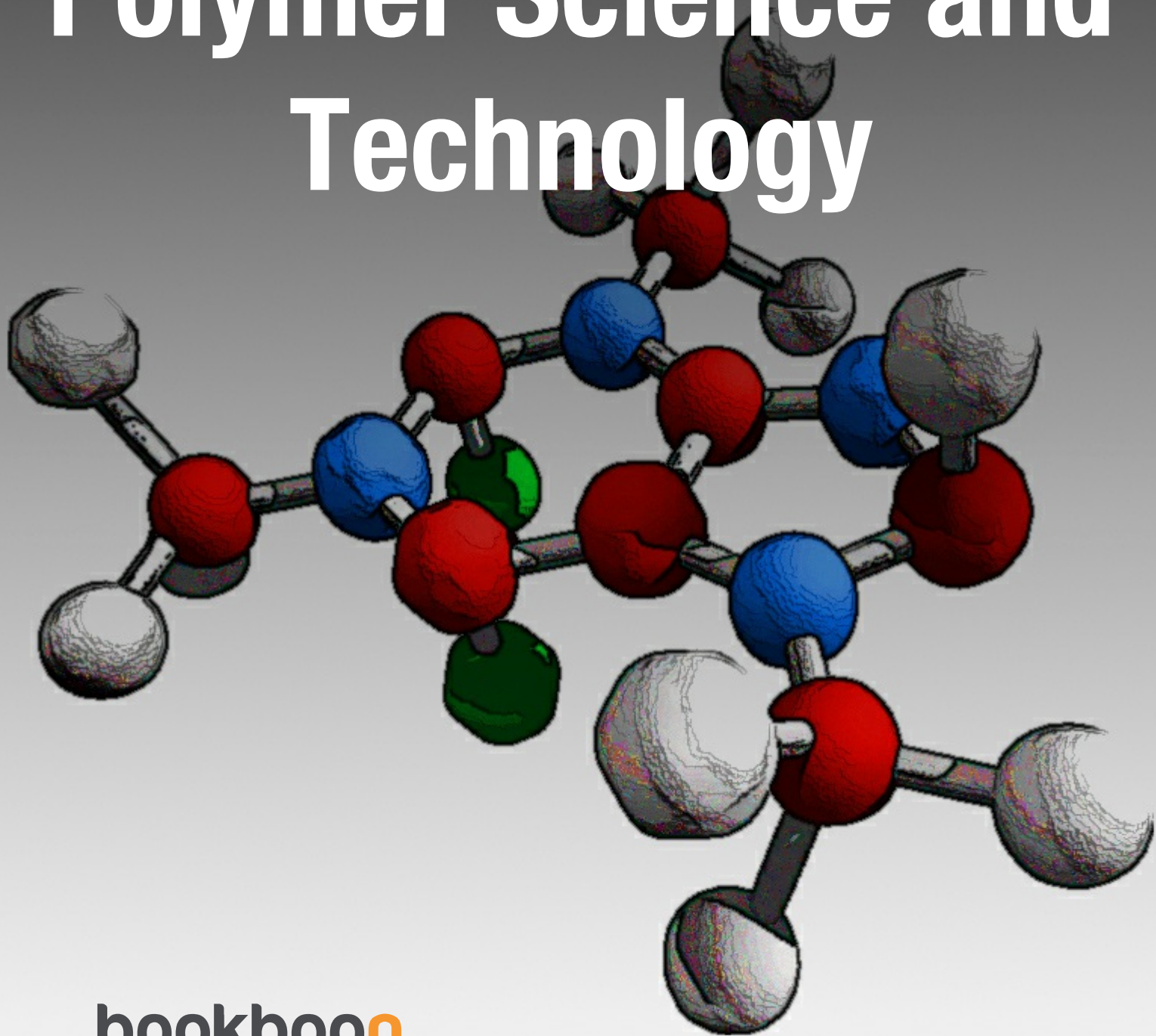


Mustafa Akay

Introduction to Polymer Science and Technology



Mustafa Akay

Introduction to Polymer Science and Technology

Introduction to Polymer Science and Technology

© 2015 Mustafa Akay & bookboon.com

ISBN 978-87-403-0087-1.

Contents

	Preface	8
	Acknowledgements	9
1	Introduction	10
1.1	History of the development of polymers	10
1.2	Why a clear understanding of material is important?	12
1.3	What can be achieved by appropriate selection of polymer-based materials?	17
1.4	What makes polymers versatile?	20
2	Polymerisation	31
2.1	Polymerisation mechanisms	31
2.2	Polymerisation processes	36
2.3	Polymerisation reactors	39
2.4	Catalysts	42
2.5	Molecular weight and molecular weight distributions	47
2.6	Self-assessment questions	50

3	Polymer processing	54
3.1	Concept of rheology	54
3.2	Processing and forming thermoplastics	56
3.3	Processing and forming thermosetting polymers	98
3.4	Self-assessment questions	109
4	Microstructure	111
4.1	Stereoregularity	112
4.2	Morphology in semi-crystalline thermoplastics	113
4.3	Degree of crystallinity	116
4.4	Crosslinking	124
4.5	Copolymer arrangements	126
4.6	Domain structures	127
4.7	Degree of molecular orientation	128
4.8	Self-assessment questions	130
5	Behaviour of polymers	133
5.1	Degradation of Polymers	133
5.2	Viscoelasticity	134
5.3	Relaxation transitions	150
5.4	Self-assessment questions	158

6	Mechanical properties	163
6.1	Introduction	163
6.2	Tensile properties	166
6.3	Flexural properties	179
6.4	Compressive properties	184
6.5	Shear properties	186
6.6	Hardness	187
6.7	Impact properties and fracture toughness	189
6.8	Bearing strength	196
6.9	Environmental stress cracking	199
6.10	Fatigue and wear	202
6.11	Self-assessment questions	206
7	Thermal properties	209
7.1	Differential scanning calorimetry	210
7.2	Thermogravimetric analysis	218
7.3	Thermomechanical analysis	221
7.4	Dynamic mechanical thermal analysis	225
7.5	Determination of softening temperature	248
7.6	Self-assessment questions	257
	References	261

To my parents (Rahmetullahi Aleyhima), to my wife, and to Mevlüde, Latifa and Melek, the apples of my eye

Preface

Learning involves acquiring knowledge, which is encouraged in all traditions. For example, the Quran urges people to seek knowledge and to use it for the well being of society:

“My Lord, increase me in knowledge”, Al-Quran 20:114.

Knowledge should be applied in a safe, responsible and ethical manner not only to benefit us personally but also to improve the lot of the people we live with. It is also a duty to ensure that our surrounding habitat is not endangered. This sometimes requires knowledge of the local culture to help achieve a desirable outcome. Martin Palmer’s presentation on BBC Thought for the Day programme, 17/06/2006, on the subject of the protection of the oceans included:

“To many around the world the environmental movement and its proffered solutions - usually economic - are alien ways of thinking and seeing the world, and can be interpreted as telling people what is best for them whether they like it or not. Let me tell you a story. Dynamite-fishing off the East African coast is a major problem. Environmental organisations have been addressing it for years, from working with Governments, to sending armed boats to threaten those illegally fishing. None of this worked because it had no relationship to the actual lives or values of the local fishermen all of whom are Muslims. What has worked off one island, Misali, is the Qur’an. In the Qur’an, waste of natural resources is denounced as a sin. Once local imams had discovered this, they set about preaching that dynamite fishing was anti-Islamic, non-sustainable and sinful. This ended the dynamite fishing of the Misali fishermen because it made sense to them spiritually.”

The subject of this book is covered in seven chapters. The chapters are arranged in an attempt to reflect the three pillars of materials science and technology: in materials, there is a strong link between processing, microstructure and properties. Changing one affects the others and this has enabled scientists/engineers to tailor materials to suit purposes. Nature provides many examples of how materials comply with the processing-microstructure-properties relationship, e.g., one of the wonders of the world, the Giant’s Causeway consists of regular columns of polygonal slabs of volcanic basalt deposition juxtaposed the same material in rubble form with no recognisable shape. Based on the prevailing conditions, particularly that of temperature and the rate of cooling, the lava has solidified in regular as well as irregular forms. The processing-properties link is also highlighted by Leo Baekeland, the inventor of the first commercial plastic:

“I was trying to make something really hard, but then I thought I should make something really soft instead, that could be molded into different shapes. That was how I came up with the first plastic. I called it Bakelite.”

Chapter 1 in this book is introductory and includes a history of the development of polymers; the importance of the knowledge of materials for engineers and technologists; what makes polymeric materials attractive over conventional materials and a description of the versatile nature of polymers. The subsequent two chapters deal with the polymerisation processes and the processes employed in the conversion of polymeric raw materials into products. Chapter 4 covers the microstructural features in polymers, including lamellae, spherulites, crosslinking, and the measurements of degrees of crystallinity and molecular orientation. The viscoelastic nature of polymers, the time/temperature sensitivity of viscoelasticity and how this manifests itself in the form of creep, stress relaxation and mechanical damping are covered in Chapter 5. Glass transition and its dependence on molecular features are also covered in Chapter 5. The last two chapters cover various aspects of mechanical and thermal properties of polymers. Writing this book has been educational, and I thank BookBoon for giving me the opportunity.

Mustafa Akay, N. Ireland, February 2015

Acknowledgements

The book emerges from my work at the Ulster Polytechnic/University of Ulster, where I met and worked with various characters and personalities and I would like to mention Lesley Hawe, the late Archie Holmes and Myrtle Young who epitomise for me the constant kindness, help and support I received from the academic, technical and secretarial staff over the years.

The book incorporates material taken from various sources, including my lecture notes, research outcomes of my postgraduate students, some of them have become friends for life, and some excellent text books, research papers/news, industry/company/organisation literature and web material that we are so fortunate to have access to. The sources of the materials used are gratefully acknowledged and are listed as references, however, over the years material permeates into teaching notes that is not always possible to trace the references for. I apologise, therefore, for any such material that has no accompanying reference and I express my thanks and gratitude to the people concerned.

A special thank you goes to my wife for the offers of regular walks to blow away the cobwebs and visits to “Mugwumps” for coffee.

1 Introduction

1.1 History of the development of polymers

“Genius is one percent inspiration and ninety-nine percent perspiration.” **Thomas A. Edison**, 1847-1931.

Edison, one of the most prolific inventors in history, has appreciated the work of others, believed in team working, and has stated, “I start where the last man left off.” Over time, the work of the pioneers of polymer science, some listed below, has been gratefully acknowledged by others and developed upon.

1839 Eduard Simon discovered **polystyrene**.

1843 Hancock in England and Goodyear in USA developed the **vulcanisation of rubber** by mixing it with sulphur. Charles Goodyear epitomizes the 99% perspiration attitude: toiled all his life in spite of many set-backs and disappointments.

1854 Samuel Peck produced “union cases” for photographs by mixing shellac (produced from the secretions of the lac beetle which live on trees native to India and South-East Asia) sawdust, other chemicals and dye, and heated and pressed the mixture into a mould to form the parts of a Union Case. The term “union” refers to the material composition, i.e., synonymous with the terms mixture or blend.

1862 Alexander Parkes exhibited Parkesine, made from **cellulose nitrate**, at an International Exhibition in London.

1868 The Hyatt brothers in America produced celluloid from cellulose nitrate mixed with camphor. This was unstable and subsequently led to the development of cellulose acetate. They developed many of the first plastics mass **production techniques** such as blow moulding, compression moulding and extrusion.

1869 Daniel Spill took over the rights to manufacture Parkesine in England and established the Xylonite Company producing Xylonite and Ivoride.

1872 Eugen Baumann, one of the first to invent **polyvinyl chloride (PVC)**.

1897 Spitteler in Germany patented casein, marketed as Galalith, made from protein from milk mixed with formaldehyde.

1907 Leo Baekeland produced **phenol-formaldehyde**, the first truly synthetic plastic, Bakelite. Cast with pigments to resemble onyx, jade, marble and amber it has come to be known as phenolic resin.

1910 The Dreyfus brothers perfected **cellulose acetate lacquers** and plastic film.

1912 Fritz Klatte discovered **polyvinyl acetate** and patented the **manufacturing** process for PVC.

- 1924 Rossiter produced urea thiourea formaldehyde, marketed as Linga Longa or as Bandalasta ware by British Cyanides.
- 1928 Otto Rohm in Germany stuck two sheets of glass together using an acrylic ester and accidentally discovered safety glass, and production of some articles began in 1933.
- 1933 ICI discovered **polyethylene**.
- 1933 **Melamine formaldehyde** resins were developed through the 1930s and 1940s in companies such as American Cyanamid, Ciba and Henkel.
- 1935 **Wallace Carothers**, working for DuPont, invented poly(hexamethylene-adipamide), Du Pont named this product **nylon**. Carothers did not see the widespread application of his work in consumer goods such as toothbrushes, fishing lines, and lingerie, or in special uses such as surgical thread, parachutes, or pipes, nor the powerful effect it had in launching a whole era of synthetics. Sadly, he died in early 1937 at the young age of 41.
- 1936 **Polymethyl methacrylate sheet**, Perspex, was cast by ICI, and shortly after it was employed in aircraft glazing.
- 1936 The Wulff brothers in Germany produced commercially viable **polystyrene**.
- 1937 Otto Bayer patented **polyurethane**.
- 1938 Roy Plunkett working for DuPont accidentally discovered **poly(tetra fluoroethylene)**, PTFE, trademarked Teflon.
- 1941 Commercial development of **polyesters** for moulding began in the USA.
- 1941 **Polyethylene terephthalate** (PET), a saturated polyester patented by John Rex Whinfield and James Tennant Dickson.
- 1948 **Acrylonitrile butadiene styrene** (ABS).
- 1951 Paul Hogan and Robert Banks of Phillips Petroleum discovered **high-density polyethylene** and **crystalline polypropylene**.
- 1953 Polyethylene polymerisation was achieved at low pressures using Ziegler **catalysts**.
- 1954 Giulio Natta succeeded in “stereospecific” polymerisation of propylene with Ziegler-type catalysts. Karl Ziegler and Giulio Natta received the Nobel Prize in Chemistry for their work in 1963.
- 1958 **Polycarbonate** was put into mass manufacture.
- 1964 Stephanie Louise Kwolek of DuPont developed Kevlar fibre from **polyaramide** (an aromatic polyamide).
- 1987 BASF in Germany produced a **polyacetylene** that has twice the electrical conductivity of copper.

ICI published the book entitled “Landmarks of the Plastics Industry: 1862-1962” to mark the centenary of Alexander Parkes’ invention of the world’s first man-made plastic, and to pay tribute to those who have helped to establish the modern plastics industry and to those who are working towards its improvement and expansion.

Products, machinery and constructions all require the employment of materials and energy. What materials are used depends on availability, cost and, of course, suitability for purpose. As metal replaced wood in many consumer products, plastics were developed as an even cheaper alternative. The cost of casting metal increased sharply after World War II, while plastic could be formed relatively cheaply. For this reason plastics gradually replaced many things that were originally made in metal. However the choice of material requires sound judgement. Accordingly the subject of materials is taught on traditional engineering courses mechanical, civil and electrical as well as others such as sports technology and bio-medical engineering.

The importance of materials and the need for a sound awareness and understanding of materials for engineering practitioners is further explored below. The website ‘whystudymaterials.ac.uk’ also includes topics of interest in this regard.

1.2 Why a clear understanding of material is important?

In days gone by, all that the designer/engineer had to work with was cast iron, a limited range of steel, some non-ferrous metals and wood. Today, we are faced with a bewildering choice of materials and the problem of comparing materials of different types and from different suppliers. As scientists and engineers a clear understanding of these materials is vital in order to:

1.2.1 Select the right material and the production process for an application

Selection involves such considerations as the material properties (mechanical, thermal, electrical, optical and chemical); service conditions (e.g., operating temperature and humidity) and service life; impact on the environment and health and safety; economics; appearance (e.g., shape, colour, surface finish, decoration); type of production (injection moulding, extrusion, compression moulding, resin transfer mouldings, etc), and production-related material behaviour (e.g., flow, shrinkage, residual stresses, weld lines, etc).

The selection sometimes can mean life or death. For instance, the Challenger, space shuttle, disaster in January 1986 apparently resulted from not choosing quite the right sort of rubber seal for the fuel system. The O-ring seal became rigid and lost its resilience/pliability at low temperatures and resulted in fuel seepage. The seal was made of silicone rubber, which can crystallise under stress. As the craft waited for launch, the O-ring remained clamped too long and its T_g increased considerably.

The Concorde crash, which occurred in July 2000, killed 113 people – all passengers on board the aircraft, nine crew and four people on the ground. The aircraft caught fire, see Figure 1.1, on take-off from Paris Charles de Gaulle Airport when one of its tyres was punctured by a strip of metal (debris from another aircraft) lying on the runway, and the burst tyre possibly piercing through the under carriage into a fuel tank. After the accident, although, the Concorde tyres were modified and the under carriage was reinforced with Kevlar (a high performance aramid fibre) Concorde flights did not quite resume service.



Figure 1.1 Concorde undercarriage on flame (source: Google images (Toshihiko Sato/AP))

Rolls Royce, one of the pioneers in the production and application of highly acclaimed carbon-fibre in the 1960s, used carbon-fibre in the manufacture of compressor blades for one of their aero-engines without, in retrospect, a full appreciation/evaluation of the mechanical properties of the material. The blades proved to be vulnerable to “bird strike”. Consequently, as stated in Wikipedia “Rolls-Royce’s problems became so great that the company was eventually nationalized by the British government in 1971 and the carbon-fibre production plant was sold off to form Bristol Composites”, <http://bit.ly/jffQt0> .

Away from aerospace examples, Ezrin (1996, p101) cites the example of high density polyethylene (HDPE) aerators in a sewage lagoon that fractured due to unanticipated environmental stress cracking (ESC) under dynamic flexural stress. The design was at fault for the selection of HDPE, which has poor ESC, and for the grade of HDPE selected, since ESC is affected by molecular weight. The failure was at the sharp bend of the four feet, which were bolted to concrete pads.

Therefore when considering new materials, assess:

- availability
- properties
- processability
- suitability/ functionality, even under extreme conditions
- aesthetics and history of the product
- environmental impact and health & safety.

Most importantly think fabrication and corrosion/deterioration.

1.2.2 Assess product liability

New plastics and grades continue to develop rapidly and long-term experience in many areas has yet to be realised. The Consumer Protection Act (1987) places special responsibility on designers of plastic products to ensure that their choice of plastic will not endanger the user by, for example, breaking prematurely or by releasing toxic constituents or fail to perform suitably under the real conditions of use. Ezrin (1996, p293) points out that “Part of the product liability problem for plastics has to be laid to their success as new, innovative materials and processes fulfilling old and new needs in many applications. The pace of technological advance has been very fast with plastics, racing ahead of the time and effort needed to fully evaluate all potential failure situations”. It is also stated that products designed and manufactured with inadequate knowledge of plastics limitations and any peculiar synergistic (or antagonistic) effects keep lawyers in business and hurt the reputation of plastics.

Considerations in design that have a direct bearing on product liability and safety are (Witherell, 1985, p174):

- function of product
- market and sales information
- design characteristics
- test considerations
- critical parts involved
- environmental considerations
- high risk uses
- reliability requirements
- maintenance and operations demands
- conformance to standards and regulatory requirements
- packaging and shipping
- end-use requirements.

1.2.3 Develop and automate production techniques

Numerous improvements have been made to various labour intensive production methods, e.g., from the bucket and brush glass-reinforced plastics (GRP) Lotus Elan sports car to the VARI (vacuum-assisted resin injection) GRP Lotus Elan.

Plastics grow on trees! Biodegradable plastics (suitable for the production of bottles and similar containers) have been grown in plants such as the mushroom plant and sugar beet by employing genetic engineering.

Monsanto are growing biodegradable plastics plants by genetic engineering.

1.2.4 Design for recyclability

Manufacturing economics and concerns about environmental pollution have combined to put pressure on the designer to re-think the approach to product design, and to consider the entire life-cycle of the product. The technical challenges associated with the recovery and recycling of the major plastic components are being addressed by the plastics industry, original equipment manufacturers (OEMs) and an emerging appliance recycling industry. A widespread recovery of valuable plastics from discarded products will provide significant life cycle benefits.

The increased use of plastics in industries, e.g., automotive, is due to advantages such as reductions in weight, cost savings, greater manufacturing flexibility and shortened lead times. One drawback, particularly in the face of stringent EU legislation, is the lack of effective separating and recycling technology, which becomes a hindrance to the realisation of the full potential of plastics.

1.2.5 Solve problems

The urgencies of war, for example, have been the driving force for many of the most remarkable developments in materials, often to provide a solution to problems which previously simply did not exist, or at least were not perceived to exist.

1.2.6 Challenge and replace traditional materials

Plastic mouldings have demonstrated their worth in a number of industries. The major benefits, as alternatives to metals, are parts consolidation (i.e., fewer materials and components in one part), lower weight, improved strength and stiffness-to-weight ratios, corrosion resistance, and reduced cost of parts. Figure 1.2 shows scenes from the Phoenix pipe-laying operation along the Shore Road, near the University of Ulster. Phoenix purchased the old Belfast gas system and used it as a conduit for inserting new pipeline. This minimised disruption and maximised productivity by limiting trench digging.

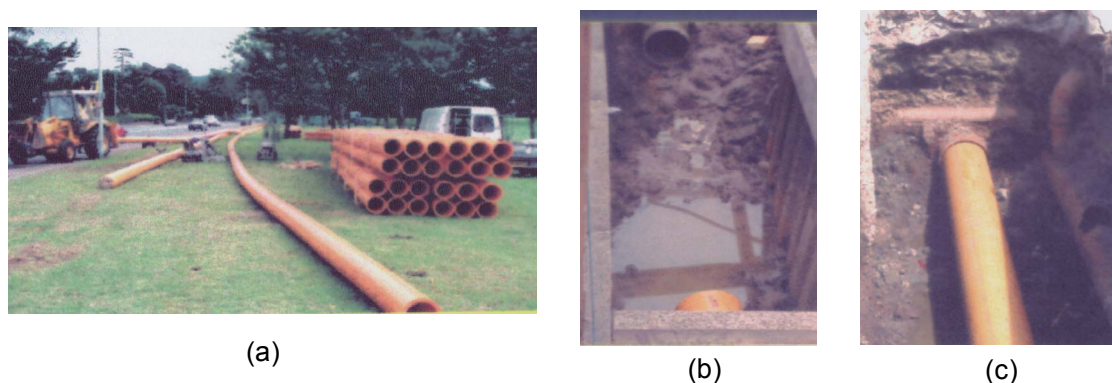


Figure 1.2 High density polyethylene (HDPE) replaces iron as gas-transmission pipes: (b) shows both old and new pipes and (c) the insertion of HDPE pipe into the old iron pipe

Replacement of metals with polymer-based materials occurs regularly in nearly all engineering sectors and is regularly forecast by practitioners: Humphreys (1997, p50) in his contribution to UK-Japan Symposium on Science and Society states, “Seventy per cent of the weight of a suspension bridge is in the steel cables. If you make the bridge longer and longer, it can no longer hold up its own suspension cables. The maximum length or span of a conventional suspension bridge is 5,000 metres. If you replace the steel ropes with carbon fibre ropes, however, then one can calculate that the maximum span goes up by a factor of three. In principle, you could have a suspension bridge which is 15, 000 metres long.” This notion was also expressed by Ramsden (2009) in his analysis of the suspension bridge over the Strait of Messina, connecting the Italian mainland to the island of Sicily. Steel cable is to be used over a 3,300 m span. However he states that longer bridges may have to consider the use of carbon and glass fibre composites.

Humphreys (1997, p48) further advocates the replacement of steel rope with carbon-fibre rope for tethering floating oil/gas rigs to the sea bed: he states that all our North Sea floating rigs have got huge buoyancy bags to keep them afloat. “At a certain depth of water, beyond 1500 m, it becomes impractical (with steel rope) to add more buoyancy bags. However, if steel rope is replaced by carbon-fibre rope, then you can go down to 3000 m, making it possible to extract oil and gas in much deeper waters. This fact, it is known, will transform the world energy scene. ...there are huge reserves of oil and gas which are now, in principle, accessible which were not accessible previously. It’s all due to the production of lighter tethers, five times lighter than steel.”

These applications foreseen a decade ago for carbon-fibre or a similar synthetic fibre rope have yet to be fulfilled but it should only be a matter of time. Some high-performance engineering ropes based on polyester, nylon and ultra-high-molecular-weight polyethylene fibres are produced by Bridon Ropes (<http://www.bridon.com/index.php>).

Examples of the replacement of metals with plastics in house-hold appliances and the advantages gained are given by Hagan & Keetan (1994).

1.3 What can be achieved by appropriate selection of polymer-based materials?

Polymeric materials offer high strength- and stiffness-to-weight ratios, corrosion resistance, moulded-in colour, safety and ease of fabrication into complex shapes, which often results in greatly reduced product costs.

1.3.1 Reduction in cost

Judicious usage of even an expensive material such as carbon-carbon composite (at the cheaper end £100-£150 kg⁻¹) can be cost-effective. Carbon-carbon raw material costs vary according to the type and geometries of fibres, the type of matrix, the end use and method of production (Savage 1993, p373). Carbon-carbon composite brakes in place of steel/cermet brakes offer significant weight savings in military and commercial aircrafts. In Concorde 600 kg was saved, which means extra payload or fuel saving.

1.3.2 Improvement in performance/safety

Most modern-day feats in sports have been possible, not least, due to the introduction of polymeric materials into sports equipment. A 120-mile-an-hour serve in tennis could not exist without polymer-matrix fibre composite rackets. Research in biomechanics has shown that the early rackets were poorly constructed to damp the high vibrational forces, which are generally regarded as the main cause of “tennis elbow”. Today’s composite constructions improve the racket’s strength and durability, as well as damp the high impact forces involved in these sports.

Huge increases in height achieved by leading pole vaulters depend on the use of carbon-fibre/epoxy and glass-fibre/epoxy prepregs in the construction of modern pole vaults.

Recent successes in cycling are strongly associated with high-tech racing bikes of carbon-fibre composite disc wheels with improved aerodynamics, lightness, rigidity and conservation of momentum.

A Formula-1 car is likely to be subjected to a number of different forms of severe impact loading during a race. These events include strikes from track debris, collisions of various types and impact with the track due to a combination of bumps and perturbations with the aerodynamic down force. Since the early 1980s the construction of Formula-1 racing cars has been dominated by the use of carbon fibre reinforced composite materials.

When carbon fibre composite chassis were first introduced by McLaren, in conjunction with Hercules, a number of designers expressed concern as to the suitability of such brittle materials for this purpose. Indeed, some even went so far as to attempt to have them banned on safety grounds! An incident in the 1981 Italian Grand Prix at Monza went a long way to dispelling these fears and removing the doubt as to the safety of carbon fibre structures under impact. John Watson lost control of his McLaren MP4/1, smashing heavily into the Armco barriers. The ferocity of the crash was sufficient to remove both engine and transmission from the chassis. The remains of the monocoque were catapulted several hundred yards along the circuit until finally coming to rest. The Ulster man was able to walk away from the debris completely unscathed. The wrecked chassis clearly demonstrated the ability of the composite structure to absorb and dissipate kinetic

energy. The high stiffness of the chassis allowed the impact to be absorbed by the structure as a whole rather than being concentrated at the point of impact. Furthermore, the composite material was able to absorb the energy of impact by a controlled disintegration of the structure. By contrast, the forces generated from the impact of a vehicle constructed from a ductile metal such as aluminium are sufficient to exceed the material's elastic limit. In an aluminium car the monocoque would have remained in one piece, but collapsed until all of the energy had been absorbed. The driver would doubtless have been killed.

In their web publication entitled "The compelling facts about plastics 2007", the organisation of PlasticsEurope (2007) highlights that "plastics protect us from injury in numerous ways, whether we are in the car, working as a fire fighter or skiing. Airbags in a car are made of plastics, the helmet and much of the protective clothing for a motorcycle biker is based on plastics, an astronaut suit must sustain temperatures from -150 to 120 °C and the fire-fighter rely upon plastics clothing which are protecting against high temperature, and are ventilating and flexible to work in. Plastics safeguard our food and drink from external contamination and the spread of microbes. Plastics flooring and furniture are easy to keep clean to help prevent the spread of bacteria in e.g., hospitals. In the medical area plastics are used for blood pouches and tubing, artificial limbs and joints, contact lenses and artificial cornea, stitches that dissolve, splints and screws that heal fractures and many other applications. In the coming years nanopolymers will carry drugs directly to damaged cells and micro-spirals will be used to combat coronary disease. Artificial blood based on plastics is being developed to complement natural blood".

1.3.3 Reduction in weight

Weight, particularly in the context of improvements in strength and stiffness-to-weight ratios, has had the most enormous effects. For example, in aircrafts and other means of transport, in conventional structures, in oil platforms, etc. Improved fuel economy in cars, trucks and aeroplanes due to lighter-weight bodywork (e.g., sheet moulding-compound GRP and glass-mat thermoplastics (GMT) panels in Lotus sports car and in various truck cabs and advanced polymer-matrix composites in structural parts for aircrafts) must account for billions of pounds worth of fuel saving and the associated reduction in atmospheric pollution from exhaust fumes.

The special demands of water-based sports, e.g., competition boat hulls, can only be met by the employment of composite materials. Most types of hulls rely on polymer/glass fibre, often with Kevlar or carbon fibres for extra toughness and strength. A good racing hull, for example, may typically consist of a sandwich construction based on alternate layers of glass fibre mat and Kevlar woven fabrics bonded with a suitable core. The core material is a cellular polymer and provides lightness without loss of stiffness.

Decreases in weight will also continue to occupy the efforts of bicycle manufacturers, particularly for racing bicycles. The Japanese have recently announced the first all paper bicycle! The frame of this bike is constructed from hand-laid-up paper and epoxy resin. The resulting cellulose fibre alignment provides a strength which is 60% of that of carbon fibre (CF) composites, no mean feat! The resulting frame has a mass of only 1.3 kg. A thin plastic coating encases the paper to ensure that the bike does not collapse into a soggy heap in the rain!

Americans developed a bullet-proof vest for the Vietnam War from a laminate of ceramic plate backed with fibre glass-polymer composite $\approx 60 \text{ kg/m}^2$! These days much lighter body armours are produced from Kevlar or Dyneema.

1.3.4 Resistance to corrosion

Plastics replace metals in many applications because they do not rust. Figure 1.3 shows an area of a swimming-pool plant room where the use of sodium hypochlorite solution, a strong oxidant, as water purifying disinfectant accelerates the rusting of metal pipes and valves. During maintenance periods, the practice is to replace corroded metal pipes with plastic ones. However, it should also be recognised that plastics can suffer discolouration, crazing, cracking, loss of properties and melting or dissolution in the presence of energy sources, radiation or chemical substances.



Figure 1.3 An example of metal corrosion and replacement of a length of corroded metal pipe with a plastic alternative

1.3.5 Electrical insulation/conduction

The electrical insulating quality inherent in most polymers has long been exploited to constrain currents flowing along chosen paths in conductors and to sustain high electrical fields without breaking down. Polymers have also been employed in more demanding applications, for instance, polyethylene insulation in coaxial cables for radar and television. Polymers also provide high-performance thin films for capacitors.

Fluorinated polymers (a permanently polarised dielectric material) are used as very low-conductive materials in electret microphones.

Polymers are good insulators, but a lightweight, readily mouldable conducting plastic would also be desirable. Thus carbon black mixed polymers are used commonly as a conductive medium. Even a slight degree of conduction which allows charges to leak away to earth would be desirable to alleviate static charges from manufactured articles.

All the above listed desirable/attractive features of polymeric materials are due to their versatility.

1.4 What makes polymers versatile?

Polymers offer a diversity of molecular structures and properties and thus lend themselves to be employed in a variety of applications. They increasingly replace or supplement more traditional materials such as wood, metals, ceramics and natural fibres. Ordinary polymers offer sufficient scope for most applications, however technological progress and concerns over environmental pollution (often translated into legislation) and health and safety at work introduce further demands to improve/modify existing polymers and synthesise new ones.

Polymers possess extensive structural features, some of which are delineated below.

1.4.1 Intra-molecular features (single molecules)

Polymers are organic materials and consist of **chain-like molecules**, which are the most salient feature of polymers. A macromolecule is formed by linking of repeating units through covalent bonds in the main backbone. The size of the resultant molecule is indicated as molecular weight (degree of polymerization). The monomers or the **repeating units** in the chain are covalently linked together. Rotation is possible about covalent bonds and leads to rotational isomerism, i.e., **conformations**, and to irregularly entangled, rather than straight molecular chains, see Figure 1.4.

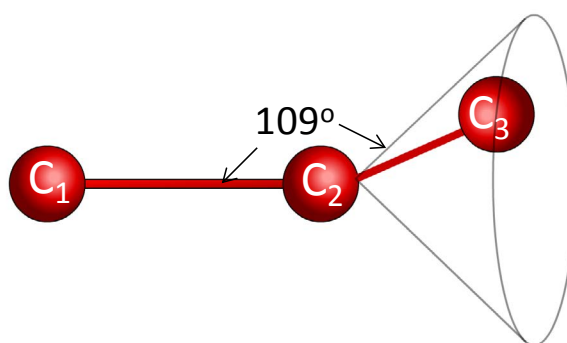


Figure 1.4 The third carbon may lie anywhere on the circle shown (i.e., the locus of the points that are a fixed distance away from a given point). In this case the locus is the circle at the base of the cone, which forms by revolving C_2-C_3 bond around the C_1-C_2 axis, maintaining the valence angle of 109.5° .

Trans and **gauche conformations** are exhibited as rotation occurs about C – C single bonds, e.g., in a butane molecule consider each molecular segment ($-\text{CH}_2 - \text{CH}_3$) being placed on a disk such that a C atom is placed at the centre of the disk, and the two hydrogen atoms and the methyl group are distributed evenly around the circumference. The rotation of one of the disks over the other produces eclipsed (highest repulsive energy between the methyl molecules when they overlap) and progressively staggered conformations (gauche being where the methyls are in a closest stagger and trans where methyls are furthest apart and experience minimum repulsive energy).

Configurations and/or **stereoisomers** describe the different spatial arrangement of the side chemical elements or groups of elements about the backbone molecular chains. Unlike conformations, the configurations cannot be changed by rotation about the covalent bonds and are established during polymerisation, when the monomer units are combined to form chains. Configurations (**cis and trans**) describe the arrangements of identical atoms or groups of atoms around a double bond in a repeat unit, e.g., cis- and trans-polyisoprene. Natural rubber contains 95% cis-1, 4-polyisoprene.

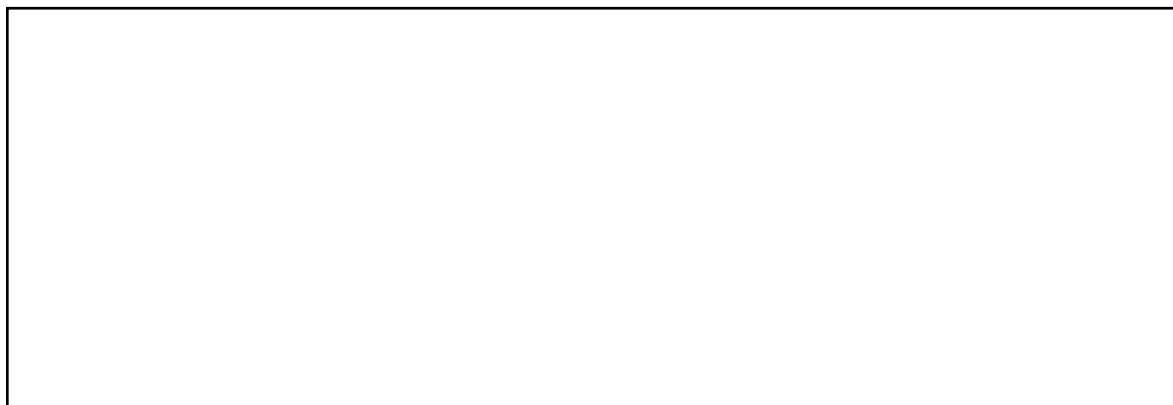
Stereoregularity (tacticity) describes the arrangement of side elements/groups around the asymmetric segment of the vinyl-type repeat units, $-\text{CH}_2 - \text{CHR}-$, consequently, three different forms of polymer chain results from head-to-tail addition of the monomers: **atactic**, **isotactic** and **syndiotactic**. Stereoregularity and configurations influence crystallisation and the extent of crystallinity in polymers. It is worth noting that by remembering specific chemical formulae for the general term “R”, one can easily reproduce the chemical expressions for the repeat units of various well-known thermoplastic polymers: e.g., when R becomes H, CH_3 , Cl, CN or a benzene ring then, respectively, the formula represents PE, polypropylene, PVC, polyacrylonitrile and polystyrene.

Conjugated chains contain sequences of alternating single and double bonds (unsaturation). Highly crystalline, stereoregular conjugated polymers exhibit appreciable electrical conductivity. A conductivity of 0.1 S/m has been obtained with a thin film of trans-polyacetylene ($-\text{CH}=\text{CH}-$)_n. The conductivity can be magnified by doping.

The terms and concepts covered in this section are explained in detail in the polymer science dictionary by Alger (1989) and in text books such as Fried (1995) and Young (1991).

Branched chains consist of a linear back-bone chain with pendant side chains. Branching occurs quite readily where the **functionality** (*f*) of the monomers > 2 . It can also occur during the polymerisation of monomers with $f = 2$ by free radicals abstracting hydrogens from a formed polymer chain, thereby generating new radicals along the backbone which initiates side chains. The presence of branches reduces the ability of the polymer to crystallise, and also affect the flow behaviour of molten polymer. Branching can be controlled by using specific catalysts.

Molecular mass indicates the number of repeat units in a polymer molecule, see the box below. The molecular mass must reach a certain value for the development of polymer properties.



Polymerisation produces chains of different lengths, thus the molecular mass is expressed as an average value (e.g., \overline{M}_n , \overline{M}_w), and the distribution of the molecular mass is indicated by $\overline{M}_w / \overline{M}_n$. A narrow distribution, e.g., in polyethylenes, gives better impact strength and low-temperature toughness whilst a broad distribution gives better moulding and extrusion characteristics.

Aromatic polymers (e.g., polycarbonate (PC) and polyether ether ketone (PEEK)) are identified by backbone chains which contain benzene rings and/or its derivatives; they are so called because of the strong odour and fragrance of the associated chemicals such as benzene. By contrast, in **aliphatic polymers** (e.g., PE and polyvinyl chloride (PVC)) the elements along the backbone chain are arranged in a linear manner. Aromatic polymers have good thermal stability, which can be further improved by heterocyclic arrangements. **Heterocyclic polymers** (e.g., polyimides) have both aromatic (benzene) and non-aromatic ring arrangements along the backbone chain. These are rigid materials with high-temperature resistance (high softening and melting points) and conductive properties. Some aromatic polymers remain crystalline in solution and in a molten state, i.e., they are “liquid crystalline polymers”. Mechanical stiffness and thermal stability of both aliphatic and aromatic polymers can be considerably increased by achieving **ladder-like** molecular structures along the backbone chains.

The intra-molecular features influence final material properties and the transition temperatures (e.g., the glass-transition temperature (T_g), secondary T_g and melting point, T_m), which indicate the temperature limits in applications. T_g indicates the temperature at which a rigid (glass-like) material becomes flexible (rubber-like) as it is being heated. The bulk structure and the behaviour of polymers are also dictated by the intra-molecular features, for example, the functionality and the frequency of the reactive sites along the backbone chain of macromolecules result in thermoplastics (TP), thermosets (TS) or elastomers. Depending on the stereoregularity and polarity along the backbone chain, crystallinity or amorphousness predominate in thermoplastics.

1.4.2 Intermolecular features (molecules in bulk)

Thermoplastics consist of a large number of independent and intertwined molecular chains. When heated these chains can slip past one another and cause plastic flow. In some thermoplastics as the polymer melt solidifies, the chains of molecules form into an orderly arrangement. These are **semi-crystalline** thermoplastics (e.g., PE, polypropylene (PP) and polyamide (PA)). The term semi-crystalline is used because the crystalline structure does not exist throughout the polymer.

The regions where the molecules do not form crystallites are referred to as **amorphous**, i.e., without morphology/shape. Non-

crystalline polymers are more readily swollen by solvents and therefore more susceptible to solvent crazing (minute cracking). Some thermoplastics (e.g., PC, polymethyl- methacrylate (PMMA) and, atactic polystyrene (PS)) are normally totally amorphous.

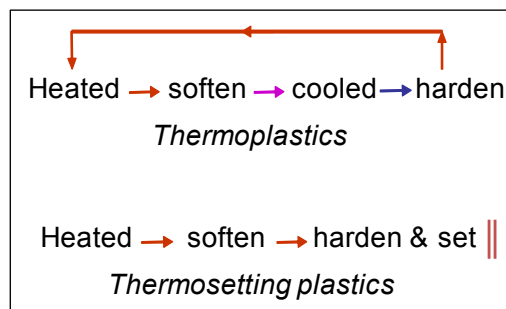
The crystalline structure comprises of **unit cells** (dimensions <1nm) and **lamellae** (i.e., approximately 10-20 nm thick platelets that are formed by an orderly packing of folded chain segments). Lamellae grow from **nuclei** in a radial fashion into a larger morphological unit, known as the **spherulite** (approximately 1-100 μm radius). Spherulite size and its uniformity influence mechanical and optical properties. During the blow moulding of PET (polyethylene terephthalate) bottles, the processing conditions are controlled to suppress spherulite formation while orientation and crystallisation occurs. Spherulites will reduce the transparency of the bottles, which is not desirable for marketing the product and also large spherulites embrittle the material.

Amorphous thermoplastics (in the absence of light scattering crystalline entities) are transparent and can be used as glass replacement, e.g., PVC glazing for skylight, acrylic ware in chemistry laboratories, PMMA front and rear car lenses or light clusters (here lower weight is also an advantage over inorganic glasses), PC headlamps and PC riot and anti-vandal shields.

Thermosets should be considered where polymers with higher rigidity (i.e., higher elastic modulus) are required. However, they suffer from being brittle and as a result are often used in a reinforced form as load-bearing solids. Thermoset (TS) formation requires that at least one of the monomers (reagents) must be trifunctional or greater. Thermosets (e.g., phenol formaldehyde resins (PF), epoxy resins, polyurethane (PU)) differ from TP in that their molecular chains are crosslinked together by primary bonds (covalent) and they are wholly amorphous. A characteristic common with most elastomers, with the important distinction that the **crosslink density** is much lower in elastomers. Varying crosslink density allows control of, in particular, mechanical and chemical properties. The generic term **network polymer** includes both elastomers and thermosets.

	T _m <input type="text"/> ; T _g <input type="text"/>
	T _m <input type="text"/> ; T _g <input type="text"/>
	T _m <input type="text"/> ; T _g <input type="text"/>

The difference between the behaviour of thermoplastics and thermosetting plastics is most obvious when being heated. As described in the textbox below, the TPs can be heated and softened repeatedly, whereas TSs can only be softened during the initial heating and no further.



The micro-structural variations in polymers reflect themselves in mechanical properties; see Figure 1.5, showing stress-strain curves for different types of polymers at room temperature.

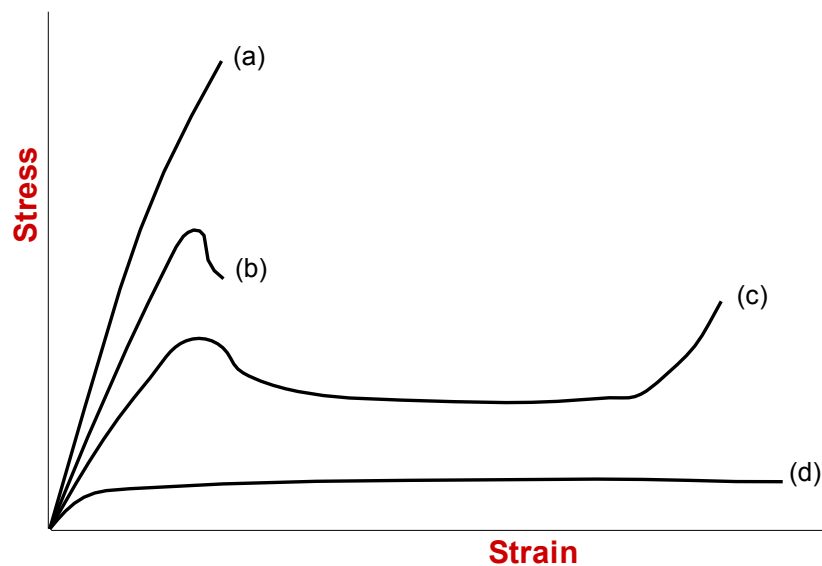


Figure 1.5 Stress-strain curves for polymers at room temperature:

- a) Low ductility polymer , e.g., PMMA or a rigid TS (e.g., PF)
- b) A ductile polymer (e.g., PVC)
- c) A ductile polymer capable of cold drawing (e.g., PP)
- d) A polymer with long-range elasticity (e.g., natural rubber)

Elastomers exhibit large reversible extensions up to ten times the original length. They are polymers that have long flexible chains with a low intermolecular attraction to enable a high localised mobility of segments. However, permanent relative chain flow or slippage must be prevented, which is achieved by cross-linking the chains to form a three-dimensional network. Varying the cross-link density allows control of properties. For example, natural rubber, which is crosslinked with sulphur (the process is known as “vulcanisation”) can also result in ebonite (a hard, rigid thermoset) by adding more sulphur to the mix and hence increasing the crosslink density. The T_g of elastomers is usually below $-50\text{ }^\circ\text{C}$. The differences between the mechanical behaviour of a rigid plastic, flexible plastic and an elastomer can be easily demonstrated as described in the text box below.

Demonstration: the specimens shown are (a) a piece of cured epoxy resin, (b) a rubber band, and (c) a strip of linear low density polyethylene (LLDPE). Answer the following:

Specimen (a) is as rigid as a board and (b) is a very flexible elastomer, but they are both thermosets, why the difference in their mechanical behaviour?

- Upon drawing/pulling, Specimens (b) and (c) will both exhibit high levels of elongation, however, when the deforming force is removed Specimen (b) will instantly retract to its original shape and form, but Specimen (c) will remain permanently deformed, why?



Hydrogels are slightly crosslinked polymers which are insoluble but highly swollen in water. Hydrogels of hydroxyethyl/methacrylate copolymers are used as soft contact lenses.

Fibres may be defined as linear filaments of material with diameters less than $100\text{ }\mu\text{m}$ and aspect ratios greater than 100. They are polymers with uniaxial **molecular orientation** and are, thus, anisotropic, being much stronger and stiffer along the fibre axis than across it. Polymers suitable for fibre formation can be significantly drawn to produce high levels of molecular orientation and retain this orientation after the removal of the drawing force. Symmetrical (stereoregular) and unbranched linear polymers of sufficiently high molecular weight that would lead to a high degree of crystallinity are desirable in fibres. Atactic amorphous polymers can also prove useful, if there are intermolecular forces present. Dipolar

interaction between the neighbouring molecules due to polar side groups/elements such as (CN and Cl) serves to improve the molecular alignment considerably. This interaction stabilises orientation during fibre production and enhances the fibre forming potential of mainly amorphous polymers such as polyacrylonitrile and PVC. Other important factors to consider in polymers for fibre production include: T_g , T_m , moisture absorption and dyeability.

Liquid crystalline polymers such as aromatic polyesters and aromatic polyamides lend themselves to the formation of fibres with enhanced mechanical performance. Liquid crystalline polymers maintain their rod-like molecular form in solution (hence liquid crystalline) and, thus, during the solution spinning high alignment of the molecules is readily achieved in the fibre direction. The orientation is retained in the solid fibre, enhancing strength and stiffness.

Versatility of polymers can be further increased by copolymerisation, polymer blending and additives:

Copolymerisation enables the modification of the chain structure by polymerisation in which more than one monomer type is reacted. Copolymers are classified as random, alternating, block and graft copolymers according to the way in which the repeat units are arranged in the polymer molecular chains. Copolymerisation can influence T_g , T_m , crystallinity, mechanical toughness and other properties.

Block copolymers such as styrene-butadiene-styrene (SBS) display the typical long-range elasticity of rubber, without the necessity of vulcanisation, and are known as **thermoplastic elastomers (TPE)**. At ambient temperatures these behave like conventional crosslinked rubbers but they have the additional advantage that their thermal behaviour is reversible (i.e., they behave like TP under heat). The behaviour of TPE is due to its **domain structure** such that the stiff-polymer (glassy or crystalline) aggregate domains are dispersed in a rubbery matrix as illustrated in Figure 1.6. The stiff domains act as effective cross-linking points, thereby obviating the necessity to vulcanise the material.

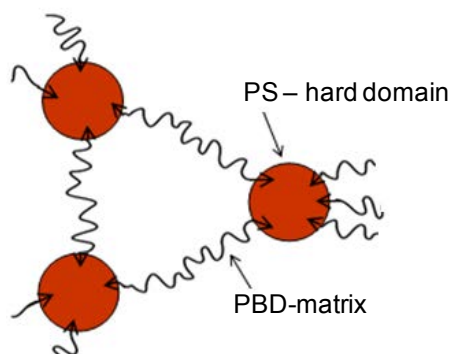


Figure 1.6 A thermoplastic elastomer of polystyrene (PS) and polybutadiene (BPD)

Polymer blends are a physical mixture of two polymers. The combining of finished thermoplastics (e.g., PE/PP; PC/PP; PC/thermoplastic PU) can be an alternative to copolymerisation in effecting variation in polymers. The advantages of crystalline polymers (chemical resistance, easy flow) and amorphous polymers (low shrinkage, impact strength) can be combined in a single material. Most blends are two phase systems, compatibilisers can be added to control the extent of phase mixing/separation, and usually result in properties intermediate between those of the individual component polymers. Blending can be used to tailor properties for certain applications and to achieve synergistic effects (i.e., the properties of the mixture are significantly better than those of the component materials).

Interpenetrating polymer networks (IPNs) are polymer blends in which at least one of the components is a crosslinked polymer. They can be prepared by mixing of the reagents and the simultaneous polymerisation of the components or by swelling of a crosslinked polymer with a second monomer, together with crosslinking agent, followed by its polymerisation to yield a mixture containing two polymers (ideally two network polymers) which are interpenetrating. Phase separation occurs to an extent depending on the compatibility of the components, but it is only to a fine scale owing to the interlocking of the networks. Often interesting modifications of the glass transition behaviour and also synergism in properties can be obtained as shown in Figures 1.7 and 1.8 for some IPNs.

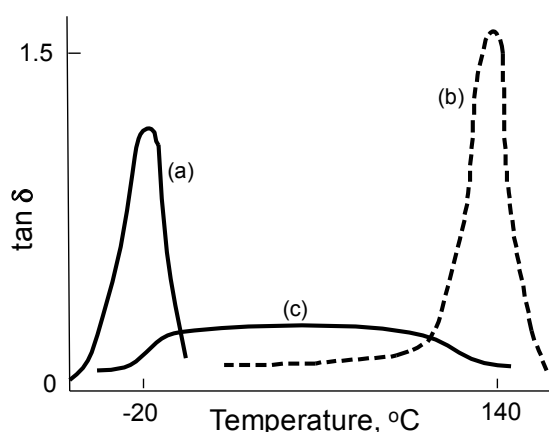


Figure 1.7 Damping term ($\tan \delta$) vs. temperature for: (a) polyurethane elastomer (PU), (b) polymethyl methacrylate (PMMA), and (c) an IPN of 70/30 PU/PMMA (adapted from Akay and Rollins (1993))

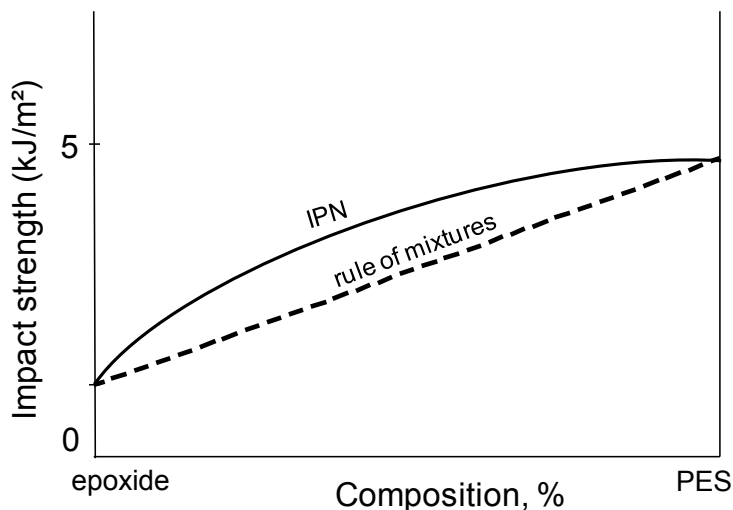


Figure 1.8 Impact strength vs. composition by weight for an IPN of epoxy resin with polyether sulphone (adapted from Akay and Cracknell (1994))

In general with the blends of polymers and IPNs the outcome can result in exhibiting one of the property correlations delineated in Figure 1.9.

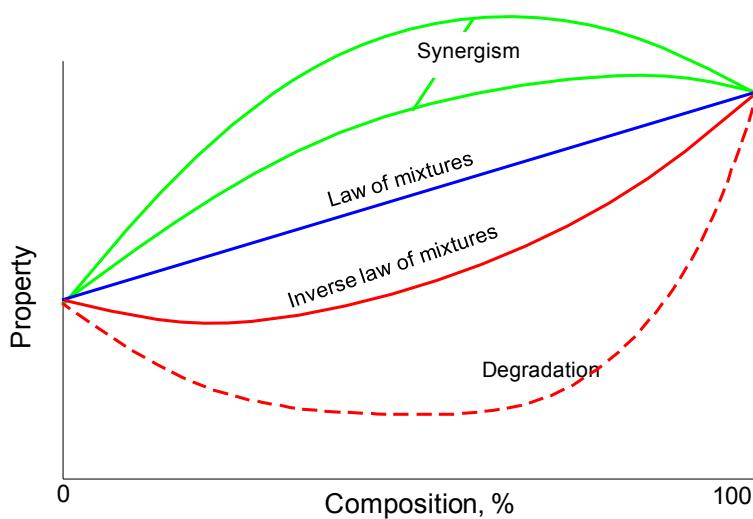


Figure 1.9 Various forms of interactions upon mixing two different types of polymers

1.4.3 Additives, reinforcements and fillers

These substances change properties of polymers and render them more adaptable and versatile. Polymers make excellent matrices for reinforcing fibres (the resultant composites are known as polymer-matrix-composites, PMC) and excellent binders for pigments such as TiO_2 in paints.

Most additives fall into one of the following categories:

- a) **modifiers**: such as plasticizers, nucleating agents, clarifiers, impact modifiers, (e.g., rubber particles) blowing agents, colourants and coupling agents,
- b) **stabilisers**: including antioxidants, heat and UV stabilisers, fire retardants, antistatic agents and fungicides,
- c) **processing aids**: lubricants, compatibilisers (e.g., Struktol in wood-plastic composites) reducers of melt temperature/pressure, etc.

Care should be exercised in the usage of additives: even the most useful additive can have detrimental effects, for example, carbon black greatly reduces the tracking resistance of a material and should be avoided in electrical applications.

Combining several types of additives into synergistic “packages” is becoming popular, also formulation of liquid systems, rather than powder, for ease of mixing.

The choice of additives must also be dictated by health and safety considerations. Much work is underway to reformulate PVC additives (incidentally the largest % of additives are used in PVC) to eliminate heavy metals such as lead, barium and cadmium. Note that Ba salts are added to baby toys for radio opacity, in case they swallow the toys. Some **phthalates**, used as plasticiser, in PVC can leach out of soft toys into the mouths of the children chewing on them, posing a risk of cancer.

1.4.4 Processing methods

A wide variety of processing and forming techniques further augment the versatility of polymeric materials. Some of these techniques are listed below and will be covered in greater detail in Chapter 3

- Injection moulding:
Machines exist with **shot capacities** ranging from a few grammes to tens of kilogrammes. The moulds can be single or family moulds. The process can be modified to produce gas-assisted injection mouldings, and it can be used as a first stage in blow moulding.
- Extrusion:
It is employed in manufacturing various profiles, pipes/tubes, cables, multi-layer packaging, fibres, blown film, calendered sheet/film, etc., and as a twin-screw extruder in compounding.
- Thermoforming/vacuum forming
- Rotational moulding
- Compression/transfer moulding
- Coating
- Reaction injection moulding
- Dispensing foam
- Machining/joining of plastics.

2 Polymerisation

“The magnitude of the atomic weight determines the character of the element, just as the magnitude of the molecule determines the character of a compound body.” **Dmitri Ivanovich Mendeleev**, 1834-1907.

The early developments in polymer technology occurred without any real knowledge of the molecular theory of polymers. The idea that the structure of polymers in nature might give an understanding of plastics was put forward by Emil Fischer, who in 1901 discovered that natural polymers were built up of linked chains of molecules. It was not until 1922 that the chemist Herman Staudinger proposed that not only were these chains far longer than first thought, but they were composed of giant molecules containing more than a thousand atoms. He christened them ‘macromolecules’, but his theory was not proved until 1935 when the first plastic was created with a predictable form. This was the first synthetic fibre, nylon.

Polymer, meaning literally many parts, is a large organic chemical molecule (macromolecule), consisting of a combination of many small chemical molecules known as monomers. For example, polyethylene (PE), $-CH_2-CH_2-CH_2-\dots-CH_2-CH_2-$, consists of many ethylene, $CH_2=CH_2$, monomers. The process of combining monomers together to yield a macromolecule is known as polymerisation.

2.1 Polymerisation mechanisms

There are two main types of polymerisation mechanisms: addition (chain-growth) polymerisation and condensation (step-growth) polymerisation. In chain-growth reaction the polymerisation proceeds in a chain-like fashion in only one direction. In condensation reaction, the chain growth is not spontaneous and usually occurs slowly: the monomers first form dimers, trimers, tetramers and oligomers. Long reaction times are necessary in order to reach polymers with high average molecular weights.

Some of the chemical formulae in Sections 2.1.1 and 2.1.2 are adapted from Clarkson (2004).

2.1.1 Addition (Chain-growth) polymerisation

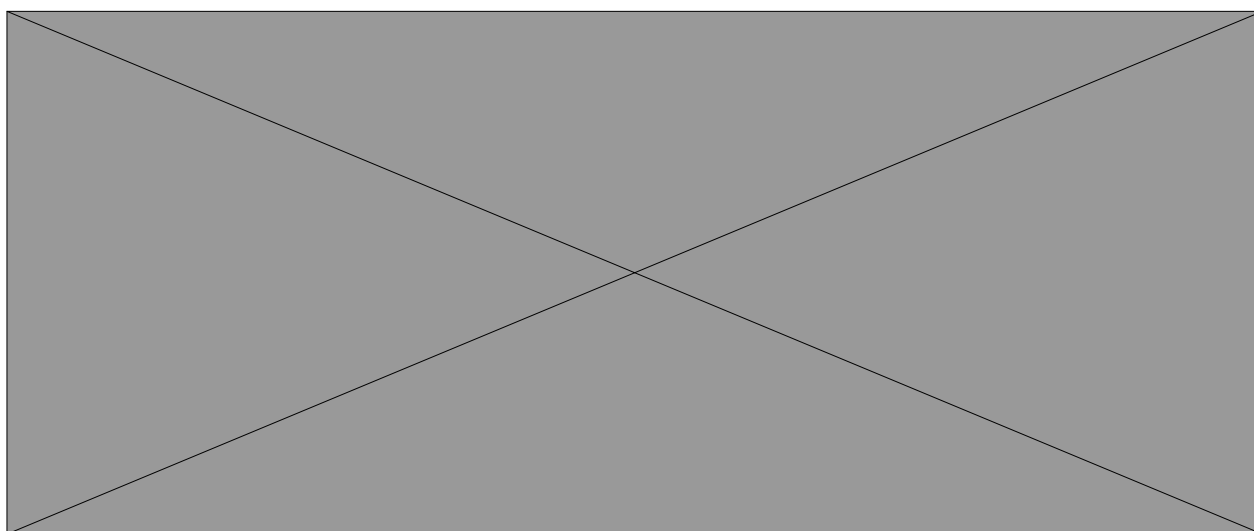
Vinyl monomers (unsaturated molecules, i.e., they contain carbon-carbon double bonds such as ethylene or styrene) react by addition polymerisation to produce long chain molecules. The mechanisms for addition polymerisation are free radical, anionic and cationic.

Free-radical, anionic and cationic polymerisations all include three stages: **initiation**, **propagation** and **termination**.

Initiation involves the splitting up of the **initiator molecules** into **free radicals** by application of heat at a certain temperature, the initiator free radicals then react with monomer molecules, beginning the formation of polymer chains.

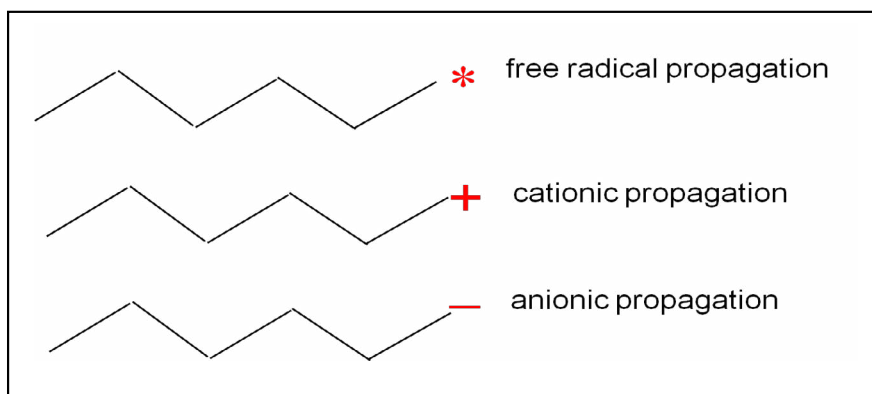
Examples of initiators include benzoylperoxide, $(C_6H_5COO)_2$ and azo-bis(*iso*-butyronitrile) (AIBN), $(NCC(CH_3)_2N)_2$.

For example, benzoylperoxide:



The vinyl monomer is unsymmetrical with respect to its ends: a **head** (the carbon atom with the R group attached) and a **tail** (the carbon atom without the R group). The addition of monomers during the propagation process is predominantly by head-to-tail bonding due to steric and resonance effects.

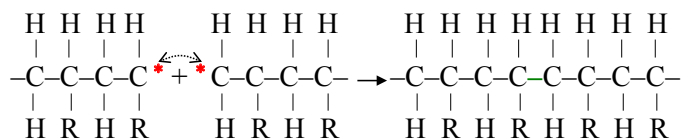
A major difference between radical polymerisation and the ionic method is that, in the latter, the incoming monomer must fit between the growing chain end and an associated ion or complex. The growing radical chain, on the other hand, has no such impediment at the growing end.



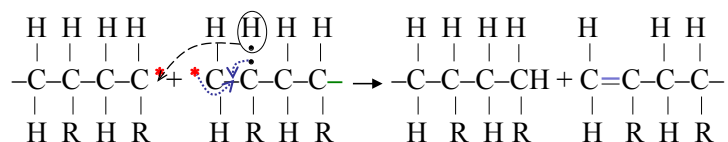
Chain transfer to polymer can also occur as a propagation step in polymerisation. This is the process where a growing chain radical is transferred to the middle of another polymer chain, forming **branches** on the polymer chains, which can lead to reduced melting point and mechanical strength for the polymer. Branching is especially prevalent in the high pressure radical polymerization of ethylene, used in the polymerisation of LDPE.

The **termination** step involves the reaction of any two free radicals with each other, either by combination or disproportionation.

Combination involves the coupling of two growing polymer chain radicals as shown below:



Disproportionation is a rather complicated way in which two growing polymer chains are rendered inactive: when two growing chain ends come close together, the unpaired electron of the chains are exchanged in such a manner that the first chain gains a H element from the second chain, and a double bond forms at the head of the second as delineated below:

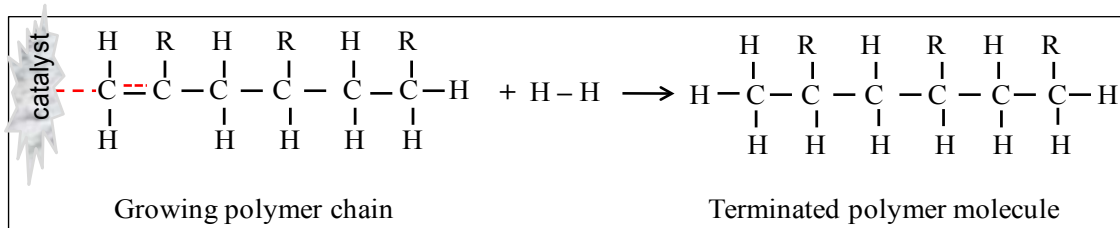


The addition polymerisation reaction mixture, at a given time, contains monomer, finished polymer, growing polymer chains, and any added reagents.

In the presence of Ziegler-Natta or other stereo-specific catalysts, a growing polymer-chain is attached to the metal atom of the catalyst and subsequent monomer addition is coordinated with the metal atom, known as coordination polymerisation, and leads to highly stereospecific polymerisation. The monomer molecule must sit in a rather specific position in order to react, enabling stereoregular polymers to be made. For example, polymerization of propylene through action of the titanium catalyst gives an isotactic product; whereas, vanadium based catalyst gives a syndiotactic product.

In coordination polymerisation the process is site based and is regulated by the type of active site, whereas in free radical polymerisation the polymerisation site moves progressively away from the initiator and is not influenced by the chemical structure of the initiator, accordingly, it is the type of monomer rather than the initiator that dictates the free-radical polymerisation process. The flexible and dynamic nature of the free-radical site can cause the formation of side branches by an internal chain transfer process known as backbiting, which generates a free radical site within the growing polymer chain. This is much less likely in the coordination polymerisation since no free-radicals are involved in this mechanism, and the active site of the growing chain is at a fixed location on the metal surface of the coordination catalyst.

Termination in coordination polymerisation is achieved by reactions of the reactive chain end with an added modifier molecule (a chain transfer agent), e.g., hydrogen, at a concentration of one hydrogen to 1000 ethylene molecules.



Use of hydrogen provides a low cost clean reaction (no residue) for controlling molecular weight. Temperature affects these processes: higher temperature increases the speed of molecules and causes more collisions, therefore increases reaction rate. However, the reaction of the hydrogen increases even faster, resulting in a higher degree of termination that produces a polymer with a low average molecular weight (high melt-flow index).

2.1.2 Condensation (step-growth) polymerisation

Multifunctional monomers react producing in steps, dimers, trimers, tetramers, oligomers (consisting of 10 to 20 monomer units) and polymer molecules. During the process, links such as ester and amide are formed and a small molecule, e.g., H_2O , is eliminated, see Figure 2.1.

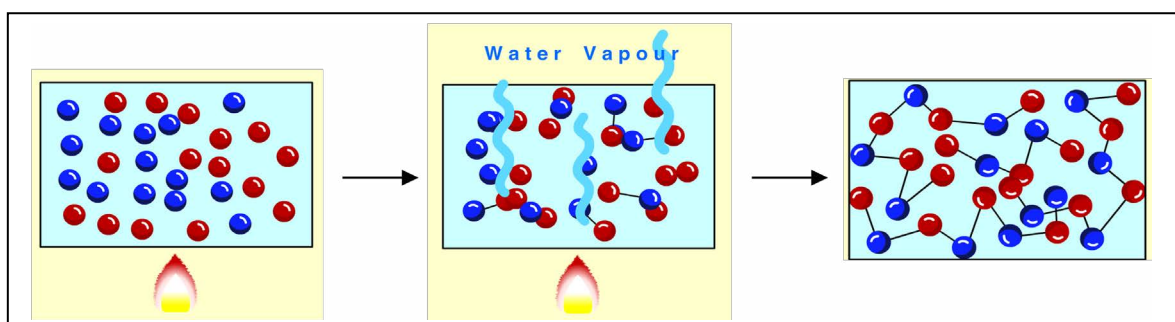
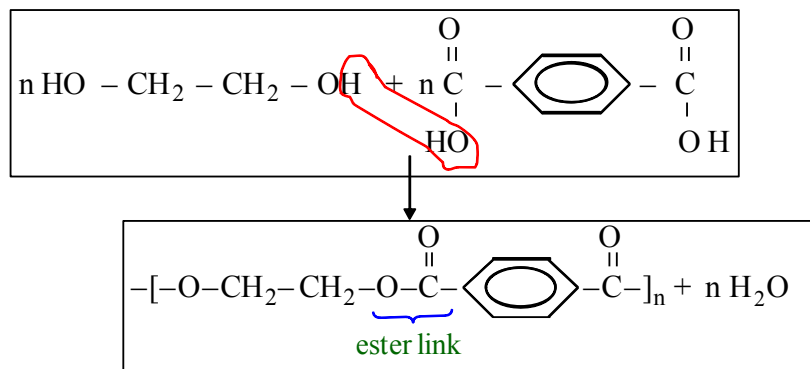
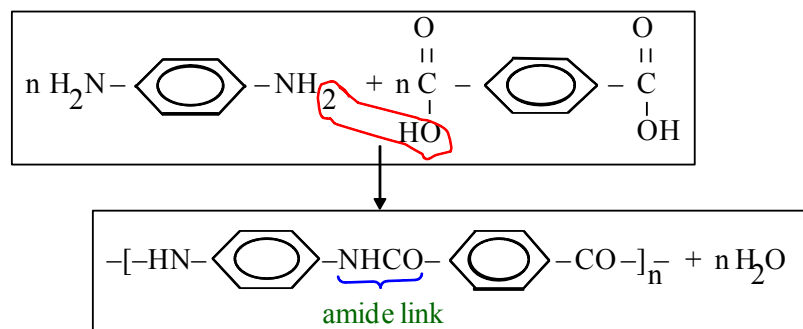


Figure 2.1 An illustration of condensation polymerisation

Polyesters contain the ester group, $-\text{COO}-$, which is formed from the reaction between a carboxylic acid and an alcohol. Both these reagents must have two reactive ends (functional groups) in order to enable a chain growth. Poly(ethylene terephthalate) (PET) made from terephthalic acid (benzene-1, 4-dicarboxylic acid) and ethylene glycol (ethane-1,2-diol):



Polyamides contain the amide group, $-\text{CONH}-$, a product of reaction between a carboxylic acid and an amine. Both these molecules must have a functionality of two, so that chain growth becomes possible. Nylons are synthetic polyamides made from a variety of dicarboxylic acids and diamines. Usually depending on the number of C atoms in the amine and the acid nylons are designated with numbers, e.g., “Nylon 4,6 or Nylon 46 or PA46” indicates that it is polymerised from a 4-carbon diamine and a 6-carbon diacid. Kevlar is another example, made from terephthalic acid (benzene-1, 4-dicarboxylic acid) and 1, 4-diaminobenzene as shown below.



2.2 Polymerisation processes

The polymerisation process requires a quantity of monomers and a suitable initiator/catalyst system to start the reaction to form polymer molecules that consist of thousands of monomers linked together. Polymerisation processes can be classified in terms of the reaction medium: bulk, solution, suspension, slurry, emulsion and gas.

2.2.1 Bulk polymerisation

Polymerisation of the pure liquid or gaseous monomer is called **bulk polymerisation**. It can be used for the production of free-radical polymers and some condensation polymers.

- In the reaction only monomer, polymer, and initiator are present and, therefore, a very pure product is obtained.
- The polymerisation is very rapid and strongly exothermic. It can lead to hazardous temperature build up and run away reactions. Overheating can cause branching and crosslinking and lead to the formation of gels
- The process produces highly transparent polymers: e.g., PS and PMMA.

2.2.2 Solution polymerisation

The monomer is added to an inert solvent with a boiling point that corresponds to the polymerisation temperature.

- During the polymerisation process some solvent evaporates and thus helps to remove the heat of polymerisation.
- Since the boiling point of the solvent is constant, this ensures a constant polymerisation temperature.
- Some difficulty lies in the separation of the residual solvent from the polymer after completion of polymerisation.

In comparison with bulk polymerisation, solution polymerisation offers easier temperature control because of the added heat capacity of solvent and lower viscosity.

2.2.3 Suspension polymerisation

Suspension polymerisation is essentially a bulk polymerisation carried out in droplets in an aqueous solution in which the monomer is dispersed. The polymer precipitates as fine spherical particles with diameters of 0.01 to 1.0 mm.

- The polymerisation begins by radical initiators in the monomer droplets.
- Protective colloids are added in order to prevent coagulation of the particles and to produce uniform polymer particles.
- The water absorbs the heat of reaction.
- It is used in the manufacture of PVC and PS.
- Residual additives need to be removed.

2.2.4 Slurry polymerisation

The process is mainly used in the production of polyolefins. The catalyst is dispersed/dissolved in a liquid diluent in which monomer is dissolved, or in the liquid monomer by itself. As in emulsion polymerisation, the polymer is not soluble in the reaction medium, and precipitates on the catalyst forming slurry.

2.2.5 Emulsion polymerisation

As in suspension polymerisation the monomer is also dispersed in water but in much smaller droplets created with the use of emulsifiers, e.g., soaps. In the presence of soapy water, the chemicals, such as the monomer droplets and subsequently formed polymer molecules are kept apart and dispersed rather than coalesce into a useless lump! The temperature control is easier, since the viscosity changes very little with conversion. Also, thermal conductivity and specific heat of water are higher than those of organic solvents.

Some of the surfactant (emulsifier) particles huddle together forming micelles, others surround monomer particles and isolate them as droplets. The micelles consist of 10 to 100 soap molecules with their hydrophilic groups on the outside in the water phase and their hydrophobic groups on the inside surrounding the hydrophobic monomers. Once the process begins, the temperature increases generating free radicals that monomers are attracted to and come out of the droplets and start adding on to that free radical site in a micelle and finally finish of producing polymer molecules that are cocooned in the micelle, see Figure 2.2 . Of course this process takes place simultaneously in many different micelles that result in many polymer particles.

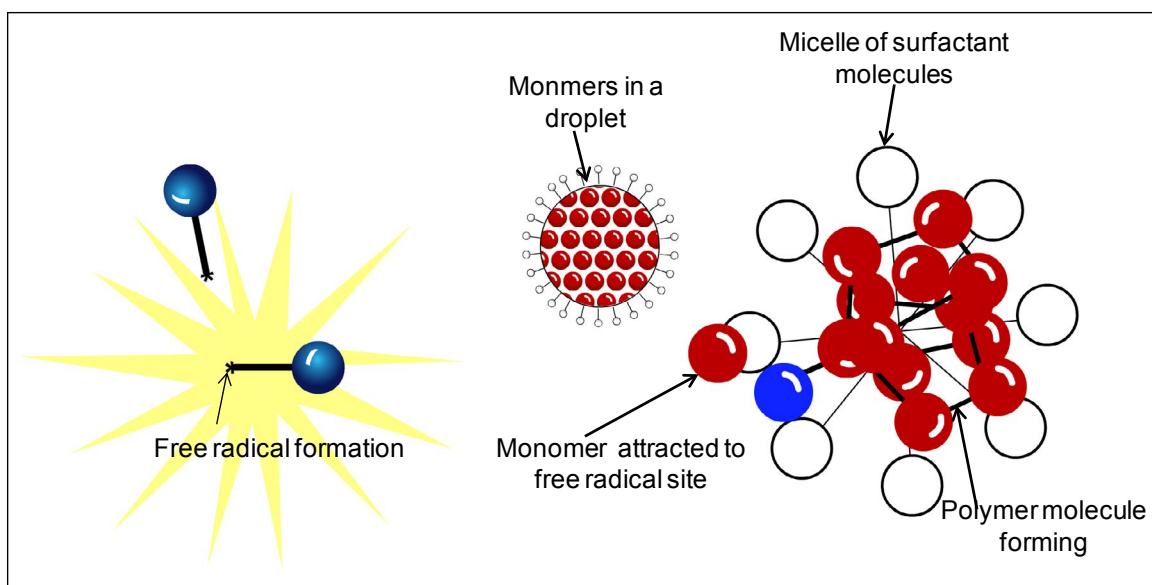


Figure 2.2 An illustration of the process of **emulsion polymerisation**

At the conclusion of the process, as well as polymer particles there are still some unreacted monomers, initiators and free radicals, which find it difficult to participate in reaction for reasons of steric hindrances. Surfactant and coagulant residues are hard to remove and also contribute to high impurity levels. Used mainly for the production of polyvinyl acetate, PMMA and PVC.

2.2.6 Gas-phase polymerisation

The monomer is in the gaseous state and a heterogeneous coordination catalyst such as a Ziegler-Natta catalyst is used. In gas-phase and slurry processes, catalysts such as Ziegler-Natta and metallocenes need to be supported on a suitable substance, e.g., SiO_2 , whereas they can be added directly in solution polymerisation. The polymer is formed on the active sites of the catalyst into a gradually expanding catalyst-polymer particle, and as in emulsion polymerisation there is one active centre in each particle. Fresh gaseous monomer diffuses through the polymer particle to reach the active site. In reactors, the catalyst is supported/uniformly dispersed by mechanical stirring or by fluidization.

Gas-phase and slurry processing techniques are used mainly for the production of polyolefins such as HDPE. Table 2.1 shows some examples of polymers that are produced under various polymerisation mechanisms and processes covered in this section.

Table 2.1 A comparison of different polymerisation methods (source: Asua 2007, p24)

Mechanism	Process	Polymer examples
Free radical	Bulk (neat)	LDPE, PMMA, PS, HIPS
"	Suspension (pearl, bead)	Expanded polystyrene, PVC
"	Emulsion	ABS, SBR, polyvinyl acetate, emulsion PVC, acrylic latexes, fluorinated polymers
Coordination	Solution	LLDPE, HDPE
"	Slurry	HDPE, i-PP
"	Gas-phase	Polypropylene, HDPE, LLDPE, bimodal LLDPE
Step-growth	Bulk	Nylon 6, Nylon 6,6, PET, PC,
"	RIM	Polyurethane, Nylon 6 (with caprolactam)

2.3 Polymerisation reactors

Industrially employed reactors include horizontal/vertical stirred tanks, high-pressure tube, loop and fluidised-bed reactors, as well as polymerisation in moulds, e.g., RIM (reaction injection moulding). The type of reactor used is dictated by the polymerisation process. For example stirred-tank reactors are suitable for suspension and emulsion polymerisations since agitation assists in controlling polymer particle size, e.g., in production of PVC.

Most of polyolefins are produced using a **fluidised-bed reactor**, illustrated in Figure 2.3.

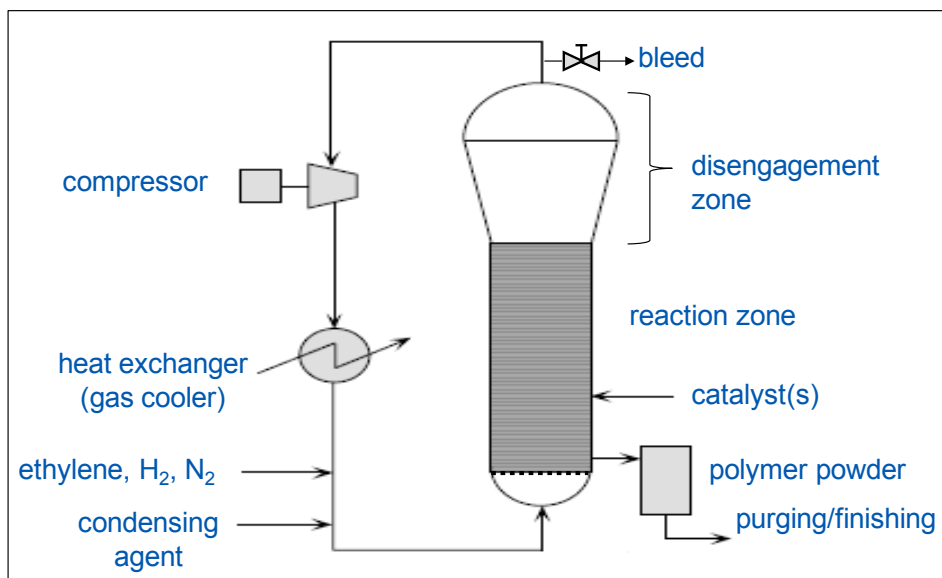


Figure 2.3 Gas-phase fluidised-bed reactor (an animation of the UNIPOL process is presented at <http://www.univation.com/unipol.animation.html>)

The design of the fluidised distributor plate at the base of a reactor is important for the efficiency of the process: fluidisation should prevent the hot polymer particles from settling onto the plate, and cause agglomeration, by maintaining sufficient recycled gas and additional feed gas flow rate through the distributor.

The gas flow, consisting of monomer/comonomer, hydrogen, nitrogen (inert carrier gas), and inert condensing agent, provides monomer/comonomer for polymerisation, agitates the bed, and removes the heat of polymerisation. The operating temperature is approximately 90 °C for LLDPE and 100 °C for HDPE and the pressure of approximately 10 bar (1 MPa). The gas with some polymer/catalyst particles rises to the enlarged domed section, referred to as the disengagement zone, where a variation in velocities occurs and entrained particles disengage from the gas, before the gas leaves the reactor, and drop back into the reaction zone. The condensing agent can be monomers and inert liquids (e.g., pentane, isopentane, butane, hexane), and its heat of vaporisation results in cooling in the reactor. The boiling point of the condensable liquid has to be lower than the operating temperature of polymerisation, for effective control of reaction. The gas leaving from the top of the reactor is condensed in the heat exchanger and returned to the reactor in liquid form.

The polymer powder passes to a purge vessel where a deactivating agent (the weight ratio of the deactivating agent to the catalyst is approximately 0.001) kills all catalyst activity, nitrogen strips off traces of monomers from hot powder, and a small amount of steam (a few kg/h) removes triethylaluminum (TEA) and other non-monomer chemicals. Finishing of the polymers includes addition of additives (e.g., heat, UV and perhaps other stabilisers, lubricants, pigments, colorants, etc.), drying, extrusion and pelletising. The polymer may enter the extruder quite hot and therefore may necessitate cooling, rather than heating, along the extruder barrel. The temperature of the cooling water for pelletisation is critical: fast and/or slow cooling/solidification can produce pellets with defects as shown in Figure 2.4. There are other causes / conditions that can generate defected pellets, which are documented by the company Black Clawson and/or Davis Standard in their company publications & technical articles, see their web sites: <http://www.er-we-pa.de/home.html>, <http://www.davis-standard.com/>

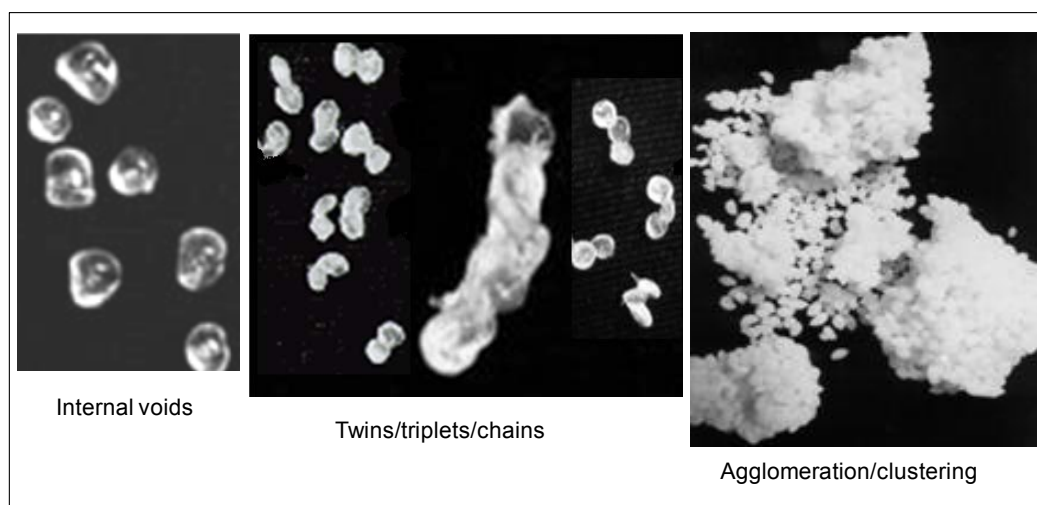


Figure 2.4 Various types of defects in pelletisation: fast cooling resulting in voids and slow cooling in agglomeration of pellets from twins to large clusters (source: http://www.er-we-pa.de/public_html/Company/pubs/EP_defects.html)

A typical **high pressure tubular process** for the production of LDPE is illustrated in Figure 2.5. In this process, the ethylene monomer is gradually compressed to a pressure level suitable for the reaction, up to 3000 bar (300 MPa) with a tubular reactor. The free radical polymerization initiates at about 150 °C, using oxygen or an organic peroxide as initiator. The temperature of polymerization reaction can peak to over 300 °C. A mixture of polymer and unreacted monomer is transported from the reaction tube to a separating and recycling part, which includes a high-pressure separator (HPS). The HPS is connected to a

low-pressure separator (LPS) for further monomer removal. The resulting molten polymer phase is passed from the LPS to a polymer finishing section for extrusion. The unreacted monomer separated in HPS gets recycled at a pressure similar to that of the outlet of the primary compressor and combines with the monomer containing feed passing from the primary to the secondary compressor. The unreacted monomer from the LPS recycles through the primary compressor.

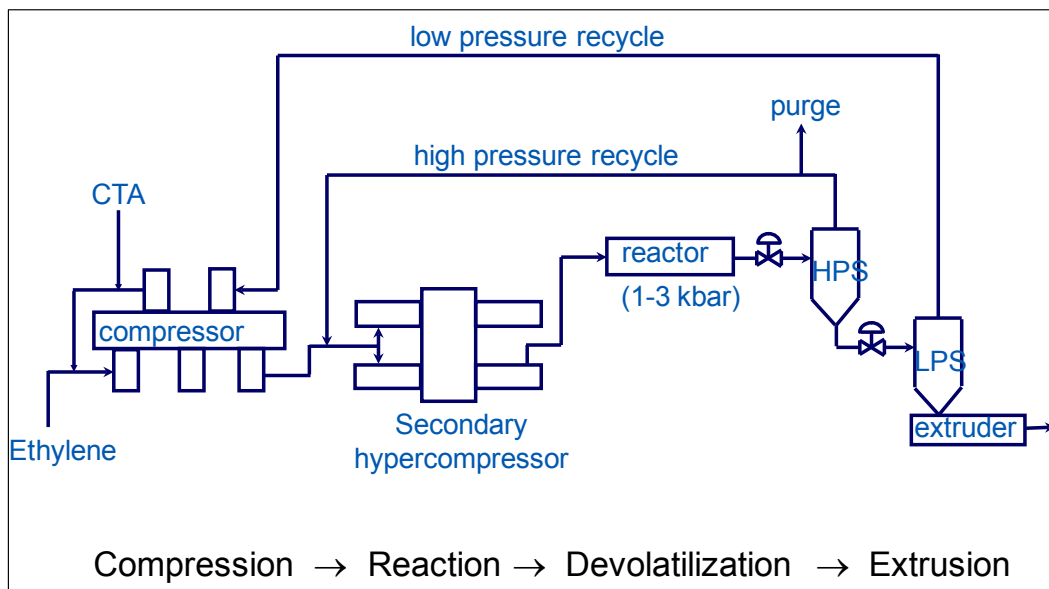


Figure 2.5 An illustration of typical high pressure LDPE process

Chain transfer agent (CTA) is also added to the circuit and conveyed to the reactor. CTA is used to reduce the molecular weight (MW) and to narrow the molecular weight distribution without changing the overall rate of conversion of monomer to polymer (using more initiator is another way to decrease MW, but the reaction rate would increase proportionally with a risk of a dangerous situation arising).

Further information on polymerisation mechanisms and processes can be found, amongst many others, in Asua 2007 and Fried 1995. A description of these processes as well as environmental, health and safety guidelines in association with these processes is also presented in a report by the International Finance Corporation 2007.

2.4 Catalysts

The employment of polyolefins enjoys a massive global increase: PE has the world's largest market closely followed by PP, which is experiencing the highest growth rate in many years. The development of polyolefins into the largest-volume family of commercially important, high-tonnage thermoplastic polymers has been made possible with the advent of **coordination catalysts**. The coordination catalyst types include Philips catalysts (supported chromium oxide catalyst), Ziegler-Natta and single-site catalysts, e.g., constraint geometry and metallocene.

2.4.1 Ziegler-Natta catalysts

The discovery of Ziegler and Natta represents the first and most significant step in the synthesis of crystalline polyolefins. The German chemist Karl Ziegler (1898-1973) discovered in 1953 that when TiCl_3 and triethyl aluminium (TEA), $(\text{C}_2\text{H}_5)_3\text{Al}$, are combined together they produced an extremely active heterogeneous catalyst (the heterogeneous catalysis has the catalyst in a different phase from the reactants, but the homogeneous catalysis has the catalyst in the same phase as the reactants) for the polymerization of ethylene at atmospheric pressure.

Giulio Natta (1903-1979), an Italian chemist, developed variations of the Ziegler catalyst and extended the method to the production of stereoregular polypropylenes. Ziegler-Natta catalysts are, now, used worldwide to produce the following classes of polymers from α -olefins:

- polyethylenes: HDPE, linear low density polyethylene LLDPE and ultra-high molecular weight polyethylene (UHMWPE)
- polypropylene: homopolymer, random copolymer and high impact copolymers
- thermoplastic polyolefins (TPO)
- ethylene propylene diene monomer polymers (EPDM)
- polybutene (PB).

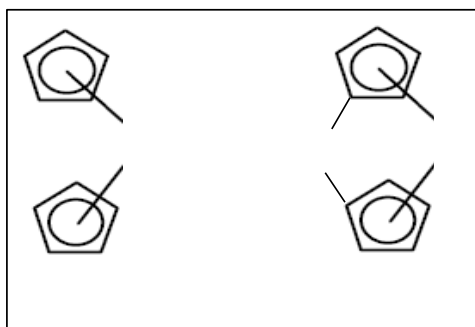
Classic Ziegler-Natta Catalyst is: $\text{TiCl}_3 + \text{Al}(\text{C}_2\text{H}_5)_3$

Polymerization is believed to occur by the repeated insertion of a double bond from the monomer into a previously formed Ti-C bond. Efficiency of such a heterogeneous catalyst can be improved significantly by impregnating the catalyst on a solid support such as MgCl_2 or MgO .

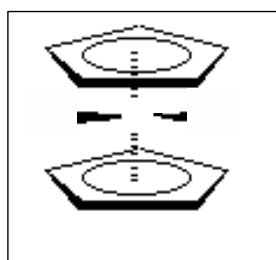
2.4.2 Metallocene catalysts

Metallocene catalysts are homogeneous and single site catalysts (SSC). Each catalyst molecule offers almost the same activity and accessibility to monomers. In α -olefins, this results in a very uniform product, and with the appropriate choice of catalysts, in a highly stereoregular product with α -olefins.

Metallocene compounds have two cyclic ligands, cyclopentadienides, bonded to a metal centre, see the following box:

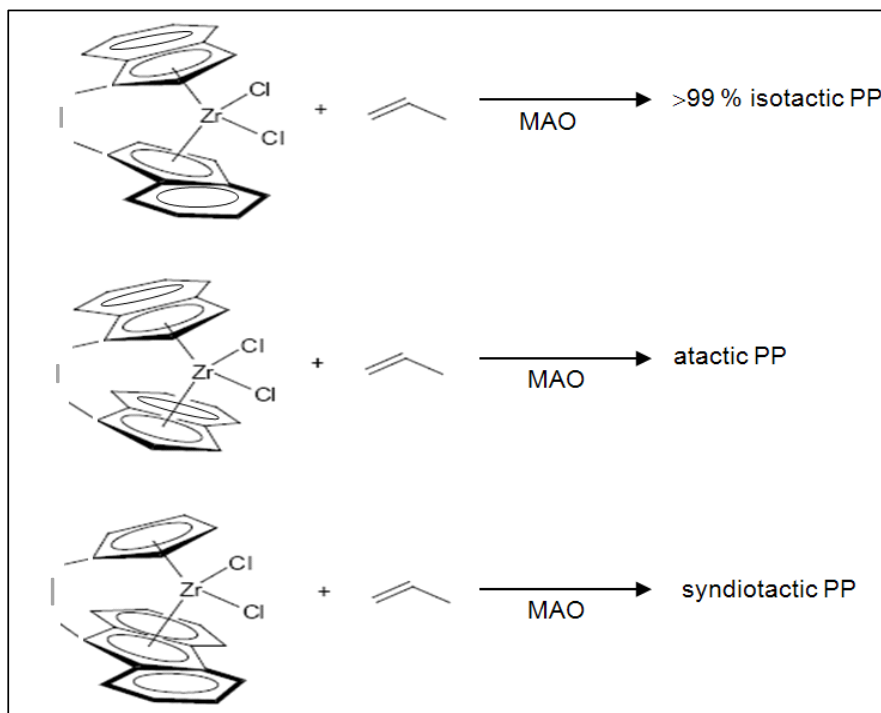


Cyclopentadienide (cp) ions have a charge of -1, so with a cation such as Fe^{+2} , two of the anions will form an iron sandwich, known as ferrocene. If a metal with a bigger valency is involved, e.g., Zr^{+4} , to balance the charge, the zirconium will also bond to two chloride ions to yield a neutral compound, bis-chlorozirconocene.



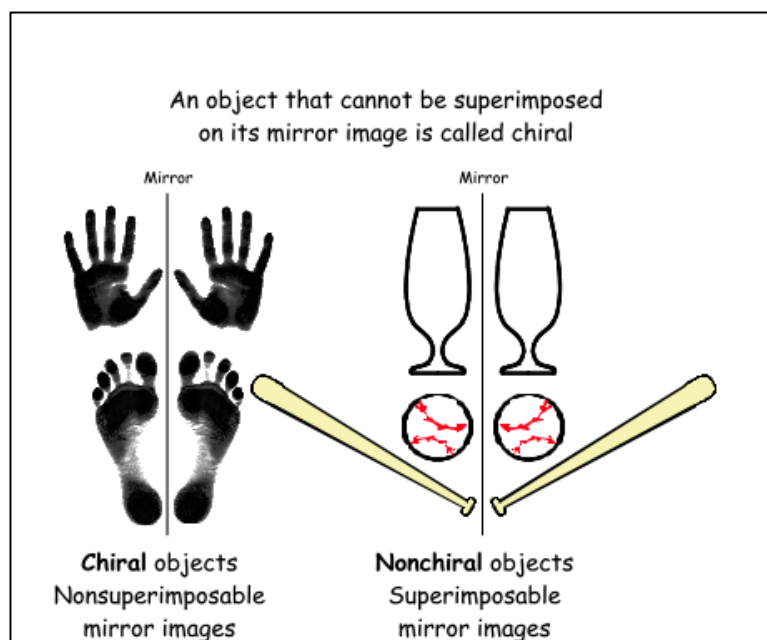
A derivative of bis-chlorozirconocene has aromatic rings fused to it. There is also an ethylene bridge, which links the top and bottom cp rings. These two features make this compound a great catalyst for making isotactic polymers.

Metallocenes by themselves are not active for polymerization. Usually, a co-catalyst is required to activate the metallocene. The activated metallocene catalysts can be used for olefin polymerization. Methylaluminoxane (MAO), $(\text{Al}(\text{CH}_3)\text{O})_n$, is used to activate the metallocene. If the catalyst is chiral, stereoregular olefin polymerization becomes possible:



source: <http://chem.rochester.edu/~chem234/lecture2.pdf>

The concept of chirality is demonstrated with some ordinary items in the box below:



source: <http://radaractive.blogspot.com/2011/01/chirality-is-reality-and-evolution.html>

Metallocene polymerization is making a big impact in the plastics business. One of the exciting outcomes is that metallocene catalysis polymerization allows one to make polyethylenes with much higher molecular weight than possible with the Ziegler-Natta catalysis. This ultra-high molecular weight polyethylene (UHMWPE), e.g., Dyneema, exhibits molecular weights up to six or seven million, and are claimed to be better than Kevlar for making bullet proof vests/armours.

Metallocene catalysts are inherently soluble catalysts (homogeneous). Therefore, the solution-polymerisation process was the first commercial process to use metallocene catalyst to produce polyethylenes. Gas phase and slurry polymerisation processes require heterogeneous catalysts. Metallocene catalysts need to be supported so that they can be employed in gas phase or slurry phase olefin polymerization processes.

Metallocene catalysts have several advantages over classical heterogeneous Ziegler-Natta catalysts:

- very high catalytic activities
- able to polymerize a large variety of olefins which were not possible with classical Ziegler-Natta catalysts
- the main chain termination mechanisms operating with metallocenes provide unsaturated chain ends that introduce additional functionality
- enable control of short as well as long chain branches with even spacings and uniform side-chain length distribution, which affect the rheological properties, thus, processing
- produce greater uniformity in micro-structural morphology, e.g., smaller spherulites of uniform size distribution in PEs
- their 'single site' nature enables these catalysts to produce extremely uniform homo and copolymers with uniform comonomer distributions with narrow molecular weight distributions and a very small fraction of extractable oligomers.

In conclusion, synthesis of vinyl polymers with stereoregular molecules was not possible until the advent of stereospecific polymerisation catalysts such as Ziegler-Natta and more recently metallocenes. Furthermore with these catalysts it is possible to produce polymer backbone chains that consist of blocks of different tacticity, e.g., a polypropylene with atactic and isotactic segments in its molecules can be polymerised by using zirconocene. The resultant polymer can be described as a thermoplastic elastomer (TPE) because of the presence of hard (crystalline) and soft (amorphous) domains. Various outcomes can be tailored by controlling the ratios of these domains.

Polymers consist of macromolecules, the size of which depends on the **degree of polymerisation**. The subject of the molecular weight of polymeric molecules is covered in the next section.

2.5 Molecular weight and molecular weight distribution

During polymerisation not all polymer chains grow to the same length and this results in a distribution of molecular weights. Accordingly, molecular weight measurements based on, for instance, viscosity and osmotic pressure produce average values. The average molecular weight of the polymer (\bar{M}) is related to the average degree of polymerisation (DP):

where, M_0 is the molecular weight of the repeat unit/monomer.

The unit for molecular weight is normally g/mol, but often it is convenient to omit the unit by expressing it as the ratio of the mass of the molecule to $1/12^{\text{th}}$ of the mass of an atom of ^{12}C .

There are several ways of expressing average molecular weight, including number average (\bar{M}_n) and weight average (\bar{M}_w) molecular weights:

\bar{M}_n is based on the number fractions of molecules with a given mass M_i (i.e., doing a weighting based on the number of molecules of a given mass), and \bar{M}_w is based on the weight fraction of molecules with mass M_i (i.e., doing a weighting based on the mass of molecules of a given mass).

where, N is the total number of chains, N_i is the number of chains with molecular mass M_i .

where, M is the total mass, m_i is the mass of molecules with mass M_i .

The other definitions for molecular weight are viscosity average (\bar{M}_v) and z-average (\bar{M}_z). The values obtained depend on the type of averaging used and they correspond to each other as follows $\bar{M}_n < \bar{M}_v < \bar{M}_w < \bar{M}_z$. Laboratory techniques for measuring molecular weight are listed in Table 2.2, which also shows the suitability of these methods at different molecular weight values. The viscosity of the polymer solution is a physical property that is closely linked to the molecular weight. The relation between the intrinsic viscosity η and the viscosity-average molecular weight:

where, K and a are polymer and solvent specific empirical constants that are obtained by calibration experiments using samples of known molecular weight and determining their $[\eta]$.

A simple alternative to viscosity measurement is the measurement of the **melt flow index** (MFI) or **melt flow rate** (MFR), which are convenient parameters used just for comparing polymer melts and polymers that are difficult to dissolve. These measure the amount of molten material that flows through a defined orifice under a certain weight. The material is extruded at a given temperature for 10 minutes and the amount of extrudate recorded in grammes. There is an inverse correlation between MFI and viscosity and/or the molecular weight of the polymer. MFR is also, confusingly, used to indicate “melt flow ratio”, the ratio between two melt flow indices under two different load levels. For clarity, this should be reported as flow rate ratio (FRR), or simply flow ratio. It is an index that can mislead, since the ratio of the totally different MFI values can produce the same ratio, commonly used as an indication of the way in which rheological behaviour is influenced by the molecular mass distribution of the material.

Table 2.2 Analytical techniques for measuring molecular weights of various ranges

Technique	Measures	Range, g/mol
End Group	M_n	up to 2500
Osmometry	M_n	15000 – 750000
Ebulliometry	M_n	up to 100000
Light scattering	M_w	20000 to 10^7
Ultra centrifuge	M_w, M_z, MWD	2000 to 10^7
Solution viscosity	M_v, M_w	15000 – 10^6
Vapour-phase osmometry	M_n	up to 25000
Gel-permeation chromatography	$M_n, M_w, M_v, M_z, \text{MWD}$	up to 10^6

\bar{M}_w / \bar{M}_n is the **polydispersity index** and indicates how uniform or otherwise the **molecular weight distribution** (MWD) is. In general, a **narrow** molecular weight distribution leads to more uniform property values, a narrower softening/melting temperature range, a lower stress cracking sensitivity, and better chemical resistance. A **broad** molecular weight distribution has advantages for processing because the low molecular weight fractions behave like lubricants. The polymer is less brittle because the low molecular weight fractions can act as plasticisers.

2.5.1 Influence of molecular weight on properties

Molecular weight influences microstructure, and both rheological/processing and end-use properties of polymers. The Polymerisation process has to proceed to a significant level in order to yield high enough molecular weight for the product to be deemed commercially viable. Polymers used as plastics, fibres, paints/adhesives and rubbers are expected to have number-average molecular weights over 10,000. Molecular weight in the range of 10,000 to 1,000,000 enables polymers to be

used in so many different applications. As molecular weight increases mechanical properties improve, but melt processing becomes difficult as illustrated in Figure 2.6. As can be seen the mechanical properties increase rapidly initially with the increasing molecular weight and then slow down reaching a steady value. It is important to keep the molecular weight at a level so that the increase in viscosity does not make processing difficult. Specific examples of the influence of molecular weight on properties for polyethylenes and polypropylene are presented in Ehrenstein (2001, p54) and Strong (1996, p162).

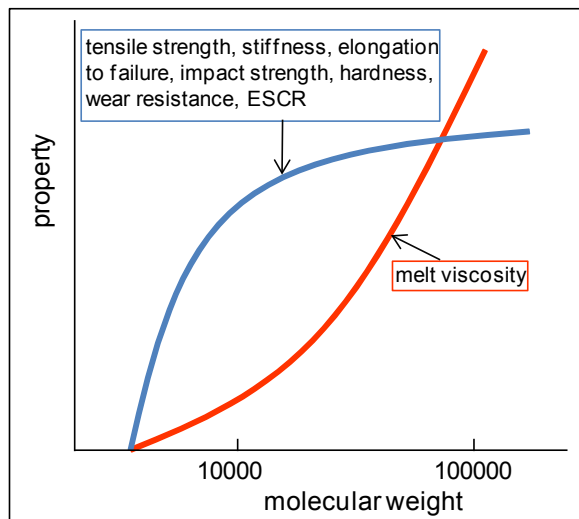


Figure 2.6 A generalised plot of property against molecular weight for polymeric materials

2.5.2 Solubility parameter

Substances can dissolve in liquids if the forces holding the molecules together in the solids can be overcome. The polymer molecules in thermoplastics are normally held together by secondary forces and physical chain entanglements. The secondary forces are much weaker than the primary covalent bonds that exist between the repeat units in the polymer molecule backbone chain, and they can be overcome by appropriate solvents to produce solutions. A measure of the strength of secondary bonds is given by the cohesive energy density (CED):

$$\text{CED} = \Delta E_v / V_1$$

where, ΔE_v is the molar energy of vaporisation and V_1 is the molar volume of the liquid.

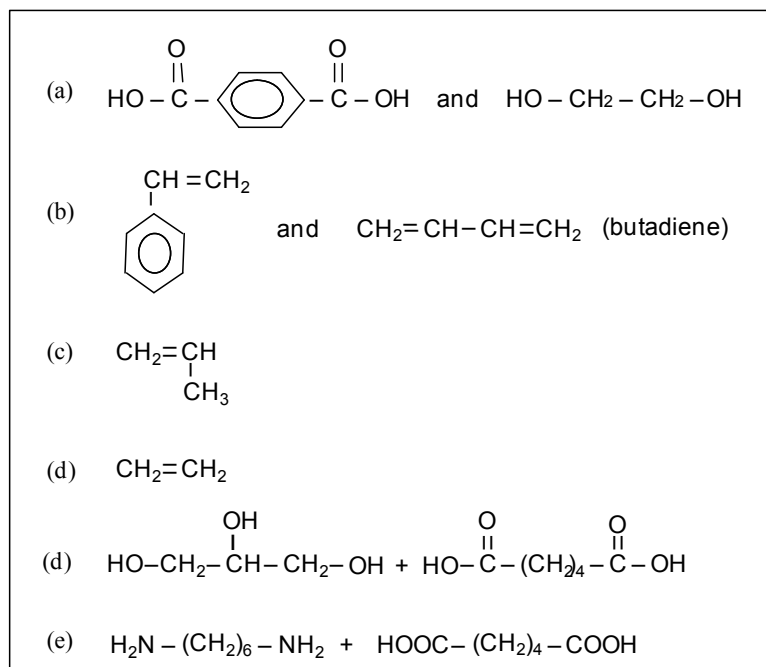
The solubility parameter is related to the CED by the equation, $\delta = (\text{CED})^{1/2}$ in $(\text{J}/\text{m}^3)^{1/2}$ or $(\text{MPa})^{1/2}$. The solubility parameter becomes a useful guide to the miscibility/compatibility of different polymers. A convenient method of estimating δ value for a polymer is to identify a solvent that causes maximum swelling in network polymers or maximum intrinsic viscosity (intrinsic ability of a polymer to increase the viscosity of a particular solvent at a given temperature) value for soluble TP polymers. It is expected that when the polymer and solvent have the same δ , the maximum swelling/expansion will occur in the polymer molecules and therefore the highest viscosity (for a given concentration) will be obtained. By measuring the viscosity of dilute solutions of a polymer in a variety of solvents, one can determine a consistent value of δ for the polymer. In a cross-linked network polymer, solution cannot occur, but swelling can occur in polymer segments between cross links. Maximum swelling is experienced when the solubilities match. Alternatively, δ can be calculated from CED values, which in turn may be calculated using the molar attraction constants (values of molar attraction constants for a number of organic chemistry groups are presented in Fried 1995, p100).

2.6 Self-assessment questions (source:Painter & Coleman 2004)

1. Styrene monomer can be polymerized by practically all chain polymerization methods. Which of these methods should be used to produce isotactic polystyrene?
 - a) free radical
 - b) anionic
 - c) cationic
 - d) coordination
2. Suspension free radical polymerization of styrene would be preferred over bulk polymerization to overcome the problem of
 - a) branching
 - b) cross-linking
 - c) isotacticity
 - d) heat of reaction during polymerization
3. In emulsion polymerization, the principal place where the monomer polymerizes is
 - a) monomer droplets
 - b) aqueous phase
 - c) swollen surfactant micelles

d) surface of reactor

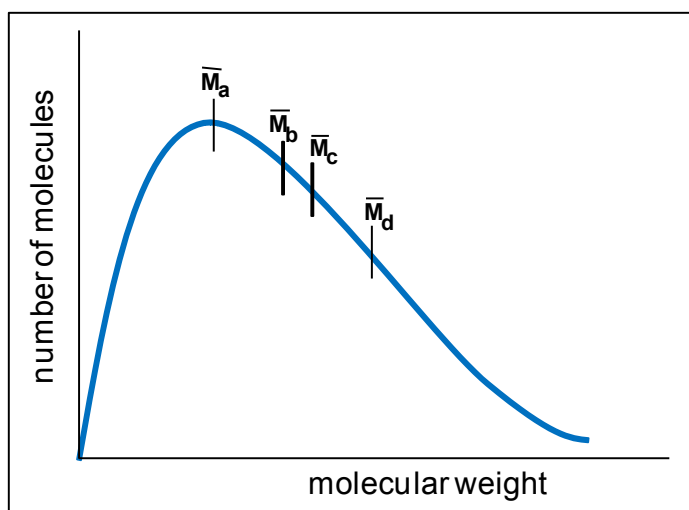
4. If a polymer chain has a molecular weight of 280,000, how many ethylene units does it contain?
5. Which of the monomers/monomer combinations in the box below polymerises by the step-wise polymerisation mechanism?



6. Which of the above monomers can be polymerized free radically at high pressures to give a polymer containing branching and what is the polymer called?
7. Which monomers in Question 5 can form polyester?
8. Which of the monomers in Question 5 containing a C=C double bond cannot be polymerized free radically?
9. Which monomers in Question 5 are used to make a thermoplastic rubber?
10. Indicate the pairs of monomers in Question 5 to make an ethylene/propylene random copolymer, and also which one of the following polymerisation mechanisms should be used to make the copolymer?
 - a) free radical polymerization
 - b) anionic polymerization
 - c) cationic polymerization
 - d) using a catalyst (coordination polymerization)
11. Which monomer or mixture of monomers in Question 5 is commercially polymerized using a catalyst to produce an isotactic polymer?
12. Which monomer or mixture of monomers in Question 5 polymerizes to form a cross-linked polymer network?
13. Which monomer or mixture of monomers in Question 5 polymerizes to form Nylon 6,6?
14. Compare the water absorption capacity of PA6,6 with PA 6,12, indicate reasons for differences.
15. Distinguish between the repeating units for addition and condensation type of polymers, and give an example of each type of polymer.

16. A polyamide polymerised from a 2-carbon diamine and a 6-carbon diacid, select its name:
- nylon 4
 - nylon 2,6
 - nylon 6,6
 - nylon 6,2
17. Which of the following polymers is least likely to be optically transparent?
- atactic polystyrene
 - isotactic polystyrene
 - an ethylene/propylene random copolymer
 - a styrene/butadiene random copolymer
18. Polyethylene is used for making carrier bags and bullet-proof vests: true or false.
19. The three commonly used metals in metallocene catalysts are
- Zr, Co and Cu
 - Zr, Hf and Ti
 - Al, Zn and Ti
 - Au, Y and Rh
20. High pressure, high temperature free-radical polymerization of ethylene produces
- HDPE
 - LDPE
 - PP
 - LLDPE

21. Calculate the molecular weights of the repeating units of polypropylene and PVC. Determine M_w for a polypropylene of average degree of polymerisation of 18,000. (Atomic masses of H = 1, C = 12, and Cl = 35).
Answer: $m(PP) = 42 \text{ g/mol}$; $m(PVC) = 62 \text{ g/mol}$; $\bar{M}_w = 756 \times 10^3 \text{ g/mol}$.
22. A polystyrene specimen has a number average molecular weight of 80,000 and a polydispersity index of 5. Calculate the weight average molecular weight.
23. The molecules of a sample of polystyrene can be divided into 5 groups in terms of their molecular weight with the same number of molecules in each group. The molecular weights of the molecules in the groups are 10,000; 20,000; 30,000; 40,000; 50,000. Calculate \bar{M}_n . *Answer: $\bar{M}_n = 30,000$.*
24. Calculate \bar{M}_w for the data given in Question 22. *Answer: $\bar{M}_w = 3.67 \times 10^4$.*
- 25.



Indicate what the subscripts (a), (b), (c) and (d) stand for on the above molecular-weight distribution curve, where M represents molecular weight.

3 Polymer processing

“Everything flows and nothing abides, everything gives way and nothing stays fixed.”

Heraclitus of Ephesus (c. 535–c. 475) describes nature and life as continuously changing and nothing remaining still, and uses the changing /flowing river image in his arguments. The propensity to change for materials and products can be desirable or otherwise: during processing the change in material is actively accelerated in order to achieve meaningful productivity, however, once the product is formed the change is not desirable. **Rheology** is the Greek word for “to stream” and is used to denote the study of the flow/deformation behaviour of material, both in liquid and solid states.

3.1 Concept of rheology

In polymer processing, viscosity is experienced under various states of deformation, for example in injection moulding the polymer melt is subjected to significant shear stresses and strains and therefore shear viscosity is of concern.

$$\text{Shear stress } (\tau) = (\eta) \times (\text{rate of strain } (d\gamma/dt))$$

$$\therefore \text{Shear viscosity } (\eta) = (\tau) / (d\gamma/dt).$$

Many low molecular weight simple liquids behave in accordance with Newton’s Law of viscosity, where the viscosity is independent of the magnitude of shear stress, τ , and strain, γ . For high molecular weight liquids, e.g., polymer melts and solutions, τ and $d\gamma/dt$ are not proportional over all ranges of τ and γ and the relationship becomes non-Newtonian. Some non-Newtonian flows are described in Table 3.1 and Figure 3.1.

Table 3.1 Different flow behaviours

Fluid type	Behaviour
Newtonian fluid	viscosity is independent of shear rate
Dilatant fluid	viscosity increases with shear rate (shear thickening)
Pseudoplastic fluid	viscosity decreases with shear rate (shear thinning)
Bingham behaviour	No flow up to a yield stress (e.g., in highly filled plastics)
Thixotropy	viscosity decreases with time under a constant shear rate
Rheopexy	viscosity increases with time under a constant shear rate

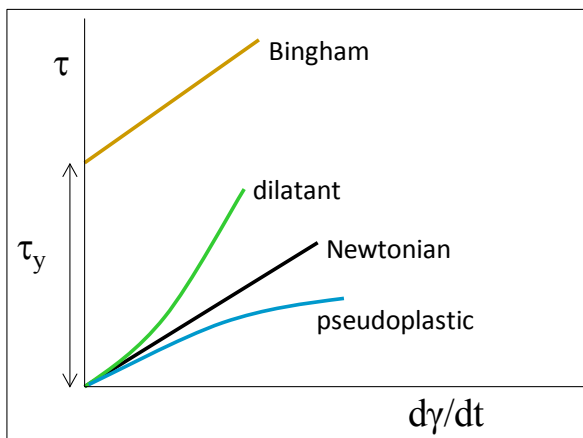


Figure 3.1 Shear stress vs. shear rate for Newtonian and non-Newtonian behaviours

Under non-Newtonian conditions that exist in polymer melts, the viscosity is no longer a material constant and therefore is termed as an “apparent viscosity”. Variation of apparent viscosity with shear rate is shown in Figure 3.2. Most polymer melts behave in pseudoplastic manner. Dilatant behaviour is experienced in mixing some pigments/fillers into polymer resins/solutions, which can cause processing difficulties. Dilatant behaviour can be demonstrated by adding water to cornstarch and stirring it.

A simple power law relationship is popularly used to describe non-Newtonian behaviour seen in polymer melts.

$$\tau = k \left(\frac{d\gamma}{dt}\right)^n$$

where, **k** and **n** are the power law indices, called the consistency index and the flow behaviour index, respectively.

For **Newtonian** liquids $n = 1$ and $k = \eta$,

$n > 1$ for **dilatant** and $n < 1$ for **pseudoplastic**.

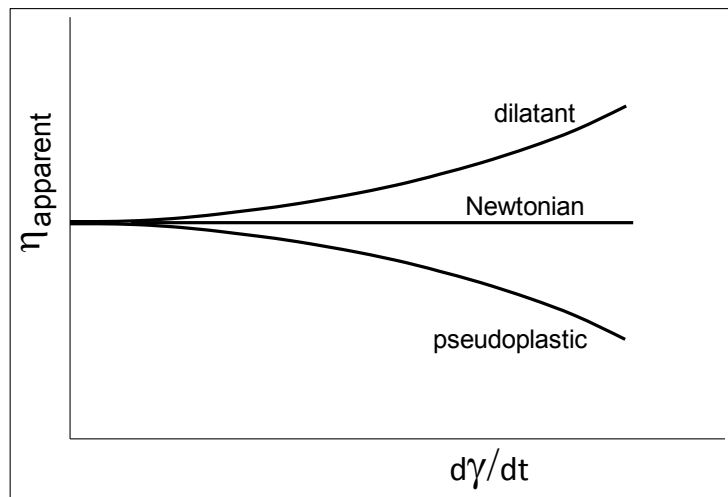


Figure 3.2 Variation of apparent viscosity with shear rate

Polymer melts are processed under different processing conditions. The rate of shearing applied to the melt depends on the type of process used as outlined in Table 3.2. Polymer melts exhibit a wide range of viscosities (10^2 - 10^6 Pa.s) mainly depending on the polymer type, shear rate and the melt temperature. At low shears polymers tend to behave like a Newtonian liquid but at high shear rates their behaviour becomes pseudoplastic.

Table 3.2 Shear rates involved in some polymer processes

Process	Shear rate, s^{-1}
Compression moulding	1-10
Calendaring	10-100
Extrusion	100-1000
Injection moulding	10^3 - 10^4

3.2 Processing and forming thermoplastics

Prior to covering processes, it might be useful to include a few basic characteristics of some common thermoplastics listed below.

- Polyethylenes
- Polypropylene
- Polystyrene
- Polyamides/nylons
- Polyvinyl chloride (PVC)
- Saturated polyesters (e.g., polyethylene terephthalate (PET))
- Acrylonitrile-butadiene-styrene (ABS) copolymer
- Others include fluorinated plastics (e.g., polytetrafluoroethylene, PTFE), polycarbonate (PC), acrylics (e.g., polymethylmethacrylate (PMMA)), etc.

Polyethylenes come in a number of different well known grades, depending on their density as influenced by the degree of micro-structural crystallinity. **Low density polyethylene** (LDPE) is flexible and very strong, used for the less expensive end of the commodity market such as bowls, buckets and bottles. It burns only slowly and softens at approximately 50 °C and, therefore, does not resist boiling water. Normally it is optically translucent. **High-density polyethylene** (HDPE) is used where more rigidity is required. It softens at approximately 80 °C. Optically it is less clear than LDPE. There are several other grades of polyethylene.

Polypropylene (PP) is similar to PEs but more versatile and sturdy; some grades only soften at as high as 140 °C, therefore, suitable as steam sterilisable hospital ware; not affected by environmental stress cracking, and exhibits outstanding resistance to fatigue on flexing. It is clear that the polyolefins (a generic name for the **aliphatic** polymers such as PEs and PPs) offer a range of plastics of increasing softening point, rigidity, gloss, and chemical resistance. Therefore why is not polypropylene used for more applications usually associated with LDPE? Mainly because of flexibility requirements and depending on market circumstances cost may become a factor.

Polyvinylchloride (PVC) is one of the few plastics to which plasticisers can be added, thus, exists as a rigid and as a flexible material. Unplasticised PVC (uPVC) is a hard, rather brittle (not as brittle as polystyrene) and resistant to many solvents (soluble in ketones, esters and chlorinated hydrocarbons). Furthermore, it is one of very few polymers with a reasonable inherent resistance to catching/spreading of flame, offers excellent electrical insulation and softens at about 80-100 °C.

Polystyrene (PS), readily identified by the metallic noise when dropped onto a hard surface, basic PS is colourless, transparent, hard and brittle, softens at 85-95 °C, resists aliphatic H/Cs, but is soluble in aromatics (e.g., benzene) and like ordinary PEs, it is not expensive. The lightweight PS (structural foam PS or expanded PS (EPS)) is an excellent heat insulator, but, since PS dissolves in aromatic solvents as display/insulation panels it should only be painted with emulsion paints.

Polyamides/nylons are extensively used in textiles and engineering, e.g., as self-lubricating bearings (especially in food processing, where the presence of lubricating oils might lead to contamination). Some nylons offer a good barrier to gas permeation, therefore used as film for packaging cheese slices, etc. Although demonstrating good chemical resistance, it is susceptible to high water absorption.

Cutting edge examples of various engineering applications of nylons and their copolymers as well as other thermoplastics such as polyester, acetal (homo- and copolymer polyoxymethylenes), polyimides and thermoplastic elastomer can be found in the DuPont knowledge centre (plastics.dupont.com) website: http://www2.dupont.com/Plastics/en_US/index.html.

The molecules of thermoplastics do not cross-link on heating and, thus, can be maintained in a softened state while being made to flow under pressure into a new shape. There are forming methods designed for thermoplastics and others for thermosets, although the barriers between these methods are becoming rather blurred. The processes/forming methods that are normally associated with thermoplastics include:

- Injection moulding
 - gas-assisted injection moulding
 - blow moulding
- Extrusion
 - blow moulding
 - calendering sheet/film
 - extrusion + thermoforming
 - fibre melt spinning
 - mesh (e.g., “Netlon”)
 - multi-layer extrusion
 - tubular film/blown film
- Thermoforming/vacuum forming
- Rotational moulding
- Coating
- Dispensing foam
- Machining/joining of plastics

Some of these processes will be expanded upon in the succeeding sections. More detailed information can be found in text books by Strong (1996), Morton-Jones (1989) and Groover (1996).

Processes of injection moulding and extrusion involve **material handling**, which basically entails the transportation of raw material often as granules/pellets in a satisfactory form.

Polymer granules undergo a series of handling steps from the raw-material producer to the processing machinery:

- conveying
- drying (typically via spin drying)
- conveying to the customer
- storage in the shipment packaging (bags or boxes)
- unloading (pneumatic conveying/silo storage)
- conveying to processing machinery
- further drying (with hygroscopic polymers)
- blending and feeding .

The transportation processes can cause deformation/degradation of pellets into undesirable products such as clumps of pellets, streamers/angel hair (thin ribbon of plastic caused by friction that melts and smears the pipe surface, which then peels off) and fines/dust, see Figures 3.3 and 3.4.



Figure 3.3 Types of degradation in delivery/conveying



Figure 3.4 granules and streamers

The presence of these degraded pellets/granules can lead to numerous problems in the subsequent processes and defects in products: e.g., clogging of filters, inconsistent feeding into the machine resulting, for example, in variations of profile and film thicknesses, gels/specs in films, colour inconsistencies and presence of black specs, and safety issues such as a greater risk of dust explosion in the dust-collection system and respiration concerns for operators. Special-purpose separators (Angel's hair separator) and elutriators (particle separator) are placed in delivery lines to remove these impurities.

Plastic particles small enough to pass through a 30 mesh screen (i.e., 30 openings or 30 wires per inch of the screen) are considered as fines and dust particles. The explosive concentration range of the plastic fines and dust is related to **particle size**. When dealing with plastic fines and dust, the important parameters are:

- the **Kst** (the deflagration index) is the maximum rate of pressure rise, which is a measure of explosion severity. There are different Kst values depending on the particle size.
- the **MIE** is the minimum ignition energy required to ignite a dust cloud.

As particle size gets smaller, the Kst values increase and the MIE values decrease. Note that deflagration means the extremely rapid burning of a material. This is much faster than normal combustion, but slower than detonation.

Plastic exposed to the atmosphere can pick up **moisture**, and can cause air pockets that hinder injection/extrusion processes, lead to poor appearance (roughness and silver-strikes in surfaces and internal bubbles) and degradation of some mechanical properties. In their susceptibility to moisture absorption, polymers are identified as hygroscopic and non-hygroscopic.

Non-hygroscopic polymers (e.g., PE, PP and PVC) do not absorb moisture; however, they can pick up surface moisture which can lead to processing problems. It can be removed with a simple hot air dryer. **Hygroscopic polymers** (e.g., Nylon, PET, TPU and PC), have a strong affinity for moisture, and water molecules can become chemically bonded to the polymer chains. Usually a dehumidifying dryer is required to remove moisture successfully from hygroscopic polymers.

3.2.1 Injection moulding

The process entails injection of molten polymer into a closed mould, which is normally cooled to facilitate rapid solidification, to produce discrete products. Thermoplastics (TPs) that can be moulded easily are PS, PE and PP, and those which require greater care are rigid PVC, nylons and PMMA. The moulds can be single or family moulds. The machines are rated by their **clamping force** and **shot capacity**. Machines exist with shot capacities ranging from a few grammes to tens of kg. Basic elements of an injection moulding machine are illustrated in Figure 3.5.

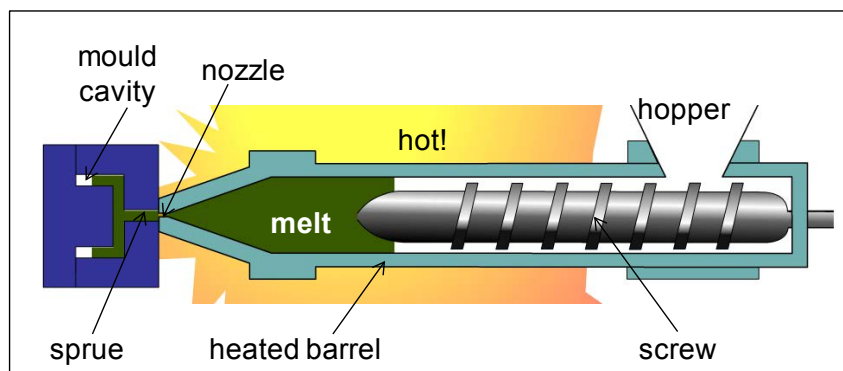


Figure 3.5 Basic elements of an injection moulding machine

The screw rotates and draws back during charging of plastics granules through the hopper, and once there is sufficient molten charge ahead of the screw, then the screw stops rotating and acts as a piston to advance the melt into the mould through the nozzle. A ring check valve is positioned in a suitable recess at the head of the screw behind the spider tip and retreats (is dragged back) onto the ring-valve seat and ensures that during the injection cycle the melt moves forward into the mould and does not leak/squeeze back onto the screw. The role of the ring is reversed during the charging when the screw rotates and retreats to leave space for the plastic melt, the ring is pushed forward by the transported melt against the shoulder of the spider openings, allowing the melt to flow over the spider openings to the space between the screw tip and the nozzle. Figure 3.6 shows the details of the spider and the sliding ring check valve.

In a typical operation the melt flows through a conduit system, which normally incorporates a **sprue**, **runners** and a **gate(s)**, prior to entering the mould cavity and taking up the shape of the product. Figure 3.7 shows a sprue and runner system with pin gates for a multi-cavity family mould for the production of eight components with one shot. Pin and tunnel (submarine and banana) gating facilitate automatic trimming of the components from the moulding. Most of the other types of gates have to be trimmed off manually, and may leave behind a sizable mark, see Figure 3.8. Much information on various gate types is given in Strong (1996, p561) or http://www.dsm.com/en_US/html/dep/gatetype.htm. Another feature of the mould is the **cold slug well(s)**, see Figure 3.7, which is an extension of the sprue and runners (where runners change direction) and traps/captures the cold leading front of the plastic melt, allowing the hotter plastic to flow into the rest of the runner system, and it can also trap any other solidified plastic that enters the mould with the melt. For example, plastic that is left in the nozzle from the previous shot and may have solidified between shots.



Figure 3.6 Photograph of a typical injection moulding screw and its spider tip and ring valve

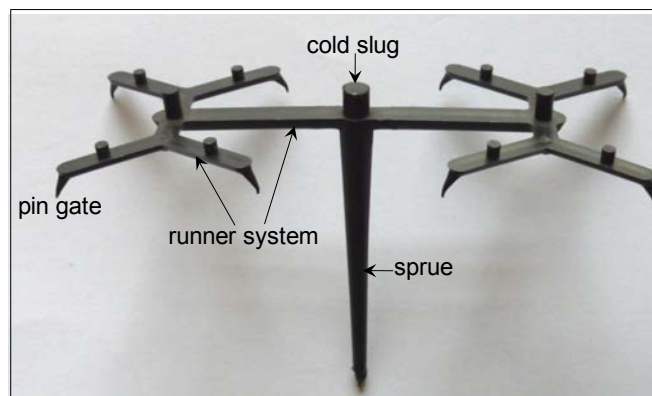


Figure 3.7 Photograph of a multi-gate sprue and runner system for a TPE product

The design of gating and the runner system in a multi-cavity mould for the production of a component should be **balanced**, i.e., the runners to all the cavities should be the same length and diameter, in order to ensure that all the cavities are filled evenly and the parts produced are uniform. Figure 3.9 shows examples of balanced and unbalanced runner layouts.



Figure 3.8 The mark left on a large moulding after trimming off the sprue runner

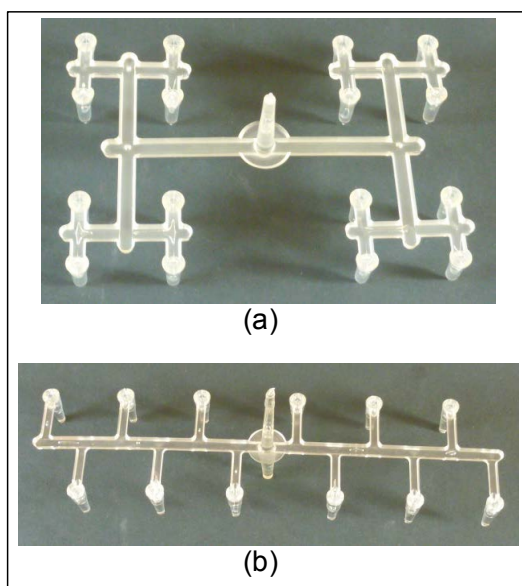


Figure 3.9 Examples of (a) balanced and (b) unbalanced runner systems

The size and positioning of gate(s) is also critical for ease of trimming and for avoidance of flaws such as jetting and weld lines or for minimising the impact of such flaws. **Jetting** is an initial squiggly narrow stream of melt which is followed by an expanding melt front, causing it to fold and gather up, see the short-shot moulding in Figure 3.10. The jetting is caused by the position of the gate such that the melt is injected straight into an open cavity and it does not make contact with the mould. By feeding the melt sideways and aiming at an obstacle as in tab gating, see Figure 3.11, the jet can be interrupted and normal mould filling should ensue.

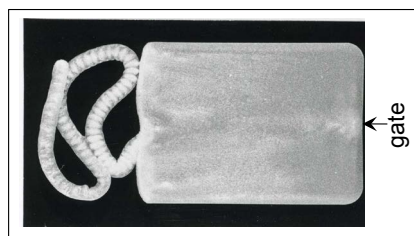


Figure 3.10 Short-shot moulding showing jetting (source: Akay (1992))

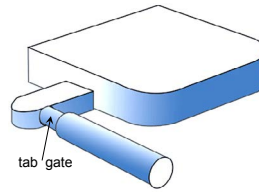


Figure 3.11 Tab gate (source: http://www.dsm.com/en_US/html/dep/gatetype.htm)

Figure 3.12 shows that jetting can also result depending on the position of the gate in the moulding: filling the cavity from the thinner end has resulted in jetting in a moulding of carbon fibre reinforced polyetheretherketone. The problem was alleviated by gating into the part from the end with the greater cross section, Akay and Aslan 1995.



Figure 3.12 Jetting when the mould is filled from the thin end (the moulding is an experimental PEEK/CF hip prosthesis)

Weld lines (knot lines) can occur where a mould requires more than one gate to fill it or the mould includes an insert that splits the melt into streams, and subsequent merging of the melt flow fronts generates a line. This can be a source of mechanical weakness in the moulding produced, particularly with polymers containing fibres, as well as an appearance problem. Figure 3.13 shows the generation of weld lines by filling a cavity using two gates, positioned for melt flow fronts to advance adjacently or head on. If the generation of a weld line is inevitable then the tool design should ensure that its potential harm is minimised. Using a mould-flow software package, the placement of a weld line may be identified. Empirically the use of **short shots** can also be informative. Short shots can also provide useful information on mould filling patterns and establishing the shot size for injection. A small shot size results in under packing and therefore sink marks and voids, and on the other hand, a large shot size can result in flashing, see Figure 3.14, and possible denting of the tool parting surfaces.

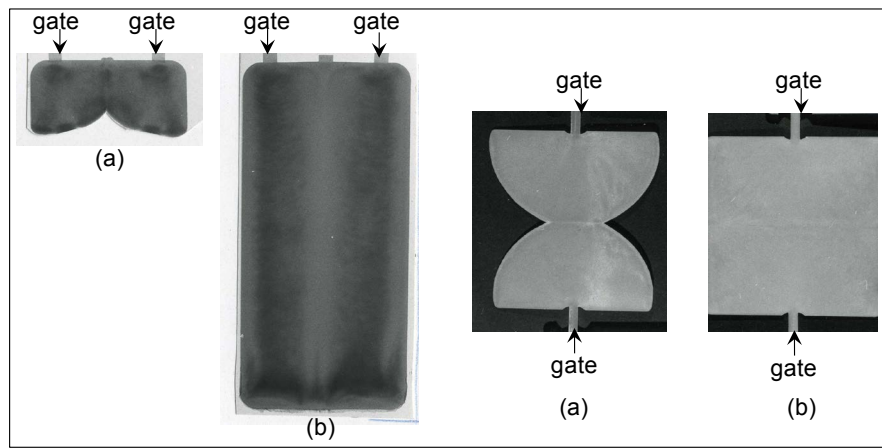


Figure 3.13 Generation of weld lines: (a) short shots and (b) complete mouldings (from Akay (1993))

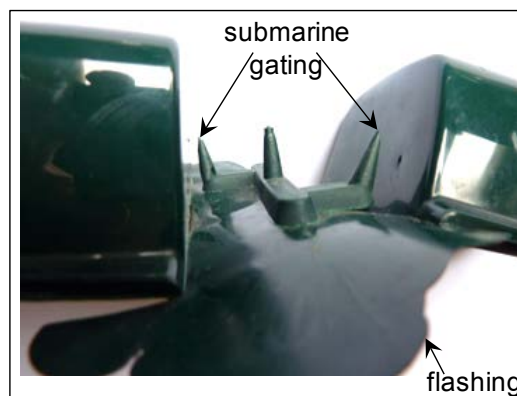


Figure 3.14 Generation of flashing, and an example of submarine gates (facilitates automatic separation of parts and runner systems)

The sprue and runner system has to be separated from the part and this generates a large amount of scrap. Therefore, sprueless gating would be desirable and is achieved with **hot runner gates**, the nozzle of the machine is extended to a sprueless mould and the melt is injected through a pinpoint gate.

Gas-assisted injection moulding has resulted in advances in the way in which injection moulded components are manufactured. Enhanced quality, reduced cycle times and component weight reductions, therefore cost reductions, can be achieved by the process.

Techniques have been developed whereby inert gas nitrogen is injected into the still molten plastic in the mould cavity. Acting from within the component shape, the gas inflates the component and counteracts the effects of the material shrinkage. The effect is to keep an internal pressure on the material until it solidifies and skin forms at the mould cavity surface. This is independent of any gate freezing. In addition, with the material being pressed against the mould surface by the gas until it solidifies, the moulding will have better surface definition and will be more likely to be dimensionally correct. In thicker components the resultant hollow core, can save up to 30% on the material used. Figure 3.15 shows the achievement of hollow cores with gas injection in some sections of a polypropylene kettle that would otherwise result in unnecessary thickness and extra weight.

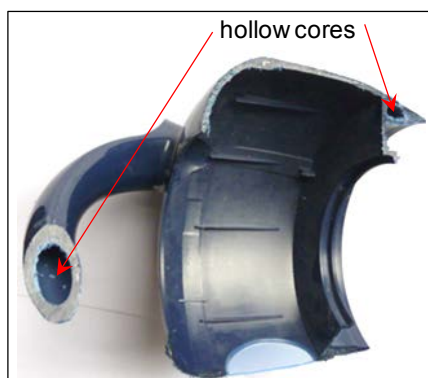


Figure 3.15 A section of a conventional kettle showing the hollow cores

Another major benefit is the reduction in machine cycle times that can be achieved. With no molten core to solidify, the material in the mould cavity solidifies quicker thus enabling the component to be ejected sooner. BPF lists benefits of internal gas injection moulding:

Inert gas nitrogen is injected into the molten plastic in the mould cavity. Acting from within the component shape, independent of any gate freezing, the gas:

- inflates the component and counteracts the effects of the material shrinkage, and therefore avoids sink marks
- keeps an internal pressure on the material until it solidifies and forms skin at the mould cavity surface
- enables reductions in product weight, power consumption and cycle time
- reduces in-mould pressures by up to 70%, and therefore reduces clamping forces, enabling larger mouldings on smaller machines
- reduces in-mould pressures, and therefore less wear on moulds
- reduces moulded-in stress, and therefore improved dimensional stability with no distortion.

The British Plastics Federation (BPF) web site provides excellent information on gas injection moulding as well as all other plastics processes for thermoplastics and thermosets. The web site includes animations that make it much easier to understand the concepts.

3.2.2 Extrusion

Extrusion is mainly used for thermoplastics, during the process the molten material is continuously forced through a shaped die by a rotating Archimedean screw. The screw is placed within a heated cylindrical barrel with just sufficient clearance for its rotation, see Figure 3.16. Well-known extruded products include PE film and pipes; PVC guttering, piping and various profiles (e.g., window frames); PS, ABS and PP sheet (gauge $\geq 250 \mu\text{m}$); nylon fibre; PP fibre and tape; PMMA light fittings and vehicle lenses, etc.

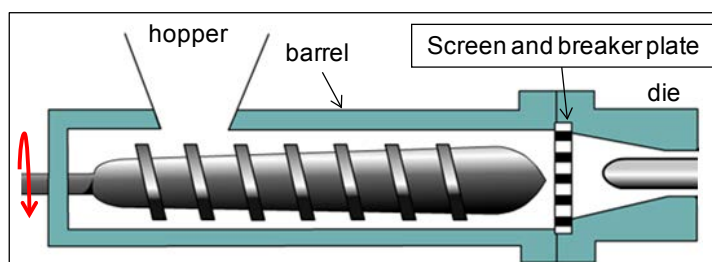


Figure 3.16 Illustration of a single-screw extruder

Polymer granules are fed into an extruder through the hopper at one end of the barrel. The hoppers are mostly just ordinary funnels but some are equipped with a vibrator in order to avoid bridging of pellets over the mouth of the hopper, particularly with long pellets (fibre containing pellets can be as long as 10 mm). Other hoppers may incorporate an auger feeder; see Figure 3.17, for uniform and consistent feeding of pellets.



Figure 3.17 Hopper with an auger facility

The screw transports and compresses the material from the hopper end to the die end along the barrel. The polymer is softened/melted with the heat generated by the shearing of the material and the heat input from the heater bands attached to the barrel. The features of the screw are outlined in Figure 3.18. The screw diameter remains constant along the barrel length with a very slight clearance between the screw flights and the inner lining of the barrel. The root diameter and therefore the channel depth decreases along the barrel to facilitate the compression of the material as it softens.

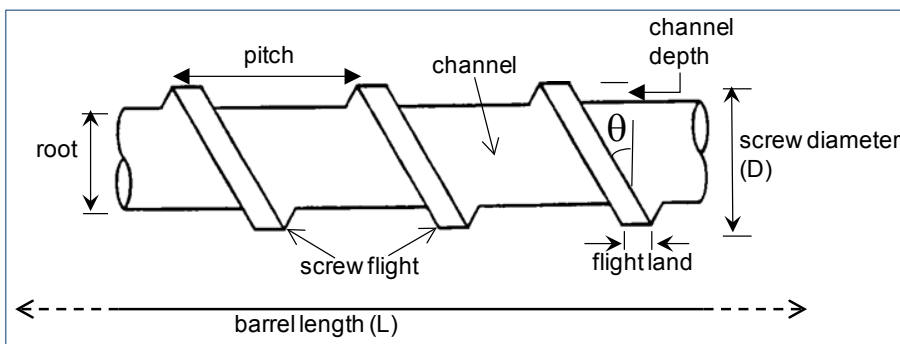


Figure 3.18 Definition of screw features

There are various screw designs that are used, depending on the type of polymer processed. Three of the basic designs are illustrated in Figure 3.19. Along these screw lengths different zones are identified. There is an increase in the screw root, hence, a decrease in volume available in passing from the feed to the transition zone – this will cause compression of the granules forcing the air between the granules back towards the hopper. Granule melting occurs in the transition zone. The melt is delivered to the die from the metering (melt) zone at a constant rate, consistency, and pressure. At the end of the metering zone there is often a screen pack or disposable continuously fed gauze and a breaker plate, which is a perforated disc. The final section within the actual extruder is the adaptor/die section.

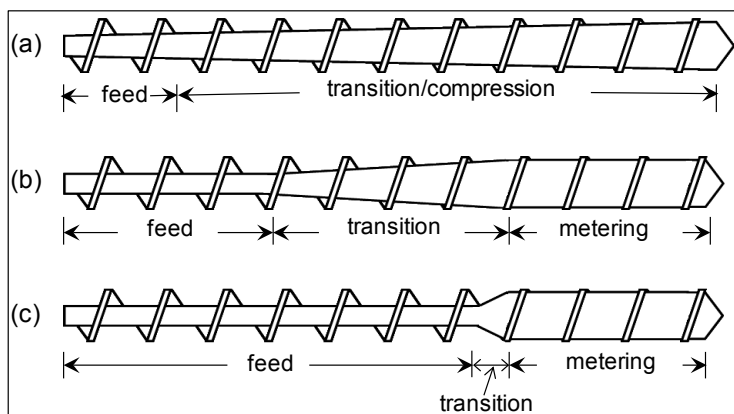


Figure 3.19 Illustration of basic screw designs and associated zones

Screw type (a) is suitable for polymers with very gradual softening temperature or shear/heat sensitive polymers, e.g., PVC, Type (b) for polymers with wide melting/softening temperature, e.g., PE, and type (c) for polymers with sharp/narrow melting temperature, e.g., nylons.

The **feed zone** begins at the hopper end and it is held at a temperature to ensure satisfactory delivery of the polymer granules to the subsequent zones. The channel depth is constant in this zone and its length controls the rate of feed of granules forward. Maximum delivery of granules by the feed zone may be achieved by having:

- deep screw channel
- low degree of friction between the polymer granules and screw surface
- higher degree of friction between the granules and the surface of the barrel wall
- optimum helix angle, $\theta = \tan^{-1} [(pitch) / (\pi D)]$

Some feed zones incorporate a grooved-feed throat. The grooves can be axial (along the barrel) or helical, and they increase the friction between the pellets and the barrel, forcing more pellets forward and hence increasing the output compared with smooth feed throat extruders. There is also less surging from grooved feed throat extruders.

The **compression zone**, where material starts to change from solid granules to a polymer melt, has a decreasing channel depth so that the softened polymer is compacted, improving heat transfer to the polymer and expelling the air that comes in with the granules back through the hopper. The material is compressed typically by a factor of three. High levels of shear/frictional heat is generated in this zone (it can exceed the barrel temperature).

The **metering zone**, where the channel depth is again constant, and where additives may be added and mixed into the melt to a homogeneous consistency and the melt is pumped forward at a uniform rate to the die region. The zone length is designed to achieve efficient mixing, especially with additives.

Other parameters in screw design include:

- Compression ratio (C. R.) = (flight depth in feed zone) / (flight depth in metering zone), or C. R. = (volume of the first full flight in the feed zone) / (volume of the last full flight in the metering zone). It is typically 3/1 for thermoplastics and 1.5/1 for rubbers.
- L/D ratio = (length of screw) / (diameter of screw). It is typically 30/1 for TPs and 5-10/1 for rubbers.

Advantages of short L/D extruders:

- less floor space
- lower equipment cost
- less torque/power requirement to operate
- less residence time in the extruder with temperature-sensitive polymers

Advantages of longer L/D extruders:

- higher throughput
- greater mixing capacity
- higher pumping pressure at die
- greater melting with less shear heating
- increased conductive heating from the barrel.

The type of screw known as **barrier screws** have a second flight added which splits the channel into two: a solids channel and a melt channel. This design offers greater energy efficiency by enabling better melting and higher output and also increases mixing capabilities.

Some applications with materials such as PVC, nylons, ABS, PC may require the use of **vented extruders** (also known as a two-stage extruder), which provide a vent hole in the barrel to remove moisture, solvents and other volatiles. As seen in Figure 3.20, the screw has a de-compression zone beneath the vent hole in order to free the volatiles and also reduce the pressure on the melt to prevent it from extruding out through the vent hole. In some cases, the venting may require vacuum assistance. The screw has a second stage compression and metering zones, after the de-compression zone.

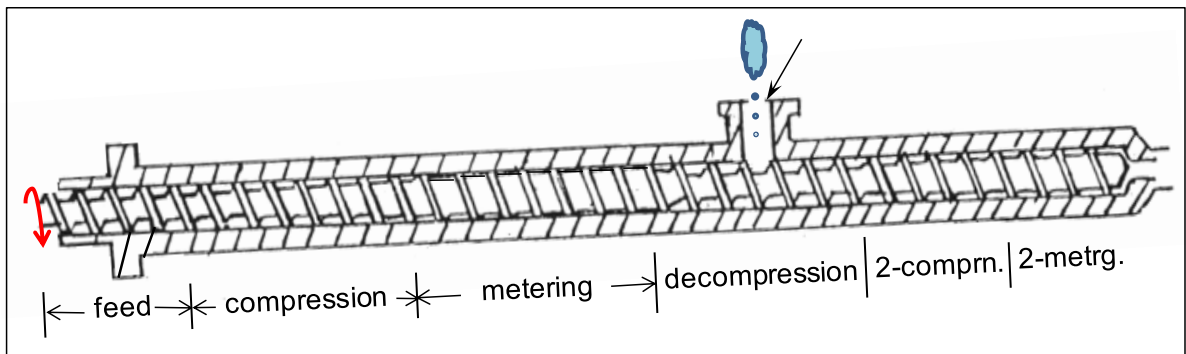


Figure 3.20 Features of a vented extruder

In the decompression zone of a two-stage screw, the root diameter is reduced and therefore presents a mechanically weak region, and the screw becomes vulnerable to fracture by torsion at this region, see Figure 3.21, if it seizes up by accidental solidification of the polymer in the barrel.

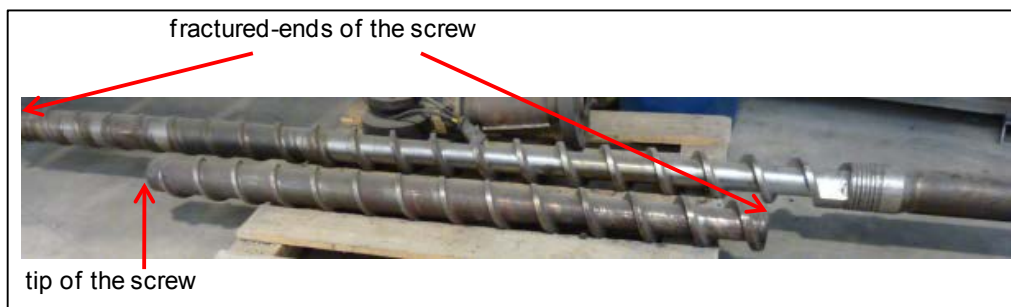


Figure 3.21 A screw which has fractured at the reduced root diameter in the de-compression zone

The melt is screened and passes through a **breaker plate** prior to entering the adaptor/die region. **Screen packs** are placed before the breaker plate (screw side) to filter unplastified material and impurities (Figure 3.22). Coarse screen (a 20-mesh screen in this illustration) is placed against the breaker plate to support the finer screens (here as 40- and 60-mesh) and also placed in front of the finer screens to collect larger particles and increase the screen pack life.

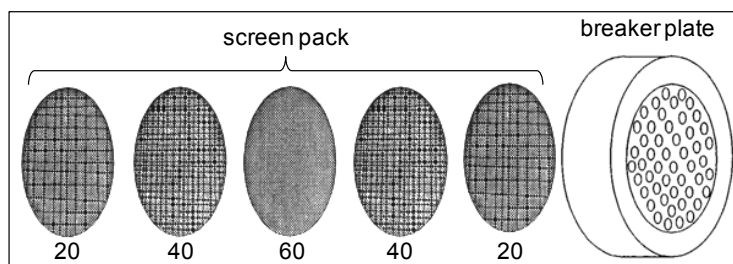


Figure 3.22 Illustration of screen pack and breaker plate

Functions of screen pack and breaker plate also include generation of back pressure to ensure that the screw is filled and the melting and mixing is efficient. The breaker plate also turns spiral /rotational flow to linear flow. An **adapter**, following the breaker plate, helps to smoothly link the barrel and the die.

The die is machined to match the profile of the product or to produce a pre-form/parison for the final product as in blow moulding of bottles or tubular film production. The land length for a die (Figure 3.23) is an important parameter: longer land lengths promote flow stability and reduce die swell and drool; however as well as the greater manufacturing costs, the disadvantages of longer land lengths include higher melt pressures and higher heat and shear histories. Generally the land length should be as short as possible, without compromising the final product characteristics. Land lengths are commonly short for wire coating and long for tubing, pipe and profile applications.

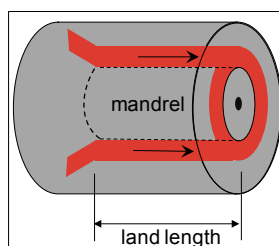


Figure 3.23 Description of a land length for a die and mandrel or pin used for a tubular product

A **gear pump** is incorporated into some extruders between the screw and the die for extrusion of some materials such as wood-flour and polymer mixtures, or to achieve accurate/uniform output from the extruder. It also reduces load on the extruder, enabling higher output and/or less wear on parts, such as thrust bearings. The use of gear pumps raises some safety concerns: the main concern being the creation of high pressures if there is a blockage ahead of the pump, since the pumping action is continued. Appropriate safety measures should be taken to avoid the risk of explosion from excessive pressure, see Strong (1996, p271) for further information. Gear pumps are expensive and are included only when it is not possible to achieve pressure/output stability and low melt temperature by screw design or other means.

Auxiliary equipment is used to pull the material from the extruder die, where the molten polymer is shaped, at an appropriate rate. The shaped molten plastic is quickly cooled in a water-cooled tank to retain the shape. Depending on the extrudate, before the cooling tank there may be vacuum-assisted calibrators and sizing plates to ensure that the roundness of the outside shape is maintained. Calibrators are usually made of brass with peripheral holes or slots in the sleeve wall to allow the surrounding

vacuum to act on the extruded tube/pipe. The inside surface should be sandblasted and may also contain shallow grooves to decrease the surface drag of the extruded tube. The inside diameter of the calibrators (sizing rings) should be between 3% and 15% wider than the outside diameter of a tubular extrudate to compensate for the subsequent shrinkage of the extrudate in the cooling tank, particularly with crystalline polymers such as PEs, PP and nylons. The actual amount of oversize, for a given polymer, depends on several factors, the most important being tube diameter and line speed. An example of this is given for Hytrel (a DuPont thermoplastic polyester elastomer) in DuPont Hytrel extrusion manual.

The extrudate moves over a set of rollers and leaves the cooling tank with an air wipe to remove water droplets present on its surface. The air wipe, therefore ensures that the water is kept in the cooling/quenching tank so that no health and safety issues arise from wet and slippery floors. It also prevents extrudate slippage in the haul-off belt of a caterpillar puller. Therefore, the haul-off pulls the extrudate from the die, through the sizing/cooling to a wind-up roll or cutter. The more accurate the haul-off speed and the caterpillar belt pressure is set, the better the dimensions of the final product will be.

Twin-screw extruders (Figure 3.24) are used where more efficient material compounding and conveying is required. The mechanism of material conveying/transportation, and therefore the output rate, is different in the twin-screw extruders compared with single-screw extruders: in single screw extruders the output rate is, basically, proportional to the inner-surface area of the barrel, whereas in intermeshing twin screw extruders it is proportional to the channel volume because the work is done mainly inside the screw channel. When intermeshed, the relative motion of the flight of one screw inside the channel of the other acts as a paddle and pushes the material from screw to screw and from flight to flight. They are, therefore, more effective for achieving high outputs. They are also better suited to processing certain polymers, e.g., PVC, which is heat sensitive and therefore prone to thermal degradation during processing. There are two types of compounding/mixing that occur in twin screw extruders: dispersive (high-shear mixing) and distributive (low-shear mixing).

Dispersive mixing breaks up large particles and disperses them as smaller particles throughout the melt, appropriate for dispersion of pigments, fillers and liquid additives into polymers, and for blending polymers. Distributive mixing facilitates uniform distribution of additives throughout the melt, and is accomplished by breaking and recombining the melt stream. It is a low shear process and therefore appropriate for the incorporation of fibres and flakes into polymers, where the mechanical degradation of these additives is not desirable.



Figure 3.24 Conveyor elements and kneading disks are assembled on the shafts of twin screws

Most twin screws have constant diameters and, therefore, form a parallel arrangement but some are conical in shape with decreasing screw diameter towards the screw end and form a conical combination. They are also distinguished with respect to their operational modes: intermeshing co-rotating (fully wiping) or counter-rotating (fully calendaring) and non-intermeshing/tangential counter-rotating. Strong (1996, p269) describes differences as, “The self-wiping nature of the co-rotating screws is much more complete than in the counter-rotating, thus in the co-rotating case there is less likelihood that material will become stagnant. Mixing is better in co-rotating systems; therefore, they are popular for compounding where good mixing is essential. In counter-rotating screws the material is brought to the junction of the two screws and builds up a material bank, most of which gets carried forward to the end of the screws, hence pumping is more efficient in counter-rotating screw systems than in co-rotating systems.”

The screws are modular, allowing different elements and screw geometries to be assembled to accomplish required mixing. A conveying element is characterized by the pitch of the flights, and is expressed as a ratio of the pitch length (P) to the screw diameter (or the inner diameter of the barrel) (D) and ranges from 0.5 to 2. The conveying rate increases with P/D . Conveying elements with low P/D values (restrictive elements) or elements with reverse flights are used at the end of the melting zone to work the material, generating higher shear heat to enhance melting.

Other screw elements that are used in twin-screw extruders include kneading and mixing elements. These elements (Figures 3.25 and 3.26) often supplied as individual pieces provide flexibility in configuring a screw. Kneading blocks perform both distributive and dispersive mixing depending on the number of elements in a block of a given length and the widths of the individual elements (disks): higher numbers increase distributive mixing and so do the narrow disks but the wider disks provide better dispersive mixing. These topics are covered in greater detail by Giles et al. 2005 and Chung 2000.

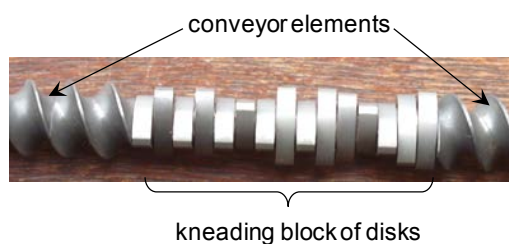


Figure 3.25 Examples of A block of kneading elements placed between conveyor elements

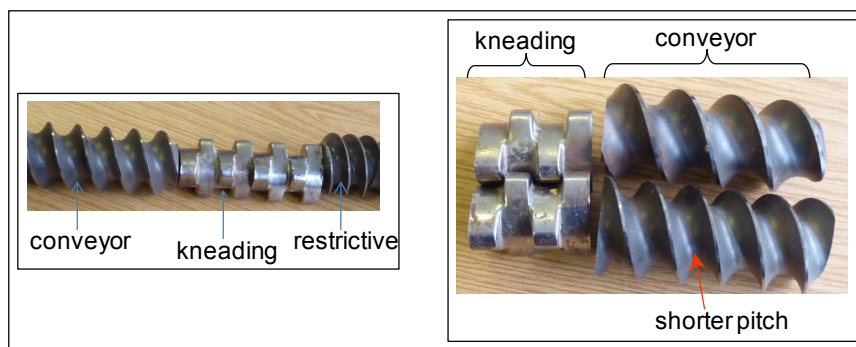


Figure 3.26 Examples of different screw elements

Mixing elements contain cut-outs and are designed to convey material forward in the barrel, while dividing and recombining the melt stream to provide mainly distributive mixing. They can suffer excessive wear, see Figure 3.27, and with some material mixes, e.g., wood flour and a polymer, this may happen in a short period of time.

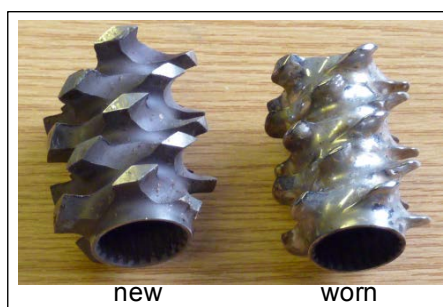


Figure 3.27 Photograph of new and worn mixing elements

Extrusion problems include excessive die swell, melt fracture, shark skin, output fluctuations (causes dimensional variations), thermal degradation (discolouration), poor mixing (streaks on the extrudate surface), bubbles (entrapped gas) and impurities. Gels (small bits of higher-molecular-weight material or overheated/degraded bits of polymer in the die or contamination that reflect and transmit light differently from the rest of the polymer) and specks (under extrusion shear forces some of these particles become elongated, referred to as “fisheyes”) are of particular concern in clear film. Detailed description of these problems and how to avoid them can be found in Strong (1996, p280) and Morton-Jones 1989.

Die swell, a function of flow and shear rates, is described by Strong (1996, p275) as, “die swell is caused by the viscoelastic nature of the polymer melt. Stress relaxation (dissipation of stresses) tends to be slow in viscoelastic materials. The compressive forces that are needed to push the polymer melt through the small die orifices are not completely relieved by the time the polymer exits the die. The polymer therefore expands when it exits the die in response to the relaxation of the residual compressive stresses, thus returning to a shape the material had just before it entered the constrictive land portion of the die. This shape recovery appears as a swelling of the polymer after the die. Die swell can be reduced by extending the land length so that the polymer has sufficient time under the compressed conditions to dissipate the compression forces. Increasing temperature will also reduce die swell as it imparts the energy needed to disentangle the molecules.”

Melt fracture can occur anywhere in an extrudate due to tensile stresses on the melt exceeding the critical shear/tear stress. When it is confined to the surface it can generate a pattern known as **sharkskin**. The sharkskin is perpendicular distortion/roughness – a pattern consisting of lines of ripples running across the flow direction. The pattern is generated by the tearing of the melt on the extrudate surface: the melt passing through the die has a parabolic flow front, i.e., the flow is faster in the centre of the die than it is near the die surfaces. Upon exiting the die the outer layer has to accelerate to maintain the flat flow front that the extrudate now assumes. Accordingly the tension increases at the extrudate surface and if it exceeds its tensile strength, the melt will tear. Tearing relieves the tension but it immediately increases again and, unless corrected, this process gets repeated.

Sharkskin can also be caused by the instability known as “stick-slip” in the die. The type of metal that the die is made from and the level of smoothness of the die surfaces can influence the occurrence of the stick-slip phenomenon, e.g., brass dies have been found to reduce sharkskin and stick-slip instabilities. Figure 3.28 shows an extrudate emerging from the die, exhibiting small magnitudes of die swell, sharkskin and melt fracture. An example of melt fracture is also shown in Figure 3.29 for a plastic-board extrudate.

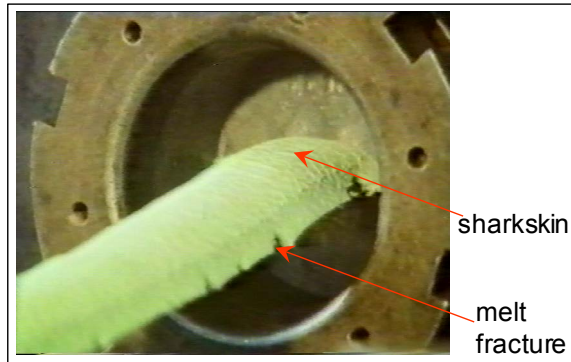


Figure 3.28 Melt-fracture and sharkskin in an extrudate

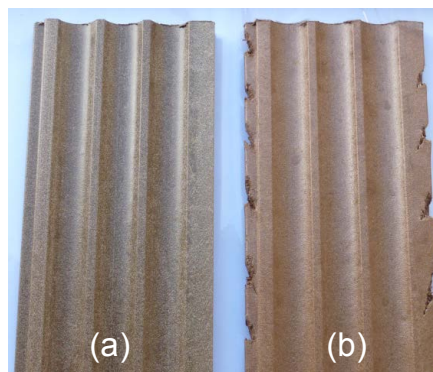


Figure 3.29 Extrudates exhibiting (a) no melt fracture and (b) melt fracture along the edges

Types of extrusion processes include:

- blown (bubble process) film
- cable coating
- cast film
- extrusion + blow moulding
- extrusion + thermoforming
- fibre
- mesh/netting
- profile extrusion
- sheet extrusion
- strand pelletising
- tube or pipe.

Some of these processes are described in more detail below.

3.2.2.1 Blown (bubble process) film

Blown-film (tubular-film) extrusion consists of extrusion of a tube of molten TP and then continuously inflating it to several times its initial diameter (Figure 3.30). Plastic melt is extruded through a ring-shaped tube die (annular gap), usually vertically, to form a thin walled tube. Air is introduced via a hole in the centre of the die to blow up the tube like a balloon. The tube of film is pulled upwards, continually cooling, until it passes through nip rolls where the tube is flattened to create what is known as a ‘lay-flat’ tube of film. During the process, the film is drawn both in radial and longitudinal directions, and the level of drawing (the extent of biaxial molecular orientation) can be controlled by changing the volume of air inside the bubble and by altering the haul off speed.

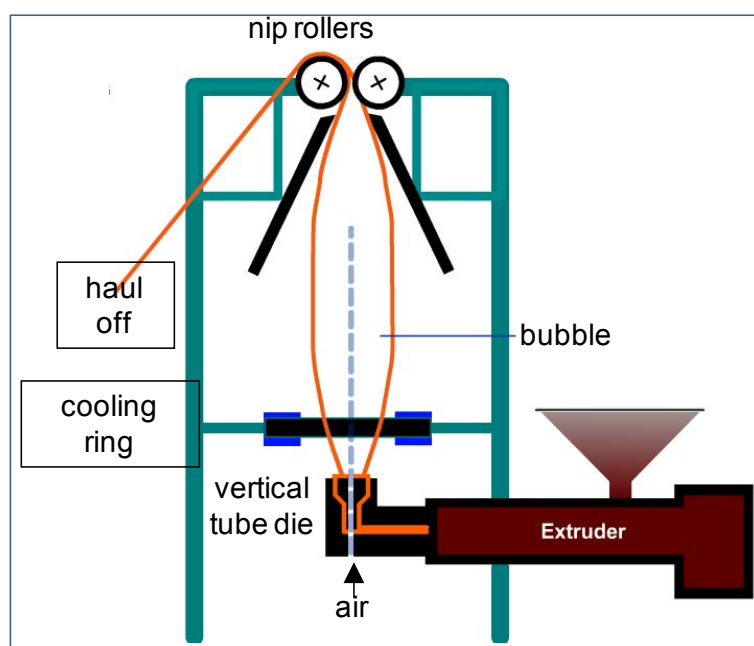


Figure 3.30 Blown-film extrusion setup

Some of the nomenclature for the bubble-process is shown in Figure 3.31.

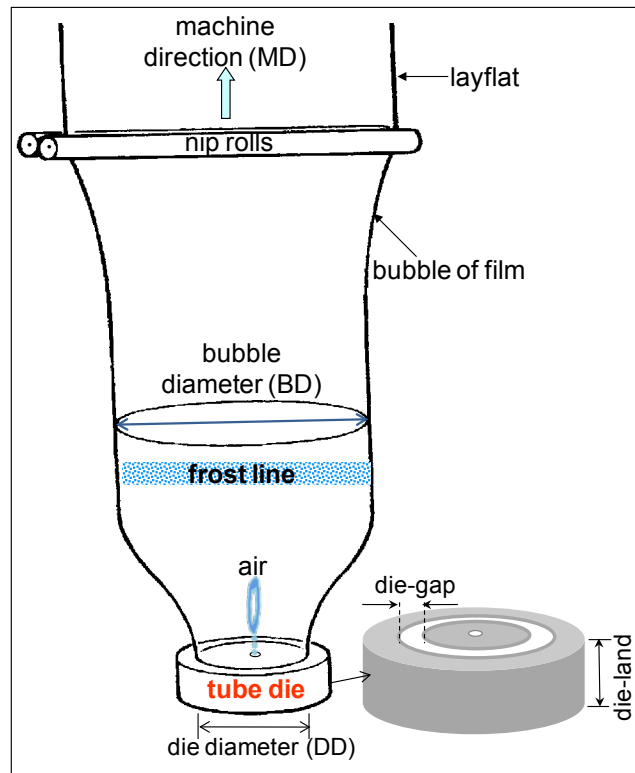


Figure 3.31 Description of a section of bubble process

Typical process parameters include:

- The blow-up ratio (BUR) = (BD) / (DD). It is simply the ratio of the final diameter of the blown tube relative to the die diameter, typically 1.5-4. The outside die diameter can be up to 2.5 m. Increasing the BUR is equivalent to working at a higher frost line height.
- Frost line (FL) height is the height above the die lips where the polymer crystallizes/solidifies. Therefore, as the temperature of the melt increases, the FL rises further up the bubble. At a given melt temperature, a high FL allows a greater relaxation of surface irregularities, resulting in a glossier and less hazy film. However, too high a FL results in slow cooling and promotion of **spherulites**/haze.
- The bubble ratio (BR) = (lay flat) / (DD)
- The ratio of the die-land to die gap varies according to material type or grade. Typically a gap of 0.6 mm for thin films and 1.6 mm for construction films. The die land is a compromise between the length required for a satisfactory melt relaxation and the length still enabling an acceptable pressure drop.
- The draw down ratio (DDR) is the ratio of the final film gauge to the die-gap opening. It controls the molecular orientation in the MD.
- The machine-direction draw ratio (MDDR), another strain related parameter associated with the film blowing process, is the ratio of the take up speed relative to the extrudate speed at the die.

The shrinkage of a blown film is affected by the deformation of the melt in the shaping die as well as by the blow-up and the take-off conditions after it emerges from the die. It can be much greater during the formation of the bubble than in the die, particularly if the blow-up ratio is high. Another problem in blown films is the entrapped air between film layers and rollers – this may cause film scratching or wrinkling, or processing problems when winding up the film due to reduced friction. One of the solutions is to use vacuum to remove entrapped air.

Large amounts of blown film are used as geomembranes (Figure 3.32). The most common polymers used for the production of membranes for ponds, lakes and lagoons are HDPE, LDPE, PP and PVC. Figure 3.33 shows an alternative application for these films – a wonderful sight to behold for sure!



Figure 3.32 A lake liner: polyester multi-split fibre gauze/scrim sandwiched between two LDPE films. (photo: Keytec Environmental Ltd)



Figure 3.33 Beauties of Ballyclare, N. Ireland

3.2.2.2 Cable coating

In **cable/wire coating** bare wire or a bundle of wires that are previously insulated is fed perpendicular to the melt extrusion direction through a mandrel that splits the melt into two. The extruded polymer melt and the wire come in contact within the die, which is a cross-head die.

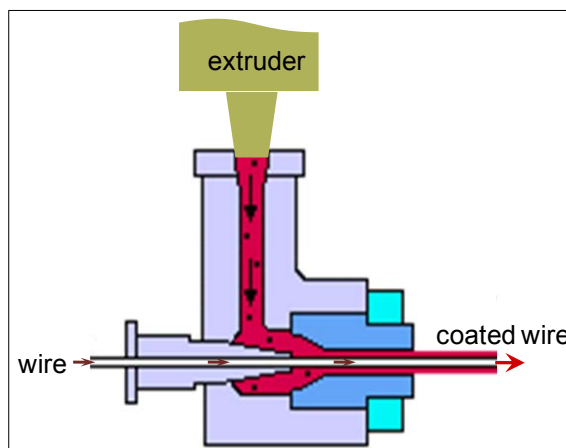


Figure 3.34 Crosshead extrusion arrangement for wire coating

3.2.2.3 Cast film/sheet extrusion

In **cast film extrusion**, the melt is extruded from a slit die onto a chill roll to produce thin film, and in **sheet extrusion**, to produce precision thin sheet/film, the extrudate passes over and through a series of rolls (Figures 3.35 and 3.36).

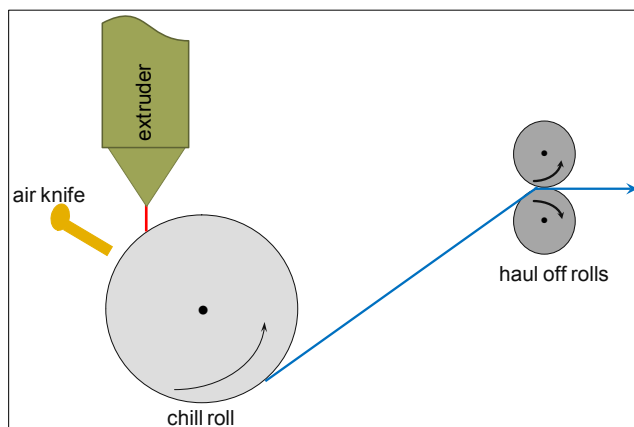


Figure 3.35 Illustration of cast-film process

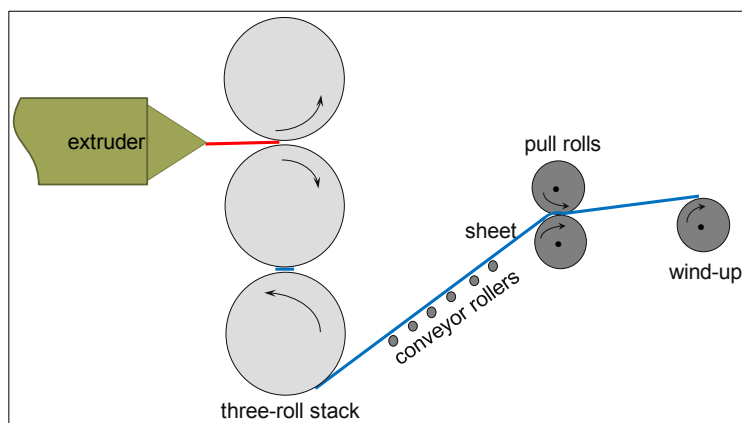


Figure 3.36 Illustration of sheet extrusion

Sheet extrusion can be set up on-line with thermoforming equipment for the production of various packaging products, particularly for the food industry. Such production lines also include labelling and/or printing facilities, and facilities for the treatment of the plastic surfaces for printability. These include corona-discharge and flame treatment processes that change the polarity and/or the chemistry of the polymer surfaces and hence enhance ink adhesion. The products include various tubs for yoghurt, coleslaw, margarine, and cups for hot and cold beverages. Many thermoplastics can be thermoformed; they include PS, PP, PET, PVC and ABS. In food packaging ethylene-vinyl alcohol (EVAL) is included in multilayer co-extruded films for its superior barrier properties.

Co-extrusions are commonly used to provide precise properties for specific applications. Multi head extruders feed into the extrusion die with the differing materials, e.g., a 5-layer sheet may consist of inner layer-tie layer-barrier layer-tie layer-outer layer construction. The microstructure of some of the polymers will determine their suitability for certain applications, e.g., amorphous PET sheets are easily thermoformed into containers with excellent clarity but are not sufficiently rigid as packaging trays for ready meals to be heated. Whereas crystalline PET, contain nucleating agents, crystallise readily under heat during thermoforming. Crystallinity renders the tray rigid and therefore prevents it from deformation when being heated and served.

Extrusion-thermoforming produces a significant quantity of scrap (it can vary from 15 to 50% of the original sheet depending on the shape of the blanks stamped out for thermoforming). Almost all the skeletal (scrap) can be reused. The chopped and regranulated skeletal is mainly used again (mixed with fresh granules) in the same production. However if this is not acceptable, for reasons of colour matching or contamination, then it can be used as feed stock for other types of productions.

3.2.2.4 Mesh extrusion

Mesh/netting extrusion can be produced by extrusion of strands through two concentric-ring dies with slots that can be rotated or oscillated with respect to one another in the modes shown in Figure 3.37 for “Netlon” products. During extrusion, when the slots of the inner and outer rings are in register the knots of the mesh are produced, and when they are out of register the strands of the mesh are produced.

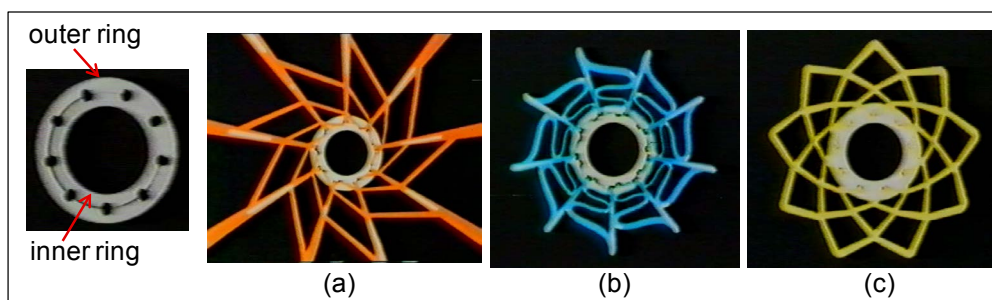


Figure 3.37 “Netlon” process alternatives using a concentric-ring die: mesh with (a) inner ring rotating, (b) outer ring stationary and inner ring oscillated, and (c) rings counter rotating

Applications of Netlon products include delicate meshes for packing fruit and vegetables, garden netting, protective sleeving for machined components, and heavy duty geogrid for civil engineering applications, e.g., soil stabilisation.

3.2.2.5 Profile extrusion

Profile extrusion produces continuous lengths of plastics of a constant cross-sectional shape and size. Figure 3.38 shows examples of PVC profile extrudates: the interior trimmings and the skirting boards include an integral flexible edge and/or a hinge that are made of plasticised PVC and produced by piggy-backing a small extruder onto the main extruder. It may not be strictly appropriate to classify structured-PC panels as profile extrusions, they are wide panels with a multitude of cells/webs in their cross section to provide thickness and, therefore, rigidity, but still render them light in weight. They come in different colours or colour combinations in order to either match the colour of the rest of the roof or to control transmission of sunlight and therefore the intensity of light and heat in the dwelling. Incorporation of 1% aluminium flakes into PC (twin screw mixing/extrusion) reduces the solar heat gain through the roof by up to 50%, but still providing a desirable level of roof-light. Some of the panels would have a membrane of UV barrier laminated on, to absorb harmful UV radiation.

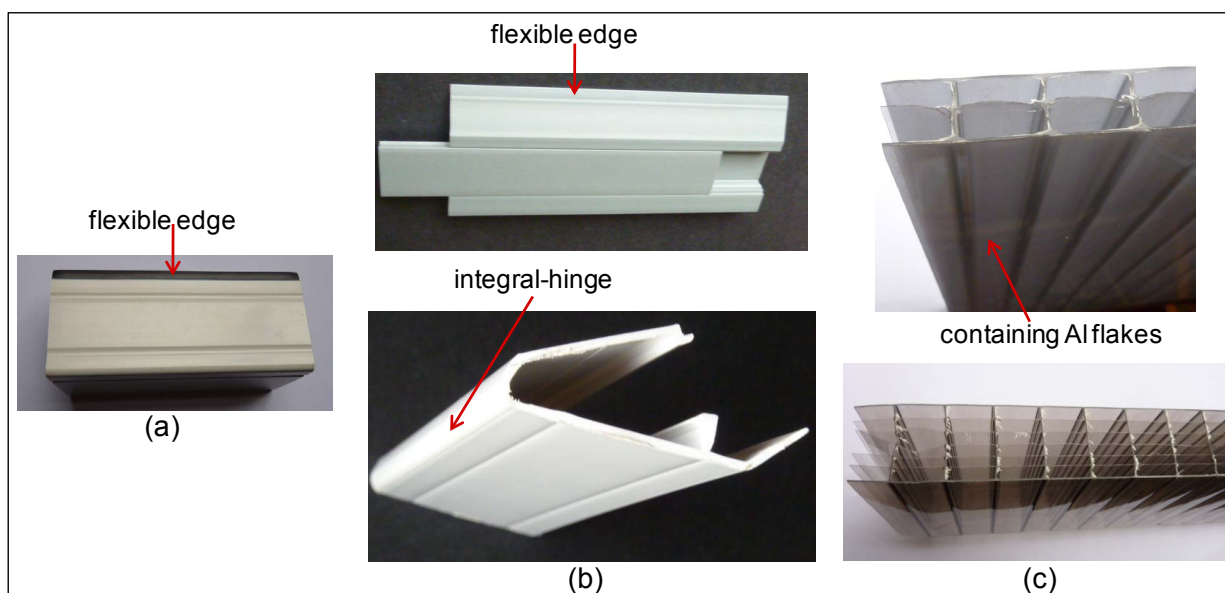


Figure 3.38 Sections of various extruded and co-extruded profiles: (a) U-PVC bus/coach interior trimming (b) a two-part and integral-hinge U-PVC skirting board for homes, caravans and auto-homes, and (c) structured-PC roofing for conservatories/gazebos

3.2.2.6 Fibre spinning

Production of **synthetic fibres** that involve the use of extruders is known as melt spinning. This term comes from the spinning (a process of overlapping and twisting short fibres) of staples of natural fibres into long threads. In melt spinning a die, known as a spinneret, a flat plate containing hundreds of small holes of a fraction of a millimetre in diameter is used. The spinneret is positioned vertically downwards and the extruded filaments/fibres are cooled by air, drawn by passing over rollers or “godets” with increasing rotational speeds to stretch the fibres and introduce molecular orientation (increasing tensile strength). A bundle of fibres, tow, can be combined with a slight twist to produce fibre yarns.

3.2.2.7 Strand pelletising

Strand pelletising entails extrusion of melt through a strand die (Figure 3.39), passing strands through a water bath, removing water from the strands (by air blowing/vacuum) after the cooling tank/trough and chopping them into pellets of a given length in a cutter. There are different types of pelletising systems: as well as pelletising using strands, many of these are done straight on the die face, including the die face-under water method for the production of micro-pellets mainly for polyolefins but can be used for almost any polymer.

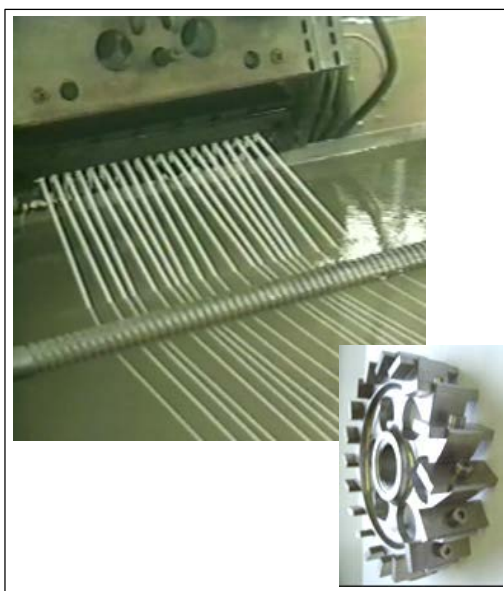


Figure 3.39 Photographs of the extrusion of strands and a cutter for pelletising

3.2.2.8 Pipe/tube extrusion

Pipe and tube extrusion entails the use of an annular slot die arrangement with an appropriate diameter and gap thickness. The annular die and mandrel/pin diameters and lengths are selected depending on the final size requirement and the type of polymer extruded. Die and pin should be accurately centralised to achieve a uniform extrudate cross-section. Polymers differ in their drawdown ratios (die drawdown ratio = (die diameter) / (final tube outside diameter); pin drawdown ratio = (pin diameter) / (final tube inside diameter)), e.g., nylons suffer greater levels of drawdown than polyolefins.

Certain applications require multilayered or striped tubes that require co-extrusion by employing a number of extruders simultaneously extruding into a single die. This enables the production of tubes/pipes with a combination of characteristics/properties, such as mechanical strength and rigidity, moisture/chemical resistance, barrier to various gases/water vapour, surface gloss, abrasion resistance/friction, transparency, etc. However, it is important to note that not all the polymers can be co-extruded. These include polymers with significantly different melting properties, e.g., PC processes at approximately 280 °C and would therefore cause degradation of PVC, which processes at 170 °C, when the two melts combine. PVC and acetals are also incompatible and are mutually destructive/explosive.

Recent developments/news on the subject of pipe and profile extrusion can be found in the pipe and profile extrusion magazine: <http://cde.cerosmedia.com/1D4cfe0f7a76b48995.cde>.

Corrugated pipes are a successful route to the production of large and rigid pipes that are obviously much lighter than the equivalent thickness of solid-walled pipes and more practical/flexible for laying. They are produced by use of a die/mandrel system that extrudes an inner smooth liner and an outer layer that gets corrugated by an on-line former. Figure 3.40 shows a corrugated pipe into which slots are cut for use in under-soil drainage.

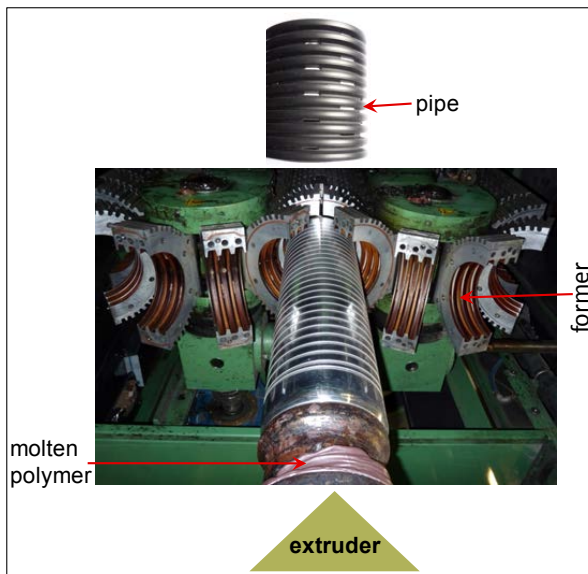


Figure 3.40 Photographs of an extrusion line, showing the corrugator/former and a length of a corrugated pipe

3.2.3 Blow moulding

This is a second stage process after extrusion or injection moulding. Some products require mechanical stretching of preforms prior to blowing with compressed air. The basic blow moulding steps beyond the processes of extrusion/injection moulding are illustrated in Figure 3.41. Injection-blow moulding involves injection moulding of the parison, which is then transferred to another machine for blow moulding. This process is suitable for small mouldings with intricate neck detail. An animation of the overall process can be seen in the BPF, *Plastipedia* web site:

<http://www.bpf.co.uk/Data/Image/Extrusion%20Blow%20Moulding.swf> or

www.bpf.co.uk/bpfindustry/process_plastics.cfm.

PP, PE, PET, PVC are used to produce bottles, jars, containers, water drums, fuel tanks for vehicles, ducting, etc. The moulds can be made from aluminium rather than tool steel, which is usually used for injection moulding; the pressures associated with blow moulding are much lower than in injection moulding, therefore, the possibility of mould deformation is reduced. Furthermore the mould wear is less likely during blow moulding; the material does not flow along the mould surface as occurs in injection moulding causing friction/wear. The levels of shrinkage associated with high temperature melt in injection moulding contribute to wear as well.

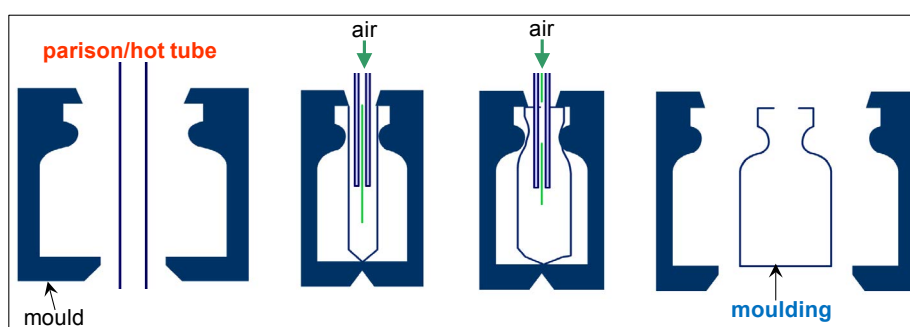


Figure 3.41 Illustration of blow-moulding process

The process produces flashing that needs to be trimmed off. Flash (pinch off scrap) on a moulding of a 2-litre HDPE milk bottle is shown in (Figure 3.42). The figure also highlights other features of the moulding

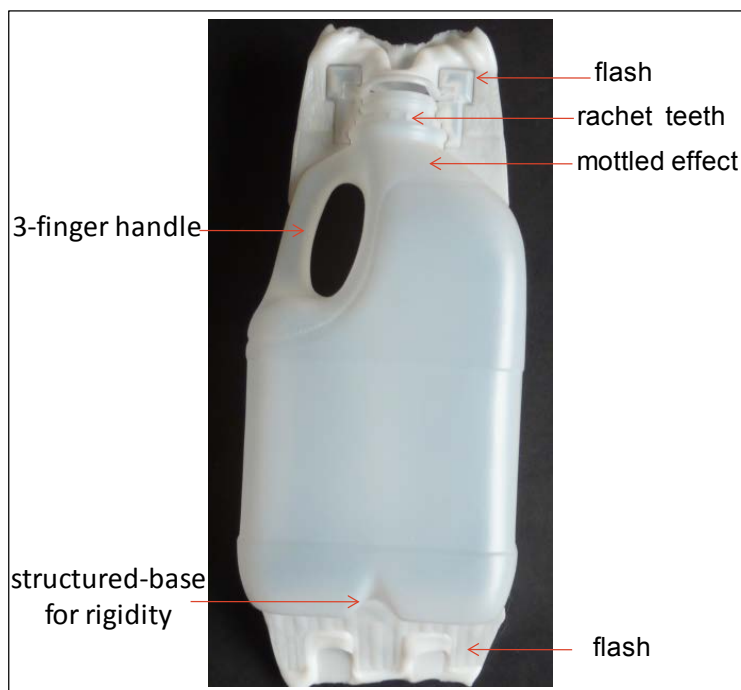


Figure 3.42 Photograph of milk-bottle moulding as it comes out of mould

Plastics have come to replace glass in many bottle products; not least because they offer advantages in terms of lower weight and material toughness. Depending on the application, there are, however, other considerations that need to be met. For example, the bottles for soft drinks should have:

- high transparency (for appeal)
- impermeability to gases (fizzy drinks must not lose CO_2 pressure too quickly)
- creep resistance (the container must not lose its shape on the shelf).

In order to meet these requirements in PET bottles, the following production steps are recommended (Newey & Weaver 1990, p285):

1. PET parison is rendered amorphous by injection moulding and rapid cooling in the mould to below T_g ($\approx 70^\circ\text{C}$)
2. the parison is heated to a temperature sufficiently above its $T_g \approx 130^\circ\text{C}$ to facilitate plastic flow but not so high that extensive crystallisation occurs
3. the parison is mechanically stretched in length, and then
4. blow-moulded into shape.

Mechanical stretching with a rod and blow moulding encourages some crystallization, about 15-20%, and biaxial molecular orientation. The crystallites are too small and not properly formed spherulites to affect clarity of the bottle, but they provide sufficient creep resistance and impermeability to CO_2 .

3.2.4 Thermoforming/ vacuum forming

The processes of thermoforming and/or vacuum forming are often referred to interchangeably. In thermoforming, however, a greater use is made of air pressure and plug assisted forming of the softened sheet. Thermoforming is often automated and thus faster cycle times are achieved than in vacuum forming, it uses plastic sheeting on rolls in a continuous operation rather than sheet blanks that are employed in vacuum forming of a discrete batch process. These processes and the differences between them are explained in detail by Strong 1996.

The materials most generally used in descending order of processing ease are PS, ABS, PVC, acrylics, PC, HDPE, PP and LDPE. The process of vacuum forming (Figure 3.43) is straightforward. A sheet blank is clamped over the vacuum box (thus sealing off the box) beneath a heater, which is often a retractable one. The heater may consist of infra-red elements mounted within an aluminium reflector plate, coiled ni-chrome resistance wire, metal rod heaters, hot air ovens, ceramic elements, or quartz tube. Once the blank becomes sufficiently pliable and begins to sag (the sag point), it is then sucked down and held tight into the mould cavity by the application of vacuum for shaping. After the part has sufficiently cooled, it is removed from the mould. Figure 3.43 shows a blank which is partially sucked into the vacuum box. In this process the mould is a female/cavity mould.

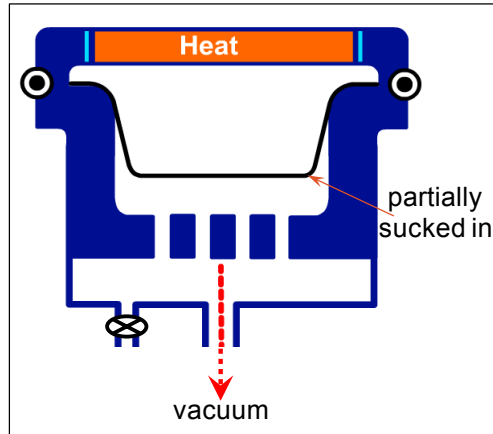


Figure 3.43 Illustration of vacuum forming

Alternatively, the heated blank is mechanically moved onto a male mould and draped over it and, simultaneously, vacuum is applied through the vent holes in the mould to force the sheet tightly onto the contours of the mould and hold it fast to give it the final shape. See Strong (1996, p378) for detailed description. In all these processes the forming operation is followed by cooling, often with air, and by a secondary operation to trim off any excess material from the moulding to obtain the finished product.

The process of stretching the sheet over the form or suction into a female mould causes thinning of the sheet, especially along the sides of deep drawn parts. The extent of draw depth is described by a parameter known as the draw ratio, which can be expressed in different ways:

draw ratio = (sheet thickness) / (part thickness);

draw ratio = (surface area of the formed moulding or part) / [(surface area of the blank) (or the footprint of the part)].

A real draw ratio is a measure of the biaxial orientation that the heated blank undergoes during forming. A linear draw ratio can be determined by scribing a line of known length onto the blank, the draw ratio then becomes the ratio of the length of the scribed line on the formed moulding to that of the scribed line on the sheet blank used to form the product. It is a measure of the overall uniaxial elongation capacity the softened plastic must have for the forming process.

The depth to which the material is to be drawn is important in determining the best technique to be used: for moderately deep draws (draw ratios less than 2:1), a basic vacuum female forming can be used. For products that require deep draw ratios, greater than 2:1, pre-stretched male forming or plug-assisted female forming is suggested to obtain the most uniform material distribution.

Pre-stretch is used to achieve “even” wall thickness. A small “bubble” is blown and the male mould is then raised into the pre-stretched sheet.

Plug assist is used for a deep draw product: a “plug” is used to push the material into the female mould during the forming process.

The BPF website (www.bpf.co.uk/bpfindustry/process_plastics.cfm) shows animations of these techniques as a stand-alone operation as well as a continuous operation that starts with feeding of the sheet from a roll onto a processing line of heating-forming-trimming-stacking, and finishes with winding of waste off-cuts (skeletal) onto a roll.

Vacuum formed products include: PS – packaging trays, egg boxes, refrigerator liners and food tubs/pots; PVC – packaging and containers; and ABS – boats, caravans, vehicle body parts, shower bases and surf boards. The moulds can be made of wood, but for extended production runs reinforced epoxy resin or aluminium is preferred.

3.2.5 Rotational moulding

The Rotational Moulding process involves the following operations (Figure 3.44):

Charging mould – a pre-determined amount of pre-compounded polymer powder is placed in the mould; the mould is closed, locked and moved into the oven.

Heating and fusion – once inside the oven, the mould is rotated around two axes. The speed of rotation is relatively slow, less than 20 rev/min. The ovens are usually air circulating ovens with gas (propane) burners and the moulds are therefore heated mainly by convection. During the process, the plastic powder/pellets remain in the bottom of the cavity of the rotating mould. As the mould becomes hotter the powder adheres to the passing mould surface of the rotating mould, begins to melt and sinter/fuse together. Mould surfaces can be insulated (see Figure 3.45) and, therefore, left cooler during the heating cycle in order to either achieve a section with lower wall thickness or a section that requires no coverage with plastic powder to leave the product completely open in that section as in most agricultural water containers and feeders, wheel barrows and trolleys but in fact nearly all products require some sort of opening in their structure. Shielding to achieve lower wall thicknesses and the openings, as in a wheel barrow (mould is shown in the figure), are achieved by a layer of insulation such as rock wool placed inside the relevant mould parts (as in the lid of the wheel barrow mould).

When the melt has been consolidated to the desired level, the mould is **cooled** either by air, water or a combination of both. The polymer solidifies to the desired shape.

De-moulding and unloading – when the polymer has cooled sufficiently to retain its shape and be easily handled, the mould is opened and the product removed. At this point powder can once again be placed in the mould and the cycle repeated.

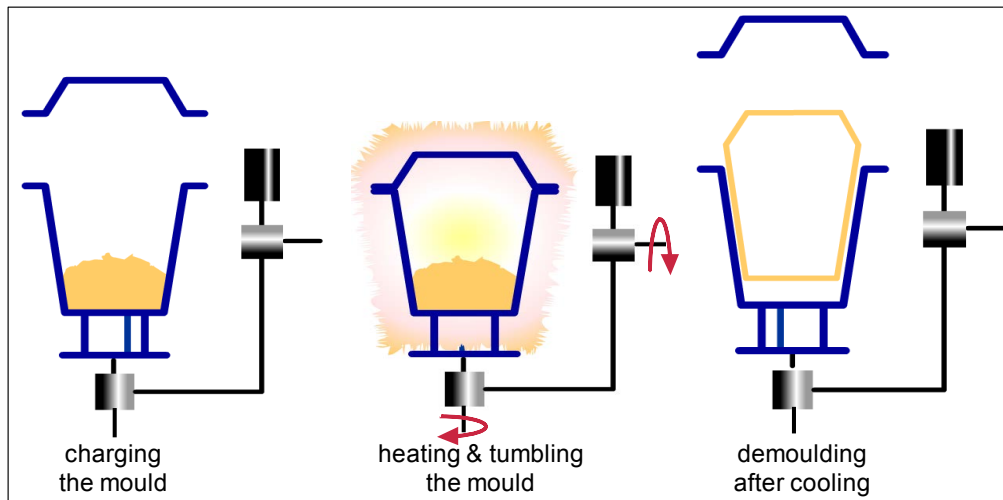


Figure 3.44 Illustration of rotational moulding

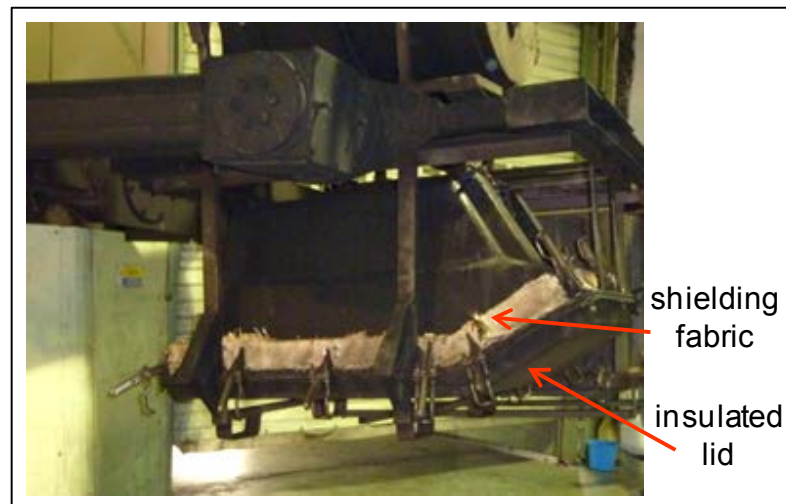


Figure 3.45 Section of a mould covered with insulation fabric

The products often require **secondary operations**, such as trimming by a router (much safer than using a Stanley knife) and vacuum lifting of the trimmed swarf for recycling; glossing/sheening the surface of products with a short passing of naked flame over it (torching/flaming); decorating/labelling; joining together the sections of a product by hot-bar, hot-gas, or ultrasonic welding, as well as many other mechanical assembly work that may require drilling, etc.

The rotational moulding process enables the production of large hollow products, which are stress-free and contain no weld-lines, using comparatively low-cost moulds. Materials commonly used are polyethylenes (LDPE, LLDPE, MDPE, and HDPE), PP, ethylene vinyl acetate and PVC. For some applications cross-linked PE is also used. Typical products include agricultural products (e.g., feeders, drinking bowls/troughs, wheel barrows, calf hutches and chicken coops (Figure 3.46)); oil and water tanks; rainwater-harvesting tanks; diesel fuel and hydraulic tanks; toys and playground items; traffic cones, and marine products(e.g., canoes and kayaks, navigation buoys and mussel floats).



Figure 3.46 Rotational moulded chicken coops (courtesy of JFC Manufacturing Ltd.)

Rotational moulding machines are specified by their swing diameter (the envelope in which rotation should occur freely when operating in heating (oven) and cooling (cooler) chambers/stations). There are two types of rotational moulder:

- 1) Drop (offset) arm/spindle (Figure 3.47-a): suitable for medium to large mouldings
- 2) Straight arm/spindle (Figure 3.47-b): suitable for multiple small mouldings

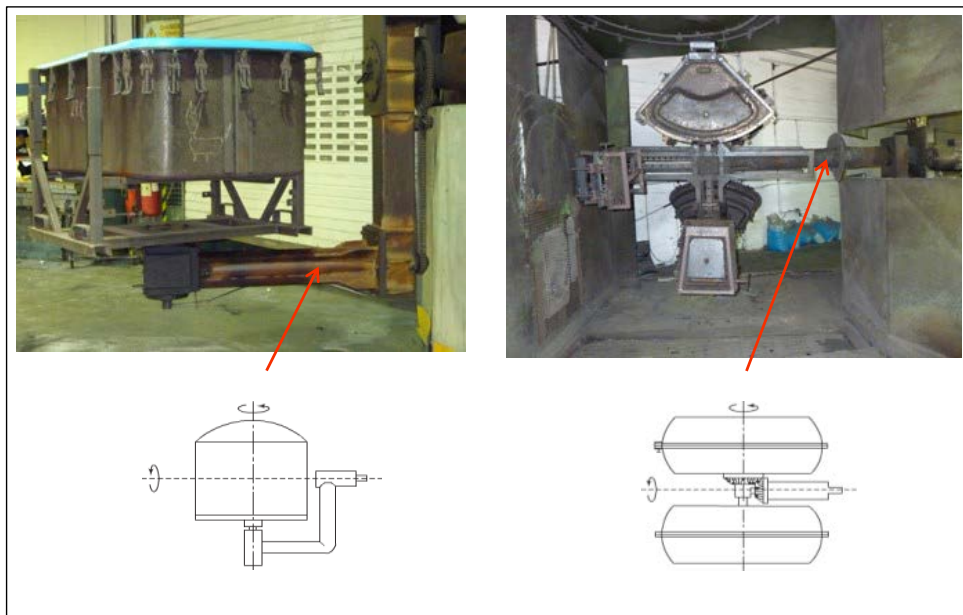


Figure 3.47 Rotational moulding machines with (a) drop arm and (b) straight arm

Most modern rotational moulding machines involve complete biaxial rotations about two perpendicular axes and the machines are classified as shuttle machines or carousel machines, depending on their modes of operation and lay out of the stations. The **shuttle machines** consist of two mould carriages, each with a single arm moulder, operating on rectilinear tracks/rails. The system includes one oven and two cooling/service stations. During the operation, the carriage/mould in the oven is moved into its own cooling/service area on straight rails, and simultaneously the other mould enters into the oven from the other cooling/service area. The use of dual-carriages improves efficiency, since the oven is always occupied by a mould while the other mould is being cooled, de-moulded and re-charged.

The **carousel machines** rotate in and out of the oven, the cooler and the service area. As long as there are extra stations available, the machine can be fitted by up to six arms of the same type or different types. Note that in a service area, the finished product is removed from the mould and then the mould is charged with fresh plastic powder ready for the next run.

The carousel machines come in two different models, fixed and independent. On a fixed machine three or four arms move in succession into and out of various stations. The moulds spend the same length of time in each operation chamber and, therefore, the fixed machines should work with the same moulds. The independent carousel machines can accommodate more arms that can be fitted with different types of moulds. Of course the arms cannot rotate past each other but they can move separately from each other and spend different lengths of times in different stations. This allows moulds of different shapes and sizes charged with different materials, with different heating and thickness requirements, to be processed. Detailed coverage of various rotational moulding machines/processes is given by Crawford & Kearns (2003).

Temperature measurement is critical for **monitoring the process**: one can establish various temperature-cycle time profiles (Crawford & Kearns 2003, p72) representing inside the oven, outer-surface of the mould, plastic and the air inside the mould with a data logger attached to the frame of the moulds and harnessed with a suitable number of the thermocouples

with sufficient length of loose thermocouple wiring to accommodate rotation of the frame. Thermocouple wires for inside the mould cavity are inserted through a filter (akin to a cigarette filter) placed inside a PTFE sleeve. The filter stops the polymer powder from falling out but allows air venting out. In the oven when the tool begins to rotate initially the temperature fluctuates ($\pm 40\text{ }^{\circ}\text{C}$) but it soon stabilises.

Processing with PE, the air temperature inside the mould reaches approximately $200\text{ }^{\circ}\text{C}$ when the air temperature inside the oven stabilises at a set temperature of $310\text{ }^{\circ}\text{C}$. The tool stays rotating in the oven for approximately 10 min, then comes out to the cooling station, continues to rotate for a further 10 min for the temperature to fall down to below $100\text{ }^{\circ}\text{C}$. The temperature-time curve (Figure 3.48) for the air temperature inside the mould cavity shows that temperature climbs up to Point A as a function of the oven temperature, where the melting begins and the smallest particles begin to adhere to the tool/mould surface. The heat is needed for melting and, therefore, the internal-air temperature increases only very slowly between Points A and B. When all the powder has melted at Point B, the internal-air temperature begins to increase again rapidly.

The sintering process, where the plastic particles on the mould surface fuse together to produce a smooth homogeneous layer, begins at Point B, reaches its optimum state at Point C and continues through into the cooling cycle until the start of crystallisation at Point D. Note that, once the tool comes out of the oven into the sintering/cooling chamber, there is still a temperature overshoot within the mould and then the temperature inside the cavity begins to decrease. The rate of fall in temperature slows down at Point D because of the contribution of the heat associated with the exothermic solidification/crystallisation process. Following complete solidification, Point E, the internal air temperature continues to fall at its normal rate. At Point F, the plastic shrinks and detaches itself from the tool face, which is accentuated by the release agent (usually silicone solution wiped on the mould), leaving a gap between the part and the tool surface. This layer of air (space) between the tool inner face and the outer face of the moulding acts as insulation and decelerates the cooling inside the tool cavity.

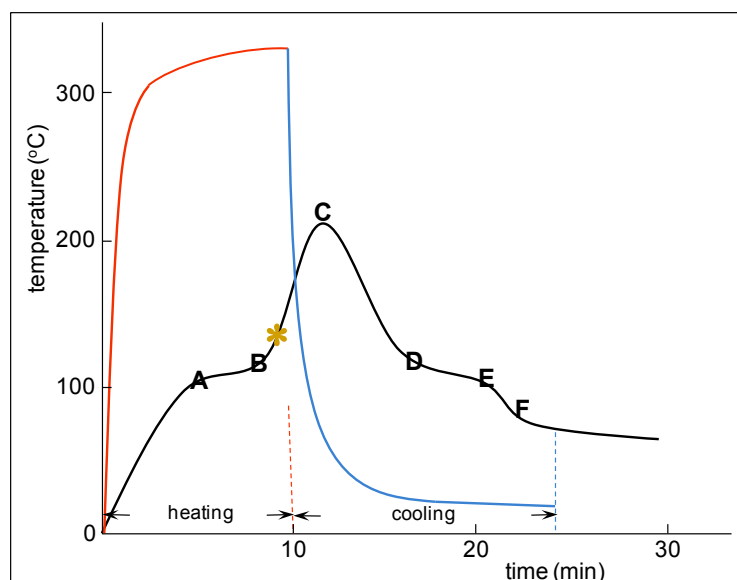


Figure 3.48 Illustration of temperature vs. time curve for a rotational moulding cycle: (— & —) oven temperature, and (—) internal-air temperature of the mould

Developments in rotational moulding seem to concentrate on multilayer structures with different types of polymers for high barrier applications, e.g., for fuel tanks, or with layers that contain fibres/fillers/nano material (e.g., nano clay), or with biodegradable and biosustainable (e.g., polylactic acid polymer) materials, skin-foam layers, conductive materials such as Cu or Al powder and the use of micropellets.

A **multi layer rotational moulding** may consist of three layers: e.g., a layer of polyethylene, with a second layer of fibre-reinforced polyethylene or foamed polyethylene and another layer of polyethylene. The multiwall or foamed mouldings are normally produced by a **multi-charge process**: with the first charge of the plastic powder, which forms the outer layer of the part, being charged into the mould in the usual way. The subsequent charges of powder/micropellets are added during the heating cycle when the temperature reaches approximately the point shown by the asterisk on the graph (Figure 3.48), and the full heating/cooling cycle is completed after the addition of the final charge.

The **single-charge method** involves placement of a plastic blend of lower and higher temperature melting point materials, or a blend of smaller and larger powder/pellet particle sizes in the mould. The principle is that the lower melting point material or smaller particles melt first and adhere/sinter onto the inner mould surface forming the outer skin/layer of the product.

The foamed rotational moulded products could be in the form of containers with walls consisting of a solid outer skin and an inner foam layer or solid inner and outer skins with foam core, or tubs and box sections (Figure 3.49) with solid outer walls completely filled with foam. I-FOAM (Insulation Foam) Ltd. produce PE pellets that contain expansion foaming agent with, apparently, up to of 40 times expansion ratios. The moulding process is a one shot method, allowing loading of all raw materials at the same time and therefore producing wholly integrated foamed products with excellent bonding between the skin and the foam.

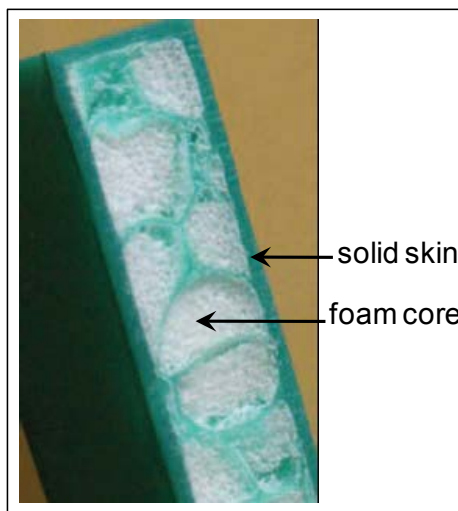


Figure 3.49 PE box section insulated with double-layer PE foam pellets (source: I-FOAM)

Micropellets are a useful alternative to powder plastic for some applications: in rotational moulding powder covers flat uncomplicated surfaces well but for complex parts micropellets give better coverage. Micropellets wash out and do not remain put on flat surfaces.

Micropellets/microgranules are obtained by fast underwater granulation: the process involves extrusion of hot strands into water (submerged) and cutting at the die face produces instantly spherical microgranules (spheres form because of the energetic tendency of the material to minimise the surface area and because of the presence of hydrostatic pressure).

One of the obvious concerns in incorporating engineering fibres such as glass fibre, natural plant fibres or nanoparticles into polymers for rotational moulding is the possibility of distortion of the finished parts, for example the walls of a box-shaped container bowing inwards. Such distortions to the mouldings are a consequence of the differences in the coefficient of thermal expansion (CTE) values for the polymer and the additives, which may result in the generation of un-balanced internal residual stresses.

When selecting polymers for rotational moulding, it is important to select grades that process easily and yield the required mechanical and physical/chemical properties, e.g., when selecting PE for oil-tank production, the important properties would be MFI (approximately a value of 4), flexural modulus and environmental-stress-cracking resistance (ESCR).

Rotational moulded products with mottled look or shot-blast or shot-peened finishes can be achieved by shot blasting the tool/mould surface with grit or very tiny billiards, often shot-blasted moulds are Teflon coated to facilitate mould release. Teflon coating involves applying/spraying a PTFE primer first. The primer contains colour so that the area covered becomes visible, and also once the PTFE coating is completed, the colour helps in spotting any subsequent damage to the coating. The primer is baked on at 110 °C, then a second ingredient is applied, then the clear PTFE solution is applied and baked at 380 °C.

3.3 Processing and forming thermosetting polymers

Thermosetting polymers/thermosets (TS) consist of a resin (linear polymer with pendant **functional groups** such as hydroxyl (OH), carboxyl (COOH), amino (NH₂) groups or containing double bonds) + **cross-linking agent** + catalyst + heat (or cold curing with a catalyst activator). Typical TS polymers include polyesters, alkyds, amino resins, epoxy resins and polyurethanes. TSs contain cross-links in their structure and in general offer greater resistance to temperature and creep cf. TPs, however, they suffer from low impact resistance.

Most thermosets are available in two forms: **resins** or as **moulding compounds**.

The resins may be used in neat form, e.g., in encapsulation processes, or as matrix in polymer-matrix composites. Moulding compounds in the forms of dough moulding compounds (DMC) and sheet moulding compounds (SMC) are a mixture of TS resins with both fillers and fibre reinforcements. In SMC longer glass strands are used. Low viscosity formulations, known as low pressure moulding compound (LPMC), are suitable for low-cost tools/moulds.

Polyester resins (unsaturated) are produced by condensation polymerisation of a polyfunctional acid with a polyfunctional alcohol.

Maleic acid (HOOC – HC = CH – COOH) contains 4 functional groups. The carboxyl groups undergo esterification (condensation) reaction with a di-alcohol (e.g., ethylene glycol), and the double bonds can enable addition reactions.



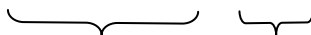
Unsaturated (i.e., containing unreacted double bonds) polyester resins are usually supplied as a solution in styrene, which acts as a solvent and also as the cross-linking agent (by reaction through the double bonds).



Therefore, unsaturated linear polyester + styrene + an activated catalyst → a cross-linked polymer.

Polyester resins are usually used with woven glass-fibre cloth or mats of chopped glass-fibre strands to produce strong laminates. DMC and SMC containing unsaturated polyester resins are widely used. Polyester DMC is of a putty-like consistency and has a very low viscosity at moulding temperatures and, therefore, can be compression moulded using low pressures. Their relatively high temperature resistance and desirable electrical properties make it attractive for the electrical industry.

Amino resins such as urea formaldehyde (UF)



and **melamine formaldehyde (MF)**, produced from melamine (Figure 3.50) and formaldehyde, which are available as neat resins, and also as moulding powders.

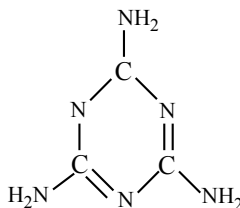


Figure 3.50 Melamine (a cyclic amino compound)

UF resins are used as adhesives for plywood and chipboard, to impart crease resistance to fabrics (it is a clear resin), and to improve the wet strength of paper. The use of melamine-formaldehyde polymers include kitchen and picnic ware (Figure 3.51).



Figure 3.51 Le Cadeaux melamine fruit-motif assorted plates

Phenol-formaldehyde (PF) resins were the first man-made plastics to be commercially used. The PF prepolymers are novolaks and resols. The novolaks are prepared using excess phenol (molar ratio of 5:4) under acidic conditions. A resol is formed by using excess formaldehyde (phenol to formaldehyde molar ratio up to 1: 2.5), normally under basic (alkaline) conditions.

Early applications were in the electrical industry. PF impregnated paper and cotton fabric laminates find application as very durable gear wheels (e.g., Tufnol products). PF and MF exhibit good flame resistance. The PF (an inherently fire resistant material with low smoke emission, like PVC) now replaces polyester in normally polyester-based products. London Transport specifies phenolic glass-fibre reinforced plastic (GRP) for use in underground rolling stock and as cladding in station escalator wells. Serious concerns were raised in the London Underground after the 1987 King's Cross Station fire regarding health and safety. Similarly, the Dusseldorf airport fire in 1999, which claimed 16 lives, focused attention on the type of materials used in public places. The victims died mainly as a result of suffocation and poisoning from the thick smoke emitted by the burning material. Other uses of PF include the weapons and equipment storage boxes on British naval ships, where, following the Falklands conflict, fire retardancy and low smoke emission were found to be essential.

Processing methods for thermosets involve the reactive processing of prepolymer/monomers with a catalyst or a curing agent as part of the shaping operation, and include:

- compression/transfer moulding
- injection moulding
- reaction injection moulding (RIM)
- vacuum infusion
- resin/foam dispensing
- autoclave and resin transfer moulding
- pultrusion
- SMC/DMC moulding
- filament winding.

3.3.1 Compression moulding

The process is suitable for moulding powders or DMC/SMC. The mould is placed in a hydraulic press and is heated (160-200 °C), being thermally insulated from the platens (Figure 3.52). The required amount of prepolymer (mixed with catalyst

or curing agent) is placed into the open mould; it is then closed and pressure is applied to cause the material to flow around the cavity. For SMC, the charge is cut into small pieces, weighed and placed in the mould cavity and pressure is applied to the hot mould to force the material to take up the shape of the cavity. After compression the mould remains closed until curing is complete and the prepolymer has cross-linked. Compression and transfer moulding, covered below, are both batch processes.

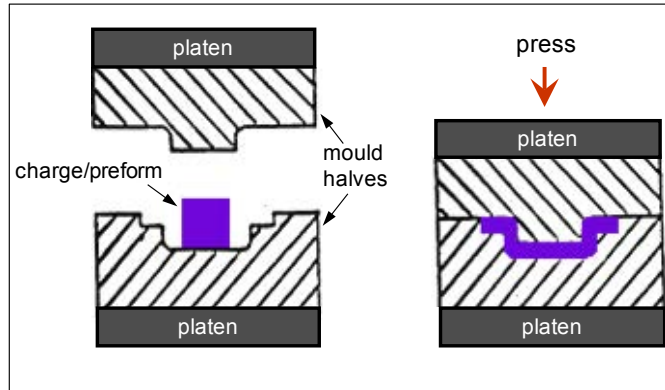


Figure 3.52 Illustration of compression moulding

3.3.2 Transfer moulding

Transfer moulding (Figure 3.53) is a variant on compression moulding, in which there is a reservoir of catalysed molten resin, an amount of which is ‘transferred’ to the mould cavity at an appropriate point in the cycle, in a fairly homogeneous state. It is better suited than the compression moulding for the applications where delicate inserts or hollow cores are required in a moulding, because the cavity is not being directly pressed. Electrical components are usually produced by transfer moulding.

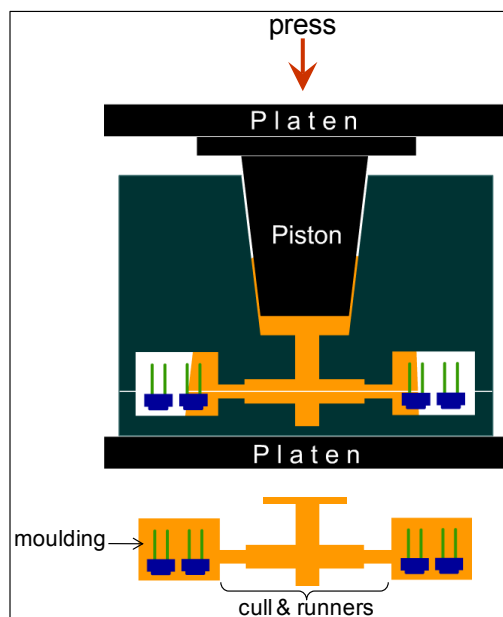


Figure 3.53 Illustration of compression moulding

3.3.3 Injection moulding

Injection moulding of thermosetting plastic is similar to the injection moulding of thermoplastics except that the plasticisation is achieved at low temperature (60-90 °C), and the curing occurs in the mould which is set at a temperature that produces rapid cross-linking (140-200 °C). The material remains in the mould until it is cured sufficiently to be stable in shape (i.e., has green strength), when it can be demoulded, although still hot. Cycle times are longer for thermosets than for thermoplastics due to the chemical reaction.

The processes of injection, compression and transfer moulding are high pressure moulding techniques, there are also **low pressure moulding** techniques that rely on specially formulated liquid resins that are used as a matrix for fibre reinforced composites. Vacuum assisted resin injection (VARI), resin transfer moulding (RTM) or vacuum infusion processes are variants of low-pressure moulding, where the catalysed resin is injected into matched moulds or bagged tools in which the reinforcement has been placed prior to mould closure. Application of vacuum ahead of resin injection assists mould filling. All these techniques depend on the easy flow of the prepolymer and good wetting of the reinforcement. For detailed information and illustration/animation of RTM and other processes, such as pultrusion and SMC, associated with fibre reinforced composites visit the BPF web site.

Many thermosetting polymers (e.g., polyurethanes, epoxides, silicone, modified polyester, phenol-formaldehyde and amino resins), and some thermoplastics (e.g., modified Polyamide 6 and certain acrylics) can be shaped directly from low-viscosity liquid monomeric or prepolymer components, which have to be mixed in stoichiometric proportion immediately before processing. Dispensing units include facilities for metering and mixing of ingredients.

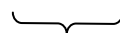
In general, thermosetting polymers have low viscosity, so when the material fills the mould cavity under pressure, some of the material will leak between the two halves of the mould and also from the vent holes for gas and air escapement, generating flash. While this problem can normally be prevented in TP injection moulding by proper mould construction and processing parameters, it cannot be avoided in TS injection moulding and needs to be removed as a secondary operation. When possible, the parts are de-flashed in an automatic tumbling operation rather than hand de-flashing to save costs. Thermoset scrap cannot be reground and mixed with virgin material for reprocessing and, therefore, when designing for recyclability, thermoplastics should be the preferred choice.

3.3.4 Expanded plastics

There are four basic means of expanding plastics: chemically – gas that causes foaming is generated by means of a chemical reaction; physically – gas is generated by means of change in the physical state of the chemicals used (e.g., boiling of the foaming agent); mechanically – rigorous mixing/agitation of the resin with air, and introduction of hollow micro spheres into the resin.

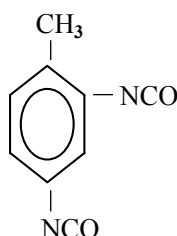
Cellular plastics find uses in industries such as furniture and bedding, flooring, automotive, building and aerospace (sandwich panels, memory foam). Polyurethane (PU) foam or expanded PS (EPS) are most widely used, phenolics, urea-formaldehyde, silicone, PVC and acrylics are also used as foams, e.g., “Rohacell” structural foam (closed-cell rigid expanded foam based on polymethacrylimide) in aircraft sandwich structures.

By way of an example, the basic chemistry of PU foam is briefly described here: a urethane link is produced as a result of the reaction between an isocyanate and a hydroxyl group.

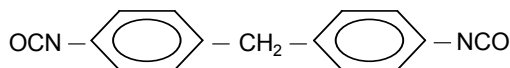


Polyurethanes are obtained if the simple isocyanate is replaced by a diisocyanate and the simple alcohol by a polyol, more generally, when isocyanates react with materials having active H atoms, e.g., OH-compounds, amines, water, and carboxylic acids.

Di-isocyanates:



Toluene - 2, 4 - diisocyanate (TDI) or alternatively (Toluene - 2, 6 - diisocyanate)



Diphenylmethane-4,4'-diisocyanate (MDI), which is a lesser health hazard.

There are other aromatic as well as aliphatic isocyanates that are used, e.g., hexamethylene diisocyanate.

Polyols: there is a wide range of polyether or polyester based polyols. For flexible foam production, high molecular weight, approximately 3000, polyether or polyester prepolymer triols are used. For rigid foam, the polyols are of higher functionality and lower molecular weight (300-1000).

Catalysts: amines or organometallic compounds, e.g., organotin, are used to promote the reaction.

Expanding (blowing) agents: CFCs such as “Freons 11 and 12” (dichlorofluoromethane) were popularly used but they are now banned, because they possess high ozone depletion potential (ODP) and destroy ozone in the stratosphere, causing “ozone-layer depletion”, and they also pose a very high global warming potential (GWP). Alternative blowing agents include hydrochlorofluorocarbons (HCFCs) and hydrofluorocarbons (HFCs), which contain C–H bonds that break down in troposphere, but these are now also scheduled to be phased out, as they both present high GWP and HCFCs also present ODP.

Other recent auxiliary blowing agents include low boiling point (< 50 °C) hydrocarbons (methylene chloride and isomers of butane and pentane) and CO₂ (liquid or gas injection). The boiling point needs to be above room temperature in some applications where a liquid foam blowing agent is required. Hydrocarbons such as cyclopentane, isopentane, and normal-pentane as well as butane isomers, which are mostly used as co-blowing agents offer the advantages of being low cost, low GWP and commercially available. The disadvantages of hydrocarbons are that they are highly flammable and they are volatile organic compounds (VOCs), and may be regulated. For further information on alternative foam blowing agents refer to Wu & Eury (2002).

Water also reacts with isocyanate and produces CO₂, thus, controls the foam density, and contributes to producing a more cross-linked rigid micro-structure.

Surfactant: usually a silicone oil to control foam cell structure and cell homogeneity.

For **processing** purposes, the raw materials of polyols, catalysts, expanding agents and surfactant are mixed together and degassed; making up Part A. Isocyanate constitutes Part B. During the production Parts A and B are mixed together and the mixture is immediately dispensed either into moulds or onto a moving belt for the **slab stock** production (Figure 3.54). The mixing in a dispenser unit is either by mechanical agitation, with a static mixer (relying on the flow of chemicals through tortuous paths) or by high speed impingement of the two streams of chemicals. The mixing/**dispensing** head must be immediately purged with solvent to avoid clogging.

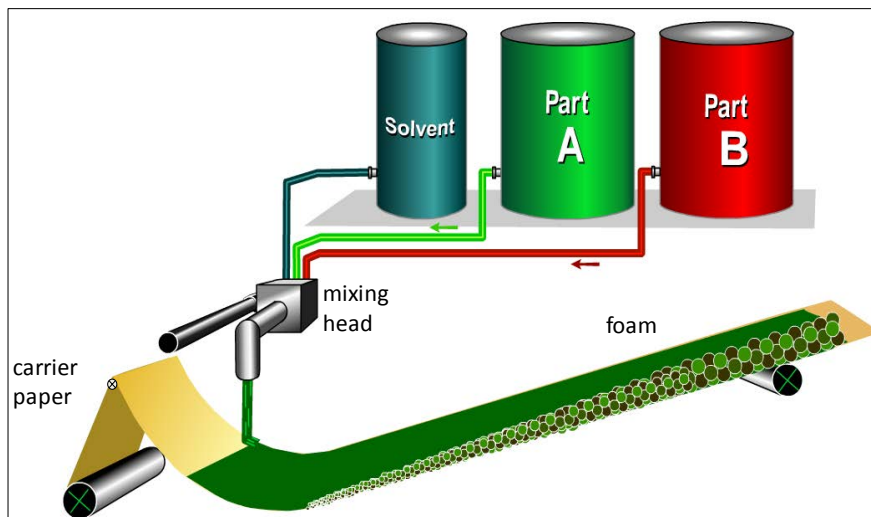


Figure 3.54 Illustration of foam-slab-stock process

Figure 3.55 shows rollers for agricultural machinery that are rotational moulded and then filled with rigid PU using a dispensing machine. The foam keeps the metal frame-shaft insert in place and avoids it from being loosened and detached from the roller with usage.



Figure 3.55 Rigid-PU foam filled agricultural rollers (courtesy of JFC Manufacturing Ltd.)

Other types of foam, besides polyurethane-based rigid and flexible foams, include:

Polystyrene and polyethylene foam: these thermoplastic foams are extensively used in packaging and building applications. Polymerisation of PS beads (by suspension polymerisation) for expansion includes pentane blowing agent in its formulation. Approximately 6 % pentane is added with monomer and following polymerisation gets trapped in polymer beads. Nucleating agent (sodium bicarbonate or citric acid) is also used to promote uniform beads with uniform pore size and structure to ensure the encapsulation of pentane gas in beads. The beads/granules are steam ($\approx 120\text{ }^{\circ}\text{C}$) expanded moulded into products of various shapes. PS foam can also be extruded in sheet form: in a post-polymerisation process, the beads and foaming agents (hydrocarbons, HCFCs, HFCs and CO_2 or their blends) are fed into an extruder where the beads expand and incorporate the blowing agent and are extruded through a flat die. The sheets can be subsequently shaped, e.g., by vacuum forming.

PE foam is mainly produced through extrusion technologies: the foam is produced by dissolving and mixing a gas (isobutane or pentane) into the molten PE, where they form small gas bubbles or cells and expand the polymer and finally cooling of the expanded polymer produces the foam. By using a suitable extrusion die, the foam can be shaped into different semi-finished products such as tubes, profiles, sheets and blocks. The expansion results in a substantial reduction of the polyethylene density: LDPE has a specific gravity of approximately 0.920, which reduces to 0.030 when it is foamed. This weight reduction is obtained by expanding the PE approximately 30 times.

Urea-formaldehyde (UF) foam: foaming is achieved by mechanical agitation. It readily absorbs a variety of liquids. Therefore used in flower arrangement: the stems of flowers easily pierce UF foam and the foam absorbs water to keep the flowers fresh.

Hollow beads may be added to plastics (as an alternative to foaming) to reduce weight.

Phenol-formaldehyde is used to produce inherently **fire retardant** foam.

3.3.5 Coating systems

Paints are used for decorative purposes but more importantly to protect and preserve materials. A liquid coating system consists of: polymer/resin (the binder) + solvent + pigment and extender. Pigment is the obliterating component because of its high refractive index compared with the binder and promotes colour. The polymer (or the resin) binds the pigment particles together as well as causing them to adhere to the substrate. The polymers employed as binders are usually solids or high viscosity liquids and require thinners (solvents) to give lower viscosities suitable for spreading.

Drying and hardening processes for the applied coating are air drying or heat drying and hardening. In **air drying** the solvent is eliminated from the applied paint by evaporation, and the film of coating is hardened by cross-linking reactions under the activation of the atmospheric oxygen. Whereas in **heat drying and hardening**, heat accelerates not only solvent evaporation but also cross-linking reactions. Paints that require heat for drying and cross-linking are known as curing or stoving paints.

Coating techniques:

- Dipping: the component is heated in an oven to a temperature such that when it is dipped, the polymer adheres to the hot metal, melts, flows, and fuses into a coherent coating. The coated article is placed back into the oven, after dipping, to ensure complete melting and fusion of the polymer.

Main stages in the dip coating are

- 1) metal preparation (e.g., degreasing, shot blasting and cleaning);
 - 2) pre-heating (e.g., 230 and 400 °C depending upon the coating thickness required and the coating material used);
 - 3) dipping;
 - 4) melting and fusion or curing.
- There are other coating techniques, e.g., a variety of spraying methods, hot metal foil stamping, and chemical and physical vapour deposition (PVD involves condensation of evaporated atoms on the substrate in a vacuum chamber, in the case of CVD a chemical interaction occurs between gases and substrate under heat to form a film on the substrate). Some of the techniques use an electric field: electrostatic and electrophoretic coating. Electrostatic coating involves spraying of an electrically grounded part with charged polymer powder. In Electrophoresis (also known as electrocoating/electroplating, used for coating a plastic with metal) the part is submerged in an immersion bath, and the process involves the motion of charged polymer (or ceramic/metallic) particles through the liquid suspension to the electrode of opposite charge, which is the substrate/part to be coated.

The dipping process is facilitated with fluidised-bed coating (Figure 3.56): a gas is passed upwards through a vertical column containing polymer powder. At some particular gas velocity, the weight of the particles will be slightly less than the **buoyant force** of the gas, and the powder becomes fluidised. Dipping objects into fluidised powder is much easier than dipping into stationary powder. Plastics powders commonly used are PEs, acrylics, nylons, PP and PVC.

Powder particle size range from a diameter of 30 to 250 μm : Particles greater than 200 μm are difficult to suspend and less than 30 μm generate too much dust from the top of the bed. The process does not involve the use of any solvent and is a very efficient method, utilising almost 100% of the coating material. The technique achieves layer thicknesses of 250 to 500 μm ; even layers of greater than two millimetres are possible in a single step.

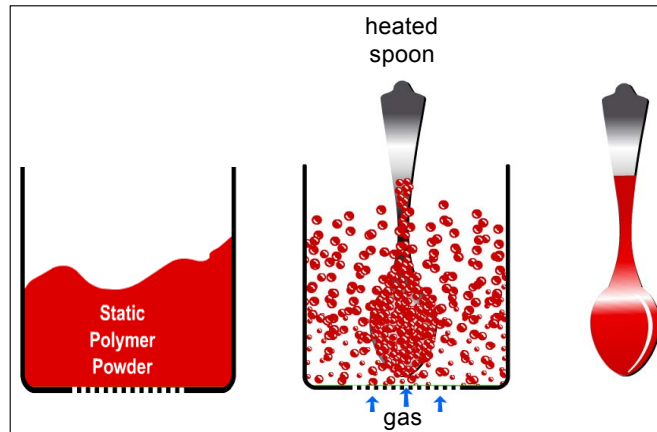


Figure 3.56 Illustration of the principle of fluidised bed coating

3.4 Self-assessment questions

1. Indicate if the viscosity of a polymer decreases with increases in (a) shear strain rate, (b) molecular weight, (c) temperature (d) pressure.
2. Does MFI of a polymer increase or decrease with increasing viscosity?
3. How are weld-lines caused in injection mouldings and how do they affect the quality of the components?
4. Indicate true or false: weld lines become a source of weakness because polymer chains diffuse very slowly.
5. Cite factors which determine the choice of fabrication techniques for polymers.
6. What two parameters are used in rating an injection moulding machine?
7. In moulding, what is the purpose of cold-wells in a mould?
8. Excess flashing could be the result of
 - a) material being too hot
 - b) mould being too hot
 - c) injection pressure being too high
 - d) all of the above conditions.
9. Why is it important to have the sections of a moulding as uniform in thickness as possible?
10. Distinguish between the screw types for the effective extrusion of Nylon 6,6 and polyethylenes.
11. On a standard extruder screw, there are three sections – what are they called?
12. What is the purpose if the tubes or passages under the surface of the feed throat?
13. What will probably happen if plastic melts too early and sticks to the screw in the feed zone?
14. Indicate two important microstructural characteristics for polymers that are considered for fibre production.
15. Why is the inside diameter of the calibrators (sizing rings) often bigger than the outside diameter of a tubular extrudate? What is the magnitude of variation and what does it depend on?
16. Die swelling occurs because of
 - a) attempting to extrude a product at too fast a rate
 - b) the chains become completely disentangled at high shear rates and expand when they re-entangle
 - c) relaxation of shear oriented molecules
 - d) the pressure of the polymer melt expands the die.
17. What processing conditions must be met in the production of PET bottles for soft drinks?
18. What processing method would you use to make a rigid plastic pipe that can be laid easily?
19. Which of the following processing methods would you use for compounding a polymer with colorants and stabilizers
 - a) injection moulding
 - b) thermoforming
 - c) single-screw extrusion
 - d) twin-screw extrusion
 - e) transfer moulding.
20. Indicate true or false: PMMA glazing for aircraft windows is biaxially stretched because this encourages crystallisation while preventing the formation of large spherulites that can scatter light.
21. Indicate the relationship between the melt temperature and the height of the frost line in blown-film production.
22. Moulds for blow moulding can be made using aluminium whereas moulds for injection moulding are usually made out of tool steel, why?

23. What processing method(s) would you use to make disposable plastic plates?
24. Describe vacuum forming/thermoforming processes. What are typical thermoformed plastic products?
25. Calculate the length \times width \times thickness of a blank sheet needed to produce a rectangular container of 100 \times 50 \times 10 cm of a 2 mm wall thickness by vacuum forming. Assume 2 cm is required all round for clamping.
Answer: 104 \times 54 \times 0.32 cm.
26. What processing method would you use to make large, hollow polyethylene playground items?
27. What processing method would you use to make a plastic traffic cone?
28. Describe a method for producing a rotational moulded part consisting of two solid layers of different materials.
29. Describe the circumstances when transfer moulding would be a better choice than compression moulding for production of polymeric parts.
30. Describe the injection moulding process and distinguish between the injection moulding of TP and TS polymers.
31. Guess what the following pattern on the floor is, how was it produced, and relate it to one of the topics covered in this chapter.



32. Describe the methods of foaming/expanding plastics.
33. Describe the fluidised-bed coating technique, outlining the parameters which influence the quality of the coating.
34. Distinguish between electrostatic and electrophoretic coating.
35. Identify and briefly describe a method for coating a plastic with metal.
36. Injection moulding scrap from the sprue and the runner system can be reground and used again for processing, explain if the same is possible with the cull and runner scrap produced in transfer moulding.

4 Microstructure

“Measure what is measurable, and make measurable what is not so.” **Galileo Galilei**, 1564-1642.

Galileo would be proud of the scientific and technological progress in telescopes and microscopy that have enabled amazing measurements to be made at the scale of heavenly bodies, which was Galileo's main field of activity, but also at the scale of atoms. In this chapter some measurements associated with the morphological and microstructural features of polymeric materials will be briefly outlined.

Polymers consist of chain like molecules, where thousands of monomers (repeat units) are strung together. The arrangement of these repeat units with respect to each other is important both in thermoplastic and in thermosetting polymers. In thermoplastics the arrangement dictates whether the polymer is crystalline (orderly) or amorphous (disorderly), and in thermosets, particularly in elastomers, it also controls the propensity of the polymer (in unvulcanised state) to be crystalline or not and, therefore, its suitability for making rubber.

4.1 Stereoregularity

Free-radical polymerisation of conjugated 1, 3-diene monomers such as butadiene, isoprene and chloroprene can produce sequences of repeat units of cis- and trans-configurations. **Configurations (cis and trans)** describe the arrangements of identical atoms or groups of atoms around a double bond in a repeat unit, e.g., cis- and trans-polyisoprene (Figure 4.1). In cis configuration the double bonds and these groups (CH_3) are on the same side of the chain, and in trans configuration they are on opposite sides or across from one another (Figure 4.2). These configurational isomers are spatially fixed and, unlike conformations, cannot be switched from one to the other by rotation about covalent bonds. Ziegler-Natta polymerisation can produce almost 100% cis- or trans-1, 4-polymers from butadiene and isoprene monomers. In general, cis-polymers show a lower T_g and T_m values than the trans polymers, as in polyisoprenes and polybutadienes, since regular (symmetrical) structure of trans polymers enable crystalline formation. Cis-1, 4-polyisoprene (natural rubber) do not normally crystallise unless highly strained and the molecules coil rather than remain linear, which gives rise to long-range rubber elasticity.

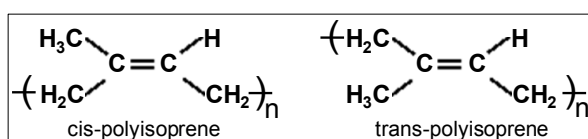


Figure 4.1 Cis-1,4-polyisoprene and trans-1,4-polyisoprene

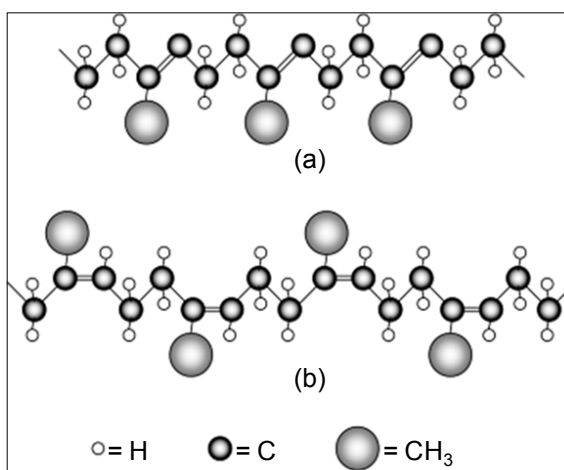


Figure 4.2 Geometric isomers: (a) cis-1,4-polyisoprene (natural rubber, e.g., from the tree *Hevea Brasiliensis*) and (b) trans-1,4-polyisoprene (gutta percha) (source: Weaver & Stevenson 2000)

Stereoregularity (tacticity) refers to spatial isomerism in vinyl polymers and describes the arrangement of side groups around the asymmetric segment of vinyl-type repeat units, ($-\text{CH}_2-\text{CHR}-$). Consequently, three different forms of polymer chain results in thermoplastics: atactic, isotactic and syndiotactic. Figure 4.3 shows the regular arrangement of the side group R in a simple vinyl polymer: in isotactic form all side groups on the same side of the polymer chain and in syndiotactic form side groups alternate regularly on either side of the chain. Atactic form describes the random attachment of the side groups about the back-bone chain. Stereoregularity influences the ability of a polymer to crystallise and also the degree of crystallinity and, in turn, significantly influences properties. For example, polystyrene has large

phenyl groups randomly distributed on both sides of the chain. This random positioning prevents the chains from aligning and packing together with sufficient regularity to achieve any crystallinity so the atactic PS is completely amorphous. However using metallocene catalysts an ordered syndiotactic PS can be produced, which is highly crystalline with a T_m of approximately 270 °C.

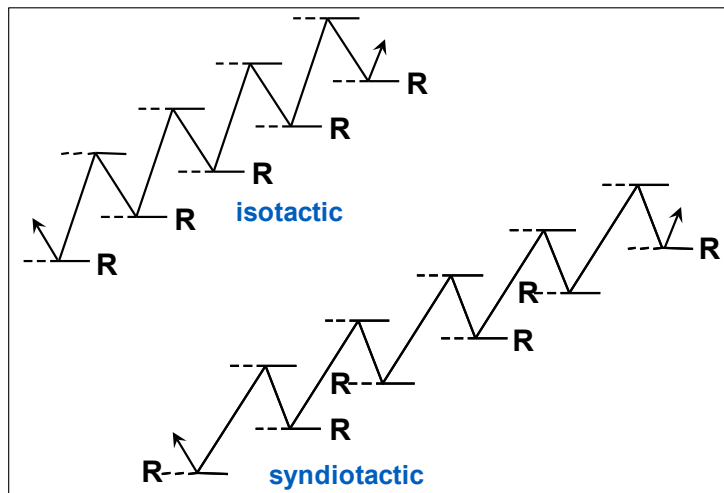


Figure 4.3 Illustration of tacticity in polymer molecules

4.2 Morphology in semi-crystalline thermoplastics

The crystalline structure of **semi-crystalline** TPs comprises **unit cells** (dimensions < 1nm) and **lamellae** ($\approx 10\text{-}30$ nm thick platelets which are formed by an orderly packing of folded chain segments). Lamellae grow from **nuclei** in a radial fashion into a larger structural unit, the **spherulite** ($\approx 0.5\text{-}100$ μm radius) (Figure 4.4). Figure 4.5 shows polypropylene spherulites of about 100 μm radius grown under controlled conditions on a microscope hot stage. But in real production situations the spherulites in thermoplastic films are imperfect in shape and much smaller in size (0.5 to 8 μm). Their size depends on production parameters such as the melt temperature, the rate of cooling/solidification, etc. Spherulite size and its uniformity significantly influence mechanical and optical properties. The interrelation of 'production parameters-spherulite size-material property' makes the on-line measurement of spherulite radius a worthwhile pursuit. An attempt was made by Akay & Barkley (1984), using the small-angle-light-scattering (SALS) technique. The principles of this technique are shown in Figure 4.6 and its adaptation for an on-line measurement of spherulite radii of clear film extrudate is illustrated in Figure 4.7.

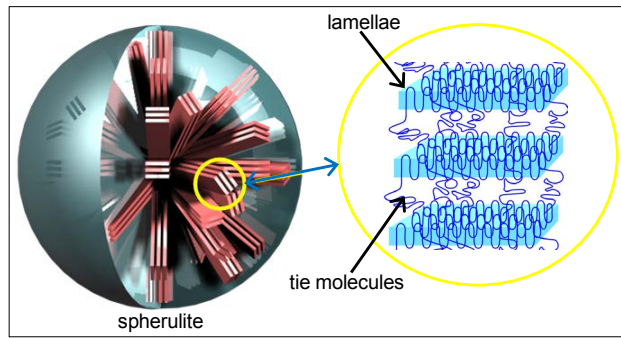


Figure 4.4 Illustration of spherulites and lamellar fibrils



Figure 4.5 An optical micrograph of PP Spherulites

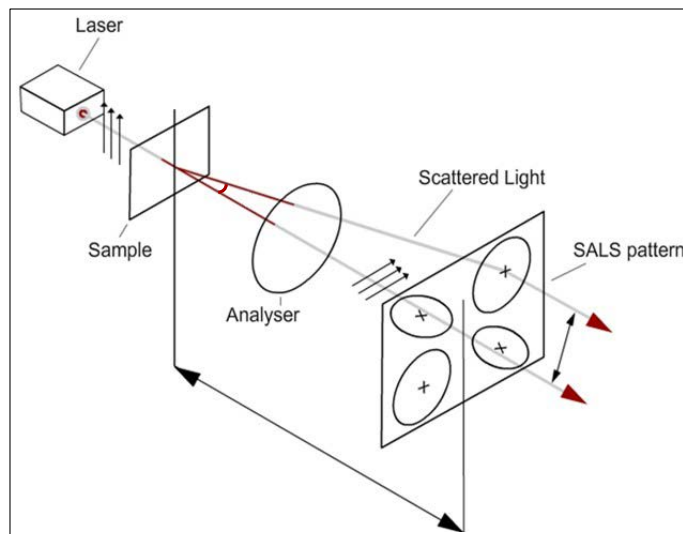


Figure 4.6 Illustration of SALS set up

Spherulite radius can be measured using the SALS set up shown in Figure 4.6: polarised monochromatic light of known wavelength, λ , impinges on a sample of film material, the light gets scattered by the spherulites and the scattered light is passed through an analyser and is captured on a photographic plate, producing a four-lobed clover leaf pattern. The average spherulite radius, R , can be calculated from the polar scattering angle, θ , using the relationship given below. The scattering angle is determined using the distances of X and Y shown in the figure. X is the axial distance between the sample and the photographic plate, and Y is half the distance between the peaks of the diagonal lobes of the SALS pattern.

$$R \approx 1.02 \lambda / [\pi \sin(\theta)],$$

where, $2\theta = \tan^{-1} (Y/X)$.

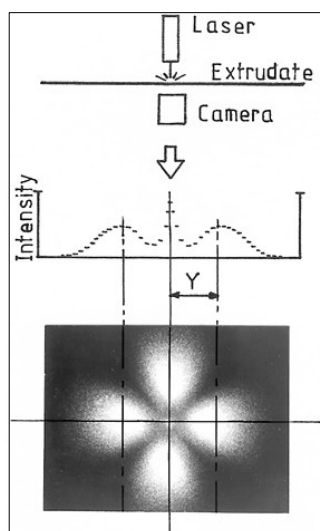


Figure 4.7 A schematic of on-line spherulite size monitoring for film extrudate (source: Akay & Barkley (1984))

The measurement of the smaller morphological unit of lamellae relies on small angle X-ray scattering (SAXS) using a suitable X-ray diffractometer. The stacks of lamellae present in spherulites produce a circular SAXS pattern shown in Figure 4.8. Although such a photographic output shows the concept well, the equipment produces digital data in the form of plots of x-ray intensity vs. diffraction angle, 2θ . The scattering is caused by the densely packed lamellae rather than the non-crystalline inter-lamellar regions. SAXS pattern therefore enables the measurement of 'long period', which represents the thickness of both a lamella and an inter-lamellar space. From the radius of the SAXS pattern and the distance between the specimen and the x-ray film (detector), the long period can be calculated using Bragg's equation

$$n\lambda = 2d (\sin\theta)$$

where, 'd' is the spacing between adjacent crystal planes (in this case the long period. L) and θ is the Bragg angle (note that 2θ is known as the diffraction angle).

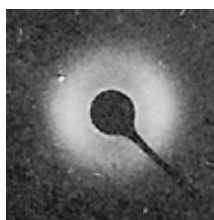


Figure 4.8 Generation of a SAXS pattern from lamellae

4.3 Degree of crystallinity

The long chain molecules in crystalline thermoplastic polymers manage to pack closely together in some regions, producing lamellae. However, the entanglements of the long molecules hinders this orderly packing in other regions giving rise to amorphous (meaning without morphology/shape) structure, as in tie molecules in the inter-lamellar spaces. Accordingly the crystalline polymers such as PEs, PP and nylons are more appropriately also referred to as semi-crystalline. This structural mix is exhibited within a spherulite, which consists of radially-grown crystalline fibrillar lamellae and the amorphous tie molecules that are irregularly entangled as delineated in Figure 4.4.

The tendency of a polymer to crystallise, the magnitude of crystallinity and the stability of crystallisation is dictated by a number of factors, including the degree of close packing and/or by the presence of **intermolecular forces**. The size and the stereoregularity of the side groups, pendant from the main backbone of the macromolecule, is a major factor in the level of packing between the neighbouring polymer chains. Small pendant groups and tacticity favour close packing of the molecules and therefore increase crystallinity.

The rate of cooling of the melt for solidification also influences the **degree of crystallinity**: during crystallization, upon cooling through melting point, polymers become highly viscous. Time is required for random and entangled chains to become ordered, slow cooling allows time for molecules to arrange themselves into an orderly structure. Intermolecular forces, such as H-bonding, also encourage crystallinity and more importantly leads to increased stability of the crystalline regions. This is why crystalline structure in Nylon 6,6 is much more stable (Figure 4.9) compared with other aliphatic thermoplastics such as PEs and PP, and hence exhibits a much higher melting point.

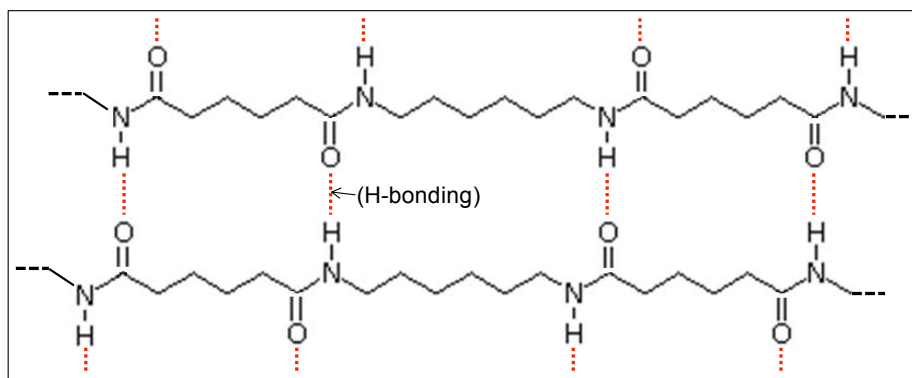


Figure 4.9 H-bonding between the amide groups in poly(hexamethylene adipamide)

The degree of crystallinity indicates the amount of the material that is structurally crystalline, and it can be measured by a number of methods such as density, x-ray diffraction, infrared spectroscopy and thermal analysis. In using all these techniques for the determination of the degree of crystallinity, certain assumptions are made: (a) polymers consist of two separable phases – crystalline and amorphous, and (b) the properties of the phases are additive, i.e., the property of the material is the sum of the properties of the phases.

4.3.1 Density method

This is the easiest of the methods used, and density has become a convenient parameter to express crystallinity as in different grades of polyethylenes: LDPE, MDPE, HDPE, UHDPE, etc.

The method uses the rule of mixtures equation for the specific volumes of phases in the material:

$$V = x V_c + (1-x) V_a$$

where, V is the specific volume, subscripts "c" and "a" represent crystalline and amorphous, and "x" is the mass fraction of crystalline phase.

$$x = (V - V_a) / (V_c - V_a) \text{ or } x = (\rho_c / \rho) [(\rho - \rho_a) / (\rho_c - \rho_a)]$$

where, ρ is the density of the polymer specimen for which the crystallinity is to be determined.

The **degree of crystallinity** can be determined as outlined below:

- V can be determined by measuring the density of the given polymer, e.g., by using a density gradient column or, more conveniently, a density balance.
- V_a from the totally amorphous form of the material (e.g., melt quenched in liquid nitrogen and its density measured).
- V_c can be determined by X-ray crystallography (i.e., crystalline unit cell dimensions are obtained by X-ray measurements).

Calculation of V_c for PE:

Five polymer chains can be associated with the unit cell: four at the corners and one through the centre, see Figure 4.10.

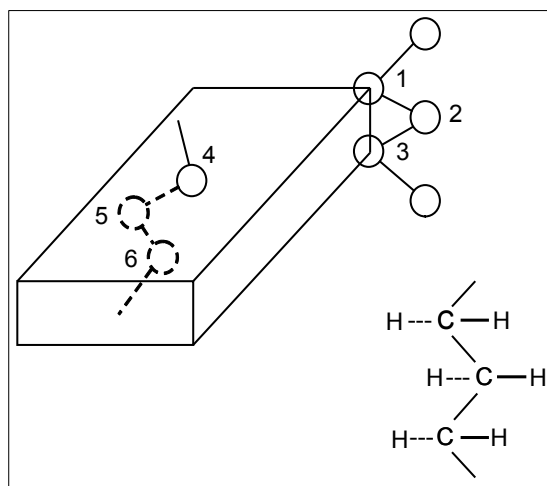


Figure 4.10 Illustration of PE unit cell

- CH₂- group in Site-1 is shared by 8 unit cells, thus, the share of each unit cell is 1/8 (CH₂).
- CH₂- group in Site-2 is shared by 4 unit cells, thus, the share of each unit cell is 1/4 (CH₂).
- CH₂- group in Site-3 is shared by 8 unit cells, thus, the share of each unit cell is 1/8 (CH₂).

each corner of the unit cell contains $\frac{1}{2}$ (CH_2).
i.e., 4 corners make up 2 (CH_2) or one monomer unit.

By the same approach, the contribution of the central chain to the unit cell is also one monomer unit.
The volume occupied by 2 monomer segments = abc , therefore, by one ethylene molecule = $(abc)/2$, where, a , b and c are the edge lengths of the unit cell.

Since there are N (Avogadro's number) molecules in 1 mole, the volume occupied by 1 mole of the substance is $N(abc/2)$.

One mole of ethylene = 28 g,

the volume occupied by 1g of crystalline PE, $V_c = N(abc) / 56$.

Density values for crystalline and amorphous components of various polymers are presented in Table 4.1.

Table 4.1 Density of some thermoplastics and their crystalline and amorphous phases

polymer type	crystallinity, %	density, g/cm ³		
		crystalline	amorphous	typical
PA 66	35-45	1.24	1.07	1.14
PA 6	35-45	1.23	1.08	1.14
POM	70-80	1.54	1.25	1.41
PET	30-40	1.5	1.33	1.38
PBT	40-50	-	-	1.3
PTFE	60-80	2.35	2	2.1
i-PP	70-80	0.95	0.85	0.905
a-PP	50-60	0.95	0.85	0.896
HDPE	70-80	1	0.85	0.95
LDPE	45-55	1	0.85	0.92

4.3.2 X-ray method

X-ray diffraction/scattering is used for polymers to characterise them in terms of their crystalline and amorphous states. The method is appropriate because X-ray diffraction/scattering produces different patterns by amorphous and crystalline regions of a polymer: a well-identifiable characteristic pattern (sharp peaks on the intensity vs. diffraction angle trace, see Figure 4.11) when scattered by the crystalline region, whereas an indistinct/diffused pattern (the amorphous halo) by the amorphous matter.

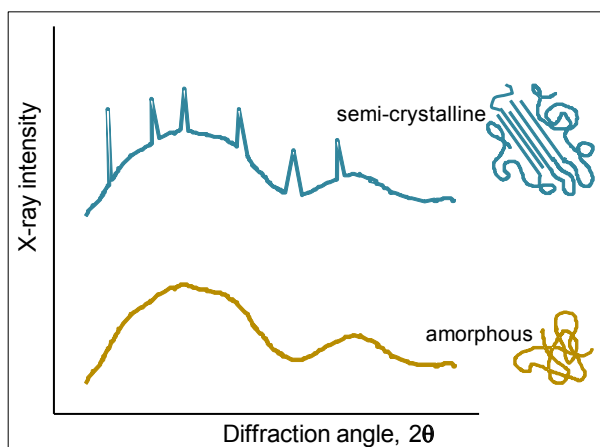


Figure 4.11 The intensity of the X-radiation scattered by the specimen vs. diffraction angle, showing Bragg diffraction peaks on an amorphous background

Wide-angle X-ray scattering (WAXS), which produces the diffraction patterns shown in Figure 4.11, is used for the determination of crystalline fraction as well as crystalline dimensions. In determination of crystalline dimensions, WAXS is used for small-scale microstructure measurements (<1 nm) such as unit cells, while SAXS is used to investigate large-scale morphological features (1 to 1000 nm) such as the lamellar long period that was covered in Section 4.2. SAXS measurements are conducted at very small scattering angles (0.022 to 2.2°) and therefore require collimators to sharply focus the incident beam and more specialised detectors than required for WAXS.

A sketch of the scattering intensity vs. angle, Figure 4.11, is used to explain the crystallinity determination.

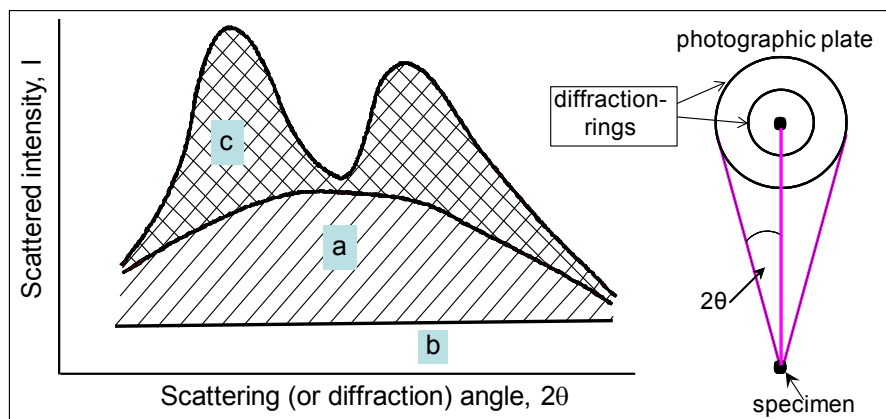


Figure 4.12 The intensity of the X-radiation scattered by the specimen vs. scattering angle

The areas indicated in Figure 4.12 are described below:

- a) scattering due to the amorphous component of the polymer
- b) background scattering (air, dust, specimen mount)
- c) scattering due to the crystalline component of the polymer.

Consider that equal masses of different substances scatter equal amounts of radiation, thus:

Crystalline fraction, $x = I_c / (I_a + I_c)$, where I_c and I_a are the scattered radiation intensities (i.e., areas under the respective regions on the graph).

4.3.3 Infra-red method

Infrared (IR) spectroscopy is also employed to determine crystallinity because the vibrations of the atoms detected by IR spectrometer are affected by the crystalline structure and appear on the spectrum at slightly higher energy levels than do more freely moving atoms in the amorphous regions.

Figure 4.13 shows a portion of the IR spectrum for semicrystalline and amorphous polypropylene specimens. On IR spectra there are crystalline, amorphous and crystalline-amorphous sensitive bands. For PP, the crystalline sensitive band is at $10.03 \mu\text{m}$ wavelength, and both the crystalline and amorphous sensitive band is at $10.29 \mu\text{m}$.

$$\% \text{ crystallinity} \approx A(10.03 \mu\text{m}) / A(10.29 \mu\text{m})$$

where, $A(\lambda)$ is the absorbance at the wavelength λ .

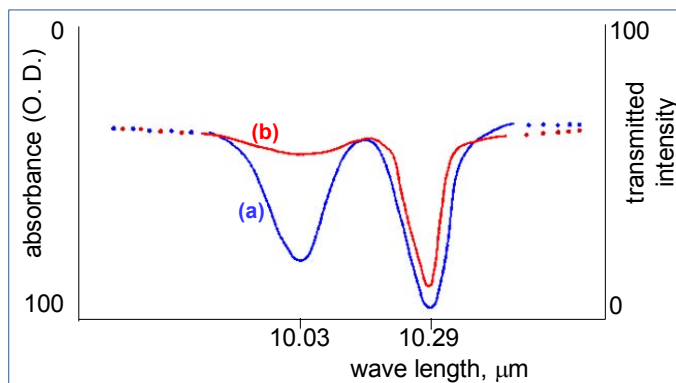


Figure 4.13 A segment of PP IR spectrum: (a) semi-crystalline film, (b) molten sample (amorphous)

4.3.4 Thermal analysis method

Differential scanning calorimetry (DSC) and its variants can be used to determine the degree of crystallinity. The method is based on extracting enthalpy values from DSC traces of materials, and using the equation below to determine the fractional crystallinity

where, ΔH_m is the enthalpy per unit weight of sample and ΔH_m^0 is the enthalpy per unit weight of a completely crystalline sample of the same polymer. ΔH_m is calculated from the area under the melting peak on the experimentally obtained DSC trace of the sample, and ΔH_m^0 values are often taken from the literature, e.g., a compilation of these values are given for some polymers in Ehrenstein et al. (2004, p15), see Table 4.2. Figure 4.14 shows a portion of the DSC trace, a plot of heat flow or power against temperature, for polyetherether ketone (PEEK). The endothermic melting peak (the hatched area) yields an enthalpy value of approximately 41 J/g, the enthalpy value for 100 % crystalline PEEK is recorded to be 130 J/g.

Table 4.2 Enthalpy values for the crystalline component of some semi-crystalline thermoplastics (note that H and C denote homo- and co-polymer for POM) (source: Ehrenstein et al. (2004, p15))

Polymer	ΔH_m^0 , J/g	T_m , °C
LDPE	293	105-120
HDPE	293	130-140
PP	207	160-165
POM-H	326	175-190
POM-C	220	140-170
PA 6	230	220
PA 66	255 or 300	260
PA 11	226 or 244	187

PA 610	208 or 284	222
PET	140	240-260
PBT	140	220-230
PTFE	82	327

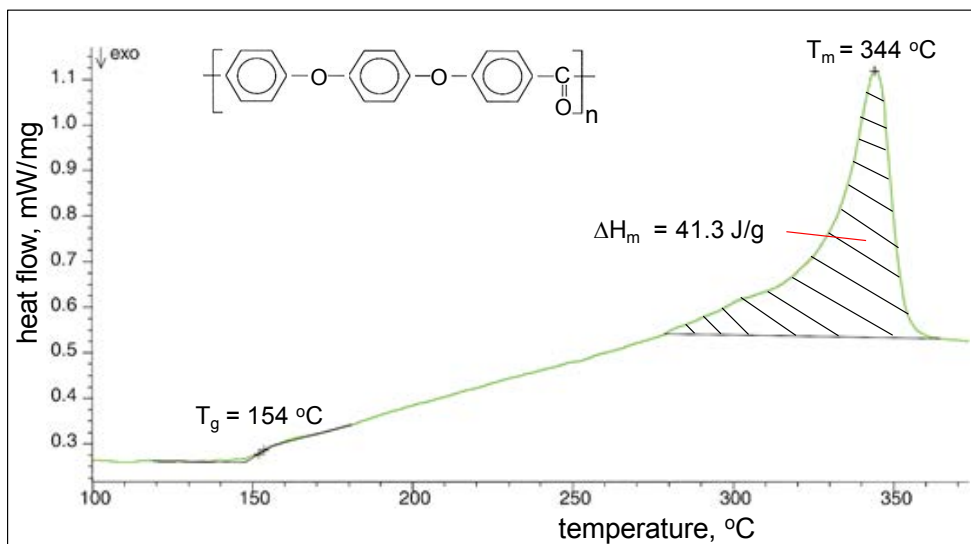


Figure 4.14 DSC trace for a PEEK specimen (source: Netzsch GmbH)

4.4 Crosslinking

In crosslinked polymers linear polymer chains are joined together by covalent bonds, either singly or mostly through crosslinking atoms or functional groups (Figure 4.15). Crosslinking may be achieved by reaction of functional groups; by vulcanisation of elastomers, using sulphur or peroxides; by reaction of unsaturated groups with atmospheric oxygen; by high energy radiation; by photolysis (using UV or visible light); or by ionic bonding.

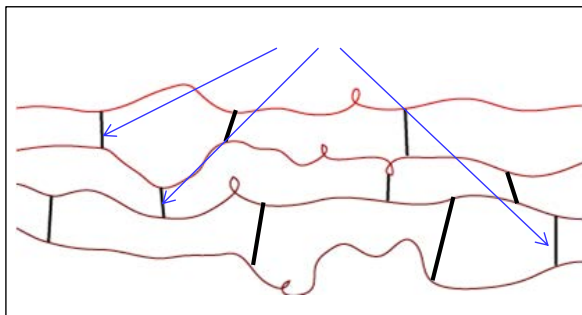


Figure 4.15 Sketch of crosslinking of neighbouring polymer chains with covalent bonds

Ionising radiation, in the form of photons, electrons, neutrons or protons, can cause both crosslinking (a free radical process) and degradation by chain scission in vinyl thermoplastic polymers. Often the nature of the side groups and their distribution will determine which reaction will dominate. PEs crosslink (LDPE with high amorphous content is most commonly crosslinked with irradiation, because radiation penetration is easier) but, for example, PVC degrade with loss of halogen, PP with methyl side group is susceptible to degradation, similarly PMMA. Crosslinking improves mechanical, chemical and thermal properties. MFI of crosslinked PE should be lower since the crosslinking holds the material together even at the crystalline melting point of the uncrosslinked phases.

The extent of crosslinking is described by **crosslink density** (degree of crosslinking), which is low in elastomers but high in thermosetting polymers. Thermosets are extensively crosslinked such that all the molecular segments are joined to each other establishing a network, hence the description of 'network polymers'. **Thermoset (network)** formation requires that monomers should be multifunctional; at least one of the monomers must be tri-functional or greater. TSs (e.g., PE, epoxy resin (see Figures 4.16 and 4.17), and PU) differ from TPs in that their molecular chains are crosslinked by primary bonds and they are amorphous – a characteristic common with most elastomers. Natural rubber consists mostly of a linear polymer that can be cross-linked to a loose network by reaction with 1 to 3% sulphur. The same polymer reacted with 40 to 50% sulphur produces ebonite, a hard material used for making, e.g., bowling balls and clarinet mouth pieces. X-link density allows control of mechanical (Figure 4.18) and chemical properties.

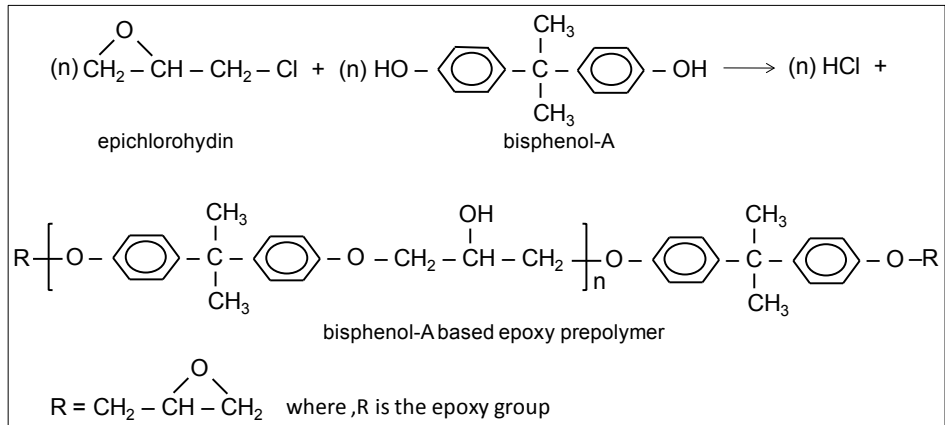


Figure 4.16 Formation of epoxy prepolymer from its monomers

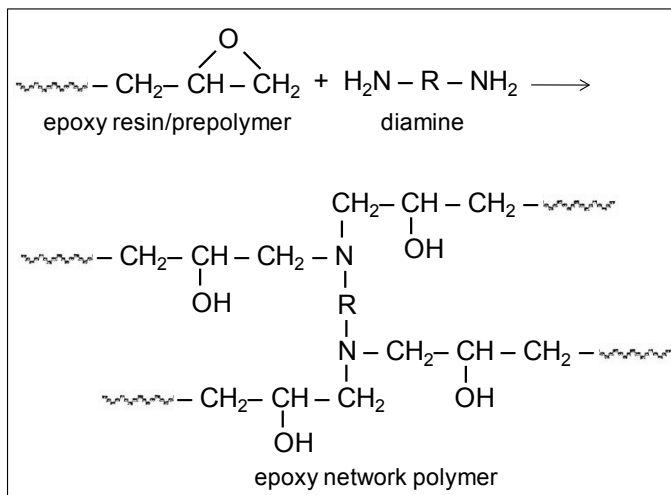


Figure 4.17 Crosslinking of epoxy resin (low molecular weight) with an amine curing agent (note that the term epoxy resin is used to describe both the network polymer and the oligomeric prepolymers)

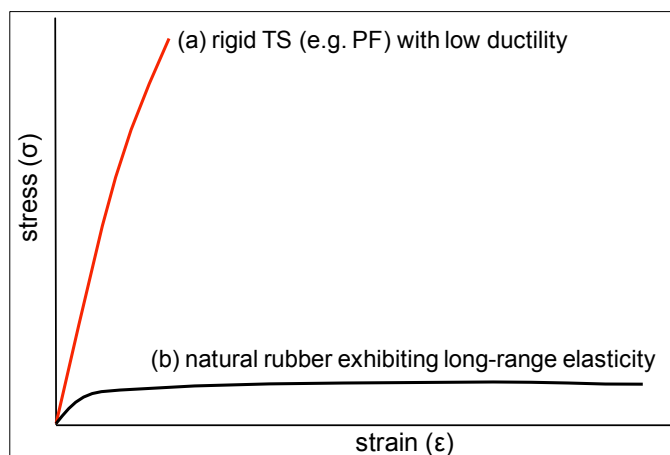


Figure 4.18 σ - ϵ curves for crosslinked polymers: (a) high X-link density, (b) low X-link density

4.5 Copolymer arrangements

Polymers can be tailored to produce unique/desirable combinations of properties by polymerising together two or more different types of monomers. The resultant polymer is called a copolymer to distinguish it from the homo-polymer that the individual monomers by themselves produce, e.g., acrylonitrile-butadiene-styrene copolymer, and polyacrylonitrile, polybutadiene and polystyrene homopolymers. While ABS is roughly twice as expensive as PS, it is more superior for its hardness, gloss, toughness, solvent resistance and electrical insulation properties. Note that copolymers should be distinguished from polymer blends.

The arrangement of different monomers within the copolymer chain leads to the formation of different structures as delineated in Figure 4.19. The terms used to describe these different basic structures are self explanatory: in the random copolymer there is no detectable regularity to the sequence of different monomers within the polymer chain, in the alternating type the monomers are ordered regularly in an alternating sequence. In Block copolymer chains, the long segment (oligomers) of each type of monomer are joined together, and similarly in graft copolymers long segments of a monomer (string of Monomer B in Figure 4.19) is covalently attached as a side branch onto the main backbone chain consisting of the second type of monomer (Monomer A in the figure).

Normally the random and alternating copolymers produce properties that are averages of the properties of homopolymers, whereas block and graft copolymers can exhibit a combination of properties that are unique to the individual homopolymers as in thermoplastic elastomers, covered in the next section.

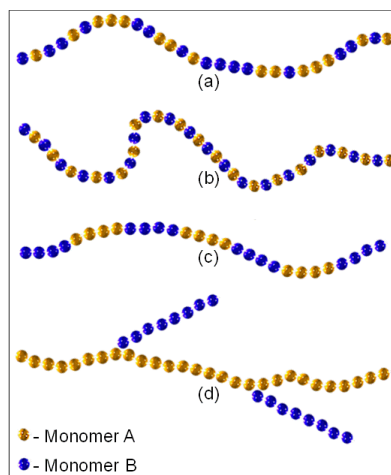


Figure 4.19 Illustration of different monomer arrangements in copolymers: (a) random, (b) alternating, (c) block, and (d) graft copolymers (source: Google images)

4.6 Domain structures

Domain structures consisting of hard and soft segments are a feature of thermoplastic elastomers (TPE). Ordinary crosslinked (vulcanised) elastomers do not melt or dissolve and cannot, therefore, be processed using processing equipment suitable for thermoplastics, and also their waste cannot be reprocessed like thermoplastics. TPEs are attractive alternatives because they can be processed as a thermoplastic.

Figure 4.20 shows an illustration of the microstructure for TPEs and also a product made from a TPE. The hard segments have T_g and T_m values well above room temperature and they perform the same function as crosslinks in thermosetting elastomers, but they are thermo-reversible physical crosslinks, making the material melt processable. The soft segments have T_g values well below ambient temperature and so exhibit good molecular flexibility at temperatures above its T_g . The soft segments impart rubbery characteristics to TPEs, as polybutadiene segments do in styrene-butadiene-styrene (SBS) block copolymer (Figure 4.20). Other examples of TPEs include thermoplastic polyurethane elastomer (TPU) in which the hard segments consist of urethane or urea groups (that include rigid aromatic rings of the isocyanate used), separated by soft blocs/segments of polyol. One particular TPU, a block copolymer of alternating soft (85 %) and hard segments, is used to produce Spandex fibre, which is popularly used to produce light-weight sports garments under such trade names as Lycra (Du Pont).

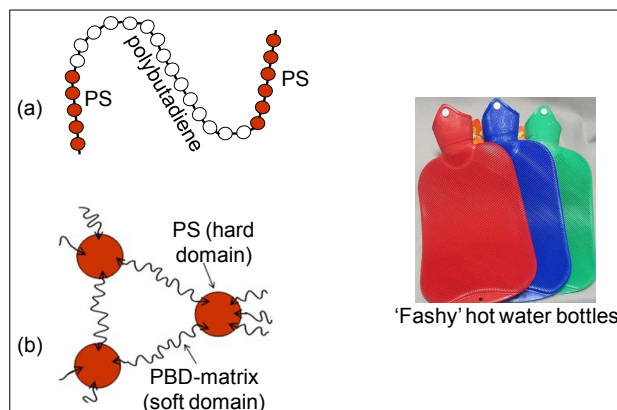


Figure 4.20 Illustration of the structure of a TPE: (a) single molecule, (b) microstructure

4.7 Degree of molecular orientation

Orientation causes alignment of the micro-structural units and polymer chains so it causes anisotropy in properties such that material becomes much stronger and stiffer along the orientation axis. Orientation is successfully exploited by industry – production of synthetic fibres depends on orientation. The packaging industry makes extensive use of uniaxial and biaxial orientation.

Measuring orientation in polymers provides valuable information about micro-structure and therefore properties. It can be measured by birefringence, sonic modulus, X-ray diffraction, infrared dichroism, laser-Raman spectroscopy, etc.

4.7.1 Birefringence

The measurement of optical anisotropy is a simple method of studying orientation in polymers. Birefringence is a measure of the total molecular orientation of a system (i.e., crystalline and amorphous components of the polymer). It is defined as the difference in the refractive index parallel, n_{\parallel} , and perpendicular, n_{\perp} , to the stretch direction for a uniaxially oriented specimen. The refractive index is a measure of the velocity of light in the medium and is related to the polarisability of the chains.

The birefringence for a uniaxial system, Δ , is therefore defined as

$$\Delta = n_{\parallel} - n_{\perp}$$

For a completely isotropic material $\Delta = 0$.

Anisotropy increases with the increased orientation in a material, and Δ increases too. To measure Δ , one method would be the direct measurement of the refractive indices, which is a tedious procedure. A more rapid method is the use of a **compensator** (e.g., Babinet compensator) to determine the phase difference between two perpendicular, plane-polarised wave motions emerging from the sample: since the sample is anisotropic, the velocity of the wave passing through the sample parallel to the stretch direction will be different than the one in the perpendicular direction. This velocity difference causes a phase difference in the emerging rays.

$\Delta \propto R$ (the retardation or phase difference as wave numbers).

Birefringence is a suitable technique for transparent samples and requires a polarising microscope fitted with a compensator for measurement.

4.7.2 Sonic technique

The orientation in polymers can be measured by propagating sound pulses through the material. This technique also gives an average orientation in the material. It is particularly suited for specimens of fibres/ribbons. The experimental set up consists of a sonic wave (pulse) transmitter and a wave detector; both placed on the sample a certain distance apart and a meter for measuring the time between the onset of the pulse and its detection after propagation. The sound velocity, v , is determined from the propagation distance and the time between the pulse and the signal detection.

The **sonic modulus**, $E = \rho (v^2)$, where ρ is the density of the material.

4.7.3 X-ray method

Wide-angle X-ray diffraction patterns of unoriented semi-crystalline polymers are characterised by a series of concentric rings. As the specimen is oriented, these rings break up into arcs and spots (Figure 4.21). From the intensity and the size of these arcs, the degree of orientation of the crystalline regions can be determined.

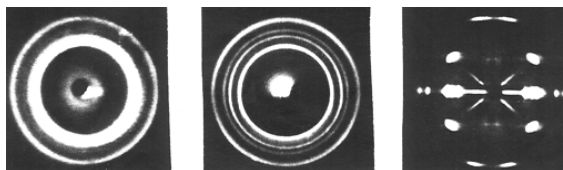


Figure 4.21 WAXS patterns for PP samples

4.7.4 Infra-red method

The infra-red dichroism is used for the determination of crystalline and amorphous orientation by studying the appropriate absorption bands.

$$\text{The infra-red dichroic ratio, } D = A_{\parallel} / A_{\perp}$$

where, A_{\parallel} and A_{\perp} are the absorbances measured with radiation polarised parallel and perpendicular to the stretch direction.

$$\text{The orientation} \propto D.$$

4.8 Self-assessment questions

1. Polymers do not crystallise easily because:
 - a) they are long chain molecules
 - b) they contain covalent bonds
 - c) the molecules are interconnected with H-bonding
2. Explain briefly the difference between crystalline and amorphous regions in a polymer.
3. What x-ray diffraction technique is used in determining crystallinity in polymers?
4. Describe crosslinking and how it affects properties in polymers.
5. What is the molecular difference between thermosetting and thermoplastic polymers?
6. Select the polymers that could show variation in tacticity: PP, PTFE, PS, and PE.
7. Indicate which of the following polymers could not exist as isotactic and syndiotactic stereo-isomers:
 - a) PP
 - b) PMMA
 - c) polyvinylidene chloride
 - d) PTFE
 - e) PS
8. Indicate if isotactic PP is
 - a) thermoset
 - b) polyolefin
 - c) an amorphous polymer
 - d) a semicrystalline TP

9. Select which of the following properties can be determined from a DSC scan:
- e) latent heat of fusion
 - f) number average molecular weight
 - g) $\tan \delta$
 - h) T_g
10. Indicate what is the effect of crosslinks in an elastomer
- a) reducing Young's modulus
 - b) increasing crystallinity
 - c) decreasing degree of crosslinking
 - d) enabling long-range elasticity
11. Indicate which of the following properties depend only on the chemical nature of its repeating units:
- a) crosslink density
 - b) T_m
 - c) chain configuration
 - d) chain conformation
12. Indicate if thermosetting polymers
- a) contain crystalline regions
 - b) are more rigid than TPs
 - c) consist of a 3D network of polymer chains
 - d) exhibit T_m
13. Indicate how neighbouring molecules are bonded in a TP:
- a) covalent bonds
 - b) H-bonds or van der Waals forces
 - c) crosslinks
 - d) primary bonds
14. The number of tie-molecules between spherulites affects:
- a) the optical properties
 - b) the impact properties
 - c) density
 - d) crystallinity
15. Indicate how to increase crystallinity in a vinyl polymer:
- a) change the tacticity from atactic to syndiotactic
 - b) stretch it
 - c) anneal it
 - d) solidify from melt at a slow rate
 - e) all of the above
16. Which of the following polymers is least likely to be optically transparent?
- a) isotactic polystyrene
 - b) atactic polystyrene
 - c) an ethylene/propylene block copolymer
 - d) a styrene/butadiene random copolymer

17. HDPE cooled slowly from 160 °C to room temperature
- remains amorphous
 - crystallises
 - remains liquid
 - crosslinks
18. A polypropylene sample is just buoyant in an alcohol of density $\rho = 0.9 \text{ g cm}^{-3}$. Calculate its mass fraction crystallinity if the density of crystalline PP is 0.99 g cm^{-3} and that of amorphous PP is 0.85 g cm^{-3} .
Answer: 39 %.
19. DCS traces of two PE samples produce melting enthalpies of 140 and 200 J/g for Specimens A and B, respectively. Using the data below, determine weight % crystallinity and the density of each specimen. Specific gravities of completely crystalline region and completely amorphous regions of PE are 1 and 0.856, and the latent heat of fusion of crystalline region is 285 J/g. *Answer: Specimen A: crystallinity 49%, density 0.92 g/cm^3 ; Specimen B: 70%, density 0.95 g/cm^3 .*

5 Behaviour of polymers

“Minds are like parachutes, they only function when they are open.” **James Dewar**, 1842-1923.

After a very brief introduction to the degradation behaviour of polymeric materials, the chapter will concentrate on describing various basic concepts in association with the viscoelastic nature of polymers, so don't shut those parachutes yet!

5.1 Degradation of Polymers

Polymers do not rust in the way metals do, but they also suffer degradation from environmental effects. The processes of degradation are different compared with metals:

- metallic corrosion is an **electrochemical** reaction
- degradation of polymers is **physiochemical** (i.e., may involve physical and/or chemical processes).

Polymers may deteriorate by **swelling** and **dissolving** – i.e., solute molecules enter and occupy positions between the polymer molecules. Note that plasticisation is achieved when this process is controlled. Polymers resist acids and alkaline solutions better than metals.

Polymers are vulnerable to **hydrocarbon liquids**, the severity of which depends on the type of polymer. Polystyrene, for instance, with a benzene side group is sensitive to aromatic and chlorinated solvents and can be readily dissolved in these solvents. It is, however, resistant to water. Some polymers such as nylons and celluloses are, on the other hand, susceptible to water.

Bond rupture in polymer molecules (i.e., scission) may result from exposure to radiation or heat, and from chemical reaction. Not all radiation is deleterious: cross-linking may be achieved by irradiation, e.g., γ -radiation is used to cross-link PE to increase its resistance to softening and flow at elevated temperatures.

Degradation resulting from outdoor exposure is known as **weathering** such that a combination of moisture, UV radiation, and heat causes deterioration by the process of **oxidation**. For example PVC can suffer degradation with the evolution of HCl under long exposure to UV. An example can be seen in Figure 5.1: the part of a clear corrugated PVC roof that was shaded by a tree has not suffered any discolouration over time in comparison with the section exposed to direct sunshine.

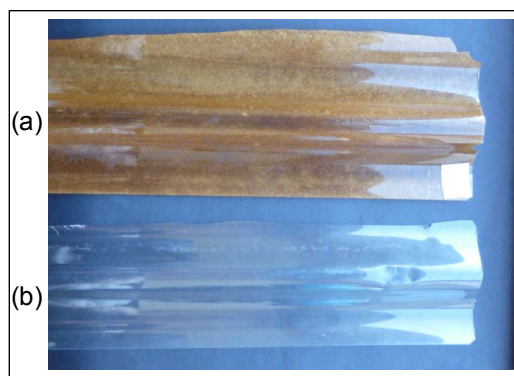


Figure 5.1 Specimens taken from a PVC clear corrugated roof: (a) represents the section of the roof exposed to sunshine, (b) represents the section of the roof shaded from the sun

Oxygen and ozone also by themselves can cause the scission of the covalent bonds within the polymer molecules, particularly in rubber due to the presence of more vulnerable double covalent bonds along the backbone molecular chain. This phenomenon can be seen in ordinary balloons that are produced by dipping porcelain formers (covered with a coagulant to coagulate the latex) into natural-rubber latex. A suitable antioxidant is added to the latex and therefore the balloons are protected against degradation by oxidation, but the protection is only effective when the balloons are not blown. The antioxidant reacts with the oxygen in the atmosphere and forms a protective layer. Once the balloons are blown up, however, the surface area increases and the protective layer breaks up. Consequently oxidation occurs and causes chain scission, which manifests itself as a sticky mass of material. This can be seen in Figure 5.2, which shows a balloon that has not been blown up and also a few balloons that were blown up tied together and left in the blown up state for a few months after a children's birthday party, suffering degradation and becoming a gooey lump.

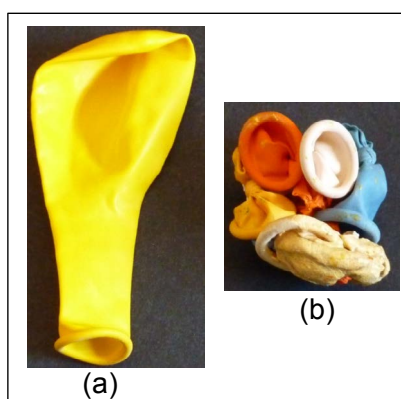


Figure 5.2 Photos of rubber balloons: (a) a fresh balloon, (b) a few degraded balloons after being left blown up for a period of time

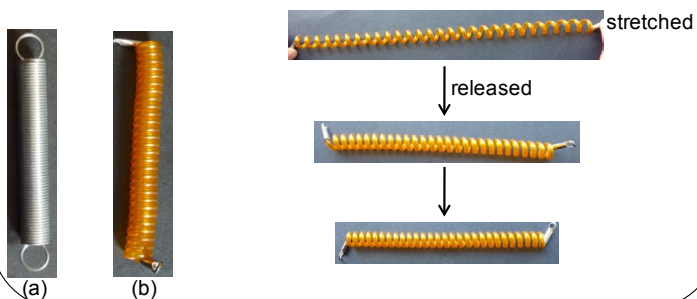
Detailed information on weathering, aging, factors affecting aging, accelerated weathering outdoors and in devices, and guidance on selecting appropriate methods of testing is presented by Kockott (1999, p697).

5.2 Viscoelasticity

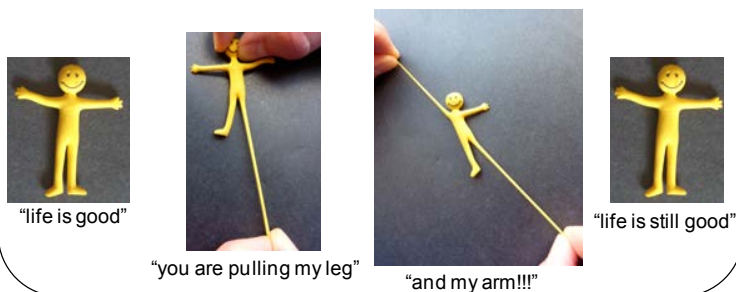
Ordinary solids such as metals are **immediate** or instantaneous in **response** to applied loads – i.e., they are **elastic**. In contrast polymers, from observation, are sluggish in response to applied loads – i.e., they are **viscoelastic**. **Viscoelasticity** is a material behaviour in which the relationship between **stress** and **strain** is **time dependent**. It should be possible to demonstrate some of these features using the items shown in the following demonstration-boxes. Demonstrations 5.1 to 5.4 are aimed to highlight the sluggish recovery of viscoelastic materials/components, and Demonstration 5.5 should exhibit rate dependency in the behaviour of viscoelastic materials such as the “Smart putty”. Smart putty can be obtained from Middlesex University, UK (www.mutr.co.uk). The human skin behaves in a viscoelastic manner – pinch the skin at the back of your hand and let go, the recovery is time dependent, particularly noticeable with the elderly.

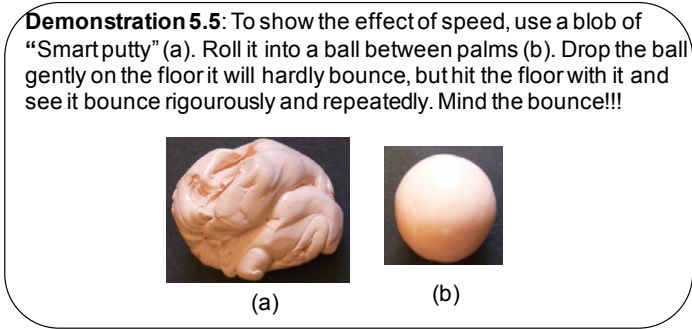
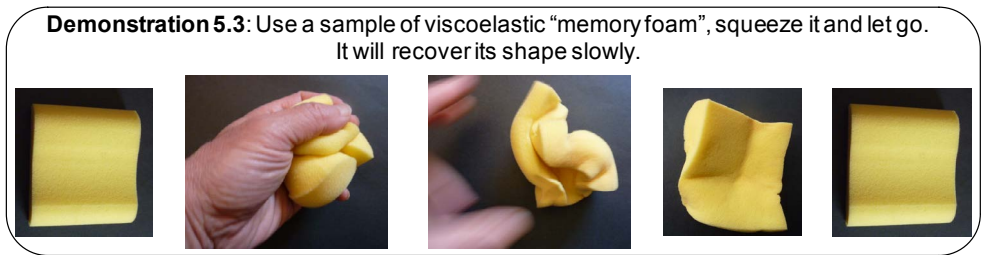
The extent of viscoelasticity depends on the **temperature** of the material. A rigid plastic has near elastic behaviour at room temperature, but at T_g (more about this later) and beyond, the behaviour changes.

Demonstration 5.1: (a) 12 mm diameter steel spring, (b) 12 mm diameter flexible polymeric cord. When the polymeric cord is pulled and released the recovery is time dependant, whereas it is instant with the metal spring. Mind the nip when releasing the metal spring.



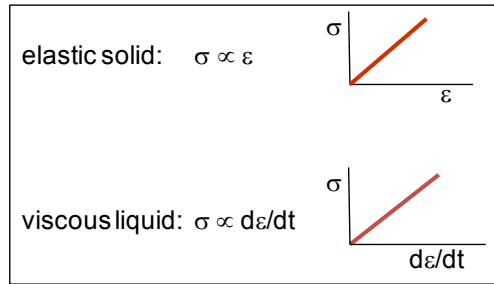
Demonstration 5.2: a little rubber man shows long range elasticity and recovers instantly with no ill effects back to its happy self.





On stressing a viscoelastic material, three deformation responses may be observed – an initial instant elastic response, then a time-dependent delayed elasticity (fully recoverable) and, finally, a viscous, non-recoverable flow. Experimental evidence for viscoelasticity is creep, stress relaxation and mechanical damping. Experimentally, thus, **viscoelasticity** is characterised by **creep** (creep compliance), **stress relaxation** (stress relaxation modulus) and by **dynamic mechanical response** (the storage and loss moduli).

Mathematical equations to describe the **stress-strain behaviour** of the linear viscoelastic materials may be derived by using **simple mechanical models** consisting of **springs** and **dashpots**. The spring represents an elastic solid (obeying Hooke’s law in its mechanical behaviour) and the dashpot, containing oil that behaves as Newtonian fluid, represents viscous liquid.



The spring and dashpot can be arranged simply in series or in parallel to illustrate the linear-viscoelastic behaviour. The assumptions for linear-viscoelastic behaviour:

- 1) Elastic strain and rate of viscous flow are directly proportional to stress.
- 2) Total deformation and stress are the arithmetic sum of viscous and elastic contributions, which may be treated independently.

5.2.1 Voigt (Kelvin) Model

Voigt model (Figure 5.3) consists of a parallel combination of a spring and a dashpot. The model at best describes the creep behaviour of a real material.

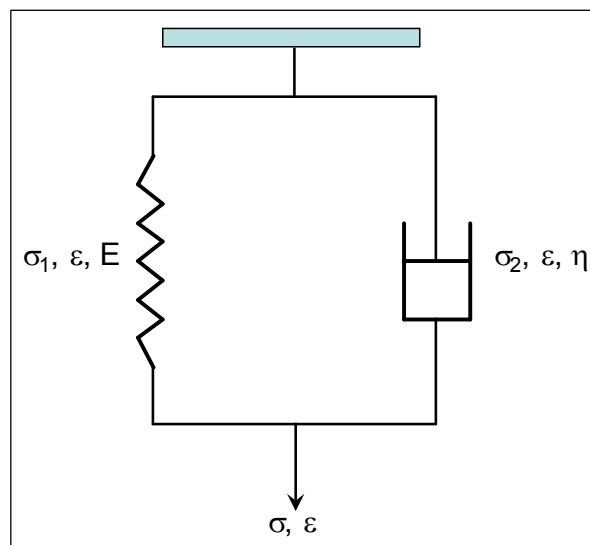


Figure 5.3 Voigt model, subjected to stress (σ) and strain (ε)

When loaded externally the model is assumed to undergo a uniform strain (iso-strain), i.e., the model and its components experience the same strain.

The stress (σ) - strain (ε) equations:

for the spring, $\sigma_1 = E\varepsilon$

for the dashpot, $\sigma_2 = \eta (d\varepsilon/dt)$

for the Voigt model, $\sigma = \sigma_1 + \sigma_2 = E\varepsilon + \eta (d\varepsilon/dt)$ (Equation 5.1)

Note that: in **creep testing** σ is constant, and ε is time dependent and therefore expressed as a function of time, i.e., $\varepsilon(t)$. Material compliance (inverse of modulus) can be determined with creep testing.

Rearranging Equation 5.1:

$$\frac{d\varepsilon}{dt} + \varepsilon \frac{E}{\eta} = \frac{\sigma}{\eta}$$

In terms of a time parameter (**retardation time**), $\tau = \frac{\eta}{E}$

$$\frac{d\varepsilon}{dt} + \frac{\varepsilon}{\tau} = \frac{\sigma}{\eta}$$

The differential equation (as expressed in Equation 5.1) can be solved as below to determine $\varepsilon(t)$:

$$\sigma = E\varepsilon + \eta (d\varepsilon / dt) \text{ or } \sigma - E\varepsilon = \eta (d\varepsilon / dt)$$

Rearranging gives:

$$(dt / \eta) = d\varepsilon / (\sigma - \varepsilon E); \text{ multiplying across by } (-E):$$

$$-E(dt / \eta) = -E[d\varepsilon / (\sigma - \varepsilon E)]; \text{ integrating:}$$

$$-E(t / \eta) = \ln(\sigma - \varepsilon E) + C.$$

Where C is the constant of integration and it can be determined by substituting initial conditions: at $t = 0$, $\varepsilon(t) = 0$, therefore $C = -\ln\sigma$.

Substituting back for C, and also for $\eta / E = \tau$:

$$-t / \tau = \ln[(\sigma - \varepsilon E) / \sigma], \text{ or } [(\sigma - \varepsilon E) / \sigma] = e^{(-t/\tau)}.$$

$$\therefore \varepsilon(t) = (\sigma/E) [1 - e^{(-t/\tau)}].$$

At $t = \tau$, $\varepsilon(t) = 0.63 (\sigma/E)$ i.e., at retardation time τ , an approximately 63% of the final deformation (viz. σ/E) occurs. τ is a characteristic material response time.

The Voigt mechanical analogue of viscoelastic behaviour is used in many engineering applications such as the shock absorbers on a mountain bike (Figure 5.4).



Figure 5.4 Shock absorber on a mountain bike frame (courtesy of www.chainreactioncycles.com)

5.2.2 Maxwell Model

In the Maxwell model (Figure 5.5) a Hookean spring and a Newtonian dashpot are linked together in series. The model at best gives only a simple description of the stress-relaxation of a viscoelastic material.

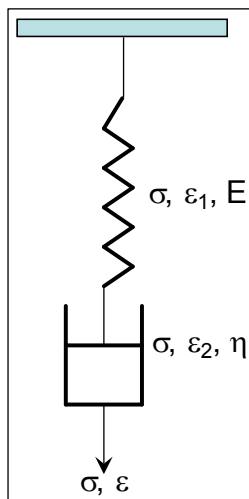


Figure 5.5 Maxwell model, subjected to stress (σ) and strain (ϵ)

Stress-relaxation behaviour of a material is similar to its creep behaviour, however, for stress relaxation measurement the material is applied a given (fixed) strain, ϵ , and stress, σ , to maintain this strain is measured as a function of time, and a relaxation modulus is determined.

The Maxwell model is assumed to undergo a uniform stress (iso-stress), i.e., the model and its components experience the same stress.

The stress (σ) - strain (ϵ) equations:

for the spring, $\epsilon_1 = \sigma/E$ or $d\epsilon_1 / dt = (1/E) (d\sigma/dt)$

for the dashpot, $(d\epsilon_2/dt) = \sigma / \eta$

for the Maxwell model, $d\epsilon/dt = (d\epsilon_1/dt) + (d\epsilon_2/dt) = (1/E) (d\sigma/dt) + \sigma / \eta$ (Equation 5.2)

The **condition** for the **stress-relaxation** experiment is that ϵ is kept constant, therefore, $d\epsilon/dt = 0$.

Substituting $d\epsilon/dt = 0$ in Equation 5.2 for the model gives:

$(1/E) (d\sigma / dt) + \sigma/\eta = 0$, rearranging

$(d\sigma/\sigma) = -(E/\eta) dt$ and integrating gives:

$\ln\sigma = -(E/\eta) t + c$

where c is the constant of integration, or:

$$\sigma = C e^{(-tE/\eta)}$$

When $t = 0$, $\sigma = \sigma(0)$, i.e., the initial stress. Substituting in the above equation gives $C = \sigma(0)$.

Substituting back for C , and also for $\eta/E = \tau$:

$$\sigma(t) = \sigma(0) e^{(-t/\tau)} \text{ or as a modulus } E(t) = [\sigma(0)/\epsilon] e^{(-t/\tau)}$$

where, **(the relaxation time)** =

At $t = \tau$, $\sigma(t) = (1/e) \sigma(0) \approx (1/2.7) \sigma(0)$, i.e., stress decays (or relaxes) down to approximately 37% of the initial stress value after a period of time known as the relaxation time.

5.2.3 Shortcomings of the simple mechanical models

The Maxwell model describes the stress-relaxation behaviour by the equation

$\sigma(t) = \sigma(0) e^{-t/\tau}$. The graphical representation of this prediction is shown in Figure 5.6.

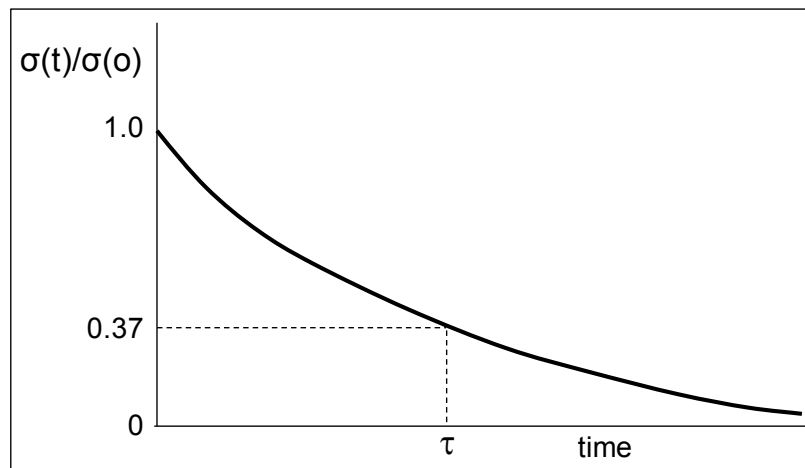


Figure 5.6 Stress (σ) vs. time (t) for a Maxwell model

According to the model the stress relaxes down to zero after a long time ($t = \infty$). In real materials, this is not necessarily so. Therefore, in this respect, a **modified Maxwell model** (Figure 5.7) may be a more appropriate model for **actual polymers**.

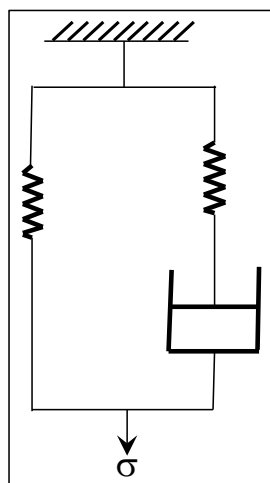


Figure 5.7 Modified Maxwell model

Furthermore, the Maxwell model is not realistic under creep conditions:

Under creep loading, $\sigma = \text{constant}$, therefore, $d\sigma/dt = 0$. Substituting this in the σ - ϵ relationship of the Maxwell model, $d\epsilon/dt = (1/E) (d\sigma/dt) + \sigma/\eta$, gives $(d\epsilon/dt) = \sigma/\eta$. The implication being that polymers behave as a viscous liquid under creep, which is not the case.

The **Voigt** model provides a very basic prediction for the creep behaviour of polymers by the equation:

—

The graphical representation of this equation is shown in Figure 5.8.

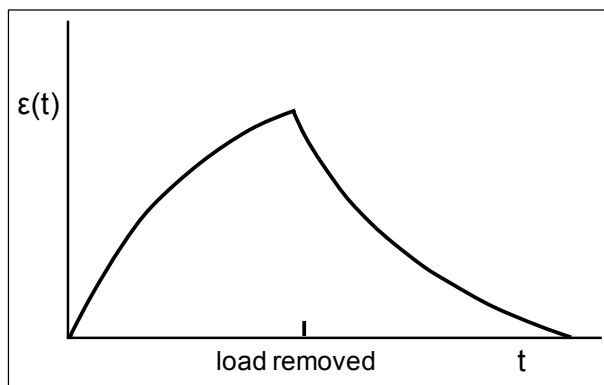


Figure 5.8 Strain (ϵ) vs. time (t) for Voigt model

The model implies that there is no elastic contribution to strain. In comparison an **experimental curve** indicates certain differences as shown in Figure 5.9.

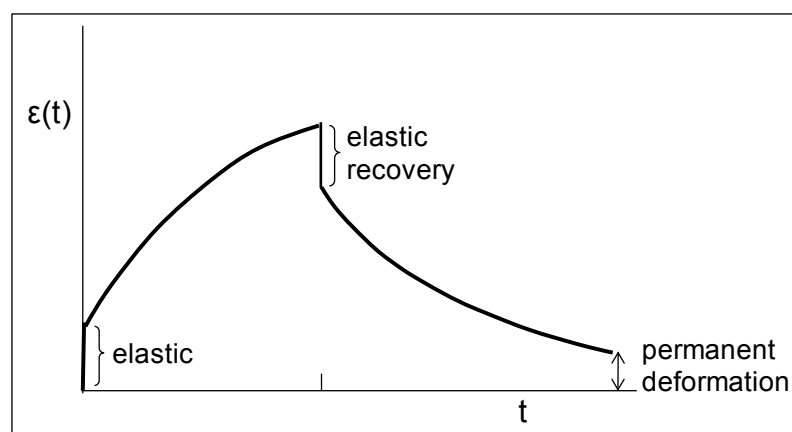


Figure 5.9 Features of a strain vs. time plot for a real specimen

The Kelvin/Voigt model needs to be **modified** to describe the creep behaviour more successfully. A comparison of the Figures 5.8 and 5.9 shows that a more accurate model needs to include elements to account for the initial elastic response of the material as well as the possibility of a permanent deformation, e.g., in the form flow of neighbouring molecular chains with respect to each other in thermoplastics. The four-element model (Figure 5.10) incorporates a spring and a dashpot in series with the Voigt unit to accommodate these two forms of deformations.

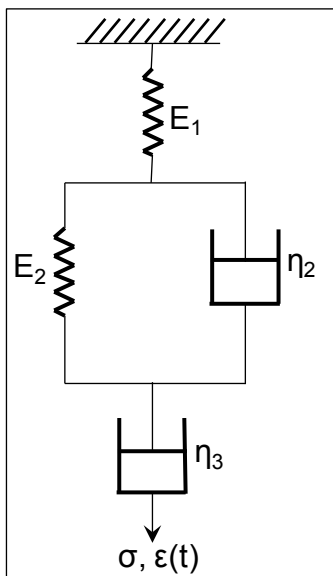


Figure 5.10 Illustration of the four-element model

Therefore the equation of the four-element model becomes:

— — —

Another short coming of the **Voigt model** is that it fails to describe the **stress-relaxation** behaviour of polymers. For stress relaxation $d\varepsilon/dt = 0$. Substitution of this condition in the Voigt model equation, — — — yields $\sigma = E\varepsilon$, which is the description of an elastic rather than viscoelastic material.

5.2.4 Dynamic mechanical thermal behaviour

Modulus measurements under dynamic conditions (e.g., sinusoidally oscillating strain and stress) can indicate the viscoelastic nature of polymers, i.e., the modulus term includes elastic and viscous components or real and loss parts.

When a viscoelastic material is subjected to a sinusoidally varying deformation (strain), the resultant stress produced in the material will also alternate sinusoidally, but will be out of phase by an angle δ , which is between 0 and $\pi/2$. Figures 5.11 and 5.12 show sinusoidally varying stress and strain curves for elastic and viscoelastic behaviours, respectively.

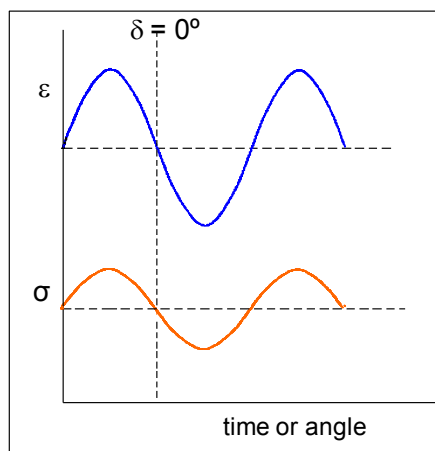


Figure 5.11 Illustration of in-phase ($\delta = 0^\circ$) oscillating stress (σ) and strain (ε) curves

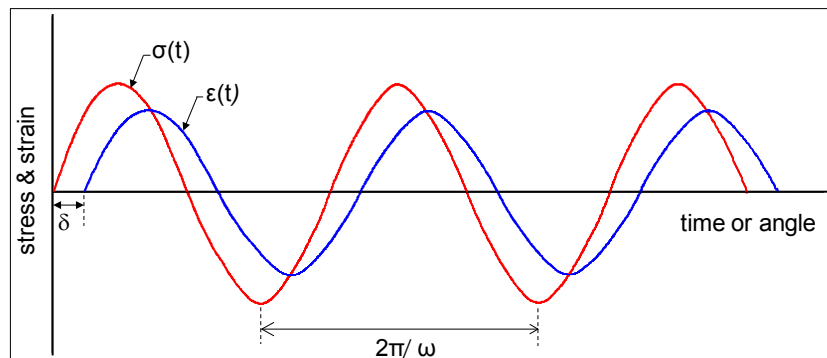


Figure 5.12 The variation of stress and strain with time for a viscoelastic material

The applied sinusoidal strain can be expressed as:

$$\varepsilon = \varepsilon_0 \sin \omega t$$

where, ε_0 is the maximum strain amplitude, ω is the angular frequency (radians per second), and t is time.

The resultant stress in the specimen is:

$$\sigma = \sigma_0 \sin(\omega t + \delta) \text{ or}$$

$$\sigma = \sigma_0 (\cos\delta \sin(\omega t) + \sin\delta \cos(\omega t)).$$

This equation implies that the stress can be separated into two components: **in phase** with strain (with a stress amplitude of $\sigma_0 \cos \delta$), and $\pi/2$ **out of phase** with strain (with a stress amplitude of $\sigma_0 \sin \delta$).

When these in-phase and out-of-phase stress amplitudes are divided by the strain amplitude ε_0 , two moduli terms emerge.

$$E' = \frac{\sigma_0 \cos \delta}{\varepsilon_0}; \quad E'' = \frac{\sigma_0 \sin \delta}{\varepsilon_0}$$

The relationship between the terms E' and E'' can be shown diagrammatically:

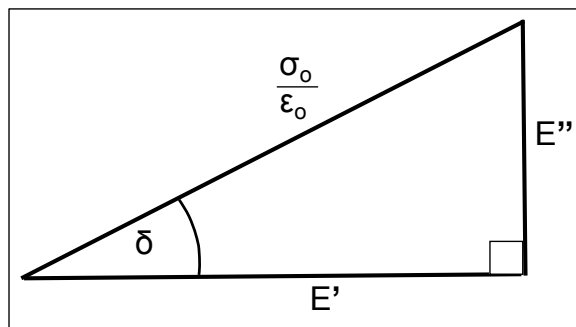


Figure 5.13 Geometric relationship between the terms E' and E''

The diagram shown in Figure 5.13 resembles an Argand diagram for a complex number and, therefore, suggests a **complex number** representation for the moduli terms such that E' and E'' are the **real** and **imaginary parts** of a **complex number** E^* . Accordingly

$$E^* = E' + i E''$$

where, E^* is described as the complex modulus, E' is the real (or the storage) modulus, and represents the elastic component of viscoelastic behaviour, E'' is the loss modulus (an energy dissipation term), and represents the viscous component of the viscoelastic behaviour, and “ i ” is the imaginary number ($i^2 = -1$).

The Argand diagram for the complex term E^* , and an indication of the level of viscoelasticity for some materials is shown in Figure 5.14, where $|E^*| = \sigma_0 / \varepsilon_0$ is the magnitude or the absolute value of E^* .

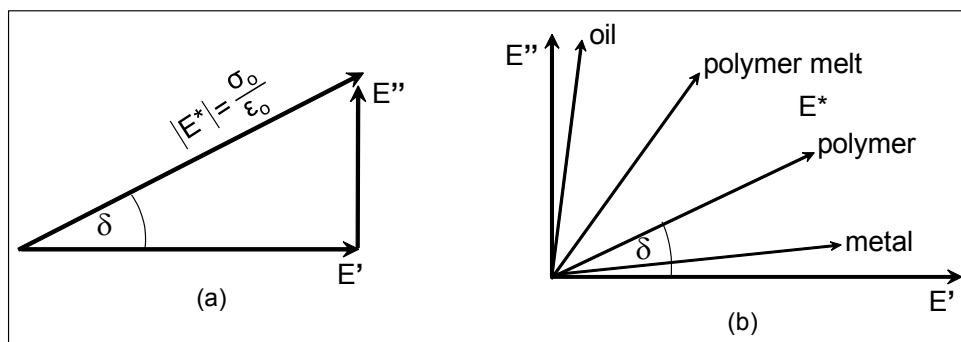


Figure 5.14 (a) Argand diagram, (b) levels of viscoelasticity in substances

The angle, δ , which reflects the time lag between the applied stress and strain can be expressed as a ratio, known as the **energy dissipation factor** or a **damping term** or the **loss tangent** such that;

$\tan \delta = E''/E'$ (i.e., the fraction of energy dissipated during each cycle of the oscillations). Damping is a consideration in engineering applications such as anti-vibration engine/motor mountings, sound attenuation, smooth movement in artificial bio-limbs, earthquake anti-tremor mountings and bridge bearings (the runaway vibrations experienced at the inaugural opening of the Millennium Bridge in London was solved by mounting dampers onto the Bridge: sparing the Millennium Bridge's blushes). Dampers are used to stop piano strings/wires from continuing to ring after moving to a new note.

Dynamic mechanical tests conducted over a wide temperature and frequency range are especially sensitive to the chemical and physical structure of polymeric materials. These tests are the most sensitive tests for studying relaxation transitions such as **glass transitions** and **secondary glass transitions** in polymers.

The instruments for dynamic mechanical thermal testing, which should produce at least a damping term and the real modulus term, may be based on **free vibration**, **resonance forced vibration**, **non-resonance forced vibration**, and **wave or pulse propagation**. Basic principles of some of these instruments are presented below.

Torsional pendulum is a free-vibration instrument and produces a decaying trace of amplitudes of vibration with time (Figure 5.15). Successive amplitudes, A_n , decrease because of the gradual dissipation of the energy into heat.

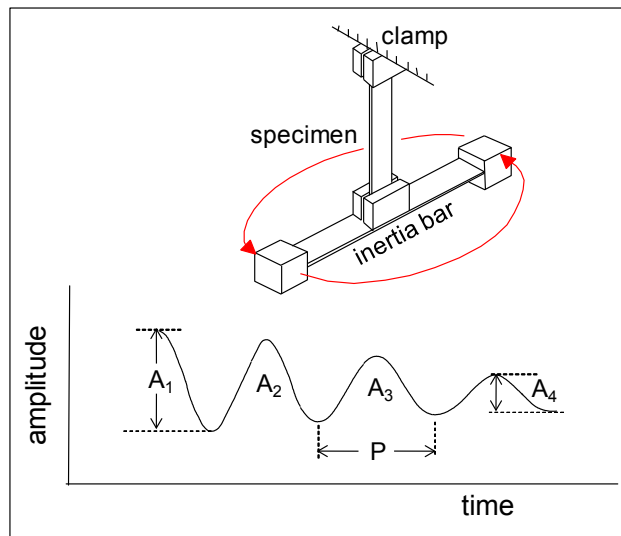


Figure 5.15 Sketch of a torsion-pendulum and amplitude of oscillations (source: Nielsen 1974, p15)

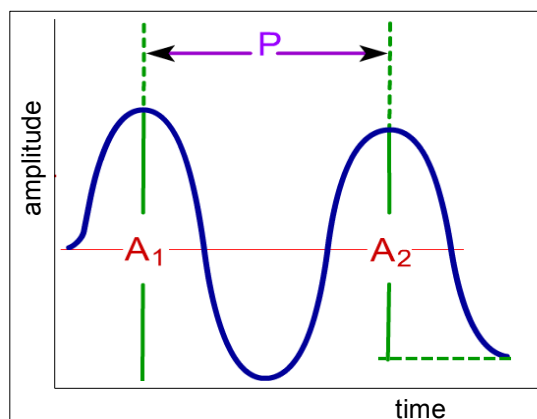


Figure 5.16 A magnified segment of the torsion amplitude vs. time trace

The **logarithmic decrement**, Δ , is a damping term that can be determined from the dynamic mechanical measurements (see Figures 5.15 and 5.16) generated on a torsion-pendulum

$$\Delta = \ln \frac{A_1}{A_2} = \ln \frac{A_2}{A_3} = \dots = \ln \frac{A_{(i-1)}}{A_i}$$

The **real modulus**, E' , can be determined using an equation which incorporates the specimen dimensions and the period (P) of the oscillations.

Vibrating reed instruments are based on forced resonance vibration: if a strip of material is excited electro-statically at different frequencies, using an audio-frequency oscillator. The specimen would respond by vibrating when the frequency of excitation approaches its resonance frequency. When the frequency reaches the natural resonance frequency of the specimen, the amplitude of the vibration of the free end of the specimen will go through a maximum. It is possible to obtain a plot of the resonance peak (i.e., an amplitude of vibration vs. frequency curve, see Figure 5.17).

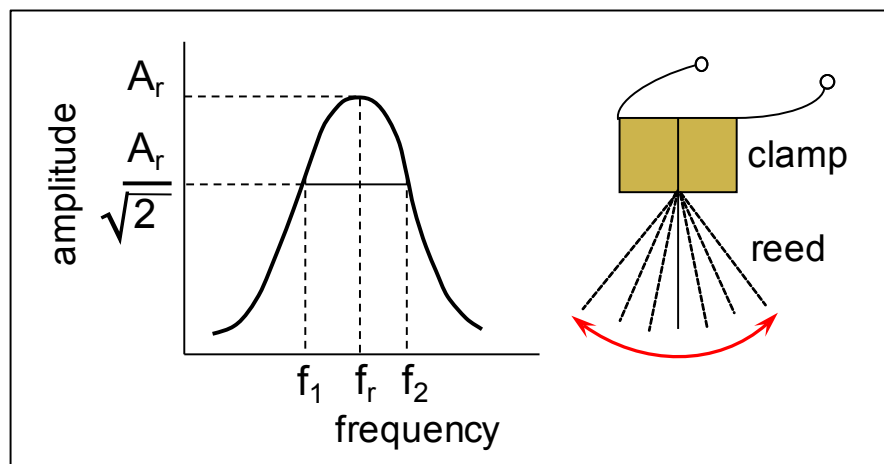


Figure 5.17 Resonance curve for the vibrating reed

The **damping** and the **real modulus** terms can be determined from the **band-width**, $f_2 - f_1$, and the **resonance frequency**, f_r , of the vibrations such that:

$$\tan \delta = \frac{f_2 - f_1}{f_r} \approx \frac{E''}{E'}, \quad \text{and} \quad E' \propto f_r.$$

Forced vibration, nonresonance, instruments, where often a flat specimen is clamped at both ends and is deformed in a sinusoidal manner, are best for tests over a wide temperature range at a fixed frequency, or for tests over a frequency range at a constant temperature. Most of the commercially available equipment is of forced vibration types.

Further coverage of various aspects of this topic is presented in Section 7.4.

5.3 Relaxation transitions

The **main relaxation transitions** for **crystalline polymers** are **melting** and for **amorphous polymers** (or for the amorphous portions of the semi-crystalline polymers) **glass transition**. Properties show profound changes in the region of glass transition. Polymers that exhibit glass transition are hard, **rigid** and glass-like below a certain temperature known as the **glass-transition temperature, T_g** . Above T_g the amorphous polymers are soft and **flexible**, and become either elastomeric or a very viscous liquid. Therefore,

for rigid polymers: $T_g >$ room temperature

for elastomers: $T_g <$ room temperature.

Mechanical properties show significant changes in the region of glass transition, e.g., the elastic modulus may decrease by a factor of 1000. Most physical properties (thermal, electrical and optical) also change rapidly in the glass transition region.

T_g of a polymer can be readily determined by using **dynamic mechanical thermal analysis** data, differential scanning calorimetry or by dilatometric measurements. Figure 5.18 shows a plot of dynamic real (storage) modulus and the damping term ($\tan\delta$) over a temperature range. The plot provides clear features for identification and determination of T_g : the point of inflection in the modulus curve or the maximum point in the damping peak can be recorded as T_g .

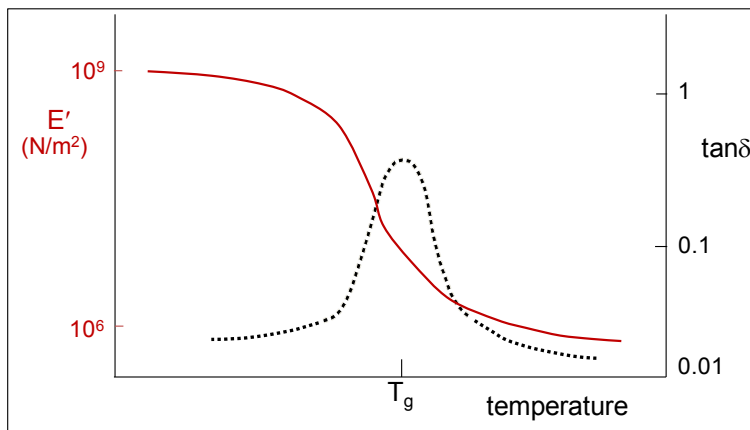


Figure 5.18 Dynamic elastic modulus and $\tan\delta$ vs. temperature

One of the basic methods of measuring glass transition temperature is **dilatometry**, where volume is measured as a function of temperature. A small piece of polymer sample of known weight is immersed in mercury in a small cylindrical glass bulb, which is attached to a graduated capillary tube. The mercury, which has a constant coefficient of thermal expansion over the temperature ranges of interest, fills part of the capillary tube as well. The dilatometer, prepared in this manner, is then placed in a water or an oil bath and heated. The rise of mercury in the capillary with temperature is recorded, which is a reflection of the expansion of the material. From this information, with calibration, the specific volume of the material can be obtained and plotted as a function of temperature. As shown in Figure 5.19, the T_g , which represents a second-order transition, is therefore the temperature where the volume-temperature curve changes slope.

Melting, however, is a first-order transition and produces a clear step/discontinuity change in specific volume at the melting point (T_m). Sometimes the change in slope is not very distinctive and, therefore, to identify the transition temperature more clearly a plot of the coefficient of thermal expansion, which is the derivative of the specific volume with respect to temperature, against temperature is plotted as in Figure 5.20 and produces a discontinuity or an abrupt change at T_g .

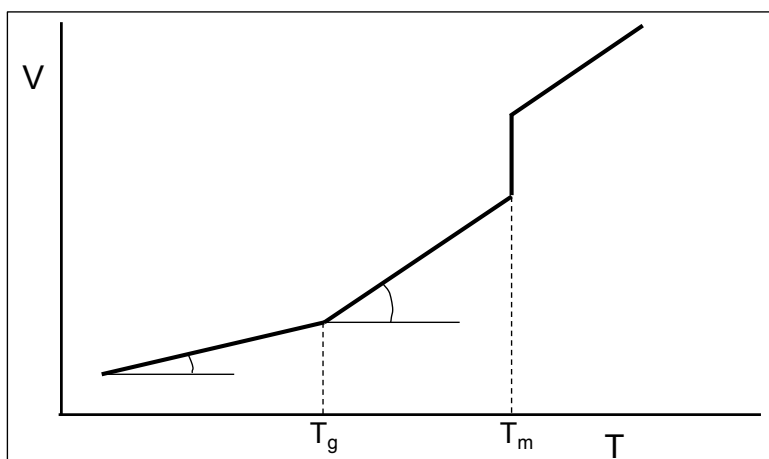


Figure 5.19 A plot of specific volume (V) vs. temperature (T) for a semi-crystalline polymer

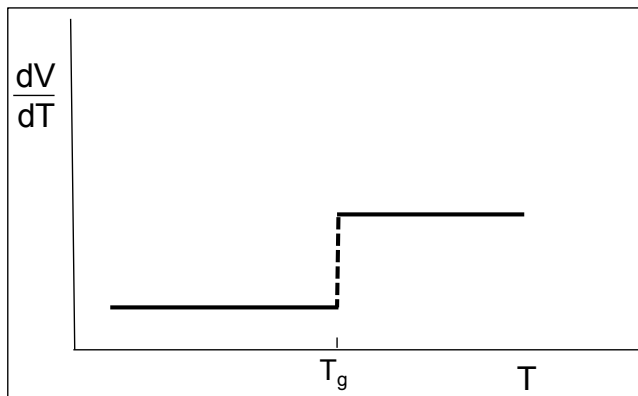


Figure 5.20 A plot of (dV/dT) vs. T

5.3.1 Dependence of T_g and T_m on chemical structure

In general any structural feature, which encourages intra molecular (i.e., within a single molecule) and inter molecular (in between molecules) motions yields low T_g and T_m and, conversely, structural features that hinder molecular motion cause an increase in T_g and T_m .

5.3.1.1 Molecular weight

Molecular weight influences both the molecular chain length and the number of molecule chains. A polymer with shorter chains will have more chain ends per unit volume, so there will be more **free volume** to accommodate molecular motion. Hence the T_g for a thermoplastic with shorter molecular chains will be lower than if the chains were longer as illustrated in Figure 5.21.

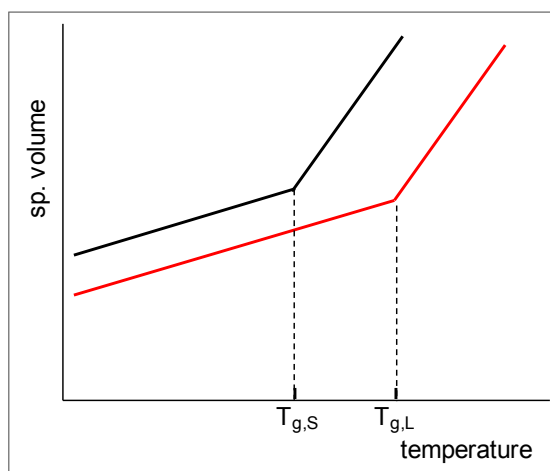


Figure 5.21 Plot of specific volume vs. temperature for short (S) and long chain (L) molecules

5.3.1.2 Composition of the backbone molecular chain

- Structure of the repeating unit:

Backbone chains with **aliphatic groups**, e.g., $-\text{CH}_2-\text{CH}_2-$ or the replacement of some of the “C” atoms by “O” (as in ether links) builds **flexibility** into a polymer, because of ease of rotation about these groups, and lowers T_g and T_m .



Conversely, **aromatic back-bone chains** (i.e., benzene rings in the chain) cause **stiffness**, for example:

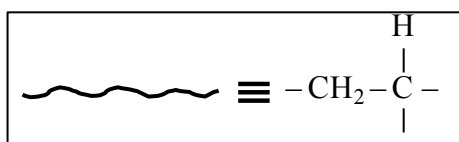
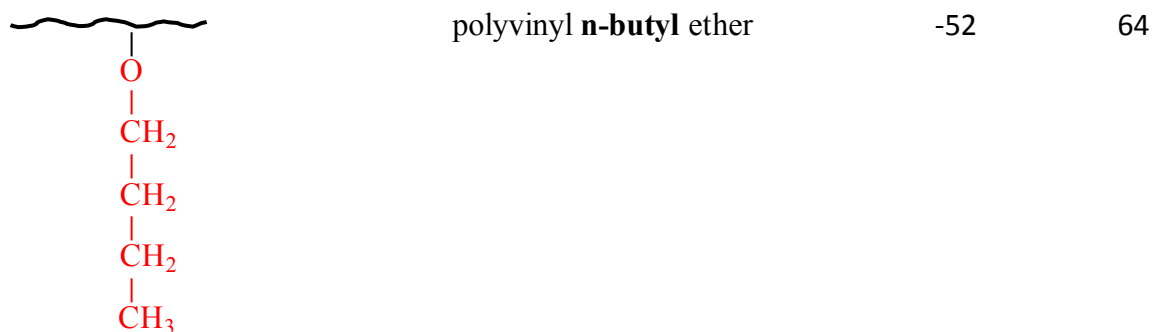
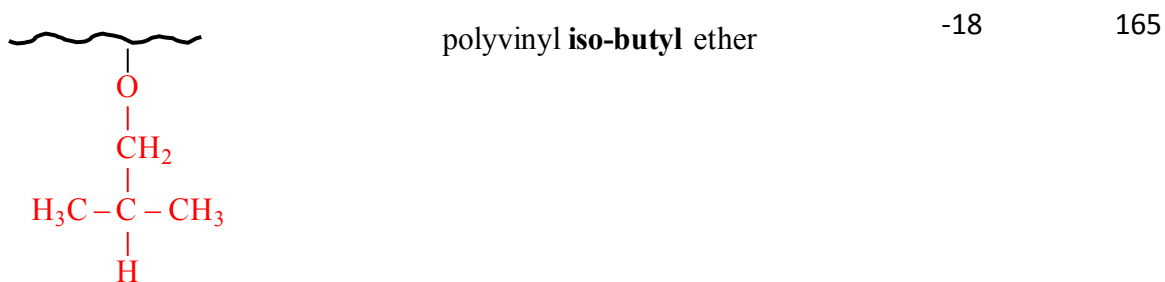
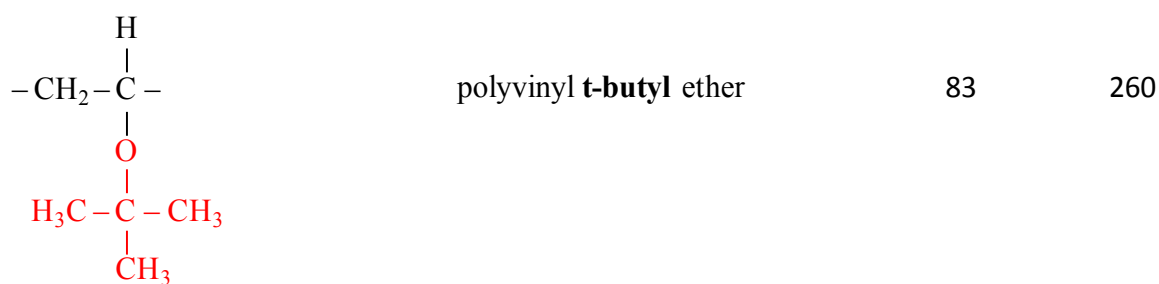
- Repeat-unit lengths and intermolecular forces:

The frequency of repeat-unit links, and the frequency and the type of intermolecular bonding (e.g., Van der Waals forces or **H-bonds**) influences T_g and T_m . In nylons, in spite of an aliphatic backbone, intermolecular H-bonds that are much stronger than Van der Waals forces hold neighbouring chains strongly together and also tend to stabilise the crystallites, therefore result in high T_g and T_m values. The melting temperature of nylons decrease as the frequency of H-bonding decreases, for example, the melting temperature of Nylon 4,6 (295 °C) > Nylon 6,6 (265 °C) > Nylon 6,10 (223 °C) > Nylon 10,10 (203 °C) , etc.

5.3.1.3 Side groups

Bulky, inflexible (rigid) side groups increase T_g and T_m by restriction of bond rotation and main chain stiffening, but **long flexible** aliphatic side groups decrease T_g and T_m . Rigid groups include aromatic and/or cyclic structures or tertiary isomeric forms.

<u>Repeat-unit</u>	<u>Polymer</u>	<u>T_g, °C</u>	<u>T_m, °C</u>
$\begin{array}{c} \text{H} \\ \\ -\text{CH}_2-\text{C}- \\ \\ \text{CH}_3 \end{array}$	PP (isotactic)	-10	170
$\begin{array}{c} \text{H} \\ \\ -\text{CH}_2-\text{C}- \\ \\ \text{C}_6\text{H}_5 \end{array}$	PS (isotactic)	100	240



t – tert or tertiary

5.3.1.4 Molecular polarity

The presence of **polar groups** such as $-\text{Cl}$, $-\text{OH}$ or $-\text{CN}$ tends to raise T_g and T_m more than non-polar groups of equivalent size. The polar interactions restrict main-chain mobility further by promoting additional intermolecular forces.

<u>Repeat-unit</u>	<u>Polymer</u>	<u>T_g, °C</u>	<u>T_m, °C</u>
$\begin{array}{c} \text{H} \\ \\ -\text{CH}_2-\text{C}- \\ \\ \text{CH}_3 \end{array}$	PP (isotactic)	-10	170
$\begin{array}{c} \text{H} \\ \\ -\text{CH}_2-\text{C}- \\ \\ \text{OH} \end{array}$	polyvinylalcohol	85	230
$\begin{array}{c} \text{H} \\ \\ -\text{CH}_2-\text{C}- \\ \\ \text{Cl} \end{array}$	PVC	87(81)	227 (273)
$\begin{array}{c} \text{H} \\ \\ -\text{CH}_2-\text{C}- \\ \\ \text{CN} \end{array}$	polyacrylonitrile (syndiotactic)	104 (130)	317

5.3.1.5 Backbone molecular symmetry

Symmetry facilitates rotation about the backbone molecular chain and, thus, causes a drop in T_g and T_m.

<u>Repeat-unit</u>	<u>Polymer</u>	<u>T_g, °C</u>	<u>T_m, °C</u>
$\begin{array}{c} \text{H} \\ \\ -\text{CH}_2-\text{C}- \\ \\ \text{CH}_3 \end{array}$	PP (isotactic)	-10	170
$\begin{array}{c} \text{CH}_3 \\ \\ -\text{CH}_2-\text{C}- \\ \\ \text{CH}_3 \end{array}$	polyisobutylene	-70	128

$ \begin{array}{c} \text{H} \\ \\ -\text{CH}_2-\text{C}- \\ \\ \text{Cl} \end{array} $	PVC	87(81)	227 (273)
$ \begin{array}{c} \text{Cl} \\ \\ -\text{CH}_2-\text{C}- \\ \\ \text{Cl} \end{array} $	polyvinylidene chloride	-19	190 (198)

As shown in the above sections, the same factors tend to raise or lower both T_g and T_m , i.e., they are related and an empirical rule exists for many polymers:

$$\frac{T_g}{T_m} = 0.5 \text{ to } 0.8 \text{ when the temperature is in } ^\circ\text{K}.$$

≈ 0.5 for symmetrical polymers, e.g., PE.

≈ 0.8 for unsymmetrical polymers, e.g., PS.

5.3.2 Secondary glass transitions

Nearly all tough ductile polymers with high impact strength exhibit prominent secondary glass transitions, e.g., polycarbonates, nylons, PVC, polysulphones, poly(ethylene terephthalate)s and epoxy resins. Secondary glass transitions are mainly associated with the motions of side groups or the backbone chain motions over short segments, and therefore require less energy and occur at lower temperatures than the main (primary) glass transition.

5.3.3 Ways of controlling T_g

Crosslinking increases T_g of a polymer by introducing restrictions on the molecular motions of the backbone chains. **Plasticisation** and **copolymerisation** also affect T_g and T_m as illustrated in Figure 5.22 for a thermoplastic.

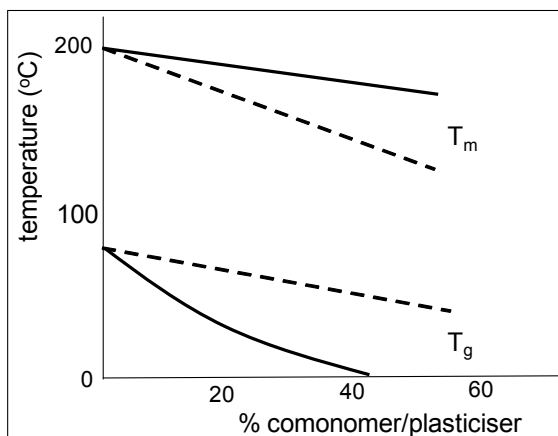
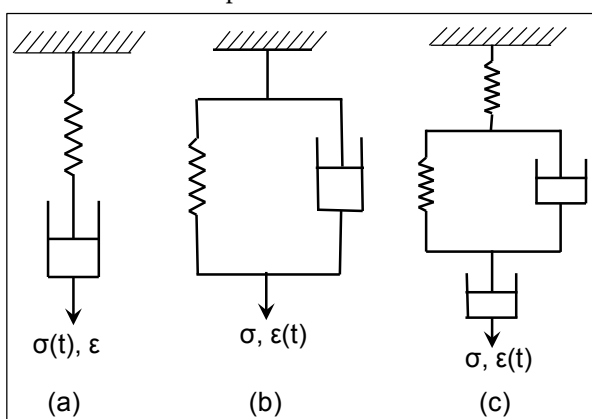


Figure 5.22 Transition temperatures vs. % comonomer (---) or % plasticiser (—) content

5.4 Self-assessment questions

1. Consider the following mechanical models, which of these models is not appropriate for describing the delayed elastic response that is characteristic of creep behaviour?



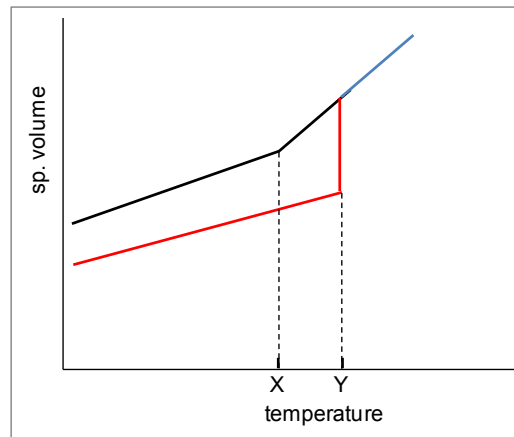
2. Which of these models (in Question 1) is not appropriate for describing stress relaxation?
3. Which of these models (Question 1) would best give a description of viscoelastic behaviour in terms of a spectrum of relaxation times?

4. The relationship below holds for the Maxwell model

$$\sigma + \tau \dot{\sigma} = E \dot{\epsilon}$$

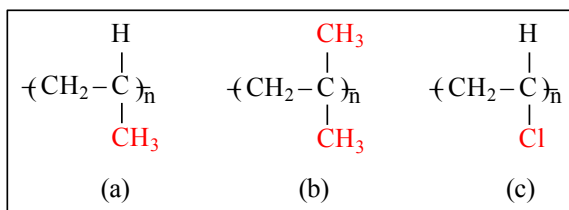
In a stress relaxation experiment which one of the following equations can be derived from this?

- i. $\epsilon = \frac{\sigma_0}{E} (1 - e^{-t/\tau})$
 - ii. $\sigma = \sigma_0 e^{-(t/\tau)}$
 - iii. $J = J_0 \{1 - \exp(-t/\tau)\}$, where J is the compliance and $\tau = \eta/E$
 - iv. $\sigma = E\epsilon$
5. Using the appropriate equation from Question 4, determine the relaxation time for a viscoelastic material that is subjected to an initial stress of 3.5 MPa, which drops to 1.5 MPa after 60 seconds.
Answer: $\tau = 70.8$ s.
6. The strain equation of a Kelvin model is $\epsilon(t) = (\sigma/E_2) (1 - e^{-t/\tau})$.
Draw a sketch of a modified Kelvin model that has the strain equation of
$$\epsilon(t) = \sigma/E_1 + (\sigma/E_2) (1 - e^{-t/\tau})$$
7. Immediately after applying the stress to the modified Kelvin model the strain is 0.001; after 1500 s the strain is 0.004; after a very long time the strain tends to 0.006. Determine the time parameter τ ?
Answer: $\tau = 1638$ s.
8. A strip of elastomer was stretched in tension and elongation was held constant. After 10 min the tensile stress in the specimen dropped by 12%. Assuming that the elastomer behaves in accordance with the Maxwell model:
- calculate the relaxation time (to the nearest whole number) (*answer: $\tau = 78$ min*)
 - show that it takes 22 min for the stress to drop to 75% of its initial value.
9. If you hang a weight from a strip of rubber so that it stretches about 300%, then heat the rubber, which of the following would happen?
- stretches some more
 - contracts
 - maintains the same length
10. Consider the two transitions from the 'solid' to the liquid or rubbery state shown below on a plot of specific volume vs. temperature. State 'true' or 'false':

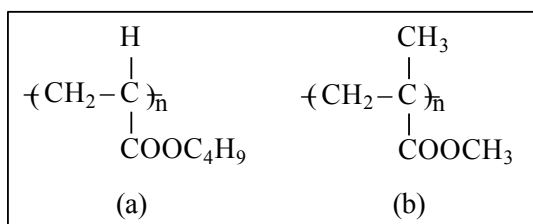


- a) the transition X is a T_g while transition Y is a crystalline melting point
- b) Y is the T_g while X is the T_m
- c) X and Y are melting points, but X is the T_m of a semi-crystalline material and Y is the T_m of an almost perfect crystal.
11. Which of the following statements are true?
- a) all polymers have a crystalline melting point
- b) all polymers have a glass transition
- c) the glass transition is a first order transition that occurs at a well defined temperature
- d) the crystalline melting point is not affected by the presence of solvent.

12. Consider the following polymers, which will have the lowest T_g ?



13. Which of the polymers in Q. 12 is polar in nature?
 14. Name polymer (c) in Q. 12.
 15. Poly(n-butyl acrylate) (a) has a lower T_g than poly(methyl methacrylate) (b), because of:



- a) weaker intermolecular attractions
 b) free volume effects due to the flexible side chain
 c) the stiffness of the side chain.
16. The general chemical structure of aliphatic polyamides is given as
- $$-\text{NH}-(\text{CH}_2)_x-\text{NHCO}-(\text{CH}_2)_y-\text{CO}-$$

Three specific nylons have values of $(x = 4, y = 6)$, $(x = 6, y = 6)$ and $(x = 10, y = 10)$; indicate which one of these nylons has the lowest and which the highest melting point.

17. A plot of DMTA damping term against temperature can be used to determine a temperature at which
- a) tensile strength becomes maximum
 b) the specific heat shows a minimum
 c) Young's modulus undergoes a significant drop
 d) the crystalline phase melts.
18. The presence of aromatic groups in a polymer chain results in
- a) intermolecular attraction
 b) potential for crosslinking
 c) increase in T_g and T_m
 d) tensile strength becomes maximum.
19. Plot and compare schematically, specific volume vs. temperature curves for PS and PP.
 20. Illustrate, with chemical formulae, the influence of the size of the side groups of a polymer molecule on T_g .
 21. A strip of rubber is set in motion on a torsional pendulum. The amplitude of vibrations decay by 15% after each complete cycle. Calculate the logarithmic decrement of the material.

Answer: $\Delta = 0.163$.

22. The amplitude of a torsional vibration decreases so that the amplitude on the 100th cycle is 13% of the amplitude on the first cycle. Determine the level of damping in terms of the logarithmic decrement.
Answer: $\Delta = 0.02$.
23. Describe the efficiency, in general, of copolymerisation and plasticisation in lowering melting points and the glass transition temperatures of polymers.
24. Briefly explain the shortcomings of a Maxwell mechanical model in describing the real behaviour of polymeric materials.
25. Which of these polymer(s), PE, PS, PMMM, PC, would be best suited for use as ice cube trays? Why?
26. Plot specific volume against temperature, on the same graph, for two polyethylenes, one with 0.99 specific gravity and 3000 degree of polymerisation (DP), and the other of 0.92 specific gravity and 2000 DP.
27. At room temperature, classify the following materials as elastomers, TP or TS polymers:
- a lightly cross-linked copolymer with $T_g = -45\text{ }^\circ\text{C}$
 - a branched polypropylene of $T_g = -8\text{ }^\circ\text{C}$
 - epoxy resin matrix in advanced composites
28. Indicate true or false:
- Aliphatic molecular backbones, such as $-\text{CH}_2 - \text{CH}_2 -$ in polymers increase T_g and lower T_m .
 - Aromatic backbone chains (e.g., benzene rings in the chain) cause stiffness, thus, increase T_g and T_m .
 - Presence of elements O or Si or both in the backbone chain impart flexibility and, thus, lower both T_g and T_m .
 - None of these are accurate.
29. How is the process of degradation in polymers described as?
- viscoelastic
 - physiochemical
 - electrochemical
 - corrosion
30. Indicate true or false:
- Polystyrene has an aliphatic side group and thus its $T_g = 100\text{ }^\circ\text{C}$
 - Plasticised PVC has a $T_g < 25\text{ }^\circ\text{C}$
 - T_g of an ordinary PVC is below $0\text{ }^\circ\text{C}$
 - The chemical formula of polypropylene is $\dots - \text{CH}_2 - \text{CH}_2 - \dots$
31. A comparison of the primary and the secondary glass transitions in polymers indicate that the secondary glass transitions
- occur at a lower temperature
 - occur at a higher temperature
 - improve impact performance in otherwise rigid plastics
 - exhibit a higher intensity of energy dissipation

6 Mechanical properties

“Satisfaction of one’s curiosity is one of the greatest sources of happiness in life.” **Linus Pauling**, 1901-1994.

Although a Nobel Laureate in Chemistry, Linus Pauling’s sentiment applies to all subjects in education, particularly to an interdisciplinary subject such as materials, which combines chemistry, physics and engineering. With various chemical compositions, microstructures, processes and properties, there is so much material to be curious about. A healthy curiosity should generate a satisfactory outcome of how best to use materials so as to benefit from the wide range of properties they possess.

6.1 Introduction

The properties of materials have been classified (Brown, 1996) as fundamental properties, apparent properties and functional properties. He distinguishes them using the example of strength. Fundamental strength of a material is that measured in such a way that the result becomes independent of test conditions. Apparent strength is that obtained by a method that has completely arbitrary conditions so that the data cannot be simply related to other conditions or specimen geometry. This classification applies to all kinds of properties (mechanical, electrical, chemical and thermal).

It is important to be aware of the purpose of testing: in establishing design data, it is mostly fundamental properties that are needed, but most mechanical tests give apparent properties. In the absence of established and verified procedures for extrapolating results to other conditions, multipoint data have to be produced under conditions likely to influence the test result. Consequently, reliable tables of properties for designers are difficult and expensive to establish

Standard test methods, giving apparent properties, are best suited for quality control, and only in relatively few cases are they ideal for design data. In recent years, the drive towards international standards has led to a close examination of long-established test methods, and it has been found that the reproducibility of many of the tests was poor. This in turn has not led to new tests but rather to the establishment of better standardisation of test procedures. There has also been a growing realisation of the need to calibrate test equipment with proper documentation of calibration procedures and results (James 1999, p8).

There has been an increase in tests on actual products, which has resulted from a greater demand to prove product performance, and from specifications more often including such tests as part of the requirements.

A test report should include information regarding the production/ preparation of the material being tested and its storage history, as well as the more obvious parameters such as test temperature and speed of test. While it is recognized that the result obtained depends on the conditions of the test, it is not always obvious that some of these conditions may have been established before the samples were received for testing. Sometimes the history of the samples is part of the test procedure, as in aged and unaged samples for example, but at other times it may not be at all clear that certain 'new' samples are already several months old, with their intervening history unknown. Degradative influences such as the action of ozone on rubber samples cannot be compensated for, but standard conditioning procedures are designed, as far as possible, to bring test pieces to an equilibrium state. The imposition of a standard thermal history before measuring the density of a crystalline polymer is a good example.

Equally test piece geometry is important, and again if comparison is to be made, a standard and specified geometry should be adhered to. Rarely is it possible to convert from one geometry to another, since polymers are complex materials. The moulding conditions for the preparation of standard specimens, for example, by injection or compression moulding, should be taken into consideration. When prepared by injection moulding, the specimens will have molecular orientation and/or fibre orientation (Akay & Barkley 1991) in reinforced mouldings with respect to the melt-flow direction. This means that many properties will be anisotropic.

Tests should be designed and conducted in a manner that allows the application of statistical principles to test results. The accuracy of the quoted results depends not only on the accuracy of the original measurements but also on the validity of the data handling. The subject is comprehensively covered by Veith (1999) in Chapter 3 of Handbook of Polymer Testing.

Engineering properties must always be accompanied by their appropriate units: the internationally recognised system of unit is the Systeme **International d'Unites** (SI, often referred to as "metric"), however, the unit system customarily used in a country no less than the U.S.A. is the imperial system. Mixing these units can result in very serious consequences, and has resulted in amazing clangers being dropped by such august establishments as NASA. The destruction, for example, of the Mars Climate Orbiter in 1999 was attributed to negligence over the units of engineering data. Press coverage on 2 October, 1999 included: "Simple maths mistake that destroyed £78m Mars mission" by R Price in Daily Mail, which read, "Converting imperial measurements into metric units is not exactly rocket science. But a failure in that most basic of calculations has been blamed for the disappearance of the Mars Climate Orbiter. An investigation has found that the engineers who built the spacecraft worked in imperial measures, while the Nasa scientists who launched it used the metric system. It is a mistake that has cost British scientists 11 years of painstaking work and the American space agency Nasa £78 million."

The article further read, “The orbiter, which was carrying a batch of British experiments, was at first assumed to have smashed to pieces in the Martian atmosphere when radio contact was lost after it flew too close to the red planet last week. But Nasa experts now suspect it was bounced back into outer space. Yesterday it emerged that while one team of scientists was busily calculating how many miles the spacecraft needed to fly to reach Mars and how many pounds of thrust its engines must generate; the second was thinking in kilometres and measuring the thrust in the metric unit of newtons. It meant the orbiter was a crucial 60 miles off course at the end of its 416 million mile journey to the dark side of Mars. Confessing what went wrong, the agency’s associate administrator Edward Weiler admitted yesterday: ‘People sometimes make errors.’ That meek explanation was met with disbelief by Patrick Moore, the astronomer”

The Independent (London, England) article by Charles Arthur read, “Converting imperial measurements into metric units isn’t exactly rocket science. Maybe that’s why the folks at the US space agency, Nasa, messed it up, and so lost their £78m Mars climate orbiter spacecraft late last month. The orbiter is believed to have burned up in the Martian atmosphere 37.5 miles above its surface after crossing 416 million miles of space apparently without a hitch. Why? Because the space-crafts builder, Lockheed Martin Astronautics, provided data for its controlling thrusters to Nasa in imperial units instead of Newtons, the scientific metric unit. But at Nasa’s Jet Propulsion Lab (NJPL) the numbers were entered into a computer that assumed metric measurements.”

The Independent article poses the question, “Is there a difference? Yes. 1 pound-force, the imperial unit, equals 4.44 Newtons (sic), the metric unit. In interplanetary space, where the margins for error are huge, that made little difference. But closer to Mars, the orbiter was jockeying against the opposing forces of the solar wind, the buffeting of the atmosphere and the pull of the planets gravity. That made a big difference. Big enough to lead to the crafts destruction. Officials at Nasa and Lockheed were clearly ashamed at their failure. “In our previous Mars missions, we have always used metric,” said Tom Gavin of NJPL adding: “It does not make us feel good that this has happened” Lockheed admitted that it should have submitted the data in metric units, although it was reviewing the contracts to see whether Nasa specified any units. ...”

The properties of plastics at room temperature, in contrast to most metals, are time dependent. Superimposed on this are the effects of the level of stress, the temperature of the material, and its structure (molecular weight, molecular orientation, and crystallinity/density). In polypropylene (PP), for example, an increase in temperature from 20 °C to 60 °C may typically cause a 50% decrease in the allowable design stress. Also for each 0.001 g/cm³ change in density of PP, there is a corresponding 4% change in design stress (i.e., the allowable maximum stress that a machine part or member may be subjected to without failure). The material, moreover, will have enhanced strength in the direction of molecular alignment (that is, in the direction of flow in the mould) and less in the transverse direction (Design Council 1993, p15).

Because of the influence of so many additional factors on the behaviour of plastics, properties quoted as a single value will be applicable only for the conditions at which they are measured. The Design Council also points out that properties measured as single values following standard test procedures are useful primarily for quality control assessments. They are useless for design purposes, because to design a plastic component it is necessary to have complete information, at the relevant service temperature, on the time-dependent (viscoelastic) behaviour of the material over the whole range of stresses to be experienced by the component.

There are many useful web-based sources that provide data on the properties of polymers. CAMPUS, **Computer Aided Material Preselection** by Uniform Standards, is one of these. It is internationally acknowledged database software for plastics

materials, more than 40 plastics producers are participants of CAMPUS. The main feature of the CAMPUS database is to provide comparable data from participating suppliers. The acquisition and presentation of properties are based on the international standards of ISO 10350 for single-point data and ISO 11403-1, -2 for multi-point data.

6.2 Tensile properties

The standard methods for conducting tests to measure tensile properties of plastics include various parts of ISO 527, BS 2782, or the harmonised method under the designation of BS EN ISO 527, and ASTM D638 or its metric version D638M. Alternative methods for testing rubber include ISO 37, BS 903, ASTM D412, and for films/sheeting ASTM D882. The tests can be conducted using a universal test machine (Figure 6.1 (a)) of appropriate load capacity in the tensile setting, with suitable grips and an extensometer to enable accurate extension measurements. Extensometers can be contact (Figure 6.1 (b)) or non-contact types (video and laser devices). For further information on the principles of non-contact extensometers see Bennett (1980).

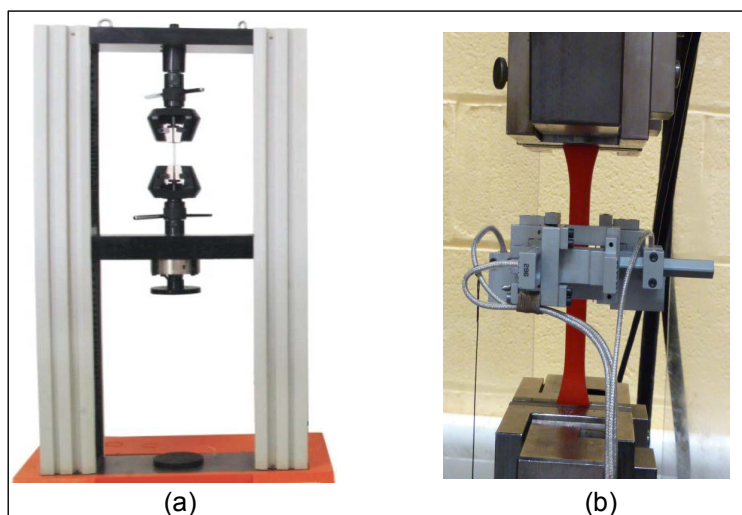


Figure 6.1 (a) a universal testing machine frame, (b) a tensile specimen with attached extensometer

Test specimens are mainly flat (sometimes cylindrical) dumbbells or flat strips: dumbbell shape is aimed at achieving failure in the narrow-waist portion of the specimen and avoid premature failure at the grips. The shape and the dimensions of the specimens vary between standards, but often aim to avoid stress concentration and/or allow for circumstances where there is limited amount of material for testing.

Important moulding conditions for the preparation of standard specimens by injection and compression moulding should be specified: when prepared by injection moulding, the dumbbell pieces will have molecular orientation along the length of the test piece and property values transverse to the orientation direction cannot be determined, unless specimens are cut from moulded plaques as described in ISO 294-5:2011.

During a test, the machine measures load or force and displacement (in this case extension) and a dedicated PC can produce force-extension plots or, by pre-loading data on the specimen dimensions, stress-strain plots (see Figures 6.2). The stress (σ) is related to force (F) and the specimen cross-sectional area (A) by $\sigma = F/A$; and extension (ΔL) and specimen

gauge length (L) to strain (ϵ) by $\epsilon = \Delta L/L$. Another parameter is the Poisson's ratio, ν , which indicates the change in the specimen cross-section as a result of axial strain and is expressed as a ratio of lateral strain to axial strain:

$$\nu = - (\Delta w/w) / (\Delta L/L)$$

where, w is the specimen width. Note that when Δw is negative, i.e., a contraction, ν becomes +ve.

For the extreme cases in isotropic materials, $\nu = -1$, when the proportions of the specimen do not change ($\Delta w/w = \Delta L/L$); and $\nu = 0.5$, when the specimen volume, V , remains constant, i.e., $\Delta V = 0$.

From $\Delta V = \Delta(AL) = L\Delta A + A\Delta L = 0$, by assuming a specimen with a square cross-section ($A = w^2$), it can be shown that $\nu = - (\Delta w/w) / (\Delta L/L) = -0.5$.

Tensile properties of Young's modulus (elastic modulus), the yield strength, the tensile strength (the maximum engineering stress, also termed the ultimate tensile strength (UTS)) and the elongation to failure can be extracted from the σ - ϵ curves. This is demonstrated in Figure 6.2, which shows a large deformation curve that includes elastic, viscoelastic and plastic deformation regions. In the elastic region, the strain is small and there is a linear relationship between stress and strain where Hooke's law holds, and material can instantly revert back to its original form when unloaded. Young's modulus, $E = \sigma / \epsilon$, is determined using the stress and strain data extracted from this elastic region. Beyond the elastic region and up to approximately the yield point, viscoelastic region, the material can recover to its original form over time.

At yield point the material begins to deform plastically, i.e., the material will undergo permanent deformation and therefore, upon the release of load only the elastic portion of the strain will recover and plastic deformation will not recover. At yield point the material begins to neck, i.e., the specimen cross-sectional area undergoes a significant reduction, further elongation causes a fall in load and, therefore, in nominal stress (engineering stress) as shown in Figure 6.2. Note that the engineering stress is computed by dividing the load with the initial cross-sectional area of the specimen and it should be distinguished from the true stress, which is computed using the actual cross-section of the specimen at the time (at the instant) during the test. Accordingly, the true stress does not decrease at necking/yielding but either remains approximately constant or rises less steeply with increasing strain, depending on the extent of cold drawing.

Cold drawing succeeds the yield point where material undergoes permanent deformation as a result of molecular slippage. Continuing extension of the waisted/narrow portion of the dumbbell specimen is achieved during drawing by causing the shoulders of the neck to travel along the specimen as it reduces from the initial cross-section to the drawn cross-section. At further elongations, the slope of the stress-strain curve increases again, due to “strain hardening”/“molecular orientation”, and finally material ruptures. These features for a tensile tested dumbbell specimen are indicated in Figure 6.3.

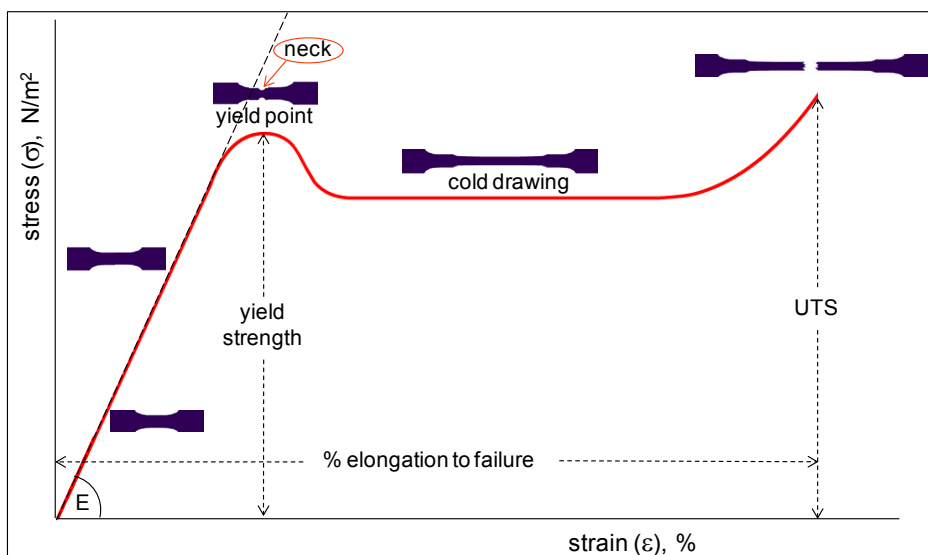


Figure 6.2 Typical stress-strain curve for a cold-drawing polymer

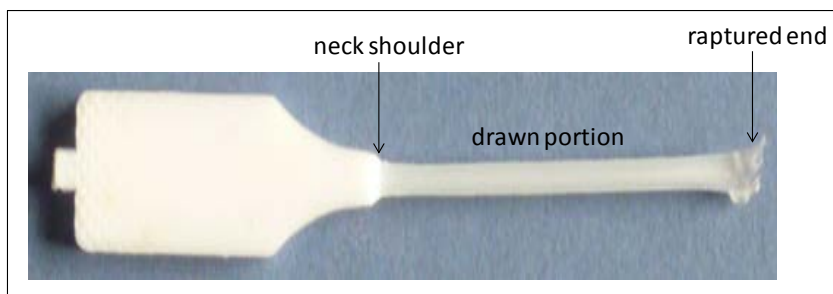


Figure 6.3 A broken half of a nylon dumbbell test piece

In the absence of a clear yield point or where the departure from the linear elastic region cannot be easily identified, an offset yield strength or proof stress is determined. The proof strength is the stress at which the stress-strain curve deviates by a given strain (offset) from the tangent to the initial straight line portion of the curve). An offset is specified as a % of strain, and it is 0.2% for metals by ASTM E8, but for plastics a higher value of 2% is also sometimes used.

Often stress-strain curves under tensile, flexure or compression may produce a spurious initial portion at the start of the curve, referred to as “toe region”, and is caused by gripping and take-up of slack in the specimen, or alignment or seating of the specimen. This artefact can be compensated as illustrated in Figure 6.4 to obtain a correct zero point for strain in order to determine accurate properties.

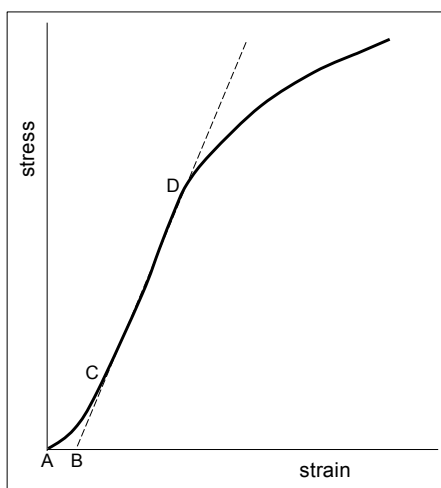


Figure 6.4 The toe compensation on a stress-strain curve: the toe region of AC is compensated for, by extending the linear/elastic portion of the curve, CD, and the intersection B becomes the corrected zero-strain point

Typical stress-strain curves for plastics with different levels of ductility are shown in Figure 6.5. Table 6.1 shows tensile properties (obtained under standard laboratory conditions of approximately 23 °C and 50 % relative humidity, and mostly in accordance with ASTM D638) for dry-as-moulded samples. Where there was access to sufficient information, the data in Table 6.1 is presented in the form of ‘the most quoted value’, succeeded by minimum and maximum values in brackets.

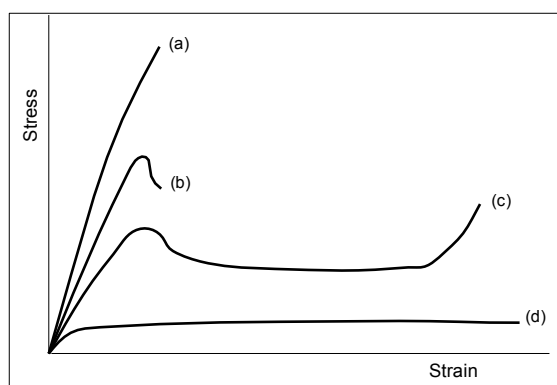


Figure 6.5 Stress-strain curves for polymers at room temperature: (a) a low ductility polymer (e.g., PMMA or a rigid TS), (b) a ductile polymer (e.g., PVC), (c) a ductile polymer capable of cold drawing (e.g., PP), and (d) a polymer with long-range elasticity (e.g., natural rubber)

Table 6.1 Tensile properties of various polymers (sources: CAMPUS, Efunda, Ehrenstein (2001, p260), Fried (1995, p474), Callister (2007, Appendix B))

Polymer type	Abbrn.	Specific gravity	Young's modulus, GPa	Yield strength, MPa	Elongation to yield, %	Tensile strength, MPa	Elongation to break, %
Commodity thermoplastics							
Low-density polyethylene	LDPE	0.92 (0.91-0.93)	0.2 (0.17-0.5)	11.5 (9-14.5)	15 (9-20)	8 -31.4	100-1000
High-density polyethylene	HDPE	0.95 (0.94-0.96)	1.1 (1.06-1.4)	21 (20-33)	10 (9-20)	18-35	10-1200
Polypropylene	PP	0.9 (0.9-0.95)	1.3 (1.1-1.55)	30 (25-38)	12	35 (21-43)	400 (20-900)
Polystyrene	PS	1.1	3.2 (2.28- 3.4)			50 (36-65)	2.5 (1.2-4)
Polyvinyl acetate	PVA	1.25 (1.19-1.34)	0.6			29-49	10-20
Polyvinyl chloride (rigid)	PVC	1.4 (1.38-1.55)	2.6 (1-4.14)	41-48	3	50 (41-75)	30 (10-100)
Styrene-acrylonitrile copolymer	SAN	1.08	3.65			70-75	3-5

Engineering thermoplastics							
Acrylonitrile-butadiene-styrene copolymer	ABS	1.05 (1.03-1.07)	2 (1.9-2.7)	35-50	3	32-50	15-40
Polyamide 6,6	PA 6,6	1.15 (1.07-1.24)	1.6 (1.4-3.8)	57 (55-85)	5-25	84 (70-95)	60 (15-80)
Polybutylene terephthalate	PBT	1.31 (1.30-1.38)	2.5 (1.93-3)	57-60	3.7-5	57-60	50-300
Polycarbonate	PC	1.2 (1.06-1.25)	2.4 (2.1-2.5)	65 (45-70)	6.2 (6-30)	63 (60-72)	110 (50-150)
Polyethylene terephthalate	PET	1.37 (1.33-1.48)	3 (2.25-4.14)	50-59	4-6	54 (47-72)	275 (30-300)
Polymethyl methacrylate	PMMA	1.2 (1.17-1.23)	3.2 (2.24-3.24)	54-73		63 (48-77)	3 (2-10)
Polyoxymethylene (acetal)	POM	1.41 (1.4-1.54)	2.6 (2.6-3.2)	64-71	11-27	65 (44-70)	40 (25-70)
Polyurethane	PU	1.16 (1-1.24)	1.31-2.07	54-76		30-62	35 (15-550)
Silicone rubber		1.1 (1.07-1.6)				4.8-10.3	100-800
Styrene-butadiene rubber	SBR	0.94-1.05	0.002-0.01			12.4-20.7	400-600
Thermoplastic urethane	TPU	1.20-1.25	0.2-0.7			30-45	400-450
Ultrahigh molecular weight polyethylene	UHMWPE	0.94	0.69-0.79	17-28		20-48	50-525
High-performance engineering thermoplastics							
Polytetrafluoroethylene (a fluoropolymer)	PTFE	2.13 (2.1-2.35)	0.5 (0.4-1.4)	13-43	7-63	25 (20-36)	200-550
Polyphenylene oxide (impact modified)	PPO	1.06	2.3-2.6			55	45
Polyetherether ketone	PEEK	1.31	1.1-3.5	91-100	5	70-103	75 (30-150)
Polyetherimide	PEI	1.27	3.0	105		97	60
Polyethersulphone	PES	1.37	2.45-2.7	90	6.3-6.7	84-87	60 (30-80)
Polyimide	PI	1.4	3.43-3.58	86-90		118-140	6-90
Polyphenylene sulphide	PPS	1.34 (1.3-1.35)	4 (3.4-4.2)			66 (33-85)	1.5 (1-6)
Polysulphone	PSU	1.24	2.6 (2.5-2.75)	75-79	5.7	65 (50-100)	25-85

Thermosets							
Epoxy resin	EP	1.4 (1.1-1.9)	4.5 (2.4-6)			40 (28-100)	4 (1-6)
Melamine-formaldehyde	MF	1.5	4.9-9.1			30	0.6-0.9
Phenol-formaldehyde	PF	1.32 (1.24-1.4)	2.76-4.83			35-62	1.5-2
Polyester (unsaturated) resin	UP	1.5 (1.2-2)	2.1 (2-4.5)			40-90	2
Polyimide resin	PI	1.43	3.2			75-100	4-9
Polyurethane casting resin	PU	1.05	4			70-80	3-6
Urea-formaldehyde	UF	1.5	7-10.5			30	0.5-1.0

Notes: The properties, in general, can be affected by many factors that are not easy to account for in tables such as this: e.g., % crystallinity, orientation and morphology in semi-crystalline polymers; degree of crosslinking/grades in TS resins; hardness of elastomers. Polyurethanes, depending on the type of polyols (polyester or polyether polyols) and the processing conditions, enable the production of a wide spectrum of products, which include flexible and rigid foams, plastics and elastomers, coatings and adhesives. TS polyester may be based on orthophthalic or isophthalic isomers: isophthalic produce higher modulus and strength. ABS has grades of medium, high and very high impact. Furthermore, the test conditions, such as the rate of straining (the cross-head speed), obviously, also affect the values measured.

The properties are affected by the weather/service conditions such as UV radiation, heat, moisture and temperature and the mechanical loading conditions, e.g., speed. These conditions can be simulated by employing accelerated-weathering devices and subjecting the specimens to one or a combination of the weathering elements for a period of time as indicated by standards (e.g., ISO 4892:2006, ASTM D256 –99 (2008), ASTM D4587–11) prior to testing and/or by placing a suitable environmental chamber on the testing machine and conducting multiple tests at different settings.

6.2.1 Effect of testing speed and temperature

The polymeric materials are viscoelastic and, therefore, their mechanical properties are time and temperature dependent. Accordingly the parameters of temperature and the speed of testing should be recorded for tests (it is a good practice to record the relative humidity as well, because of sensitivity of some polymers to moisture). Most tests are conducted under standard laboratory conditions (temperature = 23 ± 2 °C; relative humidity = $50 \pm 5\%$) on dry-as-moulded samples.

The speed of testing as recommended in the standards range from 1 to 500 mm/min and is selected depending on the property measured, for example, for the elastic modulus measurement it is normally 1 mm/min. Figures 6.6 and 6.7 show how the extension rate (speed of testing) and temperature affect the stress-strain behaviour of high-impact polystyrene (HIPS). The elongation to break decreases and the strength (both tensile and yield) increases as the temperature drops and as the deformation rate increases. The temperature effect is significantly greater than the influence of the deformation rate.

The same trends apply to other polymeric materials, therefore, one can generalise as shown in Figure 6.8. Although not very obvious in these graphs for HIPS, however, the elastic modulus trend is similar to that of strength: increases as temperature falls and/or as the speed of testing increases. Modulus variations become particularly pronounced at T_g of materials, a drop of as high as 1000 N/mm^2 can result as material changes from being glass-like to being rubber-like. This is particularly critical in amorphous thermoplastics in that the material loses its structural rigidity and hence its load bearing ability significantly. Whereas, the semi-crystalline thermoplastics and thermosetting plastics/elastomers maintain significant structural stability because of molecular crystallinity and chemical cross-linking, respectively.

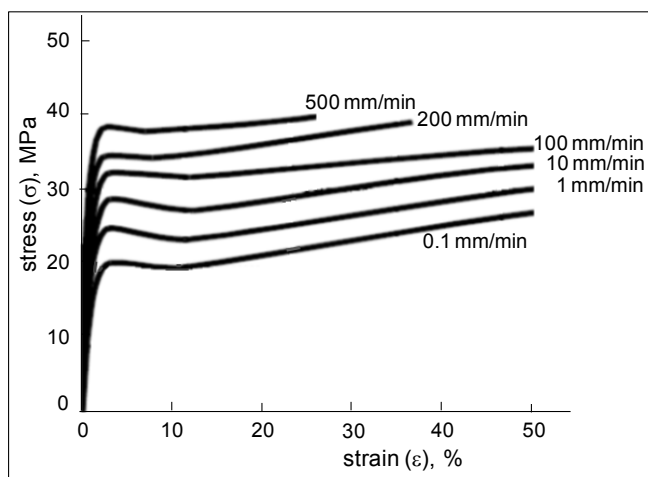


Figure 6.6 Stress-strain curves for HIPS at extension rates from 0.1 mm/min to 500 mm/min (tests conducted at 23 °C/50 % RH) (source: Ehrenstein (2001, p182))

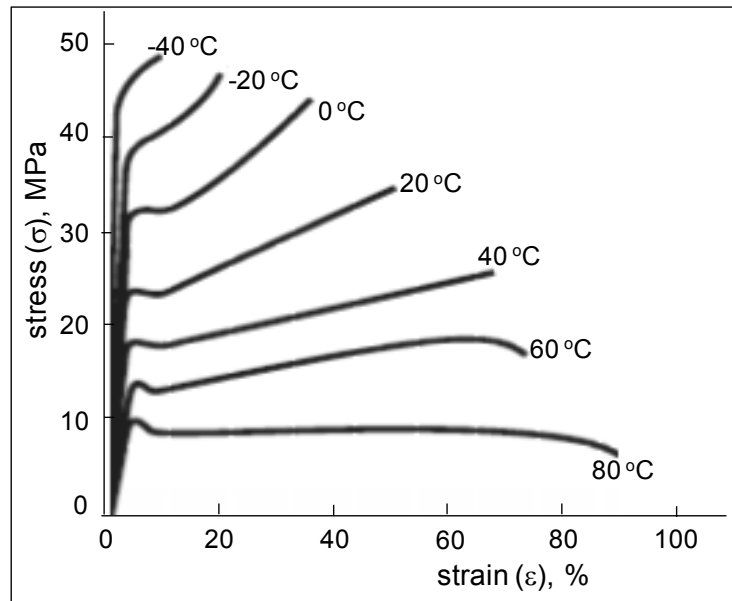


Figure 6.7 Stress-strain curves for HIPS at a range of temperatures from $-40\text{ }^{\circ}\text{C}$ to $80\text{ }^{\circ}\text{C}$ (tests conducted at 2 mm/min cross-head speed) (source: Ehrenstein (2001, p182))

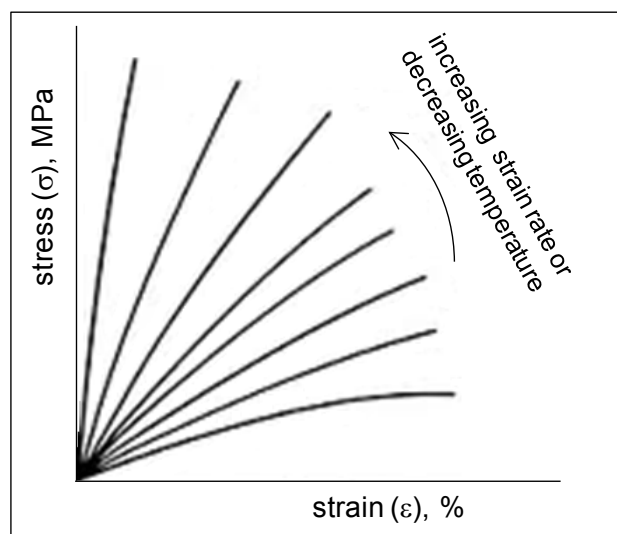


Figure 6.8 Illustration of the effect of temperature and speed of deformation on stress-strain behaviour of polymeric materials

6.2.2 Effect of water absorption

Water absorption should be a particular consideration for hygroscopic polymers. Many engineering polymers such as polyamides (nylons), ABS, polycarbonate, cellulose, and poly(methyl methacrylate). Other polymers, e.g., polyethylenes and polystyrene, do not normally absorb much moisture, but are able to carry significant moisture on their surface when exposed to water. Table 6.2 lists the water absorption values for several selected plastics as determined by ASTM D 570 after 24 h immersion at $23\text{ }^{\circ}\text{C}$. Equilibrium value for water absorption will be significantly higher for these plastics, as will water absorption values obtained at elevated temperatures (BASF-1, 2003).

Table 6.2 Water absorption values for selected plastics

Polymer	Water absorption, %
polypropylene	< 0.01
polycarbonate	0.15
nylon 11	0.25
nylon 6	1.3
cellulose acetate	1.7

Polyamides are widely used engineering materials and their water absorption has received wide coverage, e.g., Akay (1994). CAMPUS provides comprehensive data on this subject.

Figure 6.9 shows the effect of moisture on polyamide 66: as can be seen, increasing moisture content results in lowering of Young's modulus (greater flexibility) and the yield and tensile strengths but also an increase in ductility (i.e., % elongation to failure) and toughness (as indicated by the area under the stress-strain curve).

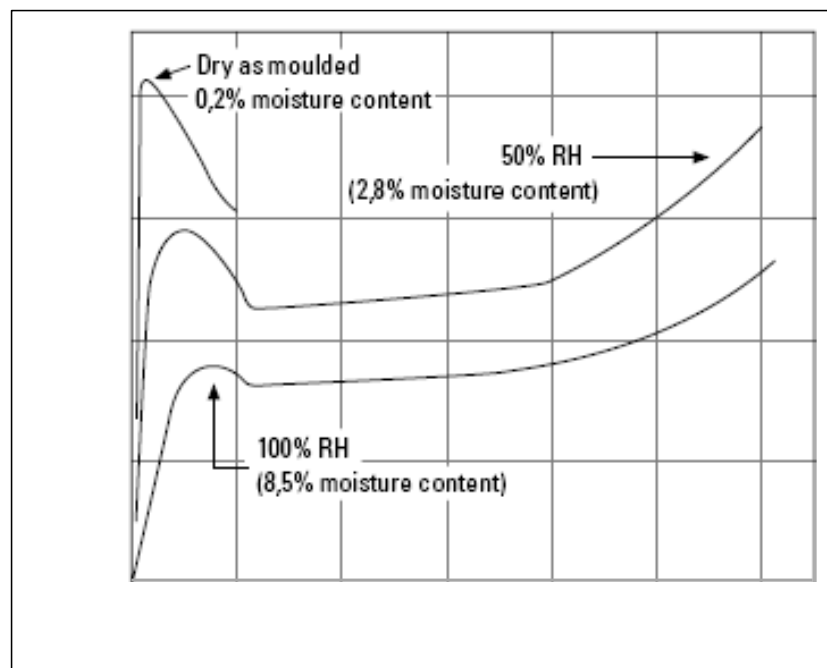


Figure 6.9 Room temperature tensile stress-strain curves for PA66 specimens with various moisture contents (source: DuPont Handbook on nylon resins, p3.1)

The extent of moisture absorption is accelerated with temperature, and obviously under hygrothermal conditions the properties suffer much greater deterioration, see Figure 6.10.

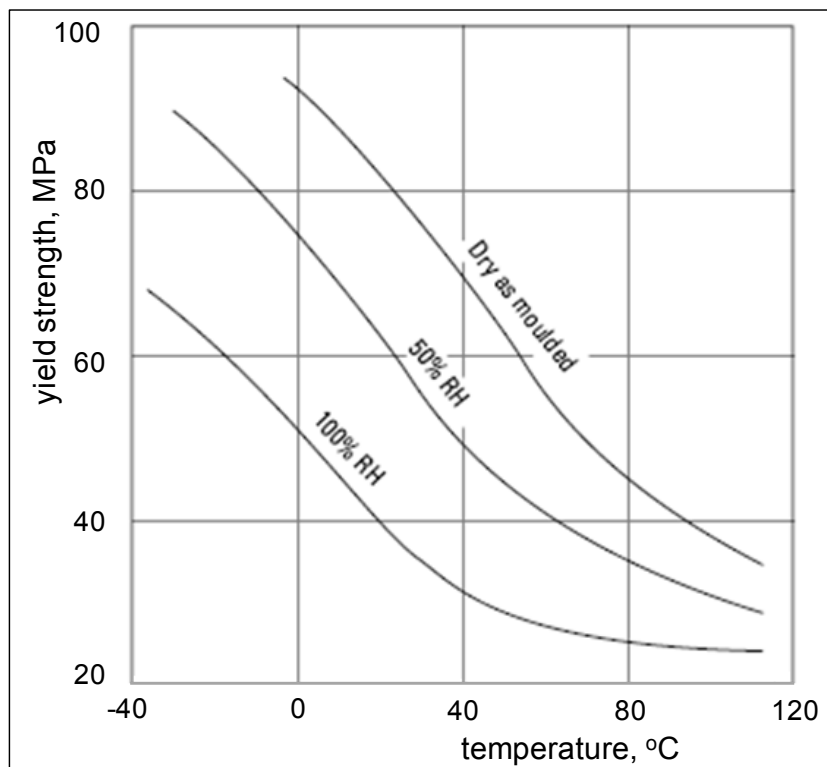


Figure 6.10 Yield strength vs. temperature for PA66 specimens with various moisture contents (source: DuPont Handbook on nylon resins, p3.1)

6.2.3 Effect of long-term loading

Viscoelastic materials will suffer gradual deformation under small loads (corresponding to below yield strength) even at room temperature. Thermoplastics, in general, are more prone than thermosets to time-dependant deformation under a given load. The long term stress-strain behaviour is described in terms of either creep (on one occasion when I was covering the subject of creep, a student who spent 6 years to get his HND in Engineering and became a good musician whispered, “a bit of a creep yourself” when the subject was dragging on a bit!) or stress relaxation (which was my response!). Creep is measured by applying a constant load (constant engineering stress) to a specimen and measuring deformation over time. Conversely, in stress relaxation the material is subjected to a constant strain and the stress to maintain this strain is recorded over time.

Creep data (i.e., strain vs. time) is usually obtained for different levels of stress and, it may also be necessary to obtain data at different temperatures. The data is of significance particularly for brittle plastics that can only support limited strain to failure. From a set of creep strain vs. time data isochronous stress-strain curves and stress relaxation curves (isometric curves) can be constructed as illustrated in Figure 6.11. Similar to an isometric curve, a creep modulus ($E(t) = \sigma(t) / \epsilon'$) vs. time curve can also be presented from the ratios of stress to strain at a given strain

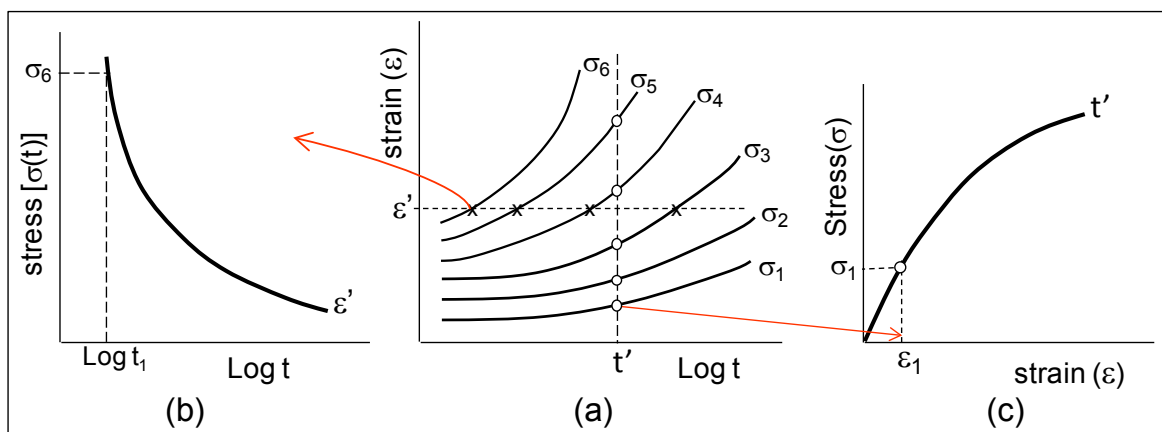


Figure 6.11 Construction of a creep isochronous σ - ϵ curve (c) and an isometric stress-time curve (b) from creep curves (a). (Isochronous indicates the same time period, and isometric indicates equal measure, here the same strain)

Isochronous curves for various polymer types and by various producers are presented in the Material Data Centre web site (www.materialdatacenter.com) as shown in Figure 6.12 for PA66.

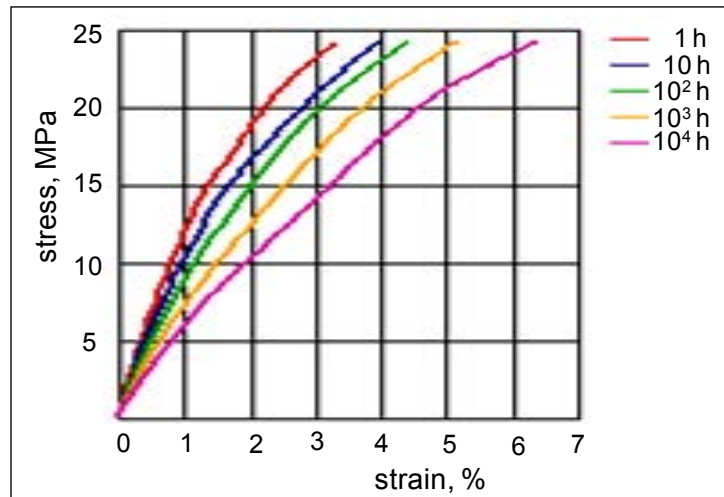


Figure 6.12 σ - ϵ isochronous curves for Zytel 101L NC010 (PA66) (cond.) at 23 °C

Temperature dependence of processes such as creep, stress relaxation as well as ageing can be described by the **Arrhenius equation**, see below, which produces a straight line when the \log_2 (change in property) is plotted against $1/T$.

$$\text{The process rate (T)} = Ae^{(-Q/RT)}$$

where, Q is the activation energy, R is the gas constant, T is the absolute temperature, and A is a pre-exponential constant.

Creep is normally determined under tensile loading for plastics, but there are also standard test methods for creep in flexure. However, creep tests for elastomers are usually conducted in compression and also in shear. The differences reflect the type of applications that these materials are employed for. Stress relaxation tests are normally conducted in tensile deformation mode, but rubber and other materials that are used as seals or gaskets are tested in compression.

The **Boltzmann superposition principle**, an aspect of linear viscoelasticity, considers the entire loading history of deformation: it states that deformation over time, $\epsilon(t)$, is dependent on the entire loading history of the material in the form of independent, discrete loading steps (these may be positive (added) or negative (removed)). Accordingly, creep after a period of time, t , due to many discrete/incremental (step) loads, $\Delta\sigma_1, \Delta\sigma_2, \Delta\sigma_3, \dots, \Delta\sigma_n$, applied at times $u_1, u_2, u_3, \dots, u_n$, becomes the sum of the contributions of every loading step:

$$\epsilon(t) = \Delta\sigma_1 J(t - u_1) + \Delta\sigma_2 J(t - u_2) + \Delta\sigma_3 J(t - u_3) + \dots + \Delta\sigma_n J(t - u_n) \text{ or}$$

where, $J(t)$ is the creep compliance, i.e., $J(t) = 1 / E(t)$.

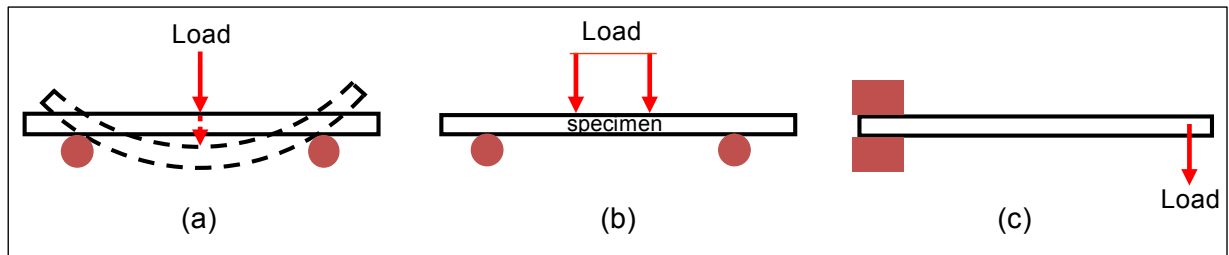


Figure 6.13 Flexural modes: (a) 3-point bending, (b) 4-point bending, (c) simple cantilever

The tests are conducted using rectangular-bar test pieces of certain dimensions on a universal test machine with suitable loading fixture (Figure 6.14).



Figure 6.14 A specimen tested in 3-point bending

For three- and four-point bending tests, the test pieces are supported on cylindrical surfaces and loaded centrally via a rounded loading nose(s) of certain diameters. The diameters are selected to avoid too much indentation and premature failure due to stress concentration under the loading nose(s). Three- point bending tests are commonly used, but in the four-point bending mode the stress is distributed over a wider span surface between the inner loading noses and, therefore, becomes more uniform rather than concentrated under the loading nose in three-point bending. **Four-point bending** is useful in testing materials that do not fail at the point of maximum **stress** in three-point bending.

ISO 178:2010 specifies two methods, Method A and Method B. In Method A, a strain rate of 1 %/min is used throughout the test. Method B uses two different strain rates: 1 %/min for the determination of the flexural modulus and 5 %/min or 50 %/min, depending on the ductility of the material, for the determination of the remainder of the flexural stress-strain curve. A variety of specimen shapes can be used for this test, but the most commonly used specimen size for ASTM is 3.2 x 12.7 x 127 mm and for ISO is 4 x 10 x 80 mm in thickness (depth), width and length, with a support span-to-depth ratio of 16. This should provide sufficient overhang to prevent the specimen from slipping through the supports during the test.

The stress and strain are not uniform through the specimen thickness: during loading the stress and strain varies gradually from a maximum compressive form on the surface in contact with the loading nose(s), through zero at the neutral plane, to a maximum tensile form on the outer surface. The maximum axial fibre stresses occur on a line under the loading nose in 3-point bending and over the area between the loading noses in 4-point bending. It is the maximum tensile stress and strain that are computed. The outcome of a test is usually a plot of load versus displacement, see Figure 6.15.

Various flexural properties can be calculated by extracting data from these plots and using the equations presented below, such as flexural modulus (modulus of elasticity in flexure), flexural strength (also known as 'modulus of rupture' when maximum stress in the outer fibres at the moment of break is recorded). Other flexural properties include yield strength, strain at yield, offset yield strength (the stress at which the stress-strain curve deviates by a given strain (offset) from the tangent to the initial straight line portion of the stress-strain curve), flexural stress at 3.5% deflection (ISO) (deflection equals to 1.5 times the thickness of the test specimen) or 5.0% deflection (ASTM), and secant modulus of elasticity (i.e., the slope of the straight line that joins the origin and a selected point on the actual stress-strain curve).

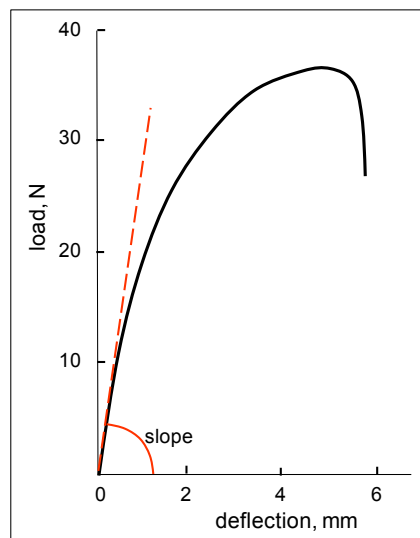


Figure 6.15 A load vs. deflection plot from 3-point bending test of a wood-plastic specimen

The equations, see the standards, for the flexural stress (maximum fibre stress) (σ_f) and strain (ϵ_f) for a rectangular-bar test piece under three-point loading are given as

$$\sigma_f = (3FL)/(2bh^2); \epsilon_f = (6hs)/(L^2)$$

where, F is the force at midspan, L is the support span, h the specimen thickness, b the width and s is the deflection of the tensile surface of the specimen at midpoint.

The modulus of elasticity (E_f), from the above equations, becomes

$$E_f = [L^3/(4bh^3)] \times (\text{slope})$$

where , 'slope ' is the slope of the tangent to the initial straight-line portion of the load-deflection curve.

The equations for a rectangular-bar test piece under four-point loading, where the load span (the distance between the two loading noses) is one third of the support span are given as

$$\sigma_f = (FL)/(bh^2); \epsilon_f = (4.7hs)/(L^2)$$

$$E_f = [0.21L^3/(bh^3)] \times (\text{slope})$$

There are equivalent equations for cylindrical test pieces.

In theory, the flexural modulus and the tensile modulus should be the same. However, as described by Hawley (1999, p320), in practice this is only approximately so, because plastic test pieces are not isotropic through their thickness. Differential cooling rates, variations in extrusion or injection rates and changes in flow patterns, all contribute to non-uniform microstructure and properties across the thickness. When coupled with non uniform stresses in flexural testing, mentioned above, that inconsistencies with tensile test can arise.

Table 6.3 shows single-point flexural data (obtained under standard laboratory conditions of approximately 23 °C and 50 % relative humidity in 3-point bending, and mostly in accordance with ASTM D790) for dry-as-moulded samples. The table, as in Table 6.1, include the most quoted value and the minimum and maximum values in brackets.

Table 6.3 Flexural properties of various polymers (sources: CAMPUS, Efunda, Plastics International)

Polymer type	Abbrn.	Flexural modulus, GPa	Flexural strength, MPa	Compressive modulus, GPa	Compr. strength, MPa	Compr. yield strength, MPa
Commodity thermoplastics						
Low-density polyethylene	LDPE	0.2-0.3				
High-density polyethylene	HDPE	1-1.6	20		19-25	
Polypropylene	PP	1.5 (1.2-1.7)	48 (40-55)	1.6 (1.1-2.1)	38-55	40
Polystyrene	PS	2.5-3.4	70 (69-101)	3.3-3.4	83-90	
Polyvinyl chloride (rigid)	PVC	1.4-3.5	41-110	2.6	55-90	66
Styrene-acrylonitrile copolymer	SAN	3.5-4.2	76-131	3.7-4	97-104	
Engineering thermoplastics						
Acrylonitrile-butadiene-styrene copolymer	ABS	2.5 (2.1-2.8)	75 (49-90)	1.4-3.1	86 (12-86)	20
Polyamide 6,6	PA 6,6	2.8 (2.8-3.2)	110 (12-124)			35-104
Polybutylene terephthalate	PBT	2.3 (2.3-2.8)	83 (83-115)	2.6	59-100	
polycarbonate	PC	2.3 (2-2.4)	90 (71-103)	2.4	69-86	86
Polyethylene terephthalate	PET	2.8 (2.4-3.1)	80-114		76-104	104
Polymethyl methacrylate	PMMA	3 (2.2-3.2)	100 (72-131)	2.6-3.2	72-124	115
Polyoxymethylene (acetal)	POM	2.8 (2.6-3.4)	97 (94-110)	4.6		108-124 (at 10% strain)
Polyurethane	PU	2 (1.3-2.1)	100 (70-104)			
Ultrahigh molecular weight polyethylene	UHMWPE	0.9-1.0		0.52		17
High-performance engineering thermoplastics						
Polytetrafluoroethylene (a fluoropolymer)	PTFE	0.5		0.41	12	7-12
Polyphenylene oxide (impact modified)	PPO	2.4 (2.3-2.8)	95 (66-97)		113	
Polyetherether ketone	PEEK	3.6-4	110-170	3.8		118

Polyetherimide	PEI	3.3	152	3.3	151	
Polyethersulphone	PES	2.6	130	2.7		100
Polyimide	PI	3 (2.5-3.5)	140 (69-199)	2.2-2.4	121-276	
Polyphenylene sulphide	PPS	3.8 (3.8-4.1)	96 (96-145)	30	110	95
Polysulphone	PSU	2.6-2.7	106-121	2.6		96
Thermosets						
Epoxy resin	EP	2.5-2.9	90-145		104-173	
Melamine-formaldehyde (cellulose filled)	MF	7.6	62-110		228-311	
Phenol-formaldehyde	PF		76-117		83-104	
Polyester (unsaturated) resin (rigid)	UP	3.0 (3.0-4.2)	100 (59-159)		90-207	
Polyimide resin	PI	4 (2.9-20)	176 (45-345)	2.9	133-227	
Polyurethane (casting)	PU	4.2	131			

6.4 Compressive properties

Plastics are subjected to compression in use, mainly as elastomeric materials and cellular plastics. Compression generates various degrees of bulging/barrelling and buckling in materials depending on the shape and size of the component and the rigidity of the material. Bulging and emaciation, depending on the mode of deformation, enables the volume of elastomers to remain constant, which is why their Poisson's ratio is approximately 0.5. The thickness of an elastomeric block dictates its stiffness under compression: a thin block will not bulge as much as a thick block and, therefore, exhibit greater stiffness. The influence of thickness on stiffness can be expressed in terms of a parameter known as the shape factor, S , such that the compression modulus, E_c , for a block of an elastomer in terms of Young's modulus, E , and shape factor becomes

$$E_c = E(1 + 2S^2).$$

S is defined as the ratio of loaded area to force-free area (bulge-prone area). Accordingly for a normal rectangular block of sides a , b and c (the height or the thickness), $S = (ab)/[2c(a + b)]$. Hence as the thickness decreases, S increases.

In rigid and semi-rigid plastics, buckling is of concern and the standard methods for conducting compression tests for plastics, ISO 604: 2002 or BS 2782: Method 345A and ASTM D695M-10, specify test pieces and fixtures to avoid buckling. In specimens prone to buckling, the specimen length may be further adjusted. Specimens recommended are rectangular prisms of 4 x 10 mm in cross section and of 10 mm length for strength and 50 mm length for elastic modulus determinations. Smaller dimensions are also specified to allow for restrictions due to the amount of material available or geometric constraints on a product/component. Normally the specimens should be conditioned and the tests should be conducted in a standard room atmosphere of 23/50.

During the test, force and the corresponding compression data is recorded. Therefore, at the outcome of the test, a plot of force vs. compression or more commonly stress vs. strain is produced, see Figure 6.16.

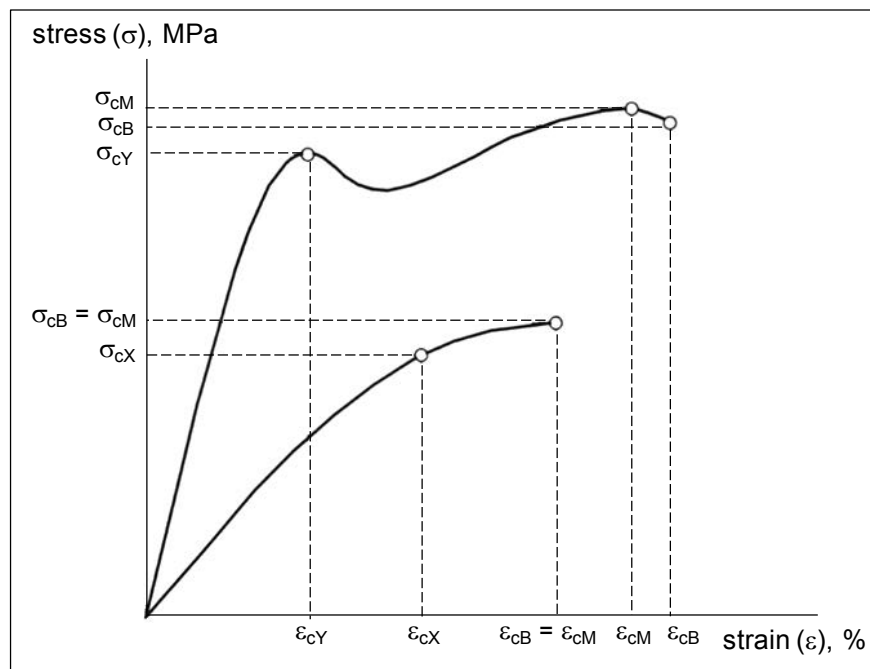


Figure 6.16 Typical compressive stress-strain curves (source: ISO 604: 2002)

Various compressive properties can be calculated by extracting data from these plots and using the equations indicated under Section 6.2 for tensile properties. The properties include compressive modulus (e.g., modulus of elasticity in compression), compressive strength, σ_{cM} (maximum stress sustained by the specimen during the test) or σ_{cB} (stress at break). Other properties include strain to break and/or to reach maximum stress, ϵ_{cB} , ϵ_{cM} ; stress and strain at yield, σ_{cY} , ϵ_{cY} ; stress at a certain % strain, σ_{cX} , etc. The values of some of these properties for some polymers are included in Table 6.3.

6.5 Shear properties

Testing for shear properties of strength and shear modulus is not so common for ordinary plastics; it is used more for elastomeric and composite materials. The standard test methods for plastics are BS 2782-3 Methods 340A and B and ASTM D732-10 for determination of shear strength by punch tool.

The specimens are in the form of disks, square plaques or rectangular bars of specified dimensions. In testing, the specimen is clamped between the two halves of an annular clamp. A round punch type of piston that fits the opening in the clamp is bolted to the specimen, and a load is applied to the specimen via the punch to push it through the clamp at such a rate that specimen fractures within 15 to 45 s. The shear strength, t , is calculated as the maximum force encountered during the test divided by the area of the sheared edge. Therefore, for a specimen that is bolted to the punch,

$$\tau_s = F / (\pi DT)$$

where, F is the force at break, D is the punch diameter and T is thickness of the specimen.

ISO 1827:2007 specifies methods for the determination of modulus in shear and adhesion strength to rigid plates for vulcanized or thermoplastic rubber, using four pieces of rubber bonded/sandwiched between four parallel plates (quadruple-shear method). Other approaches employ test pieces that consist of one-lap (a rubber layer between two metal plates) or two-lap (two layers of rubber between three metal plates) shear units.

Shear modulus, G , is determined at small strain levels where the stress-strain relationship is linear (i.e., elastic) using the equation $G = \tau / \gamma$, where τ and γ are shear stress and strain, respectively.

The elastic moduli properties obtained under different loading modes are related to each other through the constant of Poisson's ratio, ν , for example

$$E = 2(1 + \nu) G.$$

Therefore, together with Young's, the shear and the bulk moduli, Poisson's ratio becomes one of the four elastic constants.

The Poisson's ratio of isotropic, linear elastic solids cannot be less than -1 nor greater than 0.5, since moduli terms have positive values. However, it is rare to encounter engineering materials with negative Poisson's ratios: for most materials, it will fall in the range of 0.0 and 0.5. The Poisson's ratio for most metals is approximately 0.3. Rubber has a Poisson's ratio close to 0.5 and is therefore almost incompressible. Cork has a Poisson's ratio close to zero, showing very little lateral expansion when compressed and, therefore, functions well as a bottle stopper since it will not swell laterally when pushed into a bottle.

Some polymer foams have a negative Poisson's ratio; if these auxetic materials are stretched in one direction, they become thicker in perpendicular directions. Some anisotropic materials have one or more Poisson's ratios above 0.5 in some directions.

6.6 Hardness

Hardness is a measure of the level of penetration of an indenter when forced into the material under specified conditions, although the term hardness has been applied to scratch resistance and to rebound resilience as well. Brown (1999, p 226) describes the mode of deformation under an indenter as a mixture of tension, shear and compression, and not a fundamental material property. The indentation hardness is inversely related to the extent of penetration and is dependent on the elastic modulus and viscoelastic behaviour of the material. Empirical equations relating applied load, depth of indentation and indenter geometry to modulus of elasticity for different indenter geometries are presented by Brisco et al. (1994).

Hardness as a material property is used more in association with elastomers than with plastics. The results depend on the indenter geometry, the extent of indentation as well as the delay between the application of the indenter and when the hardness is recorded. Regardless of the arbitrary nature of the test, it is attractive because of its cheapness, simplicity, and applicability to finished components as well as specimens, and it is virtually a non-destructive test.

The standard test methods for plastics and rubbers are ISO 868: 2003, BS 2782-3 Method 365B and ASTM D2240-05 for determination of indentation hardness by means of a Shore durometer. The Shore hardness tester is a hand-held simple device consisting of a needle-like spring-loaded indenter, which is pressed into the specimen surface and the penetration of the needle is measured directly from a scale on the device in terms of hardness degrees. There are two types of Shore durometers with different levels of indenter stiffness; Shore A Durometer is fitted with a blunt indenter and is suitable for soft elastomers and plastics and Shore D, with a sharper-tipped indenter, for harder elastomers and plastics.

Alternative standard test methods recommend hardness testers with spherical indentors. These are ISO 2039-1: 2001, BS 2782-3 Method 365D and ASTM D2240-05. In ball indentation, the hardness is expressed in terms of the surface area of the impression left on the surface of the material by the indenter following the test, rather than the penetration of the indenter.

The Rockwell hardness tester is another ball indentation method, described in ISO 2039-2: 2001 and ASTM D785, however, here the hardness is expressed in terms of the penetration of the indenter. The method is suitable for harder thermoplastics and thermosets, and depending on the load applied and the ball diameter used different Rockwell hardness scales are defined. Table 6.4 shows a range of hardness values for various polymeric materials over hardness scales of Shore A, Shore D or Rockwell R and M.

Table 6.4 Hardness properties of various polymers (sources: ASM International (2003), Efundu)

Polymer type	Specific gravity	Hardness				
		Shore A	Shore D	Rockwell R	Rockwell M	Barcol
Commodity thermoplastics						
LDPE	0.92 (0.91-0.93)		44-50			
HDPE	0.95 (0.94-0.96)		66-73			
PP	0.9 (0.9-0.95)			80 (80-102)		
PS	1.1				60-75	
PVC	1.4 (1.38-1.55)		65-85	80		
SAN	1.08			75-83	80	
Engineering thermoplastics						
ABS	1.05 (1.03-1.07)			102-115		
PA 6,6	1.15 (1.07-1.24)			120	83	
PBT	1.31 (1.30-1.38)			117	68-78	
PC	1.2 (1.06-1.25)				70 (62-75)	
PET	1.37 (1.33-1.48)			111	94-101	
PMMA	1.2 (1.17-1.23)				68-105	
POM	1.41 (1.4-1.54)			120	92-94	
PU	1.16 (1-1.24)	75	70	100	48	
TPU	1.20-1.25	55-94				
UHMW-PE	0.94		61-63	50		
High-performance engineering thermoplastics						
PTFE	2.13 (2.1-2.35)		50-65			
PPO	1.06			115 (94-120)		
PEI	1.27				109	
PES	1.37				88	
PI	1.4			129	95; E(52-99)	
PPS	1.34 (1.3- 1.35)			123 (120-125)		
PSU	1.24				69	
Thermosets						
EP	1.4 (1.1-1.9)				80-110	
MF	1.5				120 (115-125)	
PF	1.32 (1.24-1.4)				110 (93-120)	
UP	1.5 (1.2-2)					40 (34-75)
PI	1.43				110-120	
PU	1.05		50-70			30-35
UF (cellulose filled)	1.5				110-120	

Hardness test methods that are normally used for metals, but are also used in characterising plastics, include Brinell and Vickers.

6.7 Impact properties and fracture toughness

Under impact, material is subjected to a sudden blow of a projectile or a hammer. The speed of impact testing is much higher than the strain rates encountered in the tests covered previously, which are classified as static tests. Impact tests can be conducted in the form of pendulum tests, falling mass (dart) tests and high speed tensile tests. The basic equipment at best indicate the energy absorbed in the process of specimen fracture, however, there are sophisticated equipment that are suitably instrumented to provide force-deflection traces from which more information can be gleaned as well as overall energy value at fracture.

Pendulum impact tests can be conducted in the mode of Charpy or Izod tests.

6.7.1 Charpy test

The standard test methods that describe the non-instrumented Charpy impact test include BS EN ISO 179-1: 2010 and ASTM D6110-10. Test pieces in the form of a rectangular bar may be un-notched or contain a notch centrally cut into the test piece. The notch generates stress concentration in a simulation of real application conditions. As illustrated in Figure 6.17, the specimen is supported at both ends and is struck centrally by the pendulum head at the bottom of its swing. The specimens may be tested in an edgewise or flatwise direction with respect to the impactor head. The edgewise positioning is the common practice for notch containing specimens. The ISO test pieces are 80 x 10 x 4 mm in dimension, with 2 mm depth notches of different notch-tip sharpnesses.

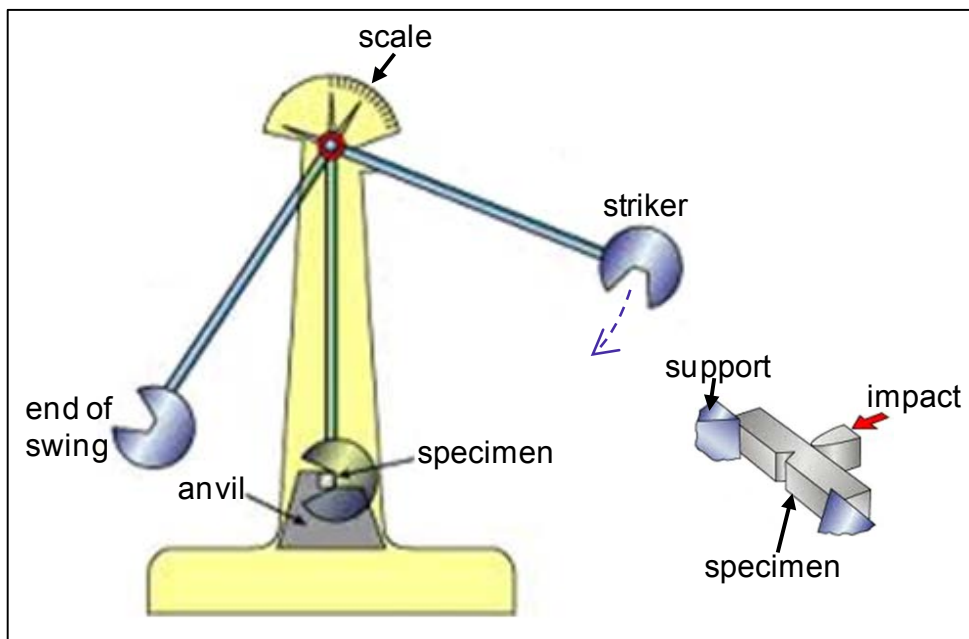


Figure 6.17 Illustration of Charpy impact test (source: The Welding Institute)

The preferred notch-tip radius is 0.25 mm, however in order to determine notch sensitivity of the material, test pieces with the sharper (0.1 mm radius) and blunter (1.0 mm radius) notches are also tested. The standard specimen for ASTM is 64 x 12.7 x 3.2 mm, and the notch depth is 2.5 mm (i.e., the depth under the notch of the specimen is 10.2 mm)

ISO impact strength is calculated by dividing impact energy with the specimen cross-sectional area behind the notch and is expressed in J/m^2 . ASTM impact energy is calculated by dividing impact energy in J with the thickness of the specimen (i.e., the notch width) and is expressed in J/m .

6.7.2 Izod test

The standard test methods that describe the Izod impact test include ISO 180: 2000 and ASTM D256-10. As illustrated in Figure 6.18, the specimen is clamped at one end as a vertical cantilevered beam with the notched side facing the striking head of the pendulum; and its free half is struck centrally by the pendulum head at the bottom of its swing. The dimensions of the test pieces are the same as for the Charpy test and the impact strength is also expressed similarly.

Charpy and Izod tests are suitable for plastic specimens that offer sufficient rigidity to avoid buckling, for specimens that are not sufficiently thick or materials that undergo high elongation to failure the tensile impact test is recommended, see ISO8256:2004 and ASTM D1822M-93.

Table 6.5 shows a range of notched impact values for various polymeric materials (obtained under standard laboratory conditions of approximately 23 °C and 50 % relative humidity on dry-as-moulded samples).

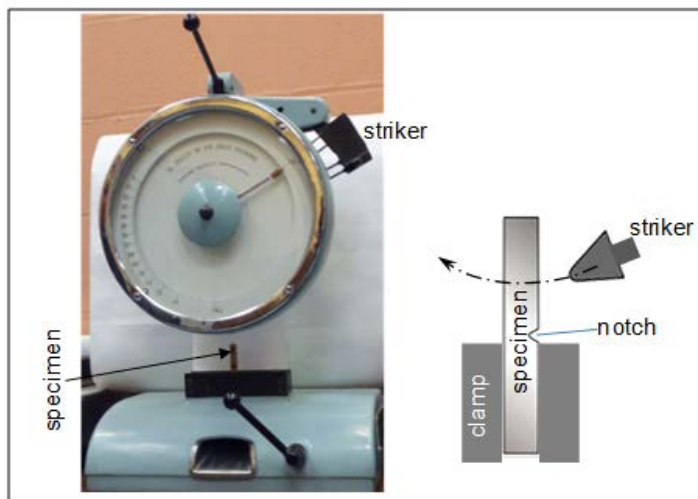


Figure 6.18 Illustration of Izod impact test

Table 6.5 Impact properties of various polymers (sources: Efunda, Plastics International, CAMPUS, Ehrenstein (2001, p260), Fried (1995, p474))

Polymer type	Abbrn.	Impact	
		Izod impact, J/cm	Charpy impact, kJ/m ²
Commodity thermoplastics			
Low-density polyethylene	LDPE	no break	no break
High-density polyethylene	HDPE	0.7 (0.2-2.1)	50
Polypropylene	PP	0.6 (0.2-0.8)	3.5 (2.5-17)
Polystyrene	PS	0.3 (0.2-1.1); (1.1 HIPS)	2-2.5
Polyvinyl acetate	PVA	1.6	
Polyvinyl chloride (rigid)	PVC	0.4 (0.2-11.7)	2-50
Styrene-acrylonitrile copolymer	SAN	0.2-0.3	2 (2-3)
Engineering thermoplastics			
Acrylonitrile-butadiene-styrene copolymer	ABS	4 (1.6-5.1)	18(7-25)
Polyamide 6,6	PA 6,6	0.6 (0.3-1.1)	6 (4-20)
Polybutylene terephthalate	PBT	0.4-0.5	5 (4-6)
polycarbonate	PC	8 (6.4-9.5)	11 (6-30); 42(with residual stress)
Polyethylene terephthalate	PET	0.4 (0.1-0.7)	4-6.5
Polymethyl methacrylate	PMMA	0.1-0.3	2
Polyoxymethylene (acetal)	POM	0.8 (0.6-1.2)	7 (6-9)
Linear polyurethane	PU	0.8-1	3
Styrene-butadiene rubber	SBR		5-13
Thermoplastic urethane	TPU	1.3-5.3	50 to 'no break'
Ultrahigh molecular weight polyethylene	UHMWPE	no break	100 (partial break)

High-performance engineering thermoplastics			
Polytetrafluoroethylene (a fluoropolymer)	PTFE	1.6-1.9	13-15
Polyphenylene oxide (impact modified)	PPO	1.9-2.7	
Polyetherether ketone	PEEK	0.8-0.9	6-7
Polyetherimide	PEI	0.5-0.6	
Polyethersulphone	PES	0.9	4.5
Polyimide	PI	0.8-0.9	5.9-7.3
Polyphenylene sulphide	PPS	0.3 (0.3-0.5)	4.6
Polysulphone	PSU	0.7 (0.5-0.9)	5.5
Thermosets			
Epoxy resin	EP	0.1-10	3
Melamine-formaldehyde	MF	0.1-0.2	1.5
Phenol-formaldehyde	PF	0.1-0.2	1.5
Polyester (unsaturated) resin	UP	0.1-0.2	2.2 (1.8-3)
Polyimide resin	PI	0.4	
Polyurethane casting resin	PU	0.2	
Urea-formaldehyde	UF	0.2	2.5

6.7.3 Falling weight test

The test consists of the release of a striker with hemispherical nose of a specified diameter from a given height on to flat circular disks or square platelets of 2 mm thickness. The test piece is supported on an annular base with a 40 mm opening for the striker to go through. There are various falling weight/dart standard test methods: ISO 6603-1: 2000, BS 2782, Method 353A, and Gardner impact test (ASTM D5420-10, ASTM D5628-10). The tests are conducted usually by a staircase approach, whereby the mass of the dart is decreased or increased incrementally on whether the failure occurs or not in the previous attempt. The test results are recorded as pass / fail and energy (J) level that causes 50% failure, E_{50} , is determined.

The standard falling weight test methods specifically for materials in film and sheet form are ISO 7765-1, BS 2782, Method 352E and ASTM D1709-09.

Instrumentation, although expensive, has enabled much more information to be obtained from an impact test. All of the impact process can be documented in terms of force and displacement, which then enables the computation of various force, deflection and energy levels. Figures 6.19 and 6.20 show instrumented falling-weight force-deflection features for unfilled and short glass-fibre reinforced polypropylene injection moulded plaques. The tests were conducted at room temperature, using a hemispherical striker tip of 5 mm radius, at a striker velocity of 4 m/s.

Instrumentation also enables detailed assessment of multi-component material assemblies such as sandwich panels, consisting of solid composite skins and honeycomb or foam cores (see Akay & Hanna 1990), and multi-component laminated films/sheets. Barkley and Akay (1992) have presented a detailed description of an instrumented impact tester and its various applications. The equipment can be fitted with a suitable camera to take flash photographs at predefined times during an impact event in order to assist in the identification of features contained in the force-deflection trace, see Figure 6.21.

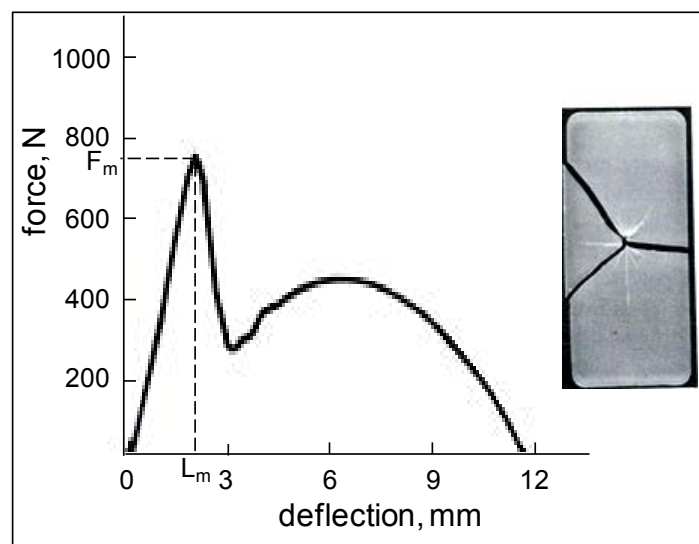


Figure 6.19 Force-deflection trace for a 3 mm thick PP plaque, and the photograph of the fractured specimen (F_m – maximum force, L_m – deflection at maximum force) (source: Akay and Barkley 1985)

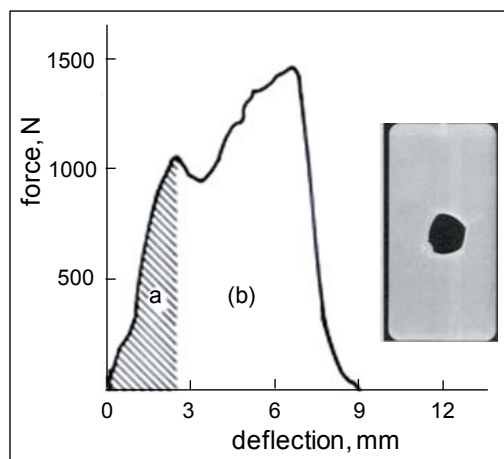


Figure 6.20 Force-deflection trace for a 4 mm thick sort glass-fibre reinforced PP plaque: (a) crack initiation (the hatched area is the energy expended up to the crack initiation), (b) crack propagation (source: Akay and Barkley 1985)

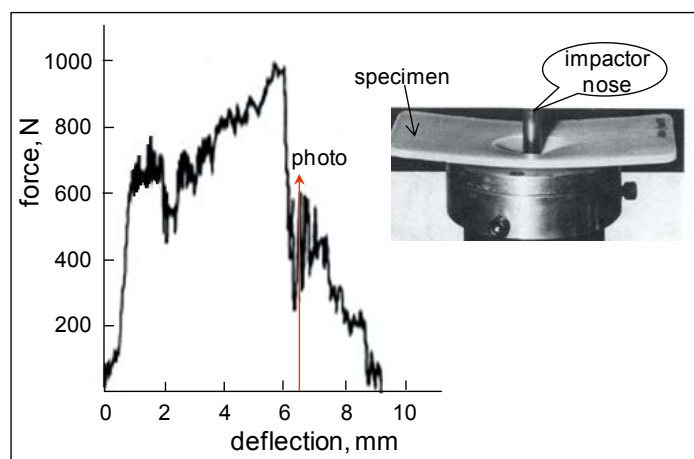


Figure 6.21 Photograph of an impact event for an injection-moulded fibre-reinforced PP plaque (the red arrow on the force-deflection trace indicates the instant of photography) (source: Barkley and Akay (1992)

The associated ISO test standard for instrumented impact testing is ISO 6603-2: 2000, but for thinner materials less than 1 mm thick ISO 7765-2: 1994 should be used. The tests produce force-deflection traces, from which various results that are indicated by the standard methods can be extracted: the maximum force, the deflection at maximum force, the energy to maximum force, the puncture force, deflection and energy to puncture, and total energy and deflection, where the force, deflection and energy are expressed in N, mm and J, respectively. The type of failure, i.e., brittle or tough/ductile, is also recommended to be recorded.

6.7.4 Fracture mechanics approach

Fracture mechanics enables a separation of the material response from specimen geometry; however there is a reluctance/scepticism in industry, particularly polymer-related industry, to use this concept. The standard notch impact tests are qualitative and produce at best a guide for ranking materials. Design against crack propagation in materials requires

determination of fracture toughness, a material property that indicates the likelihood of a particular crack to cause catastrophic failure. Fracture toughness parameters K_{Ic} indicates the minimum level of stress intensity to cause a specimen of the material containing a crack of certain sharpness to suffer fracture, and the corresponding release of the stored energy, G_c , are interrelated in the fracture mechanics equation for isotropic materials:

$$K_{Ic} = (EG_c)^{1/2} = Y\sigma_f a^{1/2}$$

where, K_{Ic} is the fracture toughness ($\text{MPa m}^{1/2}$), E is the Young's modulus (GPa), G_c is the critical energy release rate (kJ / m^2), σ_f is the nominal applied stress at fracture (MPa), a is the crack length (or one-half of an internal crack length) and Y is the dimensionless calibration (correction) factor that accounts for the geometry of the specimen containing the flaw. Y is a function of (a/W) , where W is the width or depth of the specimen. The values for the Y calibration factor are available for different specimen geometries and loading modes (Rook & Cartwright 1976). For an ideal case, where an infinitely large plate containing an internal crack length of $2a$ is under tensile load, $Y^2 = \pi$.

ASTM D5045-99 standard test method, for 'Plane-strain fracture toughness and strain energy release rate of plastic materials', is designed to characterize the toughness of plastics in terms of the critical-stress-intensity factor, K_{Ic} , and the energy per unit area of crack surface (the specific surface energy) or critical strain energy release rate, G_c , at fracture initiation. Two testing geometries are covered by these test methods, single-edge-notch bending (SENB) and compact tension (CT). Linear elastic behaviour is assumed for the cracked specimen, so certain restrictions on linearity of the load-displacement diagram are imposed. A state-of-plane strain at the crack tip is required. Specimen thickness, therefore, must be sufficient to ensure this stress condition holds. Furthermore, the crack must be sufficiently sharp to ensure that a minimum value of toughness is obtained.

Further information on testing and the determination of fracture mechanic parameters, and on various fracture toughness data for polymer types and polymer-matrix composites are presented elsewhere (Akay 1999, pp. 533-588). One of the important factors in material behaviour under mechanical loading is the presence of any frozen-in residual stresses in materials. Some polymers, such as polycarbonate, are very sensitive to the presence of residual stresses in their fracture behaviour as demonstrated in Figure 6.22, causing a variation in impact strength values: a Charpy notched impact value of 42 kJm^{-2} was obtained with specimens taken from as-moulded injection moulded plaques, which deteriorated to 6 kJm^{-2} with specimens taken from plaques that were annealed at temperatures both below and above the material's glass transition temperature ($140 \text{ }^\circ\text{C}$) (see Akay & Ozden 1996).

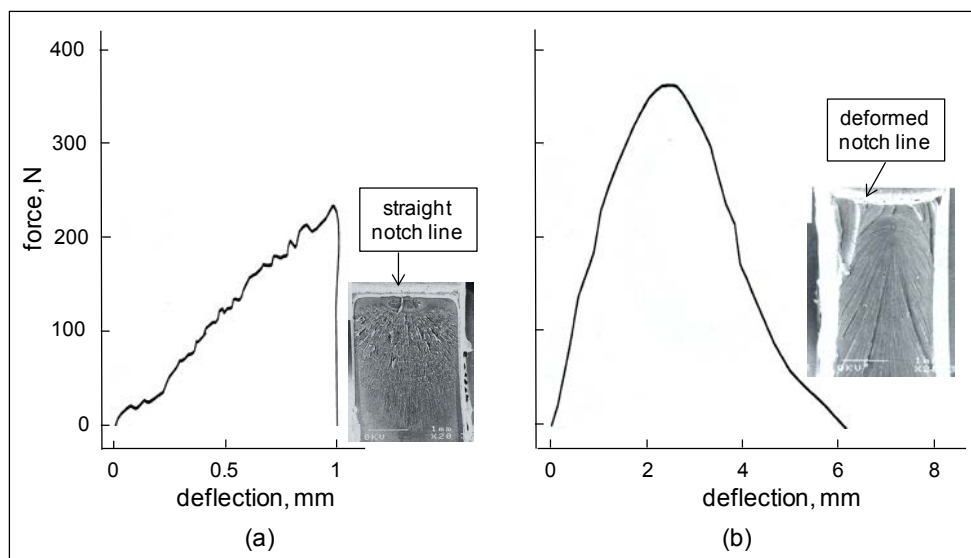


Figure 6.22 Instrumented impact force-deflection traces for notched specimens, and photograph of fracture surfaces for: (a) annealed PC and (b) as-moulded PC (source: Akay & Ozden 1996)

The presence of compressive stresses at the surface of notched specimens enhances the impact strength by promotion of the plane-stress failure, the material yields during the impact failure as can be seen from the deformed notch line in Figure 6.22 (b). Heat-treated specimens fail in a brittle manner as indicated by the straight notch line and the smoother fracture surface in Figure 6.22 (a).

However, a similar study on ABS copolymer has shown no significant variation between the impact properties of the as-moulded and annealed specimens (Akay & Ozden 1995).

6.8 Bearing strength

Bearing strength is particularly relevant in bolted joints. Successful adoption of bolted joints depends on a clear understanding of pin bearing strength, which is of critical importance since such joints are employed in critical engineering applications such as aerospace structures. The serious accident that an Airbus 300 jet aircraft suffered in 2001 during its flight from New York to Santo Domingo, Dominican Republic, claimed the death of 260 people on board and five people on the ground. The accident was attributed to the tail of the plane breaking off from the fuselage under the force of swirling wakes generated by another jetliner flying at a path, approximately 1.2 km away. The tail assembly of the aircraft was constructed from carbon-fibre (CF) polymer composite and bolted on to the fuselage and the failure had occurred in the vicinity of the bolted joints as shown in Figure 6.23.

The bolted joints are vulnerable to bearing failures, where the mode of failure is complex and depends on the factors such as the structure and properties of the materials joined together, the size and the geometry of the joint, e.g., the pin-hole diameter, thickness and width of the lug, and the level of clamping force applied to the joint (see Akay 1992 and Akay & Mun 1995). Various failure modes are possible: end-section bearing (i.e., crushing failure ahead of the bolt), net-section tension (tensile failure across the reduced section), edge-section shear (double shear out parallel to the direction of load), end-section cleavage (tear out or split forward of the bolt) and a tension-cleavage combination. Any mixture of these failure modes may also be experienced, see Figure 6.24. The figure also shows the influence of the clamping force (or constraint pressure) applied to the bolted assembly on the bearing strength and the modes of failure.



Figure 6.23 Illustration of the aircraft tail section failure at the November 2001 crash (source: TIME, November 26, 2001)

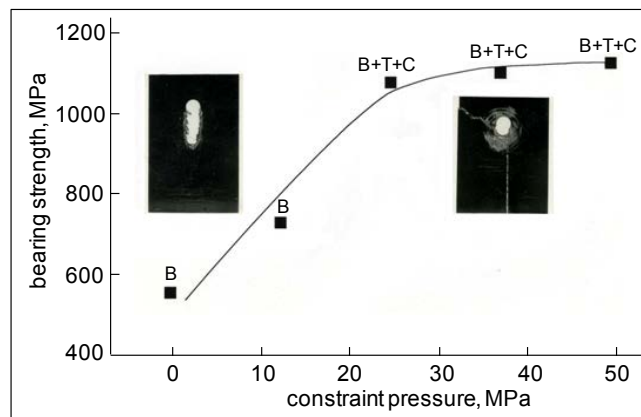


Figure 6.24 Bearing strength vs. constraint pressure for a CF/epoxy resin composite system with associated failure modes indicated as B - bearing, T - tension and C - cleavage (source: Akay 1992)

Figure 6.23 shows that the tail assembly has snapped off at the bolted joints, however without a closer inspection, it is difficult to conclude whether the failure is caused by an inherent weakness in the composite material or by an actual aspect of the joint.

A standard test method for bearing strength of plastics is given in ASTM D953-10 and for polymer-matrix composites in CRAG test methods (Curtis 1985). The tests are normally conducted in tensile mode, employing a test fixture shown in Figure 6.25. The test produces a load-displacement graph (see Figure 6.26.), from which the bearing strength properties; expressed in terms of the maximum stress sustained by the specimen, the stress at initial failure, and the stress at which the bearing hole is deformed by 4% of its diameter; may be determined.

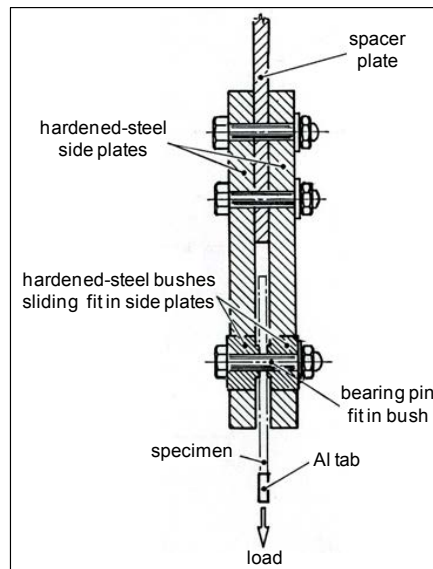


Figure 6.25 An illustration of specimen test fixture for bearing strength

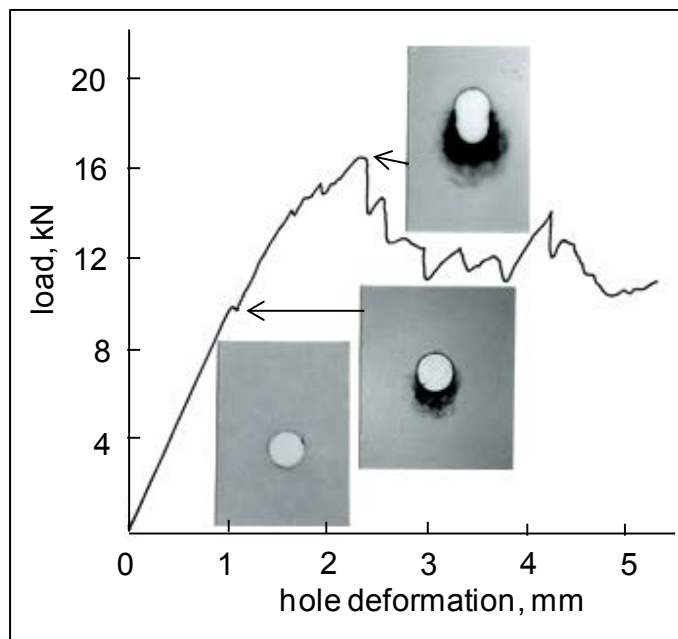


Figure 6.26 A typical load-displacement curve with associated X-ray micrographs of specimens at various levels of load on CF/epoxy composites (loading at 1 mm/min via 4.8 mm diameter pin) (source: Akay 1992)

6.9 Environmental stress cracking

Environmental stress cracking (ESC), also known as solvent cracking or stress corrosion cracking, is produced in a solid when placed in an aggressive liquid environment. The level of stress required to produce cracking/fracture is less than that required in the absence of liquid. Residual frozen-in stresses may be sufficient even in the absence of any additional applied stress to produce cracking (Alger 1989). The resistance of polymeric materials to ESC is known as environmental stress crack resistance (ESCR).

The phenomenon is responsible for many failures in plastic products/components in service (It is claimed that about 25 % of plastic part failures are relate to ESC, see Jansen 2004). A classic example of the phenomenon can be seen when one examines the history of the development of the current soft drinks PET bottle. These bottles were originally made from glass, a 2-litre bottle weighing almost 600 g, in 1980s PET bottles were introduced, using the same shape design as the glass bottles, which had a small radius between the body of the bottle and its flat bottom. This design made plastic vulnerable to ESC in the presence of the drink, creating a mess and shock in customers as the bottom fell out of them when the customers lifted the products from supermarket shelves. To alleviate the problem, the design of the bottle was changed such that the bottles had rounded hemispherical bases, but they had to be seated and glued into a separate base cup (Figure 6.27 (a)) with a flat bottom to make it self-standing. Such two piece constructions do not lend themselves to recycling and were relatively expensive in terms of material and production costs. In 1990s, the current design of bottles was introduced; having petaloid bases (multiple bulges), Figure 6.27(b), to provide a self-standing ability with a one piece construction without introducing any stress-rising sharp edges. The base cup was no longer necessary.

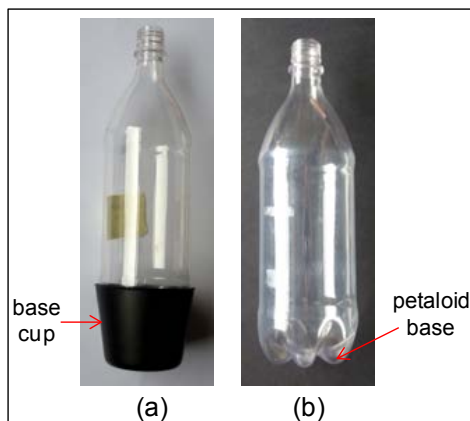


Figure 6.27 PET bottles: (a) fitted into a base cup, and (b) one-piece bottle with a petaloid base

The progression made in the design of PET bottles for carbonated beverages had many desirable outcomes: as well as exhibiting much greater ESCR, the bottles weighed less. The weight of 2-litre PET bottles was reduced from approximately 66 g in 1980s to 40 g in 2000s. This light-weighting meant material resource conservation, waste reduction and more efficient transportation of the product.

There are a variety of tests that are available for assessing the resistance of thermoplastics to ESC. These are based on the application of either constant strain or constant load (stress) to specimens and monitoring crack initiation and propagation. The equipment for constant-strain based tests tends to be simpler and less costly.

Determination of environmental stress cracking resistance of plastics by a constant pre-strain test include a bent strip method BS EN ISO 4599:1997, where the test pieces are clamped to a former of known radius before being brought into contact with the liquid at the specified temperature. Different magnitudes of strain are generated by employing formers with different radii, and the test aims to determine the minimum strain that causes a specific type of failure. An alternative method for ESC determination by means of a constant-strain test is the ball or pin impression method BS EN ISO 4600:1998. The test uses a pin or ball of known oversize, which is pressed into a reamed hole in the test piece to produce the strain. Different sized pins or balls produce a range of strains. The test is applicable to finished products and to test specimens.

Another constant strain method was developed by Bell Laboratories in the USA for testing the ESCR performance of polyethylene cable insulation and, therefore, known as the Bell Telephone Test and is detailed in ASTM D1693 – 10, entitled ‘Standard Test Method for Environmental Stress-Cracking of Ethylene Plastics’, the test involves introducing a slit/notch of a certain depth into a small rectangular strip of material and placing it in bent form into a holding clamp (a square-bracket holder with holes along its back to enable uniform exposure of the specimens to the test fluid). The assembly of the specimens are then immersed in a specified chemical solution in a test tube (Figure 6.28). The test tube is sealed and placed in a constant-temperature water bath. Specimens are inspected periodically for the development of any cracks from the notch. Cracks generally develop perpendicular to the notch, and run to the edge of the specimen. Initially crazes (tiny cracks) initiate and grow perpendicular to the notch direction in the form of a web; the crazes then coalesce and extend the notch tip. This failure repeats itself and crack propagation continues (see Jansen 2004).

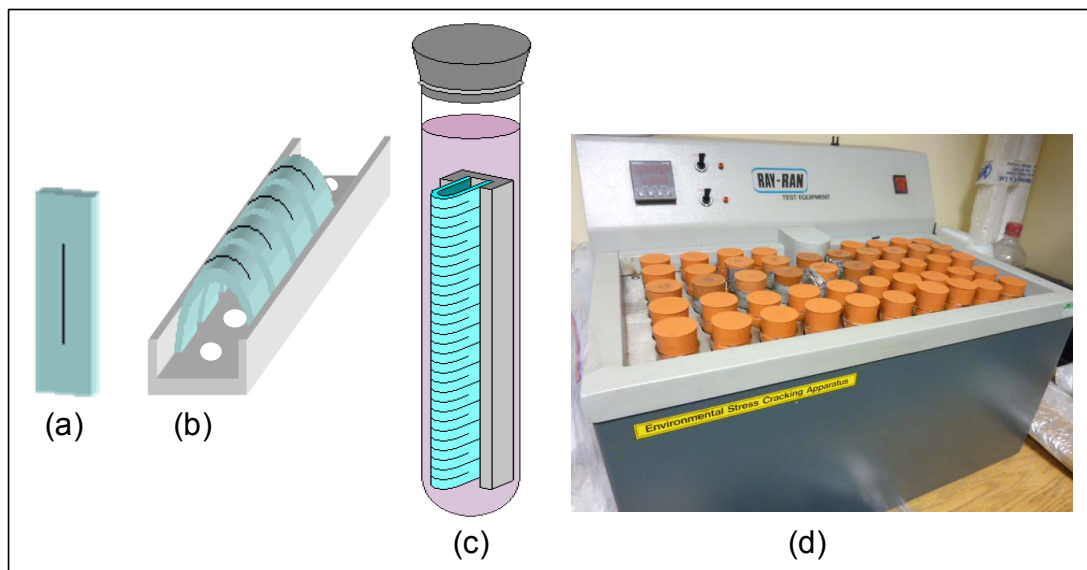


Figure 6.28 Bell telephone test: (a) notched specimen, (b) specimens assembled in the holder, (c) specimens placed in the test fluid, and (d) a battery of tubes with specimens in a hot-water bath (source: IDES)

BS EN ISO 6252:1998 is a constant tensile-stress method for the determination of ESC for plastics. A dumbbell-shaped specimen, immersed in a chemical reagent, is placed under a given tensile load until it breaks, and the time to failure is recorded.

6.10 Fatigue and wear

These properties indicate the response of the material to dynamic loading. The subject area is covered in general by Brown (1999, p245), for plastics by Hawley (1999, p334), for elastomers by Lewis (1999, p291) and with respect to fracture mechanics by Akay (1999, p541). Fatigue covers progressive weakening and ultimately breakdown of material in a component from repeated vibrations, and wear is generally taken to mean loss of material caused by repeatedly rubbing together of two surfaces, i.e., abrasion. Almost all moving parts, engineered or otherwise, could suffer from these forms of failure, for example, tyres, bearings, gears, helicopter propellers, turbine blades, engines, conveyor belts, moving shafts, limbs/equipment of sportspersons (e.g., tennis elbow), wrists/fingers of typists (an example of ‘Repetitive Stress Syndrome’, and hip and knee prostheses.

6.10.1 Fatigue

Fatigue testing, as distinct from dynamic mechanical thermal testing, takes the material/product to failure in order to estimate its expected life, and concentrates mainly on material strength, although loss of stiffness is also an important criterion in applications such as aerospace, therefore, materials would be tested for loss of stiffness under, for instance, torsion oscillations.

Fatigue testing can be conducted under any mode of loading (e.g., bending, torsion, compression, tension) and it is conducted at a given frequency between either set stress (load controlled) or set strain (strain controlled) values. The tests are normally conducted by superimposing the dynamic cycles onto a static preload or strain – this is more akin to the conditions of real applications/usage and also avoids zero strain in the cycle, which can be difficult to control. The mode of loading, therefore, may become tension-tension or compression-compression. The other obvious test variable is the wave shape selection, e.g., sinusoidal, square, saw-tooth (zigzag). Tests can also be conducted in special environments as well as under standard laboratory conditions. Of course, in certain industrial sectors, particularly where there are serious safety concerns, finished parts and the complete products are fatigue tested. Even ordinary household products such as furniture are tested for long-term strength and durability: Figure 6.29 shows the fatigue testing of an armchair, simulating sitting down, moving and getting up.

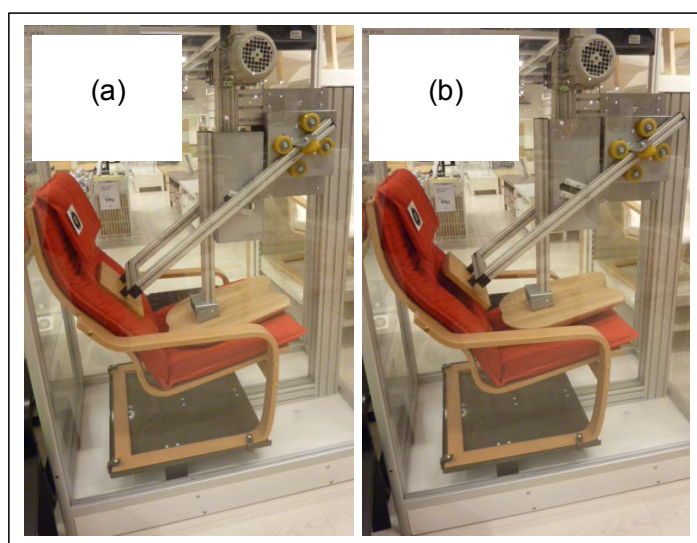


Figure 6.29 Testing home chairs for repeated (a) sitting down and (b) getting up (visit an IKEA store to see the test in action)

Compared with metals, plastics exhibit viscoelastic damping and they have lower heat conductivities and, therefore, are prone to hysteretic heating of the specimen during testing. Accordingly the tests for plastics tend to be conducted at low frequencies. Heat built up in the specimen lowers fatigue resistance, particularly if the temperature reaches the vicinity of the T_g of the material.

There is a scarcity of standard test methods on fatigue testing: ASTM E1823-10a, entitled, ‘Standard terminology relating to fatigue and fracture testing’; BS 3518-1:1993 ‘Methods of fatigue testing. Guide to general principles’; BS 7270:2006 ‘Metallic materials. Constant amplitude strain controlled axial fatigue. Method of test’ are designed for metallic materials. The only method for polymeric materials, ASTM D671-93 ‘Standard test method for flexural fatigue of plastics by constant-amplitude-of-force’ was found to be unsatisfactory and was withdrawn in 2002, and so far has not been replaced. One of the problems encountered was that the associated test machine, for cantilever bending fatigue, operated at a fixed frequency of 30 Hz!

Fatigue testing equipment are normally a servo-hydraulic system and modern machines provide flexibility for the selection of various parameters. In an actual test, conducted, for instance, in load-amplitude controlled mode, a maximum stress, S_{max} , and a minimum stress, S_{min} , is selected, giving a stress ratio $R = S_{min} / S_{max}$. The specimen is cycled at a given frequency until it fails and the number of cycles to failure, N , is noted. The tests are continued at progressively reduced values of S_{max} , maintaining the same R value and frequency, until sufficient data is collected to establish a smooth “S-N curve”, which is normally a plot of maximum stress against log (cycles to failure). The S-N curve may be constructed until a specific number of cycles are reached, or until an asymptotic limit (i.e., until there is a levelling off in the S_{max} values) is established, yielding the “endurance limit” value for S_{max} , see Figure 6.30. Note that the first data point on the S-N curve should be the static failure stress (i.e., the strength of the material under the same mode of loading). The maximum stress in the S-N curve can also be presented as normalised stress, i.e., as a fraction of the static strength of the material (UTS) (an example of this can be seen in BASF-2 (2003) for short glass-fiber reinforced PET).

Other possible outcomes for fatigue testing include “modulus decay curve”, which is determined by appropriately attaching an extensometer to the specimen, periodically stopping cycling temporarily to take data for determination of E and then resuming cycling. The test is terminated near the end of the fatigue life (i.e., prior to fracture), as estimated from S-N data.

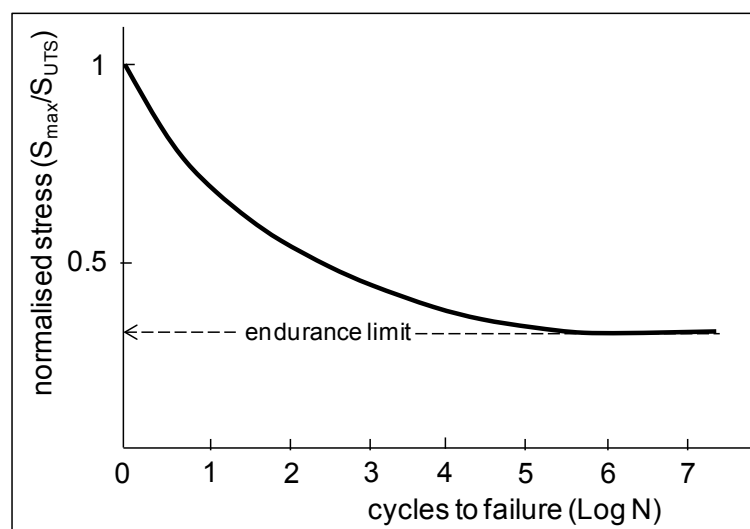


Figure 6.30 S-N curve

6.10.2 Wear

Wear is not a fundamental material property, it involves friction, localised adhesion, fatigue and tearing to various degrees depending on the material type and, therefore, at best suitable for comparing materials. Wear/abrasion tests mostly give a measure of the weight loss in the test piece, which can be converted to loss in volume if required, and sometimes loss of thickness and gloss/transparency as in coatings and laminates.

The main standard method for measurement of wear resistance of polymeric materials is the Taber Abrasion Test as specified in ISO 9352: 1995 or ASTM D1044-08. In ISO 9352: 1995 test, two rollers covered with abrasive paper abrade the surface of a rotating test specimen; see Figure 6.31, for a specified number of cycles under a specified load. The magnitude of the abrasion depends on the grade of the abrasive medium and the down force of the wheels on the test specimen, and the result is expressed as material loss given in milligrams per cycle of rotation. The ASTM D1044-08 test method specifies that the change in haze of the test specimen to be determined as a measure of abrasion resistance.

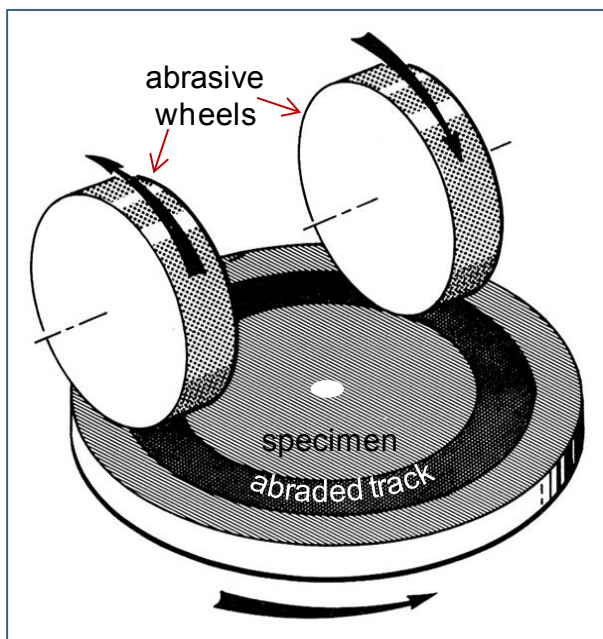


Figure 6.31 Taber abrasion set up (source: Taber Industries)

An associated property is friction, which can be defined as resistance to motion when substances slide over each other. It is proportional to the compressive normal force between the surfaces, and the property of the **coefficient of friction** is defined as the ratio of the frictional force to normal force. One of the associated standard test methods is BS EN ISO 8295:2004, “Plastics, film and sheeting. Determination of the coefficients of friction”. There are other test methods that are specific to certain applications, for example, for flooring where anti-slip characteristics are important, a swinging pendulum test is used. This was designed by the Road Research Laboratory (now the Transport Research Laboratory) of the U.K. in the late 1950s, which is standardised in BS 7976:2002 in three parts: BS 7976-1 specifies the features, dimensions and characteristics of the pendulum tester. BS 7976-2 describes a method of operation for this pendulum tester, and a method of calibration is specified in BS 7976-3. Its equivalent in ASTM is ASTM E303 - 93(2008), “Standard test method for measuring surface frictional properties using the British Pendulum Tester”.

The pendulum slider, Figure 6.32, can be fitted with a pad of either 4-S rubber or TRL rubber with different hardness and resilience values. During the test, similar to impact testing, the pendulum is released from a given height, and at the bottom of its swing it slides over a given area of the specimen surface. The energy absorbed by the sliding process is determined on the basis of the climbing height of the pendulum and results in a measure of the grip offered by the surface tested. The pendulum tester is fitted with an appropriate scale depending on the sliding length traversed on the specimen surface, and enables a direct reading of a test result in terms of a pendulum test value (PTV), which is proportional to the energy absorption and indicates the level of grip or skid resistance of the surface tested. The test is often conducted under dry or wet conditions. PTV value provides a guidance, above which the risk of slip is extremely low for able-bodied people (under standard laboratory conditions, the guidance PTV values of 65 and 75 are indicated for TRL and 4S sliders, respectively).

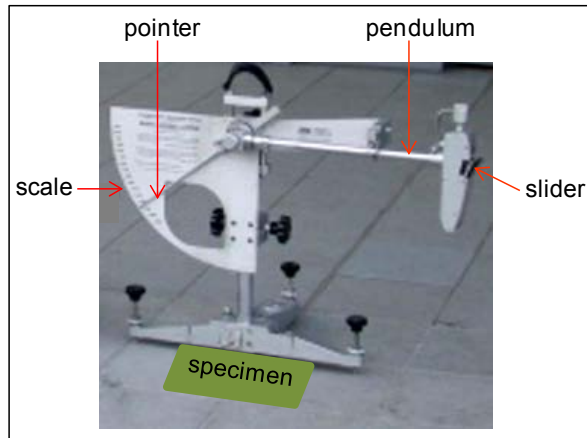


Figure 6.32 Pendulum slip resistance test

6.11 Self-assessment questions

- Compare the elongation to failure value obtained from a plot of stress-strain curve for a brittle plastic with the one obtained by measuring the length of the broken halves of the specimen. What difference would be expected and why?
- The mechanism of plastic deformation in ductile polymers is different than that in metals because:
 - it occurs by the movement of dislocation
 - it is reversible by heating
 - it takes place by stretching of cross-links
 - it takes place by slippage of chains
- Sketch on the same graph paper (on the same plot) the stress-strain curves for: (a) atactic PS, (b) HDPE, and (c) a copolymer of styrene and butadiene.
- Draw stress-strain graphs for two polymers: one is stiffer than the other and exhibits a yield point and the other shows no clear yield point but is much tougher.
- A metal ball is dropped from a height of 2 m onto a specimen cut from a plastic sheet. The specimen punctures and the damage consists of a hole about the size of the ball. The same test is conducted by dropping the ball from a height of 5 m, and this time the specimen shatters to pieces. Explain why this is so.
- From the stress-strain plots shown in Figure 6.7, determine the tensile strength, yield strength and % elongation to failure for HIPS at room temperature.
- A pillar of length L , made from a polymer-matrix composite of density, ρ , is erected upright. Show that the compressive strain under its own weight at a height of h from the ground is $\epsilon = \rho(L-h)g / E$.
Express the level of compression (the reduction in length) in terms of L and h by using the data for a composite material of density of 2000 kg/m^3 and E of 20 GPa . Show that the length of the pillar should not be greater than 5.4 m in order to avoid an average compression of $15 \mu\text{m}$.
Answer: $\Delta L = L(L-h) \times 10^{-6}$.
- Often a range of values rather than a single value are quoted for the mechanical properties of semicrystalline TPs and thermosetting plastics, why?

9. Why are some polymers hygroscopic? How are the mechanical properties affected by moisture, explain by giving specific examples of polymers and mechanical properties.
10. By using the data on Figure 6.12, draw an approximate creep curve for a Nylon 66 bar of 100 mm² cross-sectional area under a load of 2 kN for over a year.
11. Bulging and emaciation, depending on the mode of deformation, enables the volume of a rubber specimen remain constant, show that its Poisson's ratio is 0.5. Assume that the specimen is a square prism of length L and cross-section $A = w^2$.
Hint: $\Delta V = \Delta(AL) = L\Delta A + A\Delta L = 0$.
12. With the aid of Table 6.1, select a polymer that floats on water, has a minimum Young's modulus of 1 GPa and remains ductile/tough below 230 K.
13. With the aid of Table 6.1, select a polymer that is transparent, remains rigid in boiling water and has a specific gravity not greater than 1.2.
14. Determine the compression modulus of a block of rubber of a square face of 200 mm side and 50 mm thickness with a Young's modulus of 3 MPa. The rubber block is to be used as a bearing material sandwiched between two steel plates attached to its faces, what deflection would it undergo if loaded with a mass of 5 tonnes?
Answer: If c is the thickness of the block, then its deflection under load, $\Delta c = 6.8$ mm.
15. A bridge of 300 tonnes mass is to be supported by four rubber bearings of square surface areas. Each has to withstand a compression stress of 5 MPa. Calculate the dimensions of the bearing needed to ensure that under a horizontal force of 60 kN, the shear deflection does not exceed 25 mm. Assume the shear modulus of the rubber to be 1 MPa. How many steel plates should be used in each bearing in order to restrict the vertical deflection to 3 mm under the static deck load?
*Answer: the surface side of the block, $a = 380$ mm, and the thickness, $c = 61.25$ mm.
By using the shape factor parameter, S , it can be shown that the total thickness of 61.25 mm should be split into three layers so that each layer would have a thickness less than 24 mm and therefore will not compress more than 3 mm. Therefore, together with the outer plates, a total of four steel plates will be needed for the bearing.*
16. Name and sketch a simple mechanical model that will describe the stress relaxation in polymers. A sample of PVC flexible cable is tested at 27 °C to determine its stress relaxation properties. The stress decreases from 6 MPa to 1 MPa in 50 h, calculate the relaxation time.
It is intended to manufacture coiled cords for telecommunication equipment using the PVC flex, and therefore the relaxation time should not be greater than 3 h for efficiency in production. Determine what should be the minimum temperature of the processing oven to achieve this. The activation energy for this process is 20 kJ / mol and the molar gas constant = 8.314 J / (mol.K).
Answer: $\tau = 28$ h; oven temperature: 142 °C
17. Distinguish between the pendulum impact tests of Charpy and Izod.
18. "One of the important factors in material behaviour under mechanical loading is the presence of any frozen-in residual stresses in materials"; verify this statement in terms of impact behaviour of some specific plastics.
19. A brittle polymer component that has an internal crack length of 0.58 mm must not fail when a tensile load is applied. Determine the maximum stress (in MPa) that may be applied if the specific surface energy of this polymer is $G_c = 0.50$ J/m². Assume an elastic modulus of 2.9 GPa, and that the calibration factor, Y , is given as $Y^{1/2} = \pi$.
Answer: $\sigma_f = 1.26$ MPa
20. Draw a typical impact force-deflection curve for a semicrystalline polymer and describe the sort of information about the impact properties of the material that can be extracted from such a curve.

21. In a bolted mechanical joint, which property of the material is relevant for the integrity of the joint under load? What modes of failure can be expected during the failure of such a joint under tension?
22. Define ESC in polymeric products and describe how it led to the development of present-day PET bottles for soft drinks. What other desirable outcomes besides improved ESCR has resulted from the changes to the PET bottles over time?
23. Describe different ways of plotting fatigue-life expectancy curve for polymeric materials; define what is meant by the fatigue endurance limit.
24. What properties indicate the response of a material to dynamic loading? Give actual engineering examples where these properties are relevant.

7 Thermal properties

“In science there is only physics; all the rest is stamp collecting.” **Lord Kelvin (William Thomson)** (1824–1907) - Britain’s first scientific peer.

Only a Belfast-born Irish man can make such a daring statement, a challenge to the dye in the wool chemists amongst us! Lord Kelvin’s statue welcomes you to the beautiful Botanic Gardens in Belfast, next to Queen’s University Belfast, what a privilege for the people of QUB and Belfast to have such a well-kept garden in the heart of the city.

Lord Kelvin’s contribution to physics includes the fundamental concept of the Kelvin thermodynamic temperature scale, where the “infinite cold” (absolute zero) was the scale’s null point, $-273\text{ }^{\circ}\text{C}$, and which used the degree Celsius for its unit increment. The kelvin symbol is always a capital K. In the SI naming convention, all symbols named after a person are capitalized; in the case of the kelvin, capitalizing also distinguishes the symbol from the SI prefix “kilo”, which has lowercase k as its symbol.

Thermal properties of materials indicate mainly the physical response of the materials to the input of heat and the resulting change in their temperature. In the short-term the physical effects of temperature variation on the material are reversible, whereas the long-term effects are generally dominated by chemical changes and are not reversible. The long-term effects at elevated temperature are usually that of degradation/aging, causing deterioration in mechanical, physical and chemical properties.

Thermal properties include coefficient of thermal expansion (CTE), specific heat capacity, thermal conductivity, glass transition temperature (also secondary glass-transition temperatures), heat-distortion temperature, softening temperature and melting point. These properties are all interrelated, e.g., the CTE values can be significantly different on either side of T_g .

The references that cover the topic of thermal properties for polymers include a comprehensive two volume coverage by Turi (1997), general introduction of the basic principles by Brown (1999, p263), a wide range of standard test methods by Hawley (1999, p341), dynamic mechanical thermal analysis by Gearing (1999, p501), thermal conductivity, thermal diffusivity and specific heat by Hands (1999, p597) and a book that covers all the principles and the applications of the thermal analysis test methods by Ehrenstein et al. (2004).

There are a variety of standard test methods for determining thermal properties, some of which are material specific, employing equipment and techniques of different degrees of sophistication. The equipment for performing thermal analysis, i.e., monitoring of the property change with temperature, used to be basic and the tests time consuming. However, the advent of a range of instrumented and soft-ware based commercial thermal analysis equipment/techniques in the last few decades have made these tests less tedious, very accurate and very efficient with many alternative ways of presentation of the measured data. These techniques include differential scanning calorimetry (DSC), thermomechanical analysis (TMA), thermogravimetric analysis (TGA), dynamic mechanical thermal analysis (DMTA)/dynamic mechanical analysis (DMA) and dielectric analysis (DEA). These techniques and the properties and the variation of the properties with temperature that can be determined with these techniques are covered in the succeeding sections.

7.1 Differential scanning calorimetry

The differential scanning calorimeter measures change in enthalpy, i.e., the amount of heat that is either absorbed (an endothermic reaction) or released (an exothermic reaction) by a substance undergoing a physical or a chemical change. During a DSC test, the sample is subjected to a controlled temperature/time programme (e.g., 10 °C/min heating rate) and the heat flow to and from the sample is measured.

Two very identical equipment/techniques are available, viz. differential thermal analyser (DTA) and DSC:

DTA, also known as heat-flux DSC, consists of one block furnace for both specimen and reference material cells. The cells are harnessed with thermocouples, and heated or cooled simultaneously to a controlled temperature programme. The temperature difference (ΔT), between the sample and the reference material is measured while both are subjected to identical heat input, and the heat flux (i.e., heat required to bring about material transitions) is calculated from calibration data using ΔT .

DSC, power-compensated DSC, consists of two small separate furnaces/blocks housing the cells for the sample and the reference. Thermal power is supplied to the individual heaters in the blocks to maintain the sample and reference at the same temperature, even during a thermal reaction in the sample. Therefore, any variation between the furnace temperatures, due to any exothermic/endothermic reactions in the specimen, is compensated by varying the power input. Because of the direct measurement of heat flow, it is often also called heat flow DSC. Direct measurement of heat capacity and enthalpy makes this technique generally preferable for quantitative analysis. Furthermore, large single DTA furnaces heat and cool at a slower rate than the smaller DSC furnaces. For the vast majority of basic applications, the data from both types of instruments are comparable and both instruments can give good data, and in the succeeding coverage, unless required, only the term DSC will be used.

Using a differential scanning calorimeter any transition in a material that involves a change in heat content of the material can be detected and measured, accordingly, the following properties are generally determined:

T_g (glass transition temperature), the temperature at which an amorphous polymer or an amorphous part of a crystalline polymer goes from a hard brittle (glass like) state to a soft rubbery state with rising temperature.

T_m (melting point), the temperature at which a crystalline polymer melts.

T_c (crystallisation point), the temperature at which a polymer crystallises upon heating or cooling. ΔH_m (heat of fusion), the amount of energy (J/g) which a crystalline polymer sample absorbs while melting, and is used in determining % crystallinity,

ΔH_c (heat of crystallisation), the amount of energy (J/g) a sample releases while crystallising.

C_p (specific heat capacity at constant pressure), the amount of heat required to raise the temperature of a substance by 1°C, in other words, C_p indicates the amount of energy a unit of matter can hold.

DSC is also used to measure curing, cross linking, phase changes (e.g., solid-state (s-s) transitions), oxidative degradation or decomposition by vaporization or sublimation. The processes/reactions of crystallisation, curing, cross linking, oxidative degradation are exothermic, whereas melting, some phase changes and decomposition by vaporisation/sublimation are endothermic. One should, however, avoid substance decomposition in the DSC in order to prevent a subsequent cleaning problem. Substances suspected of decomposition should be tested on a TGA first.

The standard methods associated with DSC include:

ISO 11357-1:2009 Plastics – Differential scanning calorimetry (DSC) – Part 1: General principles

ISO 11357-2: 1999 Plastics – Differential scanning calorimetry (DSC) – Part 2: Determination of glass transition temperature

ISO 11357-3:2011 Plastics – Differential scanning calorimetry (DSC) – Part 3: Determination of temperature and enthalpy of melting and crystallization

ISO 11357-4:2005 Plastics – Differential scanning calorimetry (DSC) – Part 4: Determination of specific heat capacity

ISO 11357-5: 1999 Plastics – Differential scanning calorimetry (DSC) – Part 5: Determination of characteristic reaction-curve temperatures and times, enthalpy of reaction and degree of conversion

ISO 11357-6:2008 Plastics – Differential scanning calorimetry (DSC) – Part 6: Determination of oxidation induction time (isothermal OIT) and oxidation induction temperature (dynamic OIT)

ISO 11357-7: 2002 Plastics – Differential scanning calorimetry (DSC) – Part 7: Determination of crystallization kinetics

DIN 51007, Thermal analysis; differential thermal analysis; principles

DIN 53765 Testing of plastics and elastomers; thermal analysis; DSC-method

ASTM D3417-99 Standard test method for enthalpies of fusion and crystallization of polymers by differential scanning calorimetry (DSC)

ASTM D3418 - 08 Standard test method for transition temperatures and enthalpies of fusion and crystallization of polymers by differential scanning calorimetry

ASTM E793 - 06 Standard test method for enthalpies of fusion and crystallization by differential scanning calorimetry

ASTM E794 - 06 Standard test method for melting and crystallization temperatures by thermal analysis

ASTM E967 - 08 Standard practice for temperature calibration of differential scanning calorimeters and differential thermal analyzers

ASTM E1269 - 11 Standard test method for determining specific heat capacity by differential scanning calorimetry

ASTM E1356 - 08 Standard test method for assignment of the glass transition temperatures by differential scanning calorimetry

The outcome of a DSC test is usually presented in the form of a plot of heat flow against temperature and/or time. The standards use different notation of indicating exothermic (exo) and endothermic (endo) effects on a DSC trace; i.e., whether they are indicated as an upward or downward deflection on the ordinate axis. In a heat-flow DSC, the endothermic peaks (those events which require energy) point up, since the instrument must supply more power to the sample to keep the sample and reference furnaces at the same temperature. In a heat-flux DSC, these same events cause the sample to absorb heat and become cooler than the furnace, so they point down. The reverse logic applies to exothermic events where energy is released. The International Conference on Thermal Analysis and Calorimetry (ICTAC) (PerkinElmer 2010, p5) has set the convention that curves should follow this pattern. Most modern software systems enable the curves to be presented either way. Notwithstanding, it is important to clearly indicate the sense/direction of 'exo.' and 'endo.' on the graph.

The plots, as well as the usual DSC curves, may also include their derivative (DDSC curves) as a function of temperature. Figure 7.1 shows the DSC and DDSC for a semicrystalline PET specimen scanned at 20 °C/min. The derivative can be expressed with respect to temperature or time. The DDSC plots are useful in detecting/highlighting the temperature of poorly defined transitions and also the start and end points of the measured effects. It is particularly useful in converting a step in the base line of a DSC trace that occurs at glass transitions into a peak and therefore makes it easier to read off temperature. The derivative traces serve as an aid and they are not normally included in the plots that are presented.

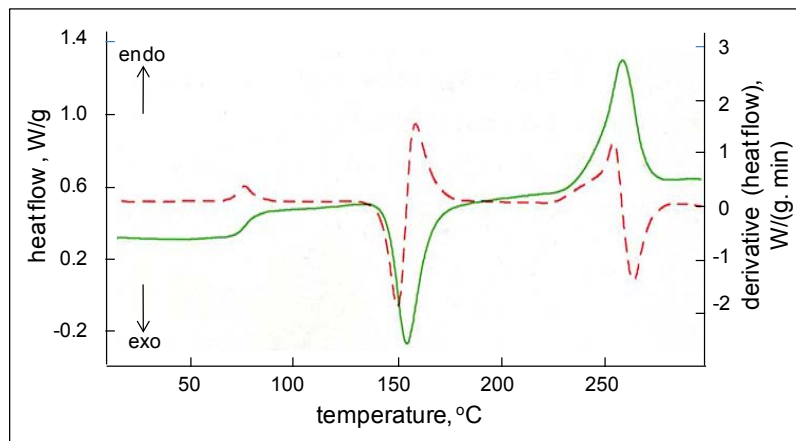


Figure 7.1 A DSC and DDSC (broken line) traces for a polymer sample (source: Netzsch GmbH)

The figure displays an endothermic shoulder at around 80 °C, an exothermic peak maximum at 150 °C and an endothermic peak maximum at 250 °C.

Temperature-modulated DSC (TMDSC) is a technique (Reading 1993), which is devised to declutter the information gleaned from a DSC run and make it easier to identify and measure properties that are not so distinctly evident on a normal DCS trace, e.g., glass transitions for semi-crystalline polymers. In TMDSC, the sample is subjected to an oscillating heating or cooling rate “forcing function”, where the mean temperature changes linearly (e.g., a sinusoidal modulation is superimposed on the underlying heating ramp). The process enables greater sensitivity and separates overlapping thermodynamic/reversing transitions (glass transition, melting) from non-reversing/kinetic events such as crystallisation, curing and decomposition. The reversing signal is associated with properties dependent upon the temperature rate of change while the nonreversing signal defines kinetic events (i.e., those associated with both time and temperature).

Other ways of affecting sensitivity/resolution include Fast Scan DSC or Hyper DSC techniques that apply very high heating rates (i.e., fast scans) to a sample to increase the sensitivity of a DSC to transitions (particularly useful with otherwise hard to detect small transitions) and to jump kinetic behaviour. As a DSC experiment is accelerated in the Hyper-DSC method, the same heat flow occurs over a much shorter period of time and provides the heat required for the event almost instantly and, therefore, the thermal event becomes magnified. This allows extremely low-energy transitions to be identified and measured with ease. The technique obscures sample changes, such as crystallisation, curing and decomposition that require time and, therefore, can occur during slow heating when using conventional DSC. During a very fast scan, the sample does not have the time to undergo any structural changes and, therefore, it is possible to maintain the material analysed in its “as-received” state.

The Hyper-DSC method is only possible with power-compensated DSC, since the single furnace DSCs cannot heat at the required rates. Fast scan heating rates range from 100-300 °C/min, whereas Hyper-DSC heating rates range from 300-750 °C/min. When heating rates of 100-750 °C/min are applied, the response of the DSC to weak transitions is enhanced and it is possible to detect very low levels of amorphous materials: the limit of detection with conventional DSC is about 10% amorphous, and with Hyper-DSC this becomes approximately 1%. High scan rates also make it possible to conduct faster tests and run many more samples.

Thermal properties that can be measured with DSC were mentioned above, and most of which are simply extracted from a DSC graph, e.g., T_g , T_c and T_m , see Figure 7.2, and others require calculations as described in the succeeding sections.

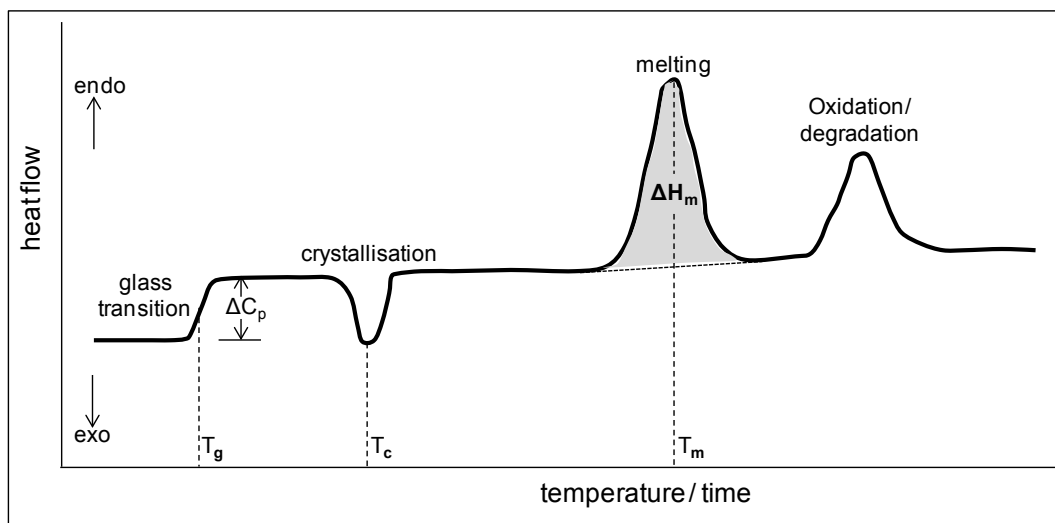


Figure 7.2 Illustration of a DSC scan for a semicrystalline polymer sample

7.1.1 Degree of crystallinity

The degree of crystallinity of a material can be calculated using the appropriate heat of fusion values:

where, ΔH_m is the area under the melting peak when heat flow is plotted against time from a DSC run, see Figure 7.2, and ΔH_m^0 is the literature value for the same material in 100% crystalline state, Table 7.1 shows the ΔH_m^0 values for some semi-crystalline polymers. The method is standardised in ISO 11357-3:2011. An example calculation of % crystallinity for a sample of PEEK is shown in Section 4.3.4.

ΔH_m is determined as shown in the following text box, when the DSC trace is a plot of “heat flow vs. temperature”.

Note that $\Delta H_m = \text{heat flow} \times \text{time} = \left(\frac{\text{heat}}{\text{time} \times \text{mass}} \right) \times \text{time}$

“Time” could be expressed in terms of temperature from the rate of heating ($^{\circ}\text{C}/\text{min}$) used in the DSC scan, $\text{time} = (\text{temperature}) / (\text{heating rate})$, and if substituted in the above equation, it gives

$$\Delta H_m = \left(\frac{\text{heat}}{\text{time} \times \text{mass}} \right) \times \left(\frac{\text{temperature}}{\text{heating rate}} \right); \text{ its unit being } \left(\frac{\text{J}}{\text{s} \times \text{g}} \right) \times \left(\frac{\text{K}}{\text{K}/\text{s}} \right) \text{ or } (\text{J}/\text{g}).$$

Alternatively, $\Delta H_m = (\text{heat flow}) \times \left(\frac{\text{temperature}}{\text{heating rate}} \right) = \left(\frac{\text{area under the DSC melting curve}}{\text{heating rate}} \right)$

“Area under the DCS melting peak” is from the plot of heat-flow vs. temperature, see Figure 7.2.

7.1.2 Specific heat capacity

Specific heat capacity, C_p , for a sample of material of mass ‘m’ that is heated for a time at a given heating rate to increase its temperature by ‘ ΔT ’ can be calculated using the following relationship:

$$\text{_____} = \frac{\text{_____}}{\text{_____} \times \text{_____}} \times \text{_____}$$

Standard test methods such as ISO/FDIS 11357-4 and DIN 53765 describe how to allow for the contribution of the empty/reference DCS pans to the heat flow in the calculations.

7.1.3 Oxidative induction time/temperature

Metals suffer from corrosion, and while plastics are immune to corrosion, they also are prone to degradation such as oxidation. Polymer producers normally add stabilizers to improve the resistance of susceptible polymers to oxidative degeneration. Polyethylene, for example, can suffer oxidation decomposition in the air at approximately 200 °C, whereas, in the absence of oxygen, in a nitrogen atmosphere, it undergoes thermal degradation at approximately 400 °C. Therefore, antioxidants are added to protect against oxidation in applications.

Determination of oxidation induction time/temperature (OIT) is the primary means of finding out the resistance of polymeric products to oxidation. OIT is a standardized test performed using a DSC. The associated standard methods include:

ISO/TR 10837:1991 Determination of the thermal stability of polyethylene (PE) for use in gas pipes and fittings

ISO 11357-6:2008 Plastics – Differential scanning calorimetry (DSC) – Part 6: Determination of oxidation induction time (isothermal OIT) and oxidation induction temperature (dynamic OIT)

ASTM D3895 - 07 Standard test method for oxidative-induction time of polyolefins by differential scanning calorimetry

ASTM D5885 - 06 Standard test method for oxidative induction time of polyolefin geosynthetics by high-pressure differential scanning calorimetry

The test essentially subjects the specimen to an accelerated oxidation environment, while monitoring for the occurrence of exothermic and endothermic reactions. Thus, the higher the values for the OIT, the more oxidation resistant the sample is. The tests follow either a “dynamic” or “static” method: in dynamic method, the specimen is heated continuously under oxygen or air flow from the start, whereas, in static procedure, a semi-crystalline plastic, is heated continuously under nitrogen flow to above its melting peak and held at that temperature, then the atmosphere is changed from N₂ (inert) to O₂ or air and the heat is maintained (isothermal heating) until the exothermic degradation peak is reached.

The dynamic method enables the measurement of the oxidative induction temperature, T_{oit} (indicating the onset of oxidation), either as an extrapolated value or an exothermic offset value. The offset of heat flow from the base-line is used when the onset temperatures are difficult to reproduce by extrapolation, and consists of drawing a line parallel to the baseline at an offset distance of $\Delta = 0.05$ W/g, as recommended by ISO 11357-6, and the intersection of this line with the exothermic peak is defined as the onset of oxidation, see Figure 7.3. The static method yields the oxidative induction time (the time period from the changeover to oxygen to onset of oxidation), see Figure 7.4. (ISO 11357-6:2008).

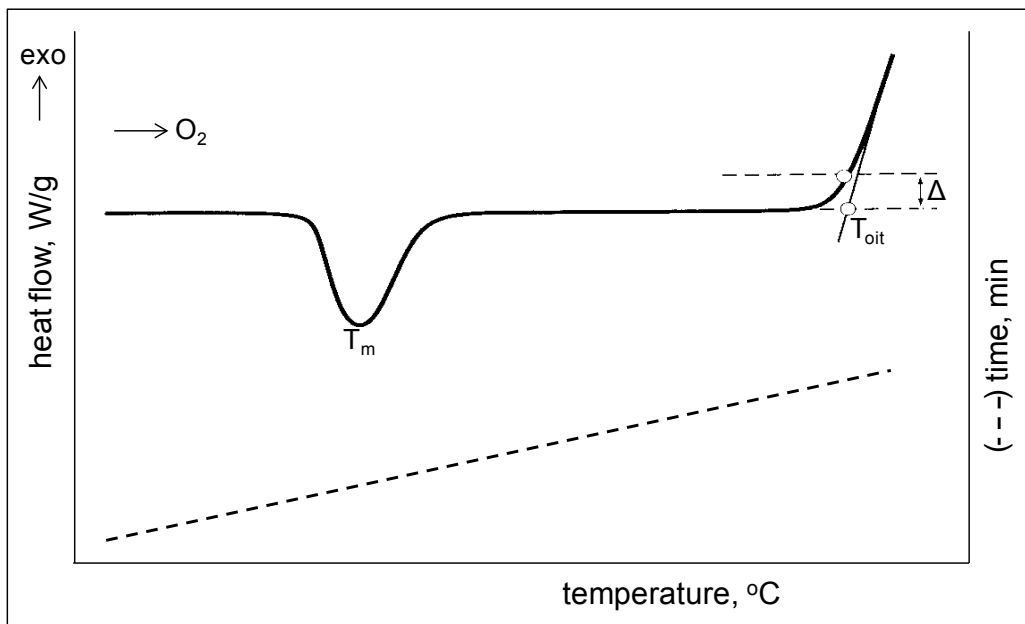


Figure 7.3 Illustration of a dynamic OIT scan for oxidation induction temperature, T_{oit}
 (source: ISO 11357-6:2008)

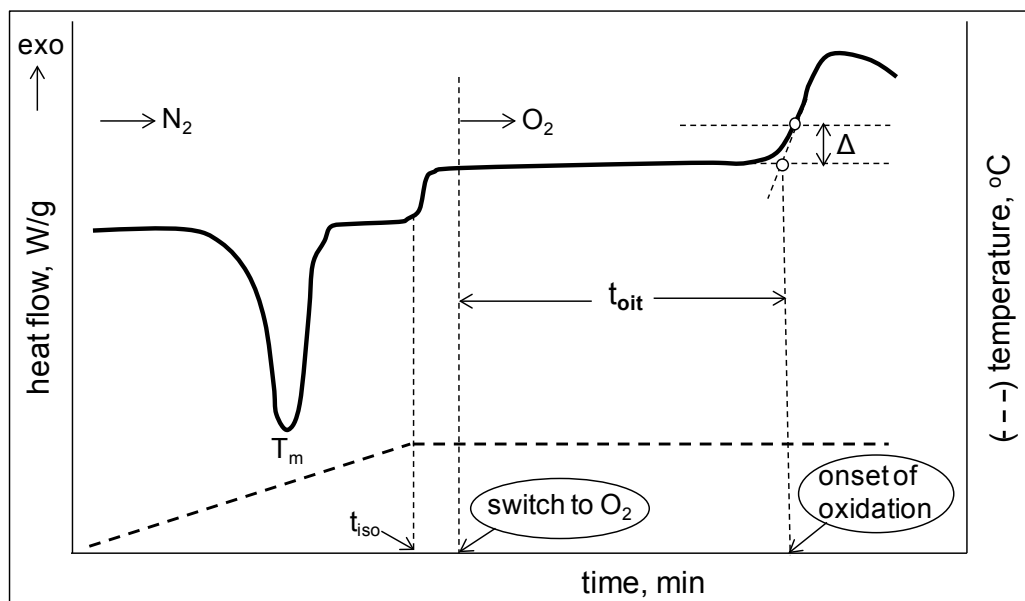


Figure 7.4 Illustration of a static OIT scan for oxidation induction time, t_{oit}

A useful application of the measurement is to find out the OIT of the unprocessed polymer and the OIT of the processed plastic. Any variation in measurements should indicate the extent of the impact of polymer processing on the reduction of oxidation resistance.

7.2 Thermogravimetric analysis

Thermogravimetric analysis (TGA) measures temperature and/or time-dependent mass changes in a sample of a material. The technique is popularly used to indicate the thermal stability of materials and to determine the composition of plastics, polymer blends and polymer-matrix composites. TGA is a convenient method of checking/verifying any modifications to material formulations.

The associated standard methods include:

ISO 11358:1997 Plastics – Thermogravimetry (TG) of polymers – General principles

ISO 9924-1: 2000 Rubber and rubber products – Determination of the composition of vulcanizates and uncured compounds by thermogravimetry – Part 1: Butadiene, ethylene-propylene copolymer and terpolymer, isobutene-isoprene, isoprene and styrene-butadiene rubbers

ASTM D6370 - 99(2009) Standard test method for rubber-compositional analysis by thermogravimetry (TGA)

ASTM E1131 - 08 Standard test method for compositional analysis by thermogravimetry

ASTM E1582 - 04 Standard practice for calibration of temperature scale for thermogravimetry

DIN 51006 (2000) Thermal analysis (TA) - Thermogravimetry (TG) – Principles

TGA tests can be conducted either in temperature scanning mode or in isothermal mode. In **temperature scanning mode**, the sample is subjected to a controlled temperature programme in a controlled atmosphere (i.e., an inert gas (N_2 or argon) or oxygen or air purge at a certain flow rate) and its mass is monitored. Constant heating rates (or temperature scanning rates) are typically in the range of 5-20 °C/min, slower scans produce better resolution of transitions, but faster rates are useful for a quick initial assessment scan. Alternatively, tests can be conducted **isothermally** and mass change is recorded against time (min). In this case the sample is rapidly heated (e.g., 100 °C/min) to the required temperature in order to avoid/minimize evaporation or reaction prior to reaching temperature. Isothermal runs are useful for studying processes such as moisture absorption or desorption, curing reactions that produce small chemicals (e.g., water or formaldehyde), and emission of HCl as PVC degrades. In TGA, the specimen size and geometry should be controlled: since for evaporation, surface area is important, and for diffusion of volatiles from the body of the specimen to its surface, the area/volume ratio is a factor. In oxidative degradation, the diffusion of oxygen into the material would also be influenced by specimen size and shape.

The test results produce thermogravimetric curves (a plot of % mass change against temperature or time). From the TGA curves, data such as mass loss (sometimes mass gain as in oxidization) and associated temperature values can be extracted. The derivative of the TGA data (DTG) can also be plotted and produces a useful curve for a clearer identification of events, particularly if these events are either too close together or are not very distinct. The point of the greatest rate of change on the mass loss TGA curves, i.e., the inflection point, is indicated by a peak on a DTG curve, which makes identification of the events and the extraction of data from the curves easier, see Figure 7.5.

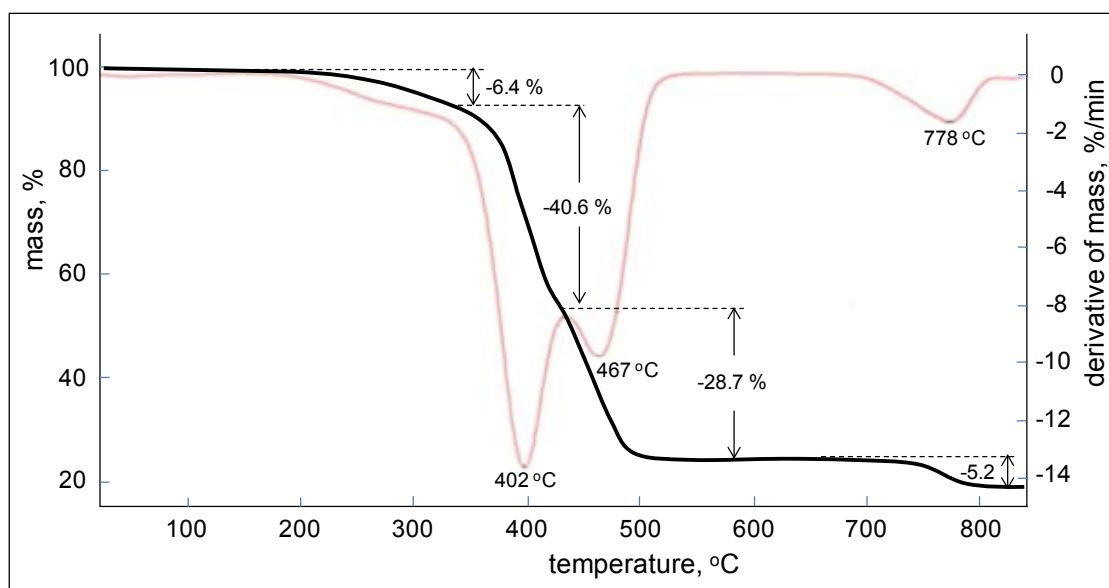


Figure 7.5 (–) TG and (–) DTG traces for a blend of natural and SBR rubber (source: Netzsch GmbH (see Reference (Kaisersberger 1994))

TGA can quantify loss or gain of water, loss of solvent, loss of plasticizer, decarboxylation (release of CO_2), composition of polymer blends, curing-related emissions, pyrolysis and related emissions, oxidation, decomposition and filler/ash content. TGA is frequently used as a quality control tool, but is also used to reverse engineer a product and to distinguish between competing products. Figure 7.5 illustrates an application, showing the TGA and DTG traces for a blend of natural rubber (NR) with SBR, used as anti-vibration mountings in the automotive industry. The TGA scan was conducted on

13 mg cuttings from NR/SBR vulcanized sheet under 10 ml/min N₂ purge, heating at 20 °C/min up to 850 °C. The graph enables one to identify the composition of the blend and quantify the amounts of the component materials. The curve shows evolution of plasticiser, with a mass of 6.4%, at about 300 °C. The pyrolysis of NR, 40.6%, and SBR, 28.7%, follows at temperatures of approximately 400 and 467 °C. At 778 °C calcium carbonate filler (the chalk) decomposes into CO₂ (5.2 %) and CaO. This information enables the calculation of the filler content as shown in the text box below.



The blend formulation also contains carbon black, which can be quantified by cooling down the sample residue to 450 °C and changing the gas to O₂ (to burn C-black) and applying a second heating scan up to 800 °C (Kaisersberger 1994, p89). Instruments with modulated thermogravimetry (MTGA) (Blaine 1998) technique are also commercially available.

TGA can also be coupled with other analytical techniques to provide simultaneous information and enable more convenient and effective analysis in a shorter period of time, using less material. Simultaneous thermal analysis (STA) technique combines DSC (or DTA) with TGA. A mass spectrometer (MS) can also be attached to the STA instrument for evolved gas analysis and provides information about the cause of mass changes. Other combination techniques are used to analyze the gas products from a TGA experiment. This approach is called evolved gas analysis, EGA, include:

TGA-FTIR is a combination of TGA with a Fourier transform infrared spectrometer (FTIR).

A sample scanned on the TGA will release volatile materials or generate combustion components as it burns. These gases are then transferred to IR cell, where the components can be identified. This technique is most useful when the evolved gases are small chemicals, such as water, carbon dioxide or common solvents which have characteristic IR spectra.

TGA-MS combination allows detection of very low levels of impurities. By heating a sample on the TGA, the sample will emit volatile materials or generate combustion components as it burns. These gases are transferred to the MS where the components can be identified. Because of its ability to detect very low levels of material, the TGA-MS is a powerful tool for quality control, safety, and product development. This technique is most useful when the evolved gases or breakdown products are known in advance but are few in number.

TGA-GC/MS combination enables the released gases to be transferred to a gas chromatograph (GC) where the components can be collected and run on GC to separate the material and the peaks can be identified by the MS. Because of its ability to detect very low levels of material in a complex mixture, the TG-GC/MS is a powerful tool for quality control, safety, and product development.

7.3 Thermomechanical analysis

Temperature-dependent dimensional changes in materials, such as thermal expansion, can be determined using a dilatometer or a thermomechanical analyser. The expansion behavior changes significantly at relaxation transitions of viscoelastic materials, therefore, the technique can also be used to determine properties such as the T_g . This was covered in Section 5.3, together with a brief description of a dilatometer. In a dilatometer, the specimen is not subjected to any external loads other than the weight of the small amount of liquid surrounding it, whereas, in thermomechanical analysis (TMA), a constant level of small load is maintained on the specimen.

The associated standard methods include:

ISO 11359-1:1999 Plastics – Thermomechanical analysis (TMA) – Part 1: General principles

ISO 11359-2:1999 Plastics – Thermomechanical analysis (TMA) – Part 2: Determination of coefficient of linear thermal expansion and glass transition temperature

ASTM E831 - 06 Standard test method for linear thermal expansion of solid materials by thermomechanical analysis

ASTM E1363 - 08 Standard test method for temperature calibration of thermomechanical analyzers

ASTM E1545 - 11 Standard test method for assignment of the glass transition temperature by thermomechanical analysis

ASTM E1824 - 09e1 Standard test method for assignment of a glass transition temperature using thermomechanical analysis: tension method

DIN 5375 Testing of plastics; determination of the coefficient of linear thermal expansion

In a standard TMA experiment, the sample is positioned on a quartz stage and a moveable quartz glass probe is placed on the top of the sample. The furnace, surrounding the sample stage and probe, provides heating/cooling during the measurement. A thermocouple adjacent to the sample monitors sample temperature, and the dimensional changes occurring as a function of time, temperature or force are monitored by a linear variable differential transformer (LVDT) attached to the probe.

There are several available probes (expansion, penetration, macro-expansion, hemispherical) which can be used to vary probe contact area and stress on the sample in order to obtain a desired mode of deformation. Normally, expansion is observed with large contact areas and low forces, and penetration with small contact areas and high forces. The larger surface area of the macro-expansion probe enables a larger contact area and therefore facilitates analysis of soft or irregular samples, powders, and films. Depending upon the probe / sample contact area and the load applied, the T_g can be detected by either an upward (expansion) or downward (penetration) movement of the probe.

Penetration measurements use an extended tip probe to focus the drive force on a small area of the sample surface for measurements of T_g , softening temperature, and melting behaviour. It is valuable for characterizing coatings without their removal from a substrate. The probe operates like the expansion probe, but provides a larger applied stress. The hemispherical probe is an alternate penetration probe for softening point measurements in solids.

TMA can also measure viscoelastic properties of creep or stress relaxation. However, the main property measurement, in expansion mode, is the coefficient of thermal expansion (CTE) for solid samples. The linear (α) and the volume (β) CTEs are defined as

$$\alpha = (\Delta L / \Delta T) / (L_0) [\mu\text{m} / \text{m } ^\circ\text{C}] \text{ or simply } ^\circ\text{C}^{-1}; \beta = (\Delta V / \Delta T) / (V_0) [^\circ\text{C}^{-1}]$$

where, L_0 and V_0 are the initial length and volume, ΔL and ΔV are the changes in length and volume, and ΔT is the change in temperature from the initial temperature associated with L_0 and V_0 . For an isotropic and homogeneous material, the CETs are related by $\beta = 3\alpha$.

Expansion and contraction of materials with temperature variation generates thermal stresses, which can cause undesirable consequences. Unstrained isotropic materials will be free of thermal stresses; however, in most practical applications the material is under restraint and therefore suffers thermal stresses. The situation becomes worse when the stress is uneven/unbalanced. The magnitude of stress resulting from a temperature change ΔT is

$$\sigma = E\alpha\Delta T.$$

The **thermal stresses** that are frozen in the material as **residual stresses**, depending on the magnitude, can cause fracture or permanent deformation. It is of concern particularly in materials with low heat conductivities such as polymers when the rate of heating or cooling is too fast, and therefore, temperature gradients form between the surface and the bulk of the material causing differential expansion or contraction: upon heating, the surface expansion is restricted by the cooler inner mass and therefore experiences compressive stresses, which are balanced by the tensile stresses induced inside; the nature of stresses are reversed upon quenching. The situation becomes more intense in composite materials, where the material is a mixture of components with different CETs, and unless the structure of the material in the product is symmetrical/balanced, then residual stresses can ensue from heat inputs involved in processing and subsequently in service.

In glass-fibre-reinforced polyester resin, for instance, the fibre and the matrix undergo a differential thermal contraction, with linear coefficients of expansion of $4.7 \times 10^{-6} / ^\circ\text{C}$ for GF and as high as $1.5 \times 10^{-4} / ^\circ\text{C}$ for polyester resin, cooling to 20°C from 120°C curing temperature produces a differential strain of approximately 1.5 % which is approximately 75 % of the elongation to failure of the resin. The carbon and Kevlar 49 fibres have -ve linear coefficients of expansion parallel to their lengths; therefore, they exert even greater thermal stresses than glass fibres on the resin along their lengths. In contrast, the expansion coefficients for carbon and Kevlar fibres in perpendicular direction to the fibre axis are +ve and this also results in differences in micro-stresses.

Figure 7.6 shows the CET values for some thermoplastics. The tests were conducted at a heating rate of $3^\circ\text{C}/\text{min}$, using 6×6 mm specimens under a macro-probe and 0.5 g load (Ehrenstein 2004, p175). The significant variations in CET are dictated by T_g in the case of amorphous thermoplastics, and by the softening temperature, which is close to melting point, in the case of semicrystalline thermoplastics.

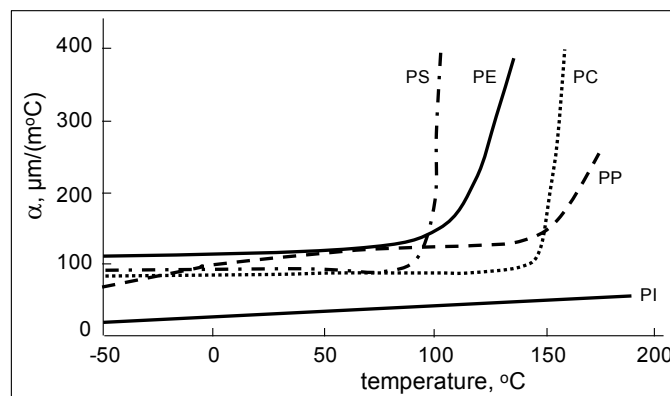


Figure 7.6 CET (α) vs. temperature for PS, PE, PC, PP and PI (source: Ehrenstein 2004, p173)

Modulated thermo mechanical analysis (MTMA) was reported by Price in 1998, and is a useful tool for determining/identifying thermodynamic and kinetic, reversing and non-reversing, changes that take place simultaneously. In MTMA, a sinusoidally varying temperature program is added to an underlying linearly changing or static temperature program. Fourier transformation of the oscillatory temperature “forcing function” produces reversing and non-reversing components for the dependent variable. The reversing signal is associated with properties dependent upon the temperature rate of change and, therefore, enhances CET and T_g measurements. The non-reversing signal contains events that relate to kinetic processes, which are both temperature and time dependent (e.g., stress relaxation, softening and heat shrinking). This ability to separate thermodynamic from kinetic events aids in the interpretation of the thermal curve, measures expansion and contraction taking place at the same time and provides a more accurate estimation of the glass transition temperature than the softening temperature.

Within the context of thermal expansion, the unusual behaviour of rubbers should also be mentioned: under normal, unstressed, conditions rubber expands like other materials as it is heated, however, when under tension it behaves differently, contracting in the loading direction, rather than expanding, as it is heated. The explanation of this behaviour lies in the contribution of entropy to the elasticity of rubber: the deformation of ordinary elastic solids are controlled by changes in internal energy (storage and release of strain energy as material is stressed and released), resulting in the increase of the inter-atomic bond lengths with rising temperature; whereas rubber elasticity is controlled by changes in entropy.

Randomly coiled/entangled rubber molecules in their equilibrium state uncoil on being stressed, and in this stressed state the input of energy in the form heating causes the rubber to contract and enable individual chain segments to recoil back to their equilibrium state, thus raising the entropy and reducing the free energy. In other words, as it is stretched, the rubber chain moves from a more probable (higher entropy) to a less probable (lower entropy) state. It is this lowering of entropy of the conformation that generates the retractive force, so rubber is described as an ‘entropy spring’.

The fact that rubbers deform elastically by the uncoiling of long, disordered molecule segments in between sparsely spaced crosslinks and/or entanglements, rather than by the stretching of individual inter-atomic bonds, is also the reason why the stiffness of rubber is so much lower than other materials. It is thus possible to predict the stiffness of a rubber solely from knowledge of its crosslink density (which dictates the chain segment length). There are approximately 500 to 1000 monomers in between cross-links in rubber. Increasing the degree of crosslinking would change the behaviour: e.g., when

the rubber band is left out for a long time, the excess UV light provides the polymer molecules with the activation energy to form more cross-links, resulting in less stretch-ability in the rubber band, the chains are prevented from uncoiling or sliding past each other, due to the higher number of cross-links. Stretching, therefore, is effectively pulling on the C-C backbone bonds of the polymer, which are very stiff and will not stretch much. Instead the rubber band snaps with very little extension.

Some oils and other chemicals have a similar effect on rubbers. However, if the initial density of cross-links is very low as in butyl rubbers, then it becomes less likely that some further cross-linking would bring it to a level sufficient for degradation, accordingly, butyl rubbers are resistant to degradation from U.V. light and from oils, and become suitable in making products such as bungee jumping cord.

7.4 Dynamic mechanical thermal analysis

Dynamic mechanical thermal analysis (DMTA) or just dynamic mechanical analysis (DMA) (although this second description may be confused with fatigue testing), places the specimen, often a small rectangular bar, under vibration, normally sinusoidally varying stress/strain, and measures mechanical properties in terms of various modulus parameters and damping as a function of temperature, time and frequency. DMTA is a powerful technique and provides information on material rigidity, mechanical damping, relaxation behaviour and material composition and structure for polymers. It must be the best technique for determining relaxation temperatures of T_g and various other secondary glass transition temperatures (and for this reason the subject matter was covered extensively in Section 5.2.3). The tests are standardized: the general principles are covered in ISO 6721-1 and ASTM 4092. The tests can also be conducted in different loading modes (the loading modes are depicted in Figure 7.7). The standards describing the test procedures under different loading modes are listed below.

The standard test methods for **tension mode** include:

ISO 6721-4:2008 Plastics – Determination of dynamic mechanical properties – Part 4: Tensile vibration -- Non-resonance method

ISO 6721-9:1997 Plastics – Determination of dynamic mechanical properties – Part 9: Tensile vibration -- Sonic-pulse propagation method

ASTM D5026 - 06 Standard test method for plastics: Dynamic mechanical properties: in tension

The test methods for **torsion mode**:

ISO 6721-2:2008 Plastics – Determination of dynamic mechanical properties – Part 2: Torsion-pendulum method

ISO 6721-7:1996 Plastics – Determination of dynamic mechanical properties – Part 7: Torsional vibration -- Non-resonance method

ASTM D5279 - 08 Standard test method for plastics: Dynamic mechanical properties: in torsion

The test methods for **flexure mode**:

ISO 6721-3:1994 Plastics -- Determination of dynamic mechanical properties – Part 3: Flexural vibration – Resonance-curve method

ISO 6721-5:1996 Plastics – Determination of dynamic mechanical properties – Part 5: Flexural vibration – Non-resonance method

ASTM D5023 - 07 Standard test method for plastics: Dynamic mechanical properties: in flexure (three-point ending)

ASTM D5418 - 07 Standard test method for plastics: Dynamic mechanical Properties: in flexure (dual cantilever beam)

The test methods for **shear mode**:

ISO 6721-6:1996 Plastics – Determination of dynamic mechanical properties – Part 6: Shear vibration – Non-resonance method

ISO 6721-8:1997 Plastics – Determination of dynamic mechanical properties – Part 8: Longitudinal and shear vibration – Wave-propagation method

ISO 6721-10:1999 Plastics – Determination of dynamic mechanical properties – Part 10: Complex shear viscosity using a parallel-plate oscillatory rheometer

The test methods for **compression mode**:

ASTM D5024 - 07 Standard test method for plastics: dynamic mechanical properties: in compression

The test methods for melt rheology and resin cure include:

ASTM D4440 - 08 Standard test method for plastics: Dynamic mechanical properties: Melt rheology

ASTM D4473 - 08 Standard test method for plastics: Dynamic mechanical properties: Cure behaviour

An aerospace-specific standard is given in DIN 65583:1999-04 Aerospace –Fibre reinforced materials – Determination of glass transition of fibre composites under dynamic load.

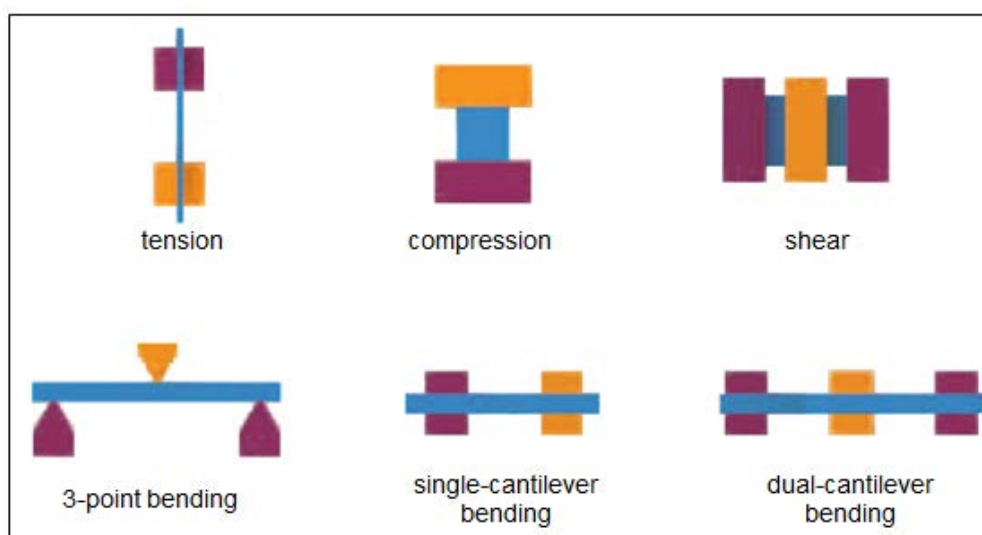


Figure 7.7 Different deformation modes (source: Mettler-Toledo AG, Analytical)

Tension mode is suitable for specimens of low cross-sectional area, compression for low elastic modulus specimens, shear for soft/flexible specimens, 3-point bending for high elastic modulus specimens, single-cantilever bending for medium modulus and high CET specimens, and dual-cantilever bending for low-to-medium modulus specimens.

Instrumental considerations, besides the modes of deformation, include many more parameters: including frequency range, temperature range, heating rate, range of amplitudes of vibration and force range. Commercially available equipment quote values of 10^{-3} to 10^3 Hz frequency range (many fixed values can be selected within this range, -170 to 600 °C temperature range, 0 - 20 °C/min heating rate, 0 - 40 °C/min cooling rate, amplitude of vibrations of ± 0.5 μm - 10 mm, and 1 mN to 40 N force range. Normally the temperature range is dictated by the type of polymer being tested and the property being measured (e.g., T_g), frequency of 1 Hz (note that the frequency can only be set on non-resonant forced vibration machines), and amplitude of vibration 50 μm are selected. The maximum frequencies differ for modes of deformation, for example a manufacturer indicates 1000 Hz for shear, 300 Hz for bending, 300 Hz for tension, and 300 Hz for compression. At very high frequencies, one should be aware of machine resonance!

Figure 7.8 shows the property vs. temperature curves for the main DMTA properties. It is also indicated that in the glassy state the elastic behaviour is energy dominated and in the rubbery state, it is entropy dominated, particularly with cross-linked polymers. Further increases in temperature beyond the rubbery state will cause flow in thermoplastics and therefore, the storage modulus (E') and the complex modulus (E^*) will drop off significantly from the rubbery plateau, leading to liquid phase, whereas, thermosetting polymers will maintain their rubbery state.

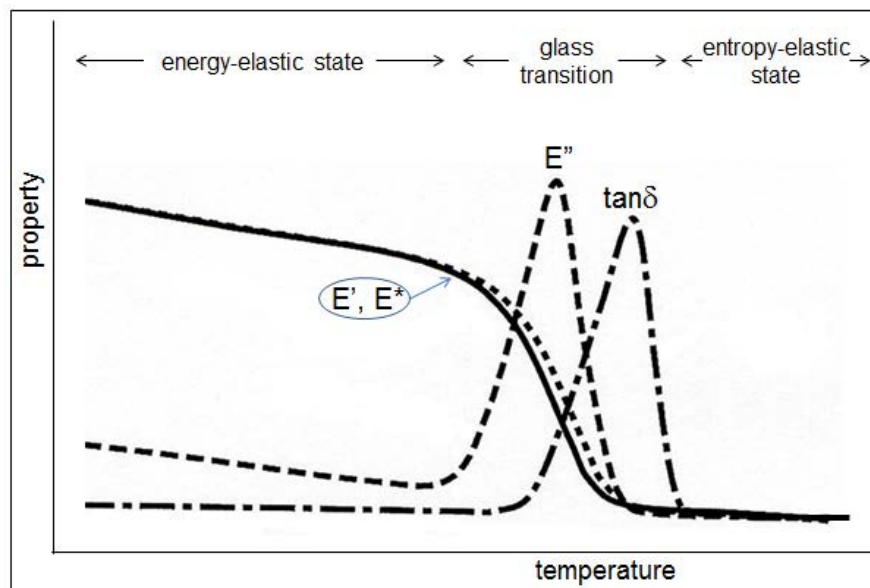


Figure 7.8. Illustration of DMTA curves for an amorphous polymer (source: Ehrenstein 2004, p239)

7.4.1 Applications

Applications of DMTA are covered widely, for example, Turi (1997), Nielsen (1974, p139), Gearing (1999, p501), Ehrenstein (2004, p236) and support notes from various well known manufacturers such as Netzsch, PerkinElmer, TA Instruments, Mettler-Toledo AG, etc. for various polymer types and polymeric products, such as coatings, adhesives and composites as well as some non-polymeric materials.

A few examples of material characterisations using DMTA are briefly described in the following sub-sections.

7.4.1.1 Molecular-relaxation transitions

Molecular-relaxation transition temperatures are summed up in Figure 7.9 for amorphous and crystalline thermoplastics and thermosetting plastics. The extent of rubbery plateau is dictated by the molecular weight (M), which dictates the degree of chain entanglement, in amorphous thermoplastics; by the degree of crosslinking in thermosetting polymers; and by the degree of crystallinity in crystalline TPs. Chain entanglements have similar effects to that of cross-links, and, therefore, with greater chain entanglement (high M) a longer rubbery region is observed, prior to the onset of flow region, where solid changes to viscous liquid and molecular chain slippage occurs readily. In the rubbery region, depending on the factors such as the degree of crosslinking and crystallinity, molecular weight and therefore the level of molecular entanglement that a slight rise in elastic modulus with increasing temperature may be observed due to entropy effects described briefly in Section 7.3.

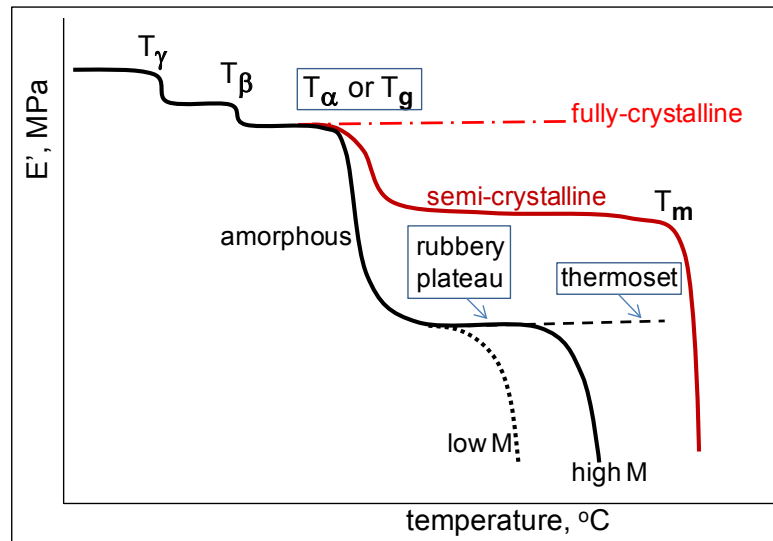


Figure 7.9 A sketch of real modulus (E') vs. temperature, showing various transitions in polymers

Not all the transitions shown on the graph would be exhibited by all the polymer types. The terms α , β and γ transitions are often used in association with both amorphous and semicrystalline polymers. In amorphous thermoplastics and in thermosets, α -transition is the glass transition, but with some semicrystalline thermoplastics the α -transition indicates a transition that may occur between T_g and T_m , and β -transition becomes the glass transition. A clearer nomenclature, however, includes sub-scripts "a" for amorphous and "c" for crystalline so that the transitions are indicated as γ_a , β_a and α_a , and the higher temperature α -transition observed between T_g and T_m is distinguished as α_c .

Suggested mechanisms for the high temperature α_c -transition in semicrystalline polymers include the shearing of the amorphous tie-molecules between crystalline lamellae and/or the rotation of polymer chain segments about their axis in the crystalline regions. In amorphous polymers β -transition is normally referred to as a secondary-glass transition, occurrence of which contributes to improvement in material toughness. Rigid polymers with high impact strength exhibit prominent secondary transitions, such as PCs, PAs, polyethersulphones, PVC, PET and epoxy resins.

The molecular relaxations that occur in the glassy amorphous regions are in the form of local motions, e.g., at the γ -transition as bending and stretching of bonds, at the β -transition as the movement of side groups, and at glass/ α -transition gradually segments of the main backbone chain is set in motion.

Energy requirement for these transitions to happen can be calculated using the **Arrhenius relationship**. A large number of processes in materials science and engineering, e.g., the diffusivity of elements in metals, creep deformation in structural materials, stress relaxation in polymers and molecular-relaxation transitions obey the Arrhenius equation, which indicates that the process rate rises exponentially with temperature.

$$\text{The process rate} = Ae^{-E_a/(RT)}$$

where, E_a is the activation energy, R is the gas constant ($R = 8.3145 \text{ J/mol.K}$), T is the absolute temperature, and A is a pre-exponential constant.

The process rate, in this case, is the frequency of specimen oscillations. The frequency is essentially a rate expression ($1/\text{time}, \text{s}^{-1}$), therefore expressing the equation in terms of frequency, F , and expressing it as a logarithmic equation gives

$$\ln(F) = \ln(A) - E_a/(RT).$$

A plot of $[\ln(\text{frequency})]$ vs. $[1/(\text{transition-temperature})]$ is the Arrhenius plot, and should yield a straight line; the slope of this line is equal to $-E_a/R$, from which the activation energy can be calculated. Examples of these calculations are given by PerkinElmer in their application notes. One of these is for α and β transitions in PMMA: a specimen of 7.3 mm length, 7.4 mm width and 2 mm thickness is DMA tested in single-cantilever bending mode at a heating rate of $2 \text{ }^\circ\text{C}/\text{min}$ at fixed frequencies of 0.1; 0.3; 1; 3 and 10 Hz. $\tan \delta$ vs. temperature curves obtained at various frequencies are shown for the β transition (Figure 7.10), and the associated Arrhenius plot with a line of best fit and the equation of that line is presented in Figure 7.11. The slope of each line is equal to the negative of the activation energy divided by the gas constant. Therefore, the activation energy for the β relaxation is calculated to be approximately 65 kJ/mol and for the glass (α) transition 368 kJ/mol.

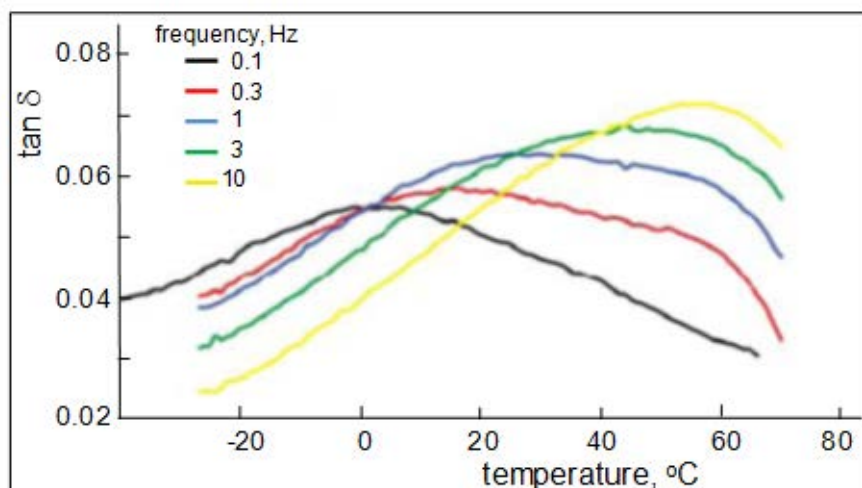


Figure 7.10 $\tan \delta$ vs. temperature at various frequencies over the β -transition of PMMA (source: PerkinElmer-1)

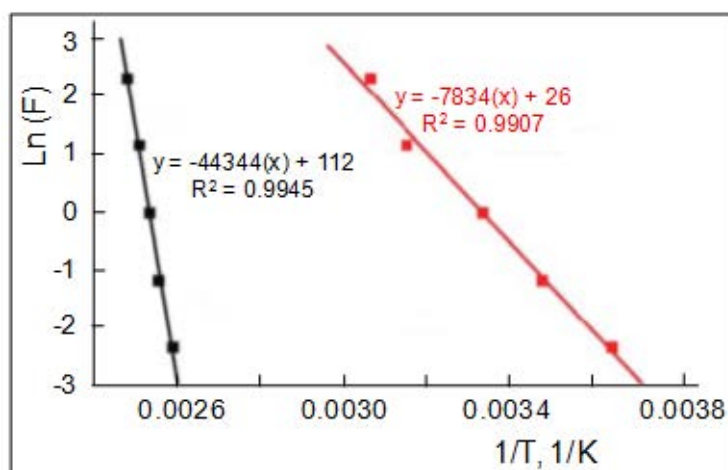


Figure 7.11 Arrhenius plots for (■) β and (■) α transitions of PMMA (source: PerkinElmer-1)

Figures 7.10 and 7.12 also demonstrate how the relaxation-transition temperatures are dependent on the strain rate (i.e., frequency). Measurements which take place over a large timescale will result in a lower glass transition temperature, and hence exhibit rubbery behaviour at lower temperatures. Measurements which take place on a short timescale will result in a higher value of T_g and hence exhibit glassy behaviour at higher temperatures. This can be seen by experimenting with silly putty at room temperature: flowing like a viscous liquid over a long timescale and breaking like glass over a short timescale.

7.4.1.2 Time-temperature superposition

It is known that there is a time and temperature equivalence for viscoelastic materials. For example, a polymer that exhibits rubber-like characteristics under a given set of testing conditions can be induced to show rigid behaviour by either reducing the temperature or increasing the rate of strain or the frequency of testing. The concept of 'shift factor', a_T , has been used to construct master curves from a limited number of tests in order to predict the viscoelastic properties of polymers over a wide range of time (or frequency) outside the range easily accessible by experiment.

Williams, Landel and Ferry (WLF) defined ' a_T ' in an equation that has become known as the WLF equation (Ferry, 1980). The equation is empirical in origin and has the form

$$\log a_T = -C_1(T - T_0) / [C_2 + (T - T_0)]$$

where, T_0 is the reference temperature, T is the measurement temperature (the temperatures are in K), and C_1 and C_2 are constants. For many amorphous polymers, $C_1 = 17.44$ and $C_2 = 51.6$ when T_0 is taken as the static T_g . The WLF expression was subsequently given theoretical basis from the free-volume theory of T_g , which is that the fractional free volume in the material increases linearly with temperature above T_g .

An application of the WLF concept is demonstrated for polycarbonate in their application brief by TA Instruments. Frequency multiplexing data (see Figure 7.12) was obtained in the glass transition region (i.e., 130 to 160 °C) at frequencies of 0.01; 0.02; 0.05; 0.1; 0.2; 0.5; and 1.0 Hz, and at amplitude of deformation (p-p) of 0.5 mm. It is recommended that a minimum of four frequencies over two decades be used when generating a master curve.

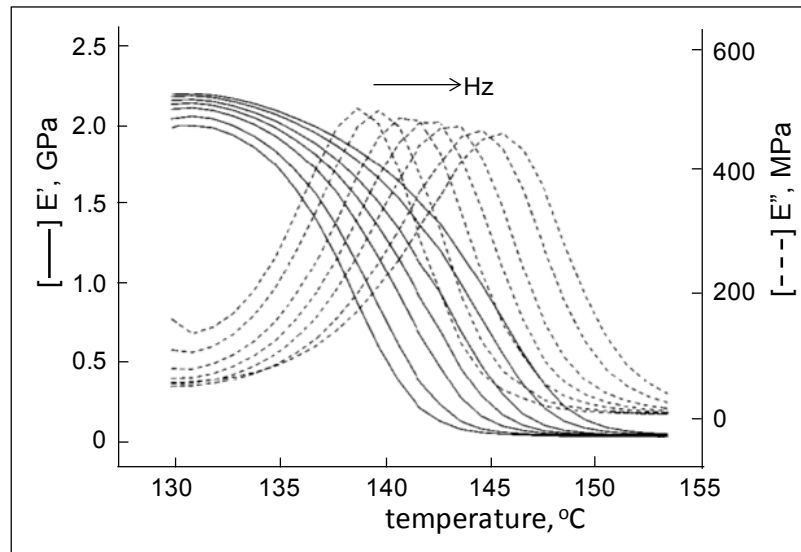


Figure 7.12 E' and E'' vs. temperature at various frequencies for PC (source: TA Instruments-1)

The loss modulus (E'') data is used to generate a master curve. Figure 7.13 is a plot of the entire individual E'' data points as a function of log frequency.

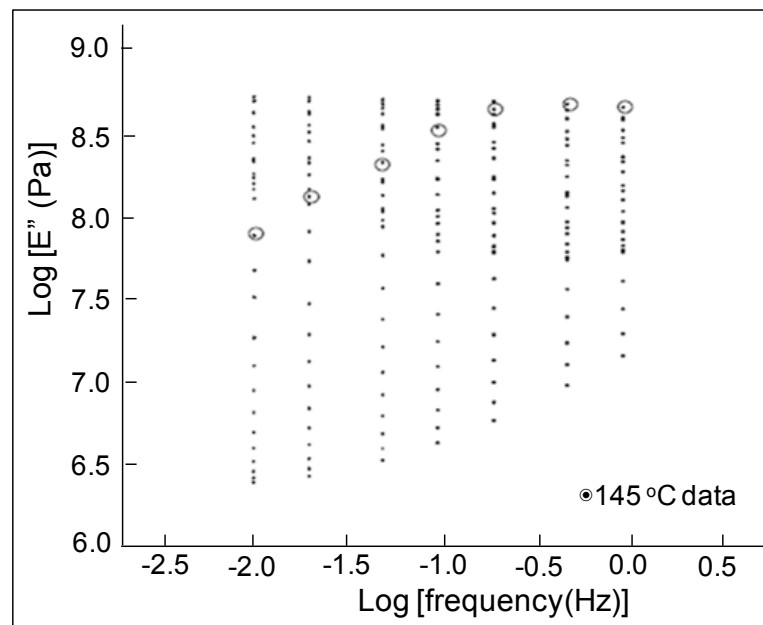


Figure 7.13 Loss modulus (E'') vs. frequency at all the test temperatures for PC (source: TA Instruments-1)

In the construction of an isothermal master curve, a reference set of data needs to be chosen. In this case, the data at 145 °C was selected and they form the initial framework of the master curve, the remaining sets of data obtained at other temperatures are shifted horizontally either to higher or lower frequencies to fall upon the chosen reference data and establish a smooth curve. The data points below the reference set of points (the data at 145 °C) will be shifted to the left

(to lower frequencies), while those above will be shifted to the right (to higher frequencies) to bring them to lie on the progressively forming master curve. During the shifting, the computer stores the shift factors, a_T . After all of the individual data points are shifted, the complete master curve is formed as shown in Figure 7.14.

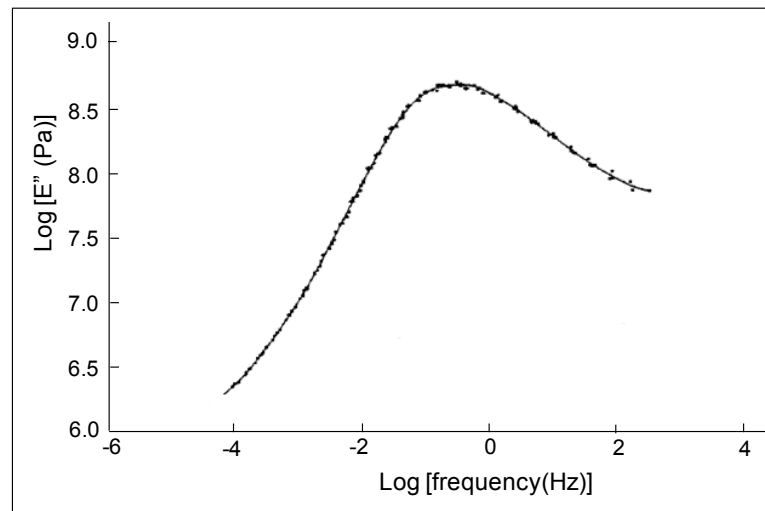


Figure 7.14 Master curve of loss modulus (E'') vs. frequency at reference temperature of 145 °C for PC (source: TA Instruments-1)

This curve shows the variation of the loss modulus with frequency over a wide frequency range (8 orders of magnitude), whereas the tests were only conducted over 10^{-2} to 10^0 frequency range. The maximum energy dissipation occurs at a frequency of 0.31 Hz at 145°C, represented by the peak maximum.

The experimental shift factors are plotted against the temperature as in Figure 7.15, and the data was fitted with WLF predictions, shown by the solid line, the WLF constants of $C_1 = 22.9$ and $C_2 = 78.8$ produce the best fit. Once the WLF constants are determined the equation can be used to predict material response at other than the reference temperature: the master curve can be transposed to any desired/service temperature by applying the model and, therefore establishing the frequency at which the maximum energy dissipation occurs at the given temperature. It is recommended, though, that the master curve be shifted only to temperatures in the range in which the data was collected.

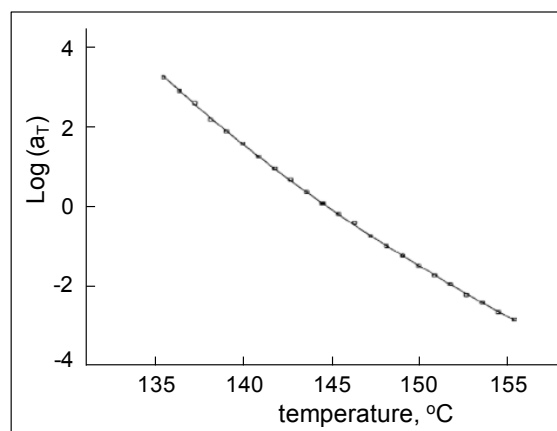


Figure 7.15 The fit of WLF equation on the experimentally obtained shift factors over a temperature range PC (source: TA Instruments-1)

A master curve for any of the other dynamic mechanical properties can be constructed; Figure 7.16 displays the master curve generated from the storage modulus data for polycarbonate. It shows the effects of frequency on the modulus of PC at 145 °C, the reference temperature. At very low frequencies (or long times) the material exhibits a low modulus and behaves similar to a rubber. At high frequencies (or short times) the PC behaves like an elastic solid and has a high modulus. This master curve again demonstrates that data collected over only two decades of frequency can be superimposed to cover eight decades.

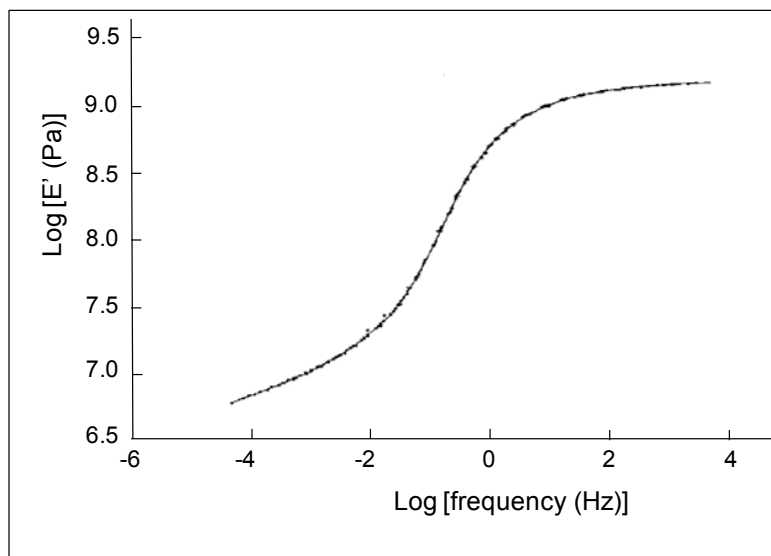


Figure 7.16 Master curve for the storage modulus (E') vs. frequency at of 145 °C for PC (source: TA Instruments-1)

Master Curves can be generated for other viscoelastic properties, e.g. stress relaxation and creep, as well as the dynamic mechanical properties measured at fixed frequencies.

7.4.1.3 Establishment of service temperature limits

DMTA provides very useful information that can help users to decide the suitability of a polymeric material for applications, particularly with respect to prevailing temperatures. An example of this is given in the PerkinElmer application notes for polyurethane foam tested under compression at 1 Hz from -80 °C to 100 °C at a heating rate of 5 °C/min.

Polyurethane foam is used for various applications, such as packaging, footwear, furnishings, that require impact absorption properties. In order to absorb energy, it is important that the foam is in its rubbery state. In glassy state, the material will be rigid and very friable due to the large proportion of void space in the structure. It is therefore important to accurately determine the T_g . Figure 7.17 shows the $\tan \delta$ and modulus response from the polyurethane sample. The T_g is at approximately -40 °C, where the desirable rubbery properties change significantly: as temperature falls the elastic modulus increases from less than 1 MPa to above 100 MPa. This material will require a low modulus to operate effectively as a shock absorbing or cushioning material. Hence, the T_g is useful in setting limits on the operation temperature of materials. Negligence on such fundamental concepts can cause serious/tragic consequences as was indicated in Section 1.2.1, concerning the rubber O-ring failure that caused the Challenger Shuttle disaster.

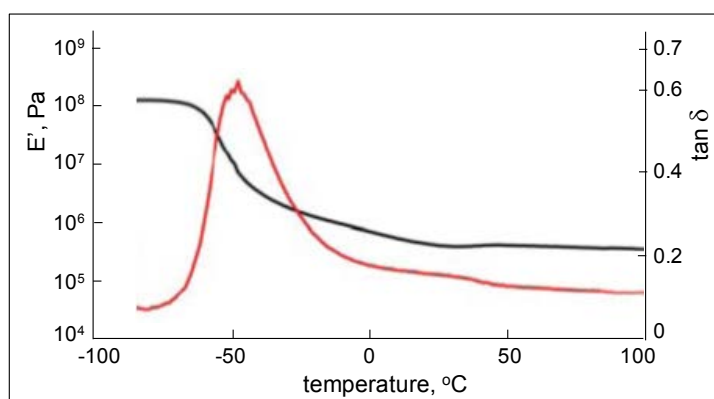


Figure 7.17 [—] Storage modulus (E') and [—] $\tan \delta$ vs. temperature for PU foam
(source: PerkinElmer-2)

7.4.1.4 Effect of crystallinity, intermolecular attraction, annealing and orientation

Relaxation transitions are processes that are associated with amorphous polymers or the amorphous regions in semicrystalline polymers, however, changes in the degree of crystallinity, crystalline size and perfection influences dynamic mechanical properties as shown in Figure 7.18. The figure shows the dynamic elastic modulus curves for Polyamide 46, which has been heat treated at various temperatures for 500 h. Heat treatment (annealing) above the glass transition temperature increases the degree of crystallinity and size and perfection of the crystallites, which in turn increases the material rigidity as indicated by the increases shown in E' in the glassy region. Crystallinity also physically holds together the polymer chains, similar in effect to chemical crosslinking, and, therefore, the drop in E' at glass transition becomes lower and the material exhibits much higher moduli values along the rubbery plateau. The curves then progressively

combine together with the curve representing as-moulded specimen as the test temperature approaches the material melting point. The specimen with the highest crystallinity, as identified with the highest annealing temperature, requires the highest temperature to reduce in stiffness to the same level of E' as that of as-moulded specimen. The associated $\tan \delta$ values exhibit significant reductions in the peak heights, and also indicate an increase in T_g .

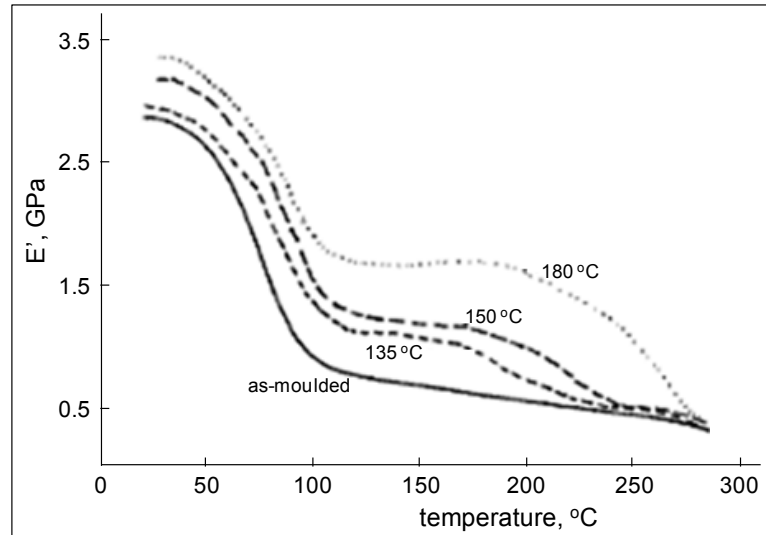


Figure 7.18 Storage modulus (E') vs. temperature for Nylon 46: as-moulded and heat treated at 135, 150 and 180 °C (source: Sepe 1997, p29)

Figure 7.19 shows the influence of intermolecular forces of attraction on the storage modulus: as the H-bonding increases, the modulus increases across the temperature range and the T_g also increases. The associated $\tan \delta$ curves (not shown here, see Ehrenstein 2004, p279), as well as showing the shift in T_g , also show a decrease in the $\tan \delta$ -peak height from the highest for PA 6, then PA 66, and to the shortest for PA 46. The $\tan \delta$ -peak height is an indicator of the amount of amorphous proportion or the degree of crystallinity in semicrystalline thermoplastics. Therefore, PA 6 is the least and PA 46 is the most crystalline of these polyamides. This is also born out by the melting points of these materials, which are about 220, 260 and 290 °C for PA 6, PA 66 and PA 46, respectively.

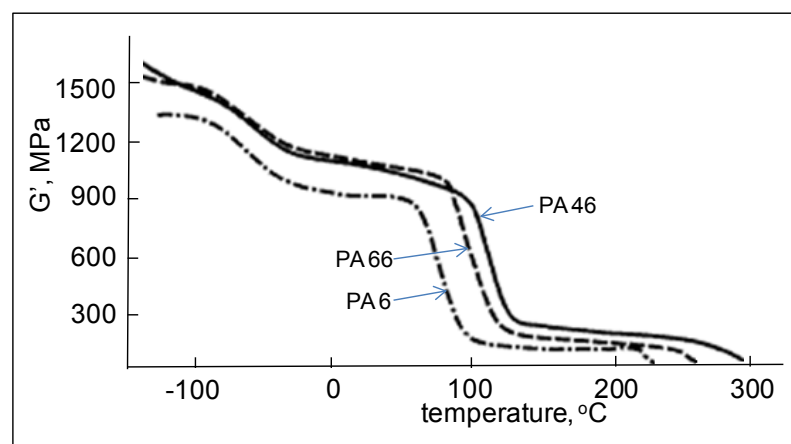


Figure 7.19 Storage modulus (G') vs. temperature for polyamides. The tests are conducted in torsion at 1 Hz frequency and 3 °C/min heating rate (source: Ehrenstein 2004, p279)

The intermolecular forces of attraction between the neighbouring polymer chains in polyamides arise from the hydrogen bonding between the carbonyl oxygen and the amide hydrogen atoms of the amide groups (links) within the polymer backbone chain. The strength of the attraction depends on the frequency of the amide groups along the chain, i.e., the ratio of amide group (NHCO) to CH_2 , and as it increases so does the level of H-bonding. In the case of PA 6, $[-(\text{CH}_2)_5 - \text{CONH} -]_n$, the amide links, therefore the H-bonds, are separated by five methylene (or methene) groups; in PA 66, $[-\text{NH} - (\text{CH}_2)_6 - \text{NHCO} - (\text{CH}_2)_4 - \text{CO} -]_n$, by six and four groups; and in PA 46, $[-\text{NH} - (\text{CH}_2)_4 - \text{NHCO} - (\text{CH}_2)_4 - \text{CO} -]_n$, by four and four ($-\text{CH}_2 -$) groups. As can be seen even such, seemingly, small variations in the chemical structure makes a clear difference in the thermal properties discussed.

Figure 7.20 shows storage modulus (E') curves over a range of temperature for polyethylene terephthalate (PET) fibres in as-spun and drawn at draw ratios of 2 to 5.5. **Drawing in fibres** causes uniaxial molecular orientation and increases crystallinity. Drawing, as well as causing increase in crystallinity also brings about a degree of alignment and reduction in free volume within the amorphous regions and therefore causes a level of constraint to the mobility of the molecular-chain segments. Such structural variations in turn bring about significant changes in mechanical and physical properties, e.g., stiffness and strength increase, T_g and T_m increase, damping reduces, etc.

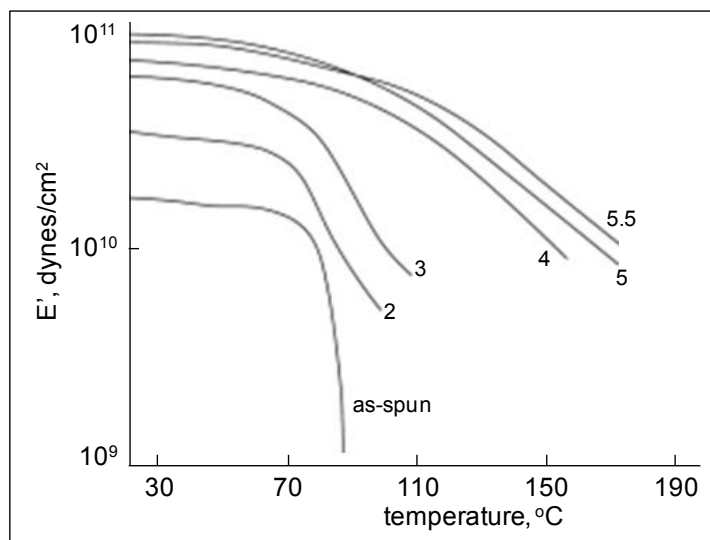


Figure 7.20 Storage modulus (E') vs. temperature for PET fibres drawn at various draw ratios. The draw ratios are indicated on the curves (note that $1 \text{ dyne/cm}^2 = 0.1 \text{ Pa}$) (source: Miller 1984)

The increase in stiffness can be clearly seen by the increases in E' with increasing draw ratio (molecular orientation), the glass-transition region broadens and becomes shallower, i.e., the extent of drop in stiffness between the glassy and rubbery states is much reduced. The changes indicated in the transition region are also present in the associated $\tan \delta$ curves: as-spun fibre specimen exhibits the sharpest and the highest $\tan \delta$ peak that occurs at the lowest temperature, and the $\tan \delta$ curves then, successively, get shallower, broader and move to higher temperatures with increasing molecular orientation.

7.4.1.5 Effect of crosslinking

Crosslinking has a dramatic effect on dynamic mechanical properties, particularly at and above T_g , as illustrated in Figure 7.21. With increasing crosslinking (indicated by the arrow on the figure), glass transition occurs over a broader temperature range and the associated drop in the storage modulus becomes much reduced, and at glass transition the damping peaks reduce in height (i.e., the damping intensity decreases), broaden and shift to higher temperatures.

These features were observed in the thermosetting acrylic systems that I studied for my PhD, some four decades ago at UMIST, under the supervision of the late Dr Eric White, a very kind and caring man, who set me off on my career. I struggled a while trying to do tests using a laboratory made vibrating reed apparatus and was, then, saved by the arrival of the Rheovibron, one of the first commercial DMTA equipment. The material tested was an acrylic system with hydroxyethyl acrylate (HEA) comonomer to facilitate crosslinking with hexamethoxymethylmelamine (HMMM). By adjusting the contents of these two ingredients, it was possible to obtain acrylic thermosets of various degrees of crosslinking. The DMTA tests were conducted on these polymer systems, using specimens in the form of rectangular film strips of approximately $30 \times 2 \times 0.03 \text{ mm}$, at 110 Hz in tension. Figure 7.22 shows plots of E' and $\tan \delta$ against temperature for formulations containing different levels of the cross-linking agent of HMMM as a % of the HEA comonomer.

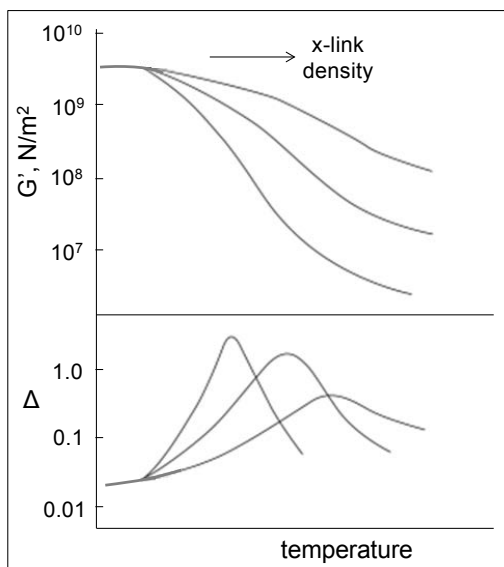


Figure 7.21 A schematic plot of the storage modulus and a damping term (Δ) against temperature, to show the effect of cross-linking in thermosetting polymers

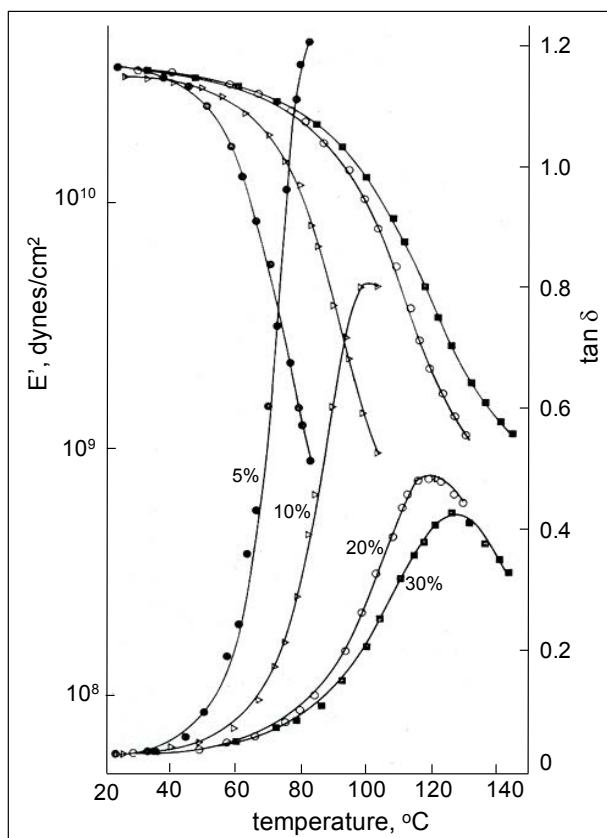


Figure 7.22 E' and $\tan \delta$ vs. temperature for a thermosetting acrylic coating system of various crosslinking agent (HMMM) content: the HMMM contents were 5%, 10%, 20% and 30% of the HEA content (source: Akay 1973)

Post-curing of thermosetting polymers at temperatures above T_g generates further crosslinking and, hence, progressively with the length of post-curing T_g increases, storage modulus increases and the peak maximum of the loss modulus and/or the damping term decreases.

7.4.1.6 Polymer blends

DMTA is an excellent method for studying and identifying polymer blends in the form of various types of copolymers, including TPEs, **interpenetrating polymer networks** (IPNs) and physical mixtures of different types of polymers. The technique is particularly useful in establishing the degree of compatibility between the polymer components, the type of relaxation-transition behaviours to be expected and the extent of variation between the stiffness of the blend and the component polymers. Figure 7.23 shows idealised plots of dynamic mechanical properties against the temperature of two compatible polymers and their blend. The glass transition of the blend is situated between the T_g s of the individual polymers in proportion to the amount of each component present in the blend. The value of the T_g for the blend can be predicted using an inverse rule of mixtures equation:

$$1/T_{g(\text{blend})} = w_1/T_{g1} + w_2/T_{g2}$$

where, w represents weight fraction and subscripts 1 and 2 represent individual polymers.

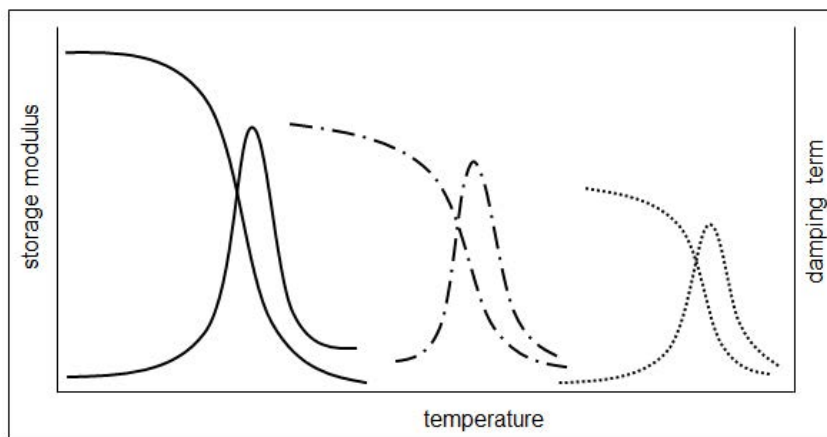


Figure 7.23 Sketches of DMTA curves illustrating the blend of two compatible polymers: (—) and (.....) for component polymers, and (- . -) for the blend

Generalised plots representing incompatible/immiscible polymers are shown in Figure 7.24. If polymers are not miscible then the resulting blend exhibits two distinctly separate glass transitions corresponding to those of the parent polymers. As already mentioned, the actual values for the dynamic mechanical properties in terms of moduli and damping terms are dependent on the types of polymers blended, i.e., amorphous and/or semi-crystalline thermoplastics, and thermosets and elastomers of various degrees of crosslinking.

Intermediate cases exist where the polymers are partially miscible so that two T_g s are still observed but they are moved towards that of the ideally miscible blend. Of particular interest are IPNs, which can produce broad glass transitions and, therefore, provide damping ability over a broad range of temperatures (and time/frequencies). Such polymers make good shock and sound absorbing materials that are not affected by reasonable ambient temperature variations.

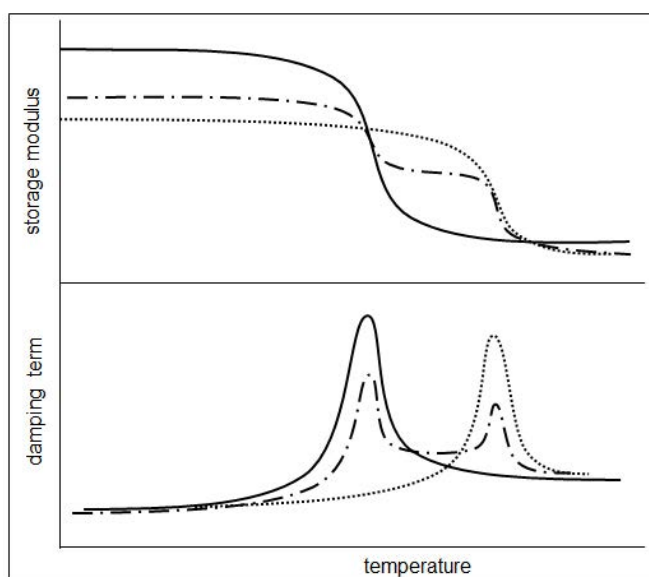


Figure 7.24 Sketches of DMTA curves illustrating the blend of two incompatible polymers: (—) and (.....) for component polymers, and (- . -) for the blend

Figure 7.25 shows the dynamic mechanical properties for PU/PMMA IPNs of various compositions. The tests were conducted in resonant frequency mode at a heating rate of 4 °C/min. test pieces were 10 mm wide and the clamp separations were adjusted according to the stiffness of the specimens. The amplitude of sinusoidal oscillations (peak-to-peak), mostly 0.3 to 0.6 mm, was also chosen according to the stiffness and thickness of the specimens. At certain compositions, in this case for around 30 to 50% by weight PMMA content, the IPNs show broad transitions of a certain damping capacity over a wide temperature range of around 100 °C, rendering the damping ability of the material almost independent of temperature variations.

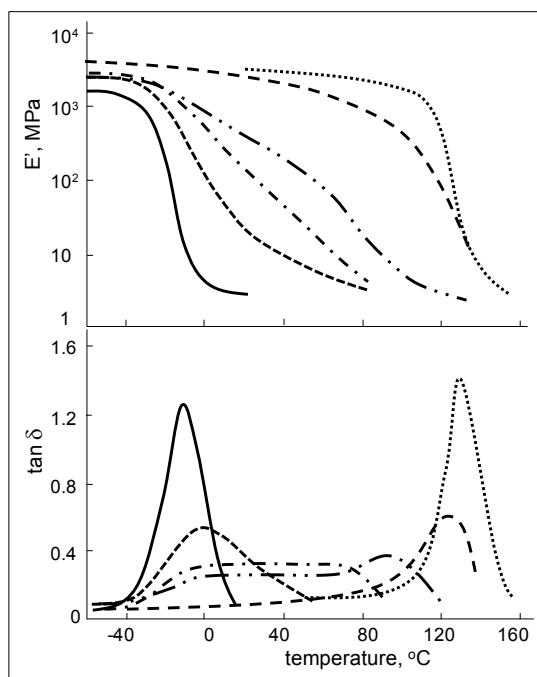


Figure 7.25 E' and $\tan \delta$ vs. temperature for PU/PMMA compositions by weight of (—) 100/0; (---) 80/20; (- . -) 70/30; (- . . -) 50/50; (- - - -) 20/80 and (.....) 0/100 (source: Akay & Rollins 1993)

Blending is practised in order to achieve certain desirable properties without significantly compromising the inherent desirable properties of component polymers. For instance, epoxy resin is used in aerospace applications as a matrix in polymer-matrix composites with high-performance fibres such as carbon fibre and although it has most of the desirable properties for applications, it sometimes requires improvement in toughness. This has been achieved by blending epoxy resin with suitable thermoplastics, one such example is the blending of epoxy resin with amorphous thermoplastic of polyethersulphone (PES) (Akay & Cracknell 1994). This study has shown that at blend compositions of 20 to 40 % by weight PES content, producing certain blend morphologies (spinodal / co-continuous), it is possible to achieve synergistic improvement in impact strength, without significantly compromising the desirable tensile properties of epoxy resin of stiffness and strength. The dynamic mechanical properties of E' , E'' and $\tan \delta$ for the component polymers and a blend is shown in Figure 7.26 for these systems.

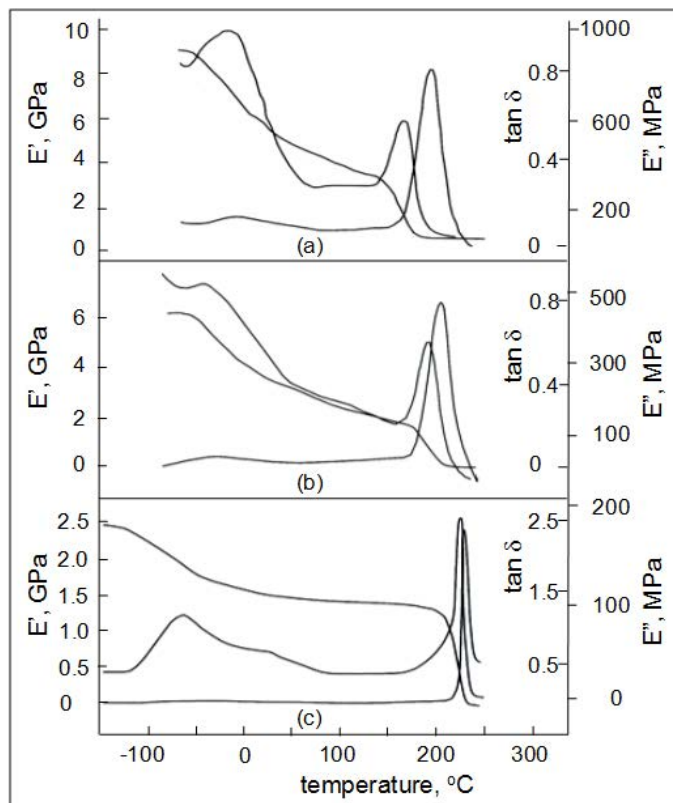


Figure 7.26 DMTA plots for: (a) epoxy resin, (b) epoxy resin / PES blend of 70/30 w/w and (c) PES (source: Akay & Cracknell 1994)

The individual graphs of E' , E'' and $\tan \delta$ have not been labelled on the figure for brevity, but should be easily identified from their customary shapes (note that the $\tan \delta$ -peak always occurs at a higher temperature than the E'' -peak). All the polymers show low temperature transitions, and a T_g at approximately 200 °C (above 200 °C for PES). Clearly the desirable property of the high temperature T_g has been maintained in the blend, the reduction in its E' value in the glassy region compared with the epoxy resin is small and in composite applications this is insignificant since the strength and stiffness in composites come from the fibre reinforcement. Therefore, blending with PES, improves the toughness of the epoxy resin (see Figure 1.8) without compromising its desirable mechanical and thermal properties.

7.4.1.7 Effect of plasticisers and moisture

Plasticisers are added to polymers to render them soft and flexible and/or to aid their processability, by lowering T_g and to a lesser extent T_m . This is exemplified for plasticised PVC in Figure 7.27: where the addition of plasticiser diethylhexyl succinate lowers T_g significantly. The figure also shows that, similar to polymer blending, the plasticisation also broadens the transition region. The broadening is also observed in the storage modulus curves which resemble in shape the ones shown for the PU/PMMA blends, see Figure 7.25. The maxima in logarithmic decrement (a damping term) peaks significantly reduce in height, as well as broaden, with increasing plasticisation; however, around 50 % plasticiser content the damping peaks become narrower and start to increase in peak height. This is probably due to overlapping of the reduced- T_g (α -transition) with the β -transition for PVC (around -75 °C) and resulting in a combined effect.

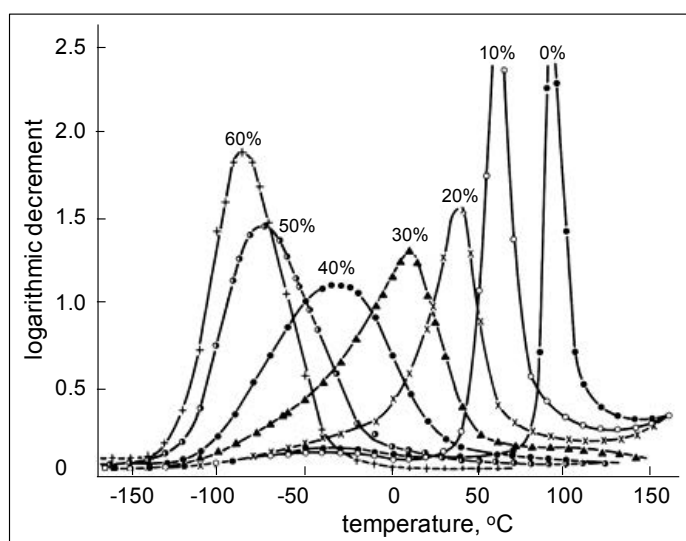


Figure 7.27 Logarithmic decrement at 1 Hz vs. temperature for PVC plasticised with diethylhexyl succinate at concentrations (by volume) indicated on the curves (source: Schmieder & Wolf 1952)

In general, the glass-transition broadening is greater with the poor plasticisers than the good ones for the polymer, therefore in PVC, a poor plasticiser such as dioctyl phthalate produces a broader and lower damping-peak height compared with a good plasticiser such as diethyl phthalate. Moisture in polymers causes similar effects to that of plasticisers. Some polymers such as polyamides are hygroscopic and can absorb large amounts of water, which alter their physical and mechanical properties, including dynamic mechanical thermal properties. This is described for PA 66 in one of TA Instruments' application brief. They have conducted DMA in resonance mode with 0.2 mm oscillation amplitude while heating at 5 °C/min over -150 to 150 °C temperature range, using rectangular specimens of 3 mm x 13 mm cross-section with clamps

separation of 19 mm. The specimens were conditioned at 0 %, 50 % and 100 % relative humidity (RH). Although the report does not mention the actual moisture uptake for the specimens, however in open literature, moisture contents (mass fraction) of approximately 0.2 % for dry as-moulded, and the saturation/equilibrium moisture level of 8.5 % at 100 % RH and 2.5 % at 50 % RH are quoted for PA 66.

Figure 7.28 shows the plots of E' and $\tan \delta$ against temperature for three specimens with different levels of moisture absorption. The $\tan \delta$ traces exhibit three peak maxima: α -transition (glass transition) due to long chain segmental motion within the main polymer chain, β -transition is attributed to localised motion within the amide segments, and γ -transition is attributed to localised segmental motion of the $(-\text{CH}_2-)$ methylene groups between amide groups in the amorphous regions. The main variation, as would be expected, is observed in T_g : a shift of around 60 °C with increasing moisture content from the “dry as-moulded” to conditioned at 100 % RH. The depression in T_g is a consequence of the disruption by water of the intermolecular hydrogen bonding. It is also worth noting that the storage modulus in the glassy region below 0 °C increases with moisture content, which has been associated with the crystallization of occluded water (Birkinshaw & Buggy 1987 and Baschek 1999).

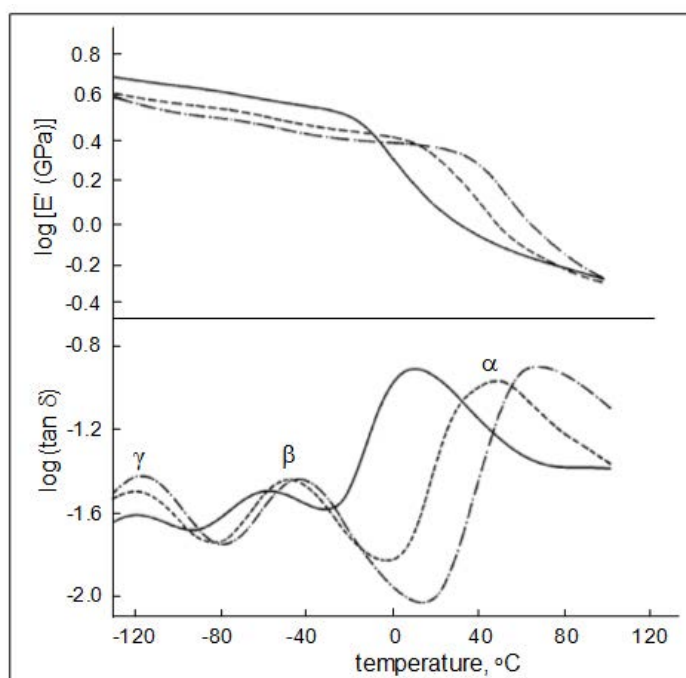


Figure 7.28 DMTA properties vs. temperature for PA66 with different moisture content: (— · —) dry; (---) conditioned at 50% RH; (—) conditioned at 100% RH (source: TA Instruments-2)

Dielectric thermal analysis (DETA), or Dielectric Analysis (DEA), is a technique similar to DMTA: dielectric measurements are the electrical analogue of dynamic mechanical measurements, where the mechanical force (stress) is replaced by an alternating voltage across the sample (a.c. electrical field) and the alternating strain becomes the stored charge (Q) or the a.c. current in the sample. Q is always measured as its derivative, $dQ/dt = I$. One can visualise the polymer specimen as being represented by a parallel combination of a resistor (conductor) and a capacitor, akin to the mechanical Kelvin-Voigt model.

The great advantage of DEA is that it can be employed in situ process monitoring as well as in laboratory testing. In a typical test, the sample is placed in between two metal electrodes (the dielectric sensor) and a sinusoidal voltage (the excitation) is applied to one of the electrodes. The resulting sinusoidal current (the response) is measured at the second electrode. The current and its phase difference with respect to the applied voltage is measured, and from this data the dielectric properties of ϵ' (the dielectric constant or the permittivity) and ϵ'' (loss factor) are calculated. Another commonly used term for expressing dielectric response is the dissipation factor or the loss tangent, $\tan\delta = \epsilon'' / \epsilon'$.

Its application in monitoring the curing behaviour of thermosetting resin systems, composite materials, adhesives and paints has been standardised in ASTM E 2038 or E 2039:

ASTM E2038-99 Standard test method for temperature calibration of dielectric analyzers,

ASTM E2039-99 Standard test method for determining and reporting dynamic dielectric properties.

The conventional thermal analysis techniques are suitable for measuring the bulk properties of materials, but for localised characterisation of materials micro and nano-thermal analysis techniques are used. These employ a displacement thermal probe attached to an atomic force microscope (AFM) and measure the probe cantilever deflection (whilst in contact with the sample surface) against probe tip temperature. The instrument is basically an AFM fitted with a tip that acts as heat source and temperature sensor. Material transitions that result in the softening of the material beneath the tip produce a downward deflection of the cantilever, similar in concept to the well established technique of thermo-mechanical analysis (TMA). Localised Thermal Analysis (LTA) can be used, for instance, to explore morphology changes across the surface of a material by measuring the localised transition temperatures. Further information on the technique can be obtained from, for example, www.anasysinstruments.com , www.tainstruments.com or Ehrenstein 2004, p300.

7.5 Determination of softening temperature

Designers and engineers need to know the maximum-use temperature, i.e., the extent of thermal stability, when selecting polymers for engineering applications. This enables them to establish the maximum temperature at which a polymer can be used as a rigid material. It is already covered that Young's modulus is a material property that indicates rigidity or stiffness and its measurement over a temperature range becomes a guide for material thermal stability by enabling the identification of the glass-transition temperature.

The softening temperature for a polymer is closely related to T_g for amorphous thermoplastics and thermosetting polymers and to T_m for crystalline polymers. Many polymers exhibit softening at a temperature between T_g and T_m , depending on the degree of crystallinity, presence of additional intermolecular force and also the method used to determine the softening temperature. The methods popularly used to establish the upper limit of safe operating temperatures for products fabricated from a given polymeric material include heat distortion temperature (HDT) or the deflection temperature under load (DTUL) and the Vicat softening temperature. The HDT/DTUL is identified as the temperature at which a standard test bar deflects a specified amount when loaded in 3-point bending, and therefore, the property can be deemed to be a mechanical-thermal property. The Vicat softening point is the temperature at which a flat-ended needle, under load, penetrates a heated sample of polymer to a certain depth. **Maximum continuous use temperature** is another parameter that is assigned to polymers as an indicator of softening temperature. This is based upon the Underwriters Laboratories (UL) rating for long-term continuous use, and is defined as the temperature at which the room temperature tensile strength of the material reduces to half its value, in the absence of any applied external stresses, as a result of high-temperature exposure for 100,000 hours. As a rule of thumb, a 10 °C increase in temperature is equivalent to a decade increase in time (Tripathy 2002, p27). For example, the maximum continuous use temperature for PP is 100 °C, which would be equivalent to 10,000 h at 110 °C or 10⁶ h at 90 °C. Therefore, certain grades of PP are suitable for short-term exposure to high temperatures at 140 °C and are used as steam-sterilisable hospital ware.

7.5.1 Heat distortion temperature

Heat distortion or deflection temperature is used to determine short-term heat resistance. It distinguishes between materials that are able to support light loads at high temperatures and those that cannot and lose their rigidity over a narrow temperature range. The standard methods for conducting HDT include:

ISO 75-1:2004 Plastics – Determination of temperature of deflection under load – Part 1: General test method

ISO 75-2:2004 Plastics – Determination of temperature of deflection under load – Part 2: Plastics and ebonite

ISO 75-3:2004 Plastics – Determination of temperature of deflection under load – Part 3: High-strength thermosetting laminates and long-fibre-reinforced plastics

ASTM D648 - 07 Standard test method for deflection temperature of plastics under flexural load in the edgewise position

The test procedure consists of positioning the specimen under the deflection measuring device for 3-point bending, see Figure 7.29. A load of 0.45 MPa or 1.80 MPa or 8.00 MPa is placed on the specimen depending on the test method

followed. The specimen is then lowered into a silicone oil bath and heated at $2\text{ }^{\circ}\text{C}/\text{min}$ until a certain deflection is reached at the centre of the support span. The level of deflection is 0.25 mm for ASTM, 0.34 mm for ISO flatwise and 0.32 mm for ISO edgewise testing.

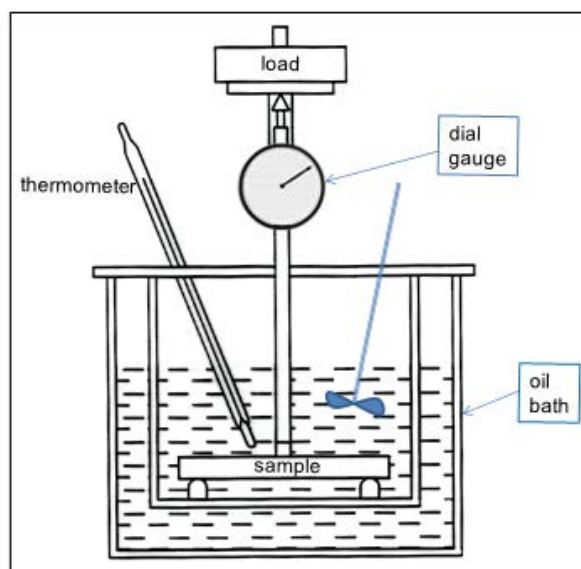


Figure 7.29 HDT test set up

The temperature at which the prescribed deflection occurs is taken to be the HDT. The high load of 8 MPa is suitable for testing TPs with very high softening temperatures, otherwise under the lower load of 1.8 MPa the test will last much longer and the HDT can be so high as to cause the decomposition of the heating oil (the silicone oil, normally used in these tests, is prone to decomposing rapidly).

In ISO standard methods, the edgewise testing (where the loading nose is placed across the thickness) uses a test bar of 120 x 10 x 4 mm with a 100 mm support span length and the flatwise testing (where the load is applied across the width) uses a test bar of 80 x 10 x 4 mm with a 64 mm support span length, similar to the normal flexural test. The ASTM method only describes an edgewise test for 5" x 1/2" x 1/4" specimens. The HDT test is essentially a flexural test, and therefore the equations for bending (see Section 6.3) apply.

The HDT test is used to determine short-term heat resistance and should not be used alone for product design to establish the upper limit of safe operating temperatures for products for long term performance. Other factors such as the time of exposure to an elevated temperature, the rate of temperature increase, and the part geometry all affect the performance. Other factors include polymer type and structure, filler/reinforcement type and loading levels, fibre orientation, oxidative stability and moulded-in residual stresses; all of which may cause the actual maximum-use temperature to be significantly different than the HDT. Accordingly it should be used together with other thermal behaviour indicators for guidance.

The techniques such as the DMTA, in comparison, produce a greater insight to the material behaviour. For instance, the HDT values for short and long glass-fibre reinforced polybutylene terephthalate (PBT) polyester are quite similar, approximately $210\text{ }^{\circ}\text{C}$ at 1.8 MPa, however, this does not reveal the actual material rigidity profile across the temperature

range as shown by the DMTA traces in Figure 7.30: as can be seen, the long-fibre reinforced PBT alternative shows a greater elastic modulus in the glassy region, which is maintained above the T_g up to the HDT.

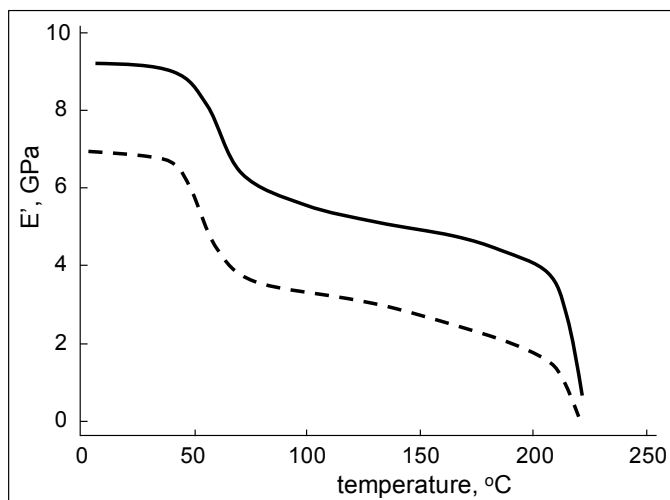


Figure 7.30 Storage modulus vs. temperature for glass-fibre reinforced PBT:
(—) long fibre; (---) short fibre

It is, however, the case that, if the differences in the elastic moduli of the materials are known, then HDT is a good indicator of the temperature where to expect a collapse in material stiffness irrespective of the stiffness characteristics at temperatures below HDT.

7.5.2 Vicat softening temperature

This is a similar method to that of HDT, but instead of a test bar, the specimen consists of a small flat piece and the Vicat softening temperature (VST) is the temperature at which a flat-ended pin of 1 mm² circular cross section, under a specified load and heating rate, penetrates the specimen to a certain depth. The standard methods for conducting VST include:

ISO 306:2004 Plastics - Thermoplastic materials – Determination of Vicat softening temperature (VST)

ASTM D1525 - 09 Standard test method for Vicat softening temperature of plastics.

The test piece is either a disk of 10 mm diameter or a square piece of 10 mm² surface area and 3 mm to 6.5 mm thickness. The alternatives in the test methods recommend employing loads of either 10 N or 50 N, and the heating rates of either 50 °C/h or 120 °C/h. The test determines the temperature at which the needle penetrates the specimen by 1 mm. The penetration is mainly an outcome of the decrease in elastic modulus, or viscous flow above T_g in lower molecular weight portions of amorphous thermoplastics. The material must become quite soft for the Vicat pin/needle to penetrate to a depth of 1 mm, therefore, for most polymers the VST values are higher than the ones obtained with other methods for measuring softening points, such as HDT, as can be seen in Figure 7.31.

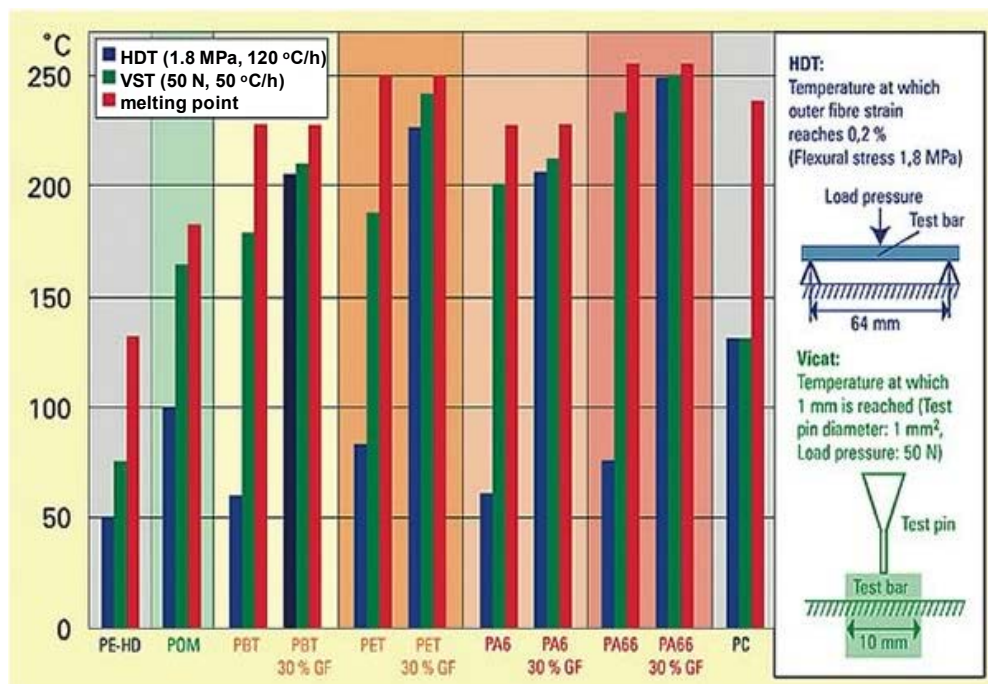


Figure 7.31 VST, HDT and T_m for various thermoplastics, showing the influence of structural variations and fibre reinforcement (source: DuPont Engineering Polymers)

The test may be open to misinterpretation when testing specimens that contain high molecular orientation. The specimens with high molecular orientation will relax and increase in thickness when heated during the test and may push the pin up or at least slow down its penetration, producing a distorted result. Similar concerns apply to the HDT test. Therefore, in such cases the material should be annealed prior to the test run.

7.5.3 Thermal conductivity

Thermal conductivity is a measure of how easily heat moves through/along a material. It is a material property that is primarily dependent on its state, temperature, density, and molecular bonding. Covalent bonding in polymer molecules are not conducive to conduction: in covalent bonding the electrons are localised and not free to move and the absence of free/mobile electrons make most ceramics and polymers poor conductors of electricity and heat. Furthermore, when heated, polymer molecules undergo random internal molecular motion absorbing/dissipating energy rather than transferring it along. Polymers, therefore, make good insulating materials, provided the application temperature is not too high as to cause thermal degradation. Crystallinity, therefore density, influences the magnitude of thermal conductivity: a material with highly crystalline/ordered structure facilitates higher conductivity than the equivalent amorphous material. In the crystalline state, the molecular vibrations to facilitate conduction are coordinated more effectively.

Thermal conductivity, k , is defined as the rate at which heat is transferred by conduction through a unit cross-sectional area of a material when a temperature gradient exists perpendicular to the area. If the uniform temperature on one face of a flat slab of a material is T and $(T-\Delta T)$ on the other face, then the rate of heat flow or heat transfer, q , through the thickness of the slab is given by Fourier's law of heat conduction:

$$q = k A (\Delta T / L)$$

where, 'A' is the heat transfer area (the surface area of the rectangular slab) and 'L' is the material thickness.

The equation is often expressed with a minus sign to indicate that the heat flows in the direction of decreasing temperature gradient. The equation can be rearranged to express for conductivity

where, ' q / A ' is known as the heat flux.

The methods for measuring thermal conductivity include the un-guarded hot plate and the guarded hot plate methods. The **unguarded hot plate** method is based on the well known Lees' disc method, see Figure 7.32. The standard test procedures for the unguarded hot plate method include:

BS 874-2.2:1988 Methods for determining thermal insulating properties. Tests for thermal conductivity and related properties. Unguarded hot-plate method

ASTM C518 - 10 Standard test method for steady-state thermal transmission properties by means of the heat flow meter apparatus.

The test is open to heat losses from the exposed edges. Ways of reducing heat loss from the exposed edges are described by Hands (1999, p602). Using thin specimens and thin heater plates with large surface areas, the side losses may be reduced. Surrounding the apparatus with a low conductivity material such as vermiculite also reduces heat loss. An improvement

on the unguarded hot plate method is the **guarded hot plate** one, which is the most accurate method available for solid materials (including foams). The associated standard test methods include:

ISO 8302:1991 Thermal insulation – Determination of steady-state thermal resistance and related properties – Guarded hot plate apparatus

ISO 8990:1994 Thermal insulation – Determination of steady-state thermal transmission properties – Calibrated and guarded hot box

BS EN 12667:2001 Thermal performance of building materials and products. Determination of thermal resistance by means of guarded hot plate and heat flow meter methods. Products of high and medium thermal resistance

BS 874-2.1:1986 Methods for determining thermal insulating properties. Tests for thermal conductivity and related properties. Guarded hot-plate method

ASTM C177 - 10 Standard test method for steady-state heat flux measurements and thermal transmission properties by means of the guarded-hot-plate apparatus

ASTM C1044 - 07 Standard practice for using a guarded-hot-plate apparatus or thin-heater apparatus in the single-sided mode

DIN 52612-2 Testing of thermal insulating materials; determination of thermal conductivity by means of the guarded hot plate apparatus; conversion of the measured values for building applications.

The guarded hot plate test, see Figure 7.33, is described in the IDES web site (http://www.ides.com/property_descriptions/ISO8302.asp): two identical samples are placed on opposite sides of the main heater. The main heater and guard heaters/rings are kept at the same temperature. Heat sinks are maintained at a lower temperature. The guard heaters minimize the amount of lateral heat transfer from the main heater. Temperatures are monitored at each surface. The heat transferred through the specimens is equal to the power supplied to the main heater. Thermal equilibrium is established when temperature and voltage readings are steady. Thermal conductivity is calculated by inserting the equilibrium values obtained into the conductivity equation:

$$k = \frac{P \cdot L}{2 \cdot A \cdot (T_h - T_s)}$$

where, P is the power supplied to the main heater ($W = VI$), A is the surface area of the specimen (m^2), L is the specimen thickness (m), T_h is the temperature of the heater and T_s is the temperature of the heat sink. Note that the power supplied is divided by 2 since there are two specimens.

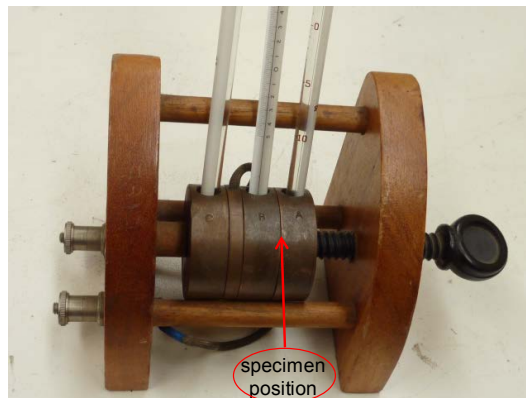


Figure 7.32 Lees' disk apparatus

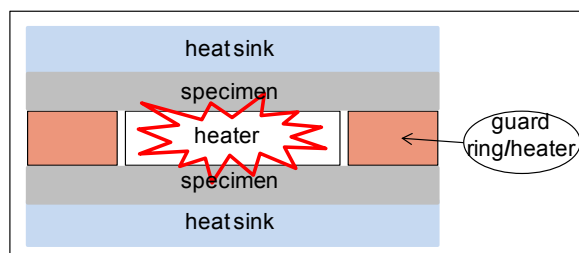


Figure 7.33 Guarded hot-plate set up

There is commercial equipment for conducting guarded hot-plate tests, e.g., GUNT WL376, designed to meet the DIN 52612-2 standard requirements is used for thermal conductivity of building materials such as polystyrene , PMMA and cork sheets, and plaster board.

Hands (1999, p597) presents a good account of testing for thermal diffusivity and specific heat as well as thermal conductivity.

Values for thermal properties of various polymeric materials (obtained under standard laboratory conditions of approximately 23 °C and 50 % relative humidity on dry-as-moulded samples) are presented in Table 7.1.

Table 7.1 Thermal properties of various polymers (sources; Netzsch, CAMPUS, Plastics International, Joel Fried (1995, p473), Ehrenstein (2001, p264))

Polymer type	T_g , °C	HDT (0.45 MPa), °C	HDT (1.8 MPa), °C	Vicat (50 N), °C	T_m , °C	ΔH_m^0 , J/g	k, W/(m.K)	C_p , kJ/(kg.K)	α , $10^{-5} \times K^{-1}$
Commodity thermoplastics									
LDPE	-120	43 (38-50)	35-37		115 (100-115)	140	0.33 (0.32-0.4)	1.8-3.4	25 (10-40)
HDPE	-120	85 (60-91)	50 (46-82)	80	130 (125-135)	293	0.48 (0.33-0.53)	1.9 (1.8-2.7)	10 (6.7-25)
PP	-20 /5	113 (90-121)	57 (50-85)	83	160 (160-175)	205 (205-209)	0.12 (0.12-0.25)	1.9 (1.8-2.1)	15 (7-18)
PS	90 (74/105)	82 (75-100)	72 (69-94)	85 (78-99)	240-260 (isotactic)		0.13 (0.13-0.18)	1.2-1.3	7 (5-15)
PVA	30 (11/40)								
PVC	81 (75/105)	82 (60-82)	60 (60-77)	75-110	273		0.16 (0.13-0.95)	0.85-1.5	7 (4-18)
SAN	100 (95/125)	100 (90-107)	88 (88-104)	106			0.13 (0.13-0.18)	1.2-1.3	7 (6-8)
Engineering thermoplastics									
ABS	95/105	101 (89-107)	88 (79-104)	94			0.16 (0.15-0.2)	1.26-1.68	8 (8-10)
PA 6,6	72 (45/90)	220 (200-235)	77 (70-105)	230 (210-250)	260 (225-265)	185 (185-300)	0.24 (0.23-0.33)	1.7	8 (4.5-14.4)
PBT	48 (45/60)	159 (116-190)	62 (50-93)	178-180	225 (220-267)	140-142	0.21 (0.18-0.29)	1.3 (1.2-2.3)	10 (6-17)
PC	145 (140/150)	138 (137-145)	130 (121-137)	138 (130-145)	230 (227-235)		0.2- 0.21	1.2 (0.9-1.5)	7 (6-12.2)
PET	68/80	80 (70-115)	80 (21-80)	185-188	255 (212-280)	140-145	0.24 (0.14-0.25)	1.05-1.17	7 (6.5-11.7)

PMMA	110 (atactic); 115(synd.); 45 (iso.)	96 (74-107)	88 (68-100)	100 (70-103)	160 (iso)		0.18 (0.17-0.25)	1.46 (1.45- 1.47)	9 (5-16.2)
POM	-17/-30	160 (124-172)	110 (100-136)	160 (151- 173)	165 (165-190)	316-335	0.23 (0.23-0.37)	1.5 (0.31- 1.5)	11 (9-18)
PU		99	88	100			1.8	0.4	6;21
SBR	-35/-55	77-89	67-85	88 (63-95)		170 (cis)	0.18 (0.18-0.25)	1.3-2	10 (7-22)
TPU	-16/ -50	86 (46-135)	47 (47-127)		135-220	3-15	1.7	0.5	10-15
UHMW- PE		68 (65-82)	42 (42-49)	80	130-140		0.33 (0.33-0.5)	1.84	20 (11-36)
High-performance engineering thermoplastics									
PTFE		121 (71-140)	46-55		325-332	82	0.25 (0.23-0.25)	1.0	12 (7-21.6)
PPO	117/210	137	123 (107-149)		257-307	50	0.22	0.25	3.3 (3.3-7.7)
PEEK	145	205-260	155-160	305- 305	335-340	130	0.25		5 (5-8.5)
PEI	215/230	207-210	197-200				0.07		4.7-5.6
PES	222 (210/230)	216-218	205 (200-230)	215			0.18	1.1-1.4	5.5 (5.2- 6)
PI	337/364	343-377	319 (238-360)		388		0.1-0.176		4.1 (3.6-5.6)
PPS	90 (85/110)	204 (199-260)	115 (100-135)		280 (275-290)		0.25 (0.08-0.29)		5 (3-7)
PSU	185/190	181 (180-183)	174 (167-175)	180			0.15-0.28	1.3- 1.4	5.3 (3.1-5.6)
Thermosets									
EP	0/180		200 (46-288)				0.19 (0.17-0.88)	1 (0.8-2.1)	6 (3.5- 11.7)
MF	20/60		180 (177-199)				0.4 (0.27-0.5)	1.2	4.5 (3.5-6)
PF	80/120	190	79 (74-150)				0.15 (0.15-0.35)	1.3-1.6	6.8 (3- 12.2)
UP	0/150	105	80 (60-204)				0.7 (0.17- 0.7)	1.2 (0.7-2.3)	7 (2-18)
PI			240-300				0.23-0.65		5 (1.5-6.3)

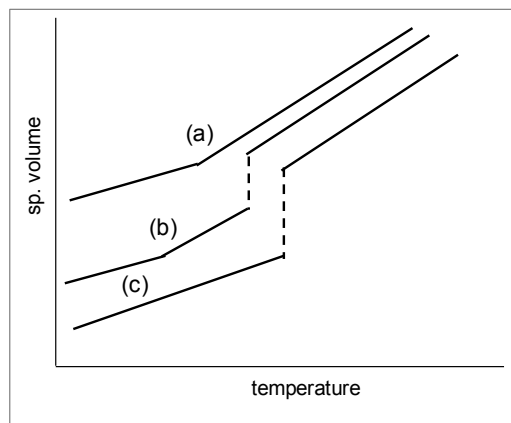
PU	10/100		90(88-93)				0.58	1.76	2-6
UF	0/30		130				0.4	1.2	5-6

Factors that affect data: crystallinity, orientation, types of copolymer, ratios of comonomers, grades of TSs, e.g., epoxy is such a generic name covering all sorts of resins with varying properties, type of curing (cold cured, stove cured at different temperatures for different lengths of times, etc.) and degree of curing. Thermosets such as MF, PF and UF mainly contain filler.

7.6 Self-assessment questions

- On the same graph paper show how the heat flow during a DSC analysis and the elastic modulus of a polymeric material changes with temperature over a temperature range that passes through the glass-transition temperature of the polymer.
- When a squash ball is immersed in liquid nitrogen and then brought out and hit immediately with a racquet against the wall, what would happen to it and why?
- Sketch, on the same graph, the plots of specific volume vs. temperature for PP and PS, both with syndiotactic stereoregularity.
- The effect that increasing the temperature of a polymer has on its elastic modulus is similar to that of
 - increasing the time under load
 - decreasing the cross-link density
 - decreasing the time under load
- What is meant by the 'free volume' of a polymer?

6. If you hang a weight from a strip of rubber so that it stretches about 300%, then heat the rubber, which of the following would happen?
- it stretches some more
 - it contracts
 - it maintains the same length
7. Consider these three labelled specific volume vs. temperature plots that may be displayed by various types of materials. Indicate the one, which best describes the behaviour expected from PP with a spherulitic structure.



8. Why is the value of T_g dependent on the method of measurement?
9. Based on the way polymer chains behave above and below T_g , why do you think glasses tend to be brittle whereas rubbers are not?
10. Explain why bungee jumping cord should be made from butyl rubber (especially if it is to be used in a sunny climate).
Hint: consider influence of u.v. light on degree of cross-linking.
11. Which of the following correctly represents the sequential change in mechanical state with increasing temperature for an amorphous polymer?
- viscous liquid; rubbery region, glass
 - glass; viscous liquid; rubbery solid
 - glass; rubbery solid; viscous liquid
 - rubbery solid; glass; viscous liquid
12. It is intended to manufacture coiled cords for telecommunication equipment using PVC flex, and for efficiency in production the relaxation time should not be greater than 3 h at the production temperature. Determine what should be the minimum temperature of the processing oven in order to achieve this relaxation time. The PVC used has a relaxation time of 28 h at 27 °C, take the activation energy for this process to be 20 kJ / mol and the molar gas constant is 8.314 J / (mol.K).
Answer: $T = 142$ °C
13. A plot of DMTA damping term against temperature can be used to determine a temperature at which
- tensile strength becomes maximum
 - the specific heat shows a minimum
 - Young's modulus undergoes a significant drop
 - the crystalline phase melts.

14. The presence of aromatic groups in a polymer chain results in
- intermolecular attraction
 - potential for crosslinking
 - increase in T_g and T_m
 - tensile strength becomes a maximum.
15. The outcome of a DSC test is usually presented in the form of a plot of heat flow against temperature and/or time, why is it useful to also present the derivative of this plot?
16. Indicate the thermal properties that can be determined using DSC. Make a definition of these properties.
17. From the definition of the specific heat capacity (C_p), derive an equation that expresses C_p in terms of DSC parameters.

Answer: _____

18. Distinguish between “dynamic” and “static” OIT methods. Briefly describe an application of OIT.
Hint: consider heating programme/conditions.
19. DSC analysis for a PA 66 sample produces a heat of fusion value of 40 J/g, with reference to Table 7.1 determine the % crystallinity for the sample.
Answer: approximately 22 %.
20. Indicate which other analytical techniques TGA can be coupled with and what would be the advantages?
21. Indicate the uses for TGA. A plastic containing a fire retardant (magnesite) is examined by TGA in order to determine the % of magnesite used. The analysis shows that, after the pyrolysis of the polymer, at approximately 600 °C, 12% CO_2 is emitted. Determine the magnesite (MgCO_3) content.
Answer: 22.8 %.
22. Describe in terms of molecular-relaxation transition, how some rigid plastics exhibit good impact strength. Give examples of such plastics.
23. Describe how the Arrhenius relationship can be used to determine the energy needed for a relaxation transition to occur. Using the Arrhenius relationship and the data for the β -transition temperature at various frequencies for a thermoplastic in the table below, determine the activation energy for the β -relaxation in kJ/mol.

Frequency, Hz	β -relaxation temperature, °C
0.1	0
0.3	15
1	25
3	45
10	55

Answer: $E_a = 61 \text{ kJ/mol}$.

24. Describe, giving an example, how annealing affects the dynamic-mechanical thermal (DMT) properties of crystalline thermoplastics.
25. Why is there a variation between the DMT properties of various nylons?
26. Compatible Polymers A and B are to be blended to achieve a glass-transition temperature of 60 °C. T_g s of Polymers A and B are 30 and 85 °C, respectively, using an appropriate equation determine the composition of the blend.
Answer: Polymer A should be approximately 23 % by weight.
27. Describe, briefly, with examples how to achieve polymers with damping properties that are not affected by changing temperature over a wide range of temperatures, and also how to improve the impact toughness of a resin widely used in aerospace applications.

28. With reference to Figure 7.27, highlight the changes that occur to the damping characteristics of PVC with plasticisation.
29. HDT is popularly used in industry to determine softening temperature for polymers, what precautions should be exercised in its use for product design to establish the upper limit of safe operating temperatures for products?
30. In comparison, which one of the methods for measuring softening points, HDT and VST, usually indicates a higher value than the other and why?
31. A fibre reinforced thermosetting polymer composite is autoclave cured at 160 °C, determine the differential strain that is generated between the component materials as the composite is cooled down to 20 °C following the curing process, and indicate if the level of strain is significant and why? The linear coefficients of expansions are $5 \times 10^{-6} / ^\circ\text{C}$ for fibre and as high as $10 \times 10^{-5} / ^\circ\text{C}$ for the resin. The resin exhibits 1.5 % elongation at failure.
Answer: approximately 1.3 %.
32. A PMMA rod, wedged in between two solid walls, parallel to the ground, suffers negligible stress at room temperature (20 °C). The rod in that position is subjected to heat, by using the data from Tables 6.1 and 7.1, determine the magnitude of the compressive stress that would be generated in the rod if the temperature reaches 70 °C?
Answer: 1.5 MPa.
33. A plane wall of 1 m² surface area is constructed from a 50 mm thick solid polymeric material of 2 W/(m °C) thermal conductivity. When the temperature is 80 °C on one side and 20 °C on the other, calculate the conductive heat transfer through the wall.
Answer: 2.4 kW.

References

- Akay, M & Aslan, N 1995, 'An estimation of fatigue life for a carbon fibre/polyether ether ketone hip joint prosthesis', *Proc. Instn. Mech. Engrs., Part H: Journal of Engineering in Medicine*, vol. 209, pp. 93-103.
- Akay, M & Barkley, D 1984, 'An assessment of processing morphology and on-line measurement of spherulite size for polypropylene film', *Plastics, Rubber and Composites Processing and Applications*, 4, pp. 247-55.
- Akay, M & Barkley, D 1985, 'Processing-structure-property interaction in injection moulded glass-fibre reinforced polypropylene', *Composite Structures*, 3, pp. 269-293.
- Akay, M & Barkley, D 1991, 'Fibre orientation and mechanical behaviour in reinforced thermoplastic injection mouldings', *Journal of Materials Science*, 26, pp. 2731-42.
- Akay, M & Barkley, D 1992, 'Jetting and fibre degradation in injection moulding of glass-fibre reinforced polyamides', *Journal of Materials Science*, 27, pp. 5831-36.
- Akay, M & Barkley, D 1993, 'Flow aberrations and weld lines in glass fibre reinforced thermoplastic injection mouldings', *Plastics, Rubber and Composites Processing and Applications*, 20, pp. 137-49.
- Akay, M, Bryan, SJ and White, EFT 1973, 'The dynamic mechanical properties of thermosetting acrylic coatings', *J. Oil Col. Chem. Assoc.*, 56, pp. 86-94.
- Akay, M & Cracknell, JG 1994, 'Epoxy resin-polyethersulphone blends', *Journal of Applied Polymer Science*, vol.52, pp. 663-88.
- Akay, M & Hanna, R 1990, 'A comparison of honeycomb-core and foam-core carbon-fibre/epoxy sandwich panels', *Composites*, vol. 21, no.4, pp. 325-331.
- Akay, M & Mun, SKA 1995, 'Bearing strength of autoclave and oven cured Kevlar/epoxy laminates under static and dynamic loading', *Composites*, vol. 26, no. 6, pp. 451-456.
- Akay, M & Ozden, S 1995, 'Influence of residual stresses on the mechanical and thermal properties of injection moulded ABS copolymer', *Journal of Materials Science*, 30, pp. 3358-68.
- Akay, M & Ozden, S 1996, 'Influence of residual stresses on the mechanical and thermal properties of injection moulded polycarbonate', *Plastics, Rubber and Composites Processing and Applications*, vol. 25, no. 3, pp. 138-144.
- Akay, M & Rollins, SN 1993, 'Polyurethane-poly(methyl methacrylate) interpenetrating polymer networks', *Polymer*, vol. 34, no. 9, pp.1865-74.

- Akay, M 1992, 'Bearing strength of as-cured and hygrothermally conditioned carbon-fibre/epoxy composites under static and dynamic loading', *Composites*, vol. 23, no. 2, pp. 101-108.
- Akay, M 1994, 'Moisture absorption and its influence on the tensile properties of glass-fibre reinforced polyamide 6,6', *Polymers & Polymer Composites*, vol. 2, No. 6, pp. 349-354.
- Akay, M 1999, 'Fracture mechanics properties', *Handbook of polymer testing: physical methods*, Brown, R (ed.), Marcel Dekker, New York.
- Alger, MSM 1989, *Polymer science dictionary*, Elsevier applied Science, UK.
- ASM International 2003, *Characterization and failure analysis of plastics*, USA.
- ASTM D2565-99(2008) Standard practice for xenon-arc exposure of plastics intended for outdoor applications.
- ASTM D4587-11 Standard practice for fluorescent UV-condensation exposures of paint and related coatings.
- Asua, JM 2007, *Polymer reaction engineering*, Wiley-Blackwell, Oxford, UK.
- Baitcher, N 2006, 'Low cost carbon fibre composites for lightweight vehicle parts',
http://www.emergingmit.com/case_studies.html or http://www.emergingmit.com/mit_docs/sbir_report.pdf.
- Barkley, D & Akay, M 1992, 'The design and evaluation of an instrumented impact tester', *Polymer Testing*, 11, pp. 249-270.
- Baschek, G, Hartwig, G & Zahradnik, F 1999, 'Effect of water absorption in polymers at low and high temperatures', *Polymer*, 40, pp. 3433-41.
- BASF-1, 2003, 'Mechanical performance of polyamides with influence of moisture and temperature – accurate evaluation and better understanding', <http://www2.basf.us//PLASTICSWEB/displayanyfile?id=0901a5e180004880> , accessed on January 2012.
- BASF-2, 2003, 'Plastics part design: low cycle fatigue strength of glass-fibre reinforced polyethylene terephthalate (PET)', BASF Corporation, New Jersey, web site: <http://www2.basf.us//PLASTICSWEB/displayanyfile?id=0901a5e18000488c> , accessed November 2011.
- Bennett, FNB 1980, 'The non-contact extensometer', *Polymer Testing*, vol. 1, issue 2, pp. 91-95.
- Birkinshaw, C, Buggy, M & Daly, S 1987, 'Plasticization of nylon 66 by water and alcohols', *Polymer Communications*, 28, pp. 286-288.
- Blaine, RL and Hahn, BK 1998, 'Obtaining kinetic parameters by modulated thermogravimetry', *Journal of Thermal Analysis*, 54, pp. 695-704.

Boustead, I 2003, *Plastics and the environment*, Andrady, AL (ed.), Wiley-Interscience, New Jersey.

BPF web site: <http://www.bpf.co.uk/Plastipedia/Default.aspx>, accessed February 2012.

Brisco, BJ, Sebastian, KS & Adams, MJ 1994, *J. Phys. D*, 27, 6, p. 1156.

Brown, R 1999, 'Effect of temperature', *Handbook of polymer testing: physical methods*, Brown, R (ed.), Marcel Dekker, New York.

Brown, R 1999, *Handbook of polymer testing: physical methods*, Brown, R (ed.), Marcel Dekker, New York.

Brown, RP 1996, *Physical testing of rubber*, 3rd edn., Chapman and Hall, London.

Burall, P 1996, *Product development and the environment*, Gower Publishing, UK.

Callister, WD 2007, *Materials science and engineering an introduction*, 7th edn., Wiley, New York.

CAMPUS® is a registered trademark of CWFG mbH, Frankfurt/Main, Germany, CWFG mbH, <http://www.campusplastics.com/>, accessed January 2012.

Carbon Trust Report (CTG019) 2010, *Industrial energy efficiency accelerator: guide to the plastic bottle blow moulding sector*, the Carbon Trust, UK.

- Chung, CI 2000, *Extrusion of polymers: theory and practice*, Hanser Publishers, Munich.
- Clarkson, RJ 2004, Chemistry rules! '03,
http://20to9.com/miscellaneous/Powerful_pdfs/OCR_6Set/Merged_OCR_Notes.pdf , accessed 23 February, 2011.
- Crawford, RJ & Kearns, MP 2003, *Practical guide to rotational moulding*, Rapra Technology Limited, Shrewsbury, UK.
- Curtis, PT (Ed)1985, 'CRAG test methods', RAE TR85099, November 1985, Royal Aerospace Establishment, UK.
- Design Council 1993, *Engineering plastics and elastomers: a design guide*, London.
- DuPont Handbook on nylon resins, 'Design information-Module II',
<http://plastics.dupont.com/plastics/pdf/europe/zytel/ZYTDGe.pdf> , accessed October,2011.
- DuPont Hytel extrusion manual, <http://bit.ly/HF8ST6> , accessed February, 2012
- Efunda: <http://www.efunda.com/home.cfm>, accessed January 2012.
- Ehrenstein, GW 2001, *Polymeric materials: structure-properties-applications*, Hanser Publishers, Munich.
- Ezrin, M 1996, *Plastics failure guide: cause and prevention*, Hanser Publishers, Munich.
- Farag, MM 1997, *Materials selection for engineering design*, Prentice Hall, Europe.
- Freegard et al. 2005, *Develop a process to separate brominated flame retardants from WEEE polymers, Interim Report 1*, The Waste & Resources Action Programme, UK.
(http://www.wrap.org.uk/downloads/RandDIntRepPLA-037_BFR.f212cb31.2201.pdf)
- Fried, JR 1995, *Polymer science and technology*, Prentice Hall PTR, New Jersey.
- Giles, HF, Wagner, JR & Mount, EM 2005, *Extrusion: the definitive processing guide and handbook*, William Andrew, Inc., New York.
- Goodwin, E 2001, 'Economy in a box', *Eureka on Campus*, Autumn 2001, p40.
- Graedel, TE & Allenby, BR 1996, *Design for environment*, Prentice Hall, New Jersey.
- Groover, MP 1996, *Fundamentals of modern manufacturing: materials, processing and systems*, Prentice Hall, New Jersey.
- Hagan, RS & Keetan, WR 1994, *Plastics: key materials for innovation and productivity in major appliances*, American Plastics Council, February 1994, pp. 1-18.

- Hands, D 1999, 'Thermal properties', *Handbook of polymer testing: physical methods*, Brown, R (ed.), Marcel Dekker, New York.
- Harold, FG, Wagner, JR & Mount, EM 2005, *Extrusion: the definitive processing guide and handbook*, William Andrew, Inc. New York.
- Hawley, S 1999, 'Particular requirements for plastics', *Handbook of polymer testing: physical methods*, Brown, R (ed.), Marcel Dekker, New York.
- Hocking, MB 1991, 'Relative merits of polystyrene foam cup and paper in hot drink cups: implications for packaging', *Environmental Management*, 15 (6), pp. 731-47.
- Humphreys, C 1997, 'Material sciences-Part one', *Science and Society, a JSPS-UK Research Council Symposium*, Pilkington Press, pp. 34-51.
- IDES, *Environmental stress-cracking resistance (ESCR) - ASTM D1693*, http://www.ides.com/property_descriptions/ASTMD1693.asp, accessed January 2012.
- I-FOAM, <http://www.ifoam.is/>, accessed February 2012.
- International Finance Corporation 2007, Environmental, health, and safety guidelines: petroleum-based polymers manufacturing, 30 April 2007, <http://tinyurl.com/chzxhlh>, accessed 28 February, 2011
- ISO 4892-2:2006 (Parts 1-4) Plastics – Methods of exposure to laboratory light sources.
- James, I 1999, 'Putting testing in perspective', *Handbook of polymer testing: physical methods*, Brown, R (ed.), Marcel Dekker, New York.
- Jansen, JA 2004, 'Environmental stress cracking – the plastic killer', *Advanced Materials & Processes*, June 2004, pp. 50-53 (http://www.madisongroup.com/publications/Janse_ASM_ESC_TMG2011.pdf, accessed February 2012).
- Kaisersberger, E, Knappe, S, Mohler, H & Rahner, S 1994, 'TA for polymer engineering: DSC, TG, DMA & TMA', *NETZSCH Annual for Science and Industry*, vol. 3, Selb, Wurzburg, Germany.
- Kent, R 2008, *Energy Management in Plastics Processing: Strategies, Targets, Techniques and Tools*, Plastics information Direct, UK.
- Kockott, D 1999, 'Weathering', *Handbook of polymer testing: physical methods*, Brown, R (ed.), Marcel Dekker, New York.
- Lewis, P 1999, 'Testing of rubber', *Handbook of polymer testing: physical methods*, Brown, R (ed.), Marcel Dekker, New York.

Loadman, J 2005, *Tears of the tree: the story of rubber – a modern marvel*, Oxford University Press.

Masters, GM & Ela, WP 2008, *Introduction to environmental engineering and science*, 3rd edn., Prentice Hall, New Jersey.

Mettler-Toledo AG, Analytical, <http://tinyurl.com/d3xmx3y> accessed February, 2012.

Morton-Jones, DH 1989, *Polymer processing*, Chapman & Hall, London.

Miller, RW & Murayama, T 1984, 'Dynamic mechanical properties of partially oriented polyester (POY) and draw-textured polyester (PTY) yarns', *Journal of Applied Polymer Science*, vol. 29, issue 3, pp. 933-39.

Newey, C & Weaver, G 1990, *Materials principles and practice*, Open University, UK.

Netzsch, 'Thermal properties of polymers',

http://www.netzsch-thermal-analysis.com/download/Poster_A1_TPfPolymers_mitLupe_1110w_539.pdf, accessed January, 2012.

Nielsen, LE 1974, *Mechanical properties of polymers and composites*, vol. 1, Marcel Dekker, New York.

Niessen, WR 1977, *Handbook of solid waste management*, Wilson, DG (ed.), Van Nostrand Reinhold Co., New York.

- Painter, P & Coleman, M 2004, *Polymer science and engineering – work book*, DEStech Publications, Inc., Pennsylvania, USA.
- Performance Comparison under Alternative Testing Standard', *Paper Number: 2000-01-1319*, BASF Corporation, New Jersey.
- PerkinElmer 2010, 'differential scanning calorimetry (DSC): a beginners guide', http://www.perkinelmer.com/CMSResources/Images/44-74542GDE_DSCBeginnersGuide.pdf [accessed 30 November 2011].
- PerkinElmer-1, 'a and b relaxations of PMMA and calculation of the activation energy', *Application notes*, http://www.perkinelmer.com/CMSResources/Images/44-74239APP_PMMAAlphaBetaRelaxations.pdf, accessed December 2011.
- PerkinElmer-2, 'Investigation into the T_g of foams', *Application notes*, http://www.perkinelmer.com/CMSResources/Images/44-74298APP_TgFoamsInvestigation.pdf, accessed December 2011.
- Plastipedia, <http://www.bpf.co.uk/Plastipedia/Processes/Default.aspx#injectionmouldinggasassisted>, accessed February 2012.
- Plastics International, http://www.plasticsintl.com/sortable_materials.php, accessed January 2012.
- PlasticsEurope 2007, The compelling facts about plastics 2007, <http://www.plasticseurope.org/Document/the-compelling-facts-about-plastics-2007.aspx?Page=DOCUMENT&FolID=2>, accessed 19 February, 2011.
- Price, DM 1998, 'Novel methods of modulated temperature thermal analysis', *Thermochimica Acta*, 315, pp. 11-18.
- Ramsden, J 2009, 'A critical analysis of the proposed bridge over the Strait of Messina', in: *Proceedings of Bridge Engineering 2 Conference*, April 2009, University of Bath, UK.
- Reading, M 1993, 'Modulated differential scanning calorimetry – a new wayforward in materials characterization', *Trends in Polymer Science*, 1, pp. 248-253.
- Rooke, DP & Cartwright, DJ 1976, *Compendium of stress intensity factors*, HMSO, London.
- Savage, G 1993, *Carbon-carbon composites*, 1st edn. Chapman & Hall, London.
- Schmieder, K & Wolf, K 1952, *Kolloid Zeit.*, 127, 65.
- Schut, JH 2006, 'Induction heated molds produce Class A thermoplastic composites', *Plastics technology*, November 2006 (<http://www.ptonline.com/articles/induction-heated-molds-produce-class-a-thermoplastic-composites>).

- Sepe, MP 1997, 'Thermal analysis of polymers', *Rapra review reports*, Report 95, Volume 8, Number 11.
- Sharpe, M 2000, 'Phthalates: a ban too far?', *Journal of Environmental Monitoring*, 2, 4N-7N.
- Shelley, T 2007, 'Induction-heated moulds slash cycle times and costs', *Eureka on Campus*, Summer 2007, pp.22-23.
- Strong, AB 1996, *Plastics materials and processing*, Prentice-Hall, New Jersey.
- Summers, J, Mikofalvy, B & Little, S 1990, 'Use of X-ray fluorescence for sorting vinyl from other packaging materials in municipal solid waste', *J. Vinyl. Tech.*, 12, No.3, pp. 161-164.
- TA Instrments-1, 'Application of time-temperature superposition principles to DMA', *Thermal Analysis Application Brief*, Number TA-144, http://www.tainstruments.com/library_download.aspx?file=TA144.pdf, accessed December 2011.
- TA Instrments-2, 'Measurement of Moisture Effects on the Mechanical Properties of 66 Nylon', *Thermal Analysis Application Brief*, Number TA-133, http://www.tainstruments.com/library_download.aspx?file=TA133.pdf, accessed December 2011.
- Taber Industries: <http://www.taberindustries.com/taber-rotary-abraser>, accessed January 2012.
- The Welding Institute, Cambridge, UK, <http://www.twipprofessional.com/content/jk71.html>, accessed January 2012.
- Tripathi, D 2002, *Practical guide to polypropylene*, Rapra Technology Limited, Shrewsbury, UK.
- Turi, EA 1997 (ed.), *Thermal characterisation of polymeric materials*, Volumes 1 & 2, 2nd edition, Academic Press, San Diego.
- Veith, A 1999, 'Quality assurance of physical testing measurements', *Handbook of polymer testing: physical methods*, Brown, R (ed.), Marcel Dekker, New York.
- Warren, CD 2008, 'Polymer composites research in the ALM materials program' (http://www1.eere.energy.gov/vehiclesandfuels/pdfs/merit_review_2008/lightweight_materials/merit08_warren_2.pdf, accessed February, 2012).
- Weaver, ML & Stevenson, ME 2000, *Introduction to the mechanical behaviour of nonmetallic materials, Mechanical testing and evaluation*, Vol. 8, ASM Handbook, ASM International, pp. 13-25.
- Williams, ML, Landel, RF and Ferry, JD 1955, *J. Amer. Chem. Soc.*, 77, 3701.
- Witherell, C 1985, *How to avoid products liability lawsuits and damages – practical guidelines for engineers and manufacturers*, Noyes Publications, New Jersey.
- Woodruff, K 1986, *The solid waste handbook: a practical guide*, Robinson, WD (ed.) Wiley-Interscience, USA.

Wu, J & Eury, S (2002), 'HCFC and HFC alternative foam blowing agents', PU China, April 2002, <http://www.arkema-inc.com/literature/pdf/217.pdf>, accessed February, 2012.

Young, RJ & Lovell, PA 1991, *Introduction to polymers*, 2nd edn., Chapman & Hall, UK.